UAB
Universitat Autònoma de Barcelona

A gill-ty parasite:
Biological aspects of the ectoparasitic flatworm Sparicotyle chrysophrii Van Beneden & Hesse, 1863 and its interactions with gilthead seabream (Sparus aurata Linnaeus, 1758)

Enrique Riera Ferrer

A gill-ty parasite:

Biological aspects of the ectoparasitic flatworm *Sparicotyle chrysophrii* Van Beneden & Hesse, 1863 and its interactions with gilthead seabream (*Sparus aurata* Linnaeus, 1758)

A thesis submitted by Enrique Riera Ferrer in fulfilment of the requirements for the dregree of Doctor of Philosophy awarded by the International Doctorate in Aquaculture, October 2024.

Author
Enrique Riera Ferrer

Supervisor
Prof. Ariadna Sitjà-Bobadilla

Supervisor
Dr. Itziar Estensoro Atienza

Supervisor
Dr. Oswaldo Palenzuela Ruiz

Academic tutor
Prof. Maite Carrassón López de Letona

Institutional support

This thesis was carried out thanks to a four-year predoctoral contract (Personal Investigador en Formación; PRE2019-087409 - MCIN/AEI/10.13039/501100011033) awarded to Enrique Riera Ferrer within the framework of the Research Project - Plan Nacional I+D+I (Spanish Ministry of Science and Innovation) SPARICONTROL - Nuevas estrategias para el control de las infecciones por Sparicotyle chrysophrii en la acuicultura Mediterránea (RTI2018-098664-B-I00, AEI/FEDER, UE) from October 2020 to September 2024. During this period, the PhD candidate undertook two research stays. The first stay was at the Instituto de Salud Carlos III (Madrid, Spain) for one month. The second stay took place at the Biology Center of the Czech Academy of Sciences (CAS; České Budějovice, Czech Republic) for a period of three months. Both stays were funded by the SPARICONTROL project.

Other research projects, including the ThinkInAzul programme supported by the Ministry of Science and Innovation of Spain and funded by NextGenerationEU funds from the European Union (PRTR-C17.I1) and the Generalitat Valenciana (THINKINAZUL/2021/022; AICO2023 - CIAICO/2022/144), the Mucosal Frontier project (PID2020-115070RA-I00), the Czech Science Foundation (no. 23-07990S), the Czech-BioImaging large RI project (LM2023050 and OP VVV CZ.02.1.01/0.0/0.0/18_046/0016045), and the Research Project - Plan Nacional I+D+I (Spanish Ministry of Science and Innovation and Universities; MICIU/AEI/10.13039/501100011033) TARGET4COTYLE, also contributed to the completion of this thesis.

A mi familia

A los que estuvieron, los que están y los que estarán; por ser la raíz, el tronco y las ramas de mi vida.

Agradecimientos | Acknowledgements | Teşekkür

Probablemente, la mayoría de las persona que se embarcan en la exigente travesía de un doctorado lo hacen con entusiasmo e ilusión, pero también con dudas y temores ante los desafíos que les esperan. Yo soy una de ellas.

A menudo, uno está tan centrado en su trabajo que no siempre es consciente de las personas que le rodean, brindándole apoyo y ánimo. Esta sección, en particular, me resulta muy especial porque refleja el profundo reconocimiento que siento hacia quienes me han apoyado en este viaje. Cada vez que he intentado escribir esta sección, me he sentido abrumado, incapaz de encontrar las palabras adecuadas para expresar toda mi gratitud.

A nivel profesional, la primera persona que siempre me viene a la mente es Francesc Padrós Bover (Sito). Sito, tú has sido un pilar fundamental en mi desarrollo profesional como veterinario. Aunque tu humildad te impida verlo de la misma manera que yo, sin tu apoyo, probablemente, no estaría donde estoy hoy. Gracias por ser mi mentor todos estos años, por todo lo que me has enseñado, por tratarme como un igual y, sobre todo, por tu amistad.

Ariadna, Itziar y Oswaldo, gracias por haberme dado la oportunidad de formar parte de vuestro equipo y por guiarme en mi desarrollo como investigador. Sois un equipo excepcional y no podría haber caído en mejores manos.

Ariadna, admiro profundamente tu extraordinaria capacidad organizativa. Estoy inmensamente agradecido por tu eficiencia, tu inagotable curiosidad y tu constante deseo de ir más allá. Gracias por tu interés, tus precisas correcciones y tu agudo pensamiento crítico. Nunca podré agradecerte lo suficiente el doble esfuerzo que has dedicado a la supervisión de esta tesis mientras también asumías la dirección del centro. Tu trabajo, tanto visible como entre bambalinas, ha sido invaluable.

Itziar, me faltan páginas para expresar todo lo agradecido que estoy. Durante estos últimos cuatro años, has sido mi apoyo diario en el trabajo. Mil gracias por las risas, tus consejos, correcciones y críticas. Gracias por haber sabido transmitirme tus conocimientos, por hacerme ver las cosas desde otra perspectiva, por tu paciencia, por escuchar mis opiniones y por aguantar mis dramas. Ya sabes que la formalidad no es mi fuerte, pero creo que esta ocasión lo merece como muestra de mi profundo respeto y admiración.

Carla, tú te has ganado el título de supervisora honorifica de esta tesis, por mucho que insistieras a tus colegas científicos que **no** eras mi supervisora. Gracias por toda tu ayuda y apoyo, por tus consejos y por enseñarmer tantas cosas.

Raquel, estoy seguro que sin tus habilidades logísiticas, capacidad organizativa y tú apoyo, mi estancia y mi experiencia en el IATS no hubiesen sido las mismas. Gracias por

haber hecho que todo fuese tan fácil.

En definitiva, gracias por tanto y lo único que deseo es que nuestros caminos se vuelvan a cruzar más pronto que tarde. ¡Sois las mejores!.

A Pepe y Lucinda del servicio de histología y al equipo de Animalario, en particular a Inma, quiero expresar mi más sincero agradecimiento por vuestro inestimable apoyo científico. Mil gracias.

A mis compañeros de despacho, David, Bea, Raquel y Soco, gracias por las risas y las charlas triviales que hicieron que cada día fuera más ameno y llevadero.

My deepest thanks to Javier Sotillo from the Instituto de Salud Carlos III and to Hynek Mazanec, Ivona Mladineo, and Roman Kuchta from the Institute of Parasitology, Biology Centre. Thanks for your hospitality, kindness, collaborative spirit, and friendship. A special thanks to Javier and Hynek for introducing me to the captivating world of extracellular vesicles.

A mis amigos de toda la vida, Lluís, César y Carlos, quiero agradeceros todos los buenos momentos que me habéis hecho vivir, a pesar de la distancia. Aunque quizás no seáis conscientes de ello, vuestra presencia ha sido un gran apoyo en este viaje.

A mi compañera de profesión, Raquel, y a su pareja Guillem, gracias por vuestra amistad. Cada vez que nos ruenimos (que lamentablemente son menos de las que me gustaría), es como si el tiempo no hubiese pasado, y eso convierte cada encuentro en algo realmente especial.

A mis padres, Claudio Julián y Esther. Gracias por ser unos padres excepcionales, por permitirme explorar y experimentar tanto, por despertar mi curiosidad y guiarme con sabiduría. Os agradezco profundamente estar siempre a mi lado en los momentos más difíciles, vuestro cariño y paciencia inquebrantables, y por dar tanto sin esperar nada a cambio. Gracias por inculcarme los valores que me han forjado y por enseñarme, en estos últimos años, que hay cosas más importantes que el trabajo. Las palabras no bastan para expresar lo mucho que os quiero.

A mi hermana Claudia, por ser un ejemplo de esfuerzo y dedicación, y por no rendirse nunca. Siempre le estaré agradecido por el impacto positivo que ha tenido en mí desde que tengo memoria, y por ser un modelo a seguir. Te quiero.

Babam İsmail ve annem Sebahat'e, beni kabul ettiğiniz, sevginiz için, her zaman beni gülümsemeyle karşıladığınız ve dil engeli bu kadar belirgin olmasına rağmen benimle ilgilendiğiniz için size her zaman minnettar olacağım. Sizi her zaman kalbimde taşıyorum.

Burçak, ister kader ister tesadüf olsun, yollarımız kesişti. Sana anında aşık oldum ve ilişkimizi herşeyin üstünde tuttmakta bir an bile tereddüt etmedim. Bazen benimle birlikte olduğun için hayattaki tüm şansımı harcadığımı düşünüyorum. Sende hayranlık duyduğum o kadar çok harika şey var ki. Cesaretin, direncin, empati yeteneğin, alçakgönüllülüğün,

cömertliğin ve sabrın. Benim için yaptığın her şey için, koşulsuz sevgin ve desteğin için benimle ilgilendigin ve karşılık beklemeden bu kadar çok şey verdiğin için her zaman minnettar olacağım. İki yıl sonra hayallerimin kızıyla evlenmiş olmak benim için inanılmaz. Bana her gün yeni bir şey öğrettiğin, öpücüklerin, kucaklamaların için teşekkür ederim. Bu tez benim olduğu kadar senin de tezin. Şimdi iyiliğe karşılık verme sırası bende ve sen yerini bulana kadar durmayacağım. Seni sonsuz seviyorum.

Resumen

La acuicultura marina de teleósteos es una industria crucial y un motor económico en la cuenca Mediterránea. Entre la gran diversidad de especies producidas en la región en las últimas décadas, la dorada (*Sparus aurata*; Linnaeus, 1758) destaca en términos de producción, no solo a nivel regional, sino también en toda la Unión Europea. España es el quinto mayor productor de dorada, pero a pesar de ser una potencia en acuicultura marina, la demanda nacional de esta especie excede ampliamente su producción, lo que obliga a importar grandes volúmenes.

Sin embargo, a pesar de la importancia de esta especie, su producción se ve gravemente afectada por *Sparicotyle chrysophrii* (Van Beneden and Hesse, 1863), un ectoparásito platelminto que infecta las branquias de su hospedador y que causa hasta un 30% de mortalidad durante la fase de engorde, principalmente en jaulas en mar abierto, siendo la principal amenaza para la acuicultura de la dorada. Esta parasitosis tiene un impacto negativo en el bienestar de estos animales y provoca pérdidas económicas directas e indirectas, obstaculizando el desarrollo, crecimiento y competitividad de las granjas acuícolas. Actualmente, el principal tratamiento contra esta parasitosis es la formalina en su formulación autorizada como quimioterapéutico desinfectante, aplicada en baños. No obstante, la formalina tiene un índice terapéutico estrecho y eficacia limitada.

Esta situación, junto a la limitada literatura científica disponible sobre *S. chrysophrii* justifica esta tesis, cuyo objetivo principal es aumentar el conocimiento sobre las interacciones entre *S. chrysophrii* y su hospedador, la dorada, así como sobre la biología del propio parásito.

En el **capítulo 1**, se presenta la dorada como una especie destacada en la acuicultura marina del Mediterráneo y de la Unión Europea. Se introducen conceptos fundamentales relacionados con el bienestar y la salud, abordando aspectos como el estrés, el dolor, la conciencia y la respuesta inmune. Posteriormente, se explora el concepto de salud branquial y se realiza un análisis exhaustivo de las principales enfermedades de etiología vírica, bacteriana y parasitaria que afectan a la dorada. En particular, se presta especial atención a los parásitos poliopiscotilos y, en particular, a *S. chrysophrii*.

En el **capítulo 2**, se establece la finalidad principal de esta tesis y ofrece una visión detallada de sus objetivos específicos, destacando las metas clave que conforman el estudio en su conjunto.

En el **capítulo 3**, se establece un modelo de infección experimental *in vivo* en un sistema de recirculación (*Recirculation Aquaculture System* - RAS) mediante cohabitación con doradas infectadas y colectores de huevos de *S. chrysophrii* para seguir la progresión de la enfermedad y modular la presión infectiva del parásito. Este modelo de infección es capaz de replicar los signos clínicos que se observan en doradas infectadas de forma natural durante su engorde en jaulas en mar abierto. Por un lado, se observaron

caídas significativas en la hemoglobina y el hematocrito alrededor de 40 días después de la exposición. Por otro lado, hubo un aumento de granulocitos eosinófilos y células caliciformes en los filamentos branquiales y de centros melanomacrofágicos esplénicos, mientras que la grasa hepática se redujo.

En el **capítulo 4**, se estudia cómo *S. chrysophrii* modula el proteoma del plasma sanguíneo de doradas infectadas experimentalmente, ofreciendo una visión global crucial de la patogénesis de la enfermedad causada por *S. chrysophrii*. Las doradas infectadas mostraron alteraciones en la concentración de hemoglobina y en las proteínas relacionadas con la hemostasia, particularmente aquellas involucradas en la coagulación sanguínea y la función eritrocitaria. Se vieron notablemente afectados el sistema inmunitario, con cambios en proteínas involucradas en la inmunidad innata, así como el metabolismo y transporte de lípidos. Específicamente, proteínas como el componente 3 del complemento y las apolipoproteínas mostraron una correlación negativa significativa con la intensidad de la infección. Los ensayos de validación, incluyendo mediciones de hemoglobina, colesterol y la actividad lítica de la vía alternativa del complemento, confirmaron los hallazgos proteómicos. En general, el estudio demostró extensos cambios fisiológicos en la dorada debido a la infección por *S. chrysophrii*, proporcionando información valiosa sobre posibles dianas para la intervención terapéutica y estrategias para mejorar la gestión en acuicultura.

En el **capítulo 5**, se explora la respuesta mucosal de la dorada frente a la infección por *S. chrysophrii*, destacando alteraciones en la diferenciación de las células caliciformes y la expresión de mucinas en los filamentos branquiales. La infección provocó la hiperplasia de células caliciformes neutras y una mayor expresión de mucinas concretas (*muc2a*, *muc2b*, *muc5a/c*, *imuc*, *muc4*, *muc18*), que presentaron patrones de glicosilación más complejos. Estas modificaciones parecen facilitar la expulsión del parásito y mejorar el intercambio de gases, mitigando así la hipoxia inducida.

En el **capítulo 6**, se exploran los mecanismos subyacentes a la respuesta inmunitaria de la dorada frente a *S. chrysophrii*, con especial atención al rol de las inmunoglobulinas, tanto a nivel local en las branquias como a nivel sistémico en el plasma sanguíneo y el bazo, tras una exposición primaria y secundaria al parásito. Se observaron cargas parasitarias significativamente inferiores y un mejor rendimiento del crecimiento en doradas que habían sobrevivido a una infección previa por *S. chrysophrii* y que fueron reexpuestas posteriormente, en comparación con doradas sanas expuestas al parásito por primera vez. Asimismo, se observó que las doradas reexpuestas presentaban niveles más altos de IgM e IgT específicas en el mucus branquial, un mayor número de células que expresaban IgM e IgT en bazo y filamentos branquiales, respectivamente. Además, se localizaron estructuras del parásito con capacidad antigénica a las que se unían IgM específicas

de plasma e IgT específicas de mucus branquial. Así pues, las doradas que superan una infección primaria por *S. chrysophrii* desarrollan una respuesta inmune adaptativa tanto a nivel mucoso como sistémico, que proporciona una protección parcial.

En el **capítulo 7**, se demuestra la presencia de grupos hemo exógenos en *S. chrysophrii*, se explora su tubo digestivo mediante microscopía óptica y electrónica de transmisión, dilucidando su morfología interna y disposición espacial, y se detectan depósitos residuales de hemo oxidado en forma de cristales de hematina en células digestivas. Asimismo, se estudia el impacto de la naturaleza hematófaga de *S. chrysophrii* en su hospedador estimando el volumen medio de ingesta de sangre para un parásito adulto, y se describe un descenso significativo de los niveles de hierro plasmático libre en hospedadores infectados. Este estudio representa la primera demostración de la naturaleza hematófaga de *S. chrysophrii*.

En el **capítulo 8**, se identifican múltiples proteínas relacionadas con la biogenésis de vesículas extracelulares (VE) a partir de datos genómicos de *S. chrysophrii*, se aislaron VE y se observaron mediante microscopía electrónica de transmisión en el tegumento sincitial de la región haptoral de *S. chrysophrii*. La caracterización proteica exhaustiva de estas VE mediante proteómica identificó proteínas relacionadas con hidrolasas peptídicas, GTPasas, proteínas con dominio EF-hand, metabolismo energético aeróbico, anticoagulante/ unión a lípidos, desintoxicación de grupos hemo, transporte de hierro, proteínas relacionadas con la biogénesis de VE, proteínas relacionadas con el tráfico de vesículas y otras proteínas relacionadas con el citoesqueleto. En particular, varias proteínas identificadas, como las leucil y alanil aminopeptidasas, la calpaína, la ferritina, la cadena ligera de la dineína, la proteína 14-3-3, las proteínas *heatshock* 70, la anexina, la tubulina, la glutatión *S*-transferasa, la superóxido dismutasa, la enolasa y la fructosa-bisfosfato aldolasa, se han propuesto como posibles dianas candidatas con fines terapéuticos o profilácticos. Este estudio supone la primera demostración de la secreción de VE por un platelminto ectoparásito, lo que proporciona nuevos conocimientos y oportunidades para el descubrimiento de fármacos y el desarrollo de vacunas contra los parásitos poliopistocotilos en la acuicultura.

En el **capítulo 9** se integran y discuten los resultados de los estudios presentados en los **capítulos 3**, **4**, **5**, **6**, **7** y **8** de esta tesis. Así pues, este capítulo ofrece una visión global y una comprensión más completa sobre los efectos de *S. chrysophrii* en su hospedador, así como sobre la biología del parásito.

Por último, el **capítulo 10** presenta una lista enumerada de las conclusiones extraídas de los resultados de esta tesis.

Resum

L'aqüicultura marina de teleostis és una indústria crucial i un motor econòmic a la conca Mediterrània. Entre la gran diversitat d'espècies produïdes a la regió en les darreres dècades, l'orada (*Sparus aurata*; Linnaeus, 1758) destaca en termes de producció, no només a nivell regional, sinó també a tota la Unió Europea. Espanya és el cinquè major productor d'orada, però tot i ser una potència en aqüicultura marina, la demanda nacional d'aquesta espècie excedeix àmpliament la seva producció, cosa que obliga a importar grans volums.

Tanmateix, malgrat la importància d'aquesta espècie, la seva producció es veu greument afectada per *Sparicotyle chrysophrii* (Van Beneden and Hesse, 1863), un ectoparàsit platihelmint que infecta les brànquies del seu hoste i que causa fins a un 30% de mortalitat durant la fase d'engreix, principalment en gàbies a mar obert, sent l'amenaça principal per a l'aqüicultura de l'orada. Aquesta parasitosi té un impacte negatiu en el benestar d'aquests animals i provoca pèrdues econòmiques directes i indirectes, obstaculitzant el desenvolupament, creixement i competitivitat de les granges aqüícoles. Actualment, el principal tractament contra aquesta parasitosi és la formalina en la seva formulació autoritzada com a quimioterapèutic desinfectant, aplicada en banys. No obstant això, la formalina té un índex terapèutic estret i eficàcia limitada.

Aquesta situació, juntament amb la limitada literatura científica disponible sobre *S. chrysophrii* justifica aquesta tesi, on l'objectiu principal de la qual és augmentar el coneixement sobre les interaccions entre *S. chrysophrii* i el seu hoste, l'orada, així com sobre la biologia del propi paràsit.

Al **capítol 1**, es presenta l'orada com una espècie destacada en l'aqüicultura marina del Mediterrani i de la Unió Europea. Es presenten conceptes fonamentals relacionats amb el benestar i la salut, abordant aspectes com l'estrès, el dolor, la consciència i la resposta immune. Posteriorment, s'explora el concepte de salut branquial i es realitza una anàlisi exhaustiva de les principals malalties d'etiologia vírica, bacteriana i parasitària que afecten a l'orada. En particular, se li presta especial atenció als paràsits poliopiscotils i, en particular, a *S. chrysophrii*.

Al **capítol 2** s'estableix l'objectiu principal d'aquesta tesi i proporciona una visió general detallada dels seus objectius específics, ressaltant les metes clau que donen forma a l'estudi en conjunt.

Al **capítol 3**, s'estableix un model d'infecció experimental *in vivo* en un sistema de recirculació (*Recirculation Aquaculture System* - RAS) mitjançant cohabitació amb orades infectades i col·lectors d'ous de *S. chrysophrii* per seguir la progressió de la malaltia i modular la pressió infectiva del paràsit. Aquest model d'infecció és capaç de replicar els signes clínics que s'observen en orades infectades de forma natural durant el seu engreix en gàbies a mar obert. Per una banda, es van observar caigudes significatives en

l'hemoglobina i l'hematòcrit al voltant de 40 dies després de l'exposició. Per altra banda, hi va haver un augment de granulòcits eosinòfils i, de cèl·lules caliciformes als filaments branquials i de centres melanomacrofàgics esplènics, mentre que el greix hepàtic es va reduir.

Al **capítol 4**, s'estudia com *S. chrysophrii* modula el proteoma del plasma sanguini d'orades infectades experimentalment, oferint una visió global crucial de la patogènesi de la malaltia causada per *S. chrysophrii*. Les orades infectades van mostrar alteracions en la concentració d'hemoglobina i en les proteïnes relacionades amb l'hemostàsia, particularment aquelles involucrades en la coagulació sanguínia i la funció eritrocitària. Es van veure notablement afectats el sistema immunitari, amb canvis en les proteïnes involucrades en la immunitat innata, així com el metabolisme i transport de lípids. Específicament, proteïnes com el component 3 del complement i les apolipoproteïnes van mostrar una correlació negativa significativa amb la intensitat de la infecció. Els assajos de validació, incloent-hi mesuraments d'hemoglobina, colesterol i l'activitat lítica de la via alternativa del complement, van confirmar les troballes proteòmiques. En general, l'estudi va demostrar extensos canvis fisiològics en l'orada a causa de la infecció per *S. chrysophrii*, proporcionant informació valuosa sobre possibles dianes per a la intervenció terapèutica i estratègies per a millorar la gestió en aqüicultura.

Al **capítol 5**, s'explora la resposta mucosal de l'orada front a la infecció per *S. chrysophrii*, destacant alteracions en la diferenciació de les cèl·lules caliciformes i l'expressió de mucines als filaments branquials. La infecció va provocar la hiperplàsia de cèl·lules caliciformes neutres i una major expressió de mucines concretes (*muc2a*, *muc2b*, *muc5a/c*, *imuc*, *muc4*, *muc18*), que van presentar patrons de glicosilació més complexos. Aquestes modificacions semblen facilitar l'expulsió del paràsit i millorar l'intercanvi de gasos, mitigant així l'hipòxia induïda.

Al **capítol 6**, s'exploren els mecanismes subjacents a la resposta immunitària de l'orada davant *S. chrysophrii*, amb especial atenció al rol de les immunoglobulines, tant a nivell local a les bràncquies com a nivell sistèmic en el plasma sanguini i la melsa, després d'una exposició primària i secundària al paràsit. Es van observar càrregues parasitàries significativament inferiors i un millor rendiment de creixement en orades que havien sobreviscut a una infecció prèvia per *S. chrysophrii* i que van ser reexposades posteriorment, en comparació amb orades sanes exposades al paràsit per primera vegada. Així mateix, es va observar que les orades reexposades presentaven nivells més alts d'IgM i IgT específiques al mucus branquial, un major nombre de cèl·lules que expressaven IgM i IgT a la melsa i els filaments branquials, respectivament A més, es van localitzar estructures del paràsit amb capacitat antigènica a les quals s'unien IgM específiques de plasma i IgT específiques de mucus branquial. Així doncs, les orades que superen una

infecció primària per *S. chrysophrii* desenvolupen una resposta immune adaptativa tant a nivell mucós com sistèmic, que proporciona una protecció parcial.

Al **capítol 7**, es demostra la presència de grups hemo exògens en *S. chrysophrii*, s'explora el seu tub digestiu mitjançant microscòpia òptica i electrònica de transmissió, dilucidant la seva morfologia interna i disposició espacial, i es detecten dipòsits residuals de hemo oxidat en forma de cristalls de hematina en cèl·lules digestives. Així mateix, s'estudia l'impacte de la naturalesa hematòfaga de *S. chrysophrii* en el seu hoste estimant el volum mitjà d'ingesta de sang per un paràsit adult, i es descriu una disminució significativa dels nivells de ferro plasmàtic lliure en hostes infectats. Aquest estudi representa la primera demostració de la naturalesa hematòfaga de *S. chrysophrii*.

Al **capítol 8**, s'identifiquen múltiples proteïnes relacionades amb la biogènesi de vesícules extracel·lulars (VE) a partir de dades genòmiques de *S. chrysophrii*, es van aïllar VE i s'observaren mitjançant microscòpia electrònica de transmissió en el tegument sincitial de la regió haptoral de *S. chrysophrii*. La caracterització proteica exhaustiva d'aquestes VE mitjançant proteòmica, va identificar proteïnes relacionades amb hidrolases peptídiques, GTPases, proteïnes amb domini EF-hand, metabolisme energètic aeròbic, anticoagulant/unió a lípids, desintoxicació de grups hemo, transport de ferro, proteïnes relacionades amb la biogènesi de VE, proteïnes relacionades amb el tràfic de vesícules i altres proteïnes relacionades amb el citoesquelet. En particular, diverses proteïnes identificades, com les leucil i alanil aminopeptidases, la calpaïna, la ferritina, la cadena lleugera de la dineïna, la proteïna 14-3-3, les proteïnes *heatshock* 70, l'anexina, la tubulina, la glutatió S-transferasa, la superòxid dismutasa, l'enolasa i la fructosa-bisfosfat aldolasa, s'han proposat com a possibles dianes candidates amb fins terapèutics o profilàctics. Aquest estudi suposa la primera demostració de la secreció de VE per un platihelmint ectoparàsit, i proporciona nous coneixements i oportunitats per al descobriment de fàrmacs i el desenvolupament de vacunes contra els paràsits poliopistocotils en l'aqüicultura.

Al **capítol 9** s'integren i es discuteixen els resultats dels estudis presentats als **capítols 3**, **4**, **5**, **6**, **7** i **8** d'aquesta tesi. Així doncs, aquest capítol ofereix una visió global i una comprensió més completa sobre els efectes de *S. chrysophrii* en el seu hoste, així com sobre la biologia del paràsit.

Per últim, el **capítol 10** presenta una llista enumerada de les conclusions extretes dels resultats d'aquesta tesi.

Summary

Marine teleost aquaculture is a crucial industry and an economic driver in the Mediterranean basin. Among the diverse species produced in the region over the past few decades, the gilthead seabream (*Sparus aurata*; Linnaeus, 1758) stands out in terms of production, not only regionally but also throughout the European Union. Spain is the fifth largest producer of gilthead seabream, but despite being a powerhouse in marine aquaculture, domestic demand for this species far exceeds its production, necessitating large-scale imports.

However, despite the importance of this fish species, its production is severely affected by *Sparicotyle chrysophrii* (Van Beneden and Hesse, 1863), an ectoparasitic flatworm that infects the gills of its host and causes up to 30% mortality during the on-growing phase, primarily in open sea cages, posing the main threat to gilthead seabream aquaculture. This parasitosis negatively impacts the welfare of these animals and causes direct and indirect economic losses, hindering the development, growth, and competitiveness of aquaculture farms. Currently, the main treatment against this parasitosis is formalin in its authorised formulation as a chemotherapeutic disinfectant, applied in baths. However, formalin has a narrow therapeutic index and limited efficacy.

This situation, coupled with the limited scientific literature available on *S. chrysophrii*, justifies this thesis, whose main objective is to increase knowledge about the interactions between *S. chrysophrii* and its host, gilthead seabream, as well as the biology of the parasite itself.

In **Chapter 1**, the gilthead seabream is highlighted as a key species in Mediterranean and European Union marine aquaculture. The chapter introduces essential concepts related to welfare and health, including stress, pain, consciousness, and immune response. Subsequently, it explores the concept of gill health, and provides a thorough analysis of the main diseases with viral, bacterial, and parasitic aetiologies affecting gilthead seabream. Special emphasis is placed on polyopisthocotylan parasites, particularly *S. chrysophrii*.

Chapter 2 establishes the primary aim of this thesis and provides a detailed overview of its specific objectives, highlighting the key goals that shape the overall study.

In **Chapter 3**, an *in vivo* experimental infection model is established in a recirculation aquaculture system through cohabitation with infected gilthead seabream and *S. chrysophrii* egg collectors to monitor the progression of the disease and modulate the parasite's infective pressure. This infection model can replicate the clinical signs observed in naturally infected gilthead seabream during their on-growing phase in open sea cages. Significant drops in haemoglobin and haematocrit were observed around 40 days post-exposure. Additionally, there was an increase in eosinophilic granulocytes and goblet cells in the gill filaments, and in splenic melanomacrophage centres, while liver fat was reduced.

Chapter 4 studies how *S. chrysophrii* modulates the blood plasma proteome of experimentally infected gilthead seabream, offering a crucial global view of the disease's pathogenesis caused by *S. chrysophrii*. Infected gilthead seabream showed alterations in the haemoglobin concentration and haemostasis-related proteins, particularly those involved in blood coagulation and erythrocyte function. The immune system was notably affected, with changes in proteins involved in innate immunity, as well as the lipid metabolism and transport. Specifically, proteins such as complement component 3 and apolipoproteins showed a significant negative correlation with infection intensity. Validation assays, including measurements of haemoglobin, cholesterol, and the lytic

activity of the alternative complement pathway, confirmed the proteomic findings. Overall, the study demonstrated extensive physiological changes in gilthead seabream due to *S. chrysophrii* infection, providing valuable insights into potential targets for therapeutic intervention and improved management strategies in aquaculture.

Chapter 5 explores the mucosal response of gilthead seabream to the infection by *S. chrysophrii*, highlighting changes in goblet cell differentiation and mucin expression in the gill filaments. The infection caused hyperplasia of neutral goblet cells and increased expression of specific mucins (*muc2a*, *muc2b*, *muc5a/c*, *imuc*, *muc4*, *muc18*), with changes towards more complex glycosylation patterns. These modifications seem to facilitate parasite expulsion and improve gas exchange, thus mitigating induced hypoxia.

Chapter 6 investigates the underlying mechanisms of the immune response of gilthead seabream against *S. chrysophrii*, with particular attention to the role of immunoglobulins at both, the local level in the gills and the systemic level in blood plasma and spleen, upon a primary and a secondary exposure to the parasite. Significantly lower parasite loads and better fitness were observed in gilthead seabream that had survived a prior *S. chrysophrii* infection and were subsequently re-exposed, compared to healthy gilthead seabream exposed to the parasite for the first time. Additionally, reexposed gilthead seabream showed higher levels of specific IgM and IgT in the gill mucus, a greater number of IgM and IgT expressing cells in the spleen and gill filaments, respectively. Moreover, specific IgM in blood plasma and specific IgT in gill mucus, bound to parasite structures with antigenic capacity. Thus, gilthead seabreams that overcome a primary infection by *S. chrysophrii* develop an adaptive immune response at both the mucosal and systemic levels which provides partial protection.

Chapter 7 demonstrates the presence of exogenous haem groups in *S. chrysophrii* and explores its digestive tract using light and electron microscopy, elucidating its internal morphology and spatial arrangement, and detecting residual deposits of oxidised haem in the form of haematin crystals in digestive haematin cells. The impact of *S. chrysophrii*'s blood-feeding nature on its host was also studied by estimating the average blood intake volume for an adult parasite, revealing a significant decrease in free plasma iron levels in infected hosts. This study represents the first demonstration of the haematophagous nature of *S. chrysophrii*.

In **Chapter 8**, multiple proteins related to extracellular vesicle (EV) biogenesis are identified from the genomic data of *S. chrysophrii*. EVs were isolated and observed through transmission electron microscopy in the syncytial tegument of the haptoral region of *S. chrysophrii*. Comprehensive proteomic characterisation of identified proteins in these EVs related to peptidase hydrolases, GTPases, EF-hand domain proteins, aerobic energy metabolism, anticoagulant/lipid-binding, haem group detoxification, iron transport, EV biogenesis, vesicle trafficking, and cytoskeletal proteins. Notably, several identified proteins, such as leucine and alanine aminopeptidases, calpain, ferritin, dynein light chain, 14-3-3 protein, heat shock proteins 70, annexin, tubulin, glutathione S-transferase, superoxide dismutase, enolase, and fructose-bisphosphate aldolase, have been proposed as potential therapeutic or prophylactic targets. This study is the first to demonstrate the secretion of EVs by an ectoparasitic flatworm, providing new insights and opportunities for drug discovery and vaccine development against polyopisthocotylan parasites in aquaculture.

In **Chapter 9**, the results of the studies presented in **Chapters 3**, **4**, **5**, **6**, **7** and **8** of this thesis are integrated and discussed. Thus, this chapter provides a comprehensive overview and a deeper understanding of the effects of *S. chrysophrii* on its host, along with the biology of the parasite.

Finally, **Chapter 10** presents a numbered list of the conclusions drawn from the results of this thesis.

Table of contents

Chapter 1

General introduction

Marine teleost Farming in the Mediterranean basin

The Mediterranean Sea, located between Southern Europe, Northern Africa, and Western Asia, is a large body of water that washes the coastline of 22 countries. It is connected to the Atlantic Ocean via the Strait of Gibraltar to the west, the Red Sea through the Suez Canal to the southeast, and the Black Sea through the Bosphorus Strait to the northeast.

In general terms, aquaculture is a fast-growing animal production industry[1], strategic for enhancing food security and boosting national economies through global trade.

Given the restricted area of the Mediterranean basin, geopolitical interests and competition for resources are inherent to the region. Such competition can be observed by the number of countries within the region having a share in teleost farming (production statistics for 19 of the 22 countries in the region are available in FishStatJ[2]). As of 2022, Türkiye (317,772 t), Greece (128,496.41 t), Egypt (110,427 t) and Spain (40,636.23 t) accounted for more than 80% of the marine teleost production in the region (**Figure 1A, B**). Moreover, another symptom of this competition is the effort to diversify the marine teleostean species being farmed[3]. From 2013 to 2022 up to 26 different species were attempted to be reared, including Atlantic bluefin tuna (Scombridae; *Thunnus thynnus*) ranching[2]. However, gilthead seabream (Sparidae; *Sparus aurata*), European seabass (Moronidae; *Dicentrarchus labrax*), and meagre (Sciaenidae; *Argyrosomus regius*) are dominant players in Mediterranean marine teleost farming, contributing over 90% of the total production in 2022 (**Figure 1C, D**).

Over the past ten years, gilthead seabream has consistently represented over 40% of teleost aquaculture production in the Mediterranean basin (**Figure 1D**), and in 2022, it led the teleost aquaculture production with 322,557.59 t according to the Food and Agriculture Organization of the United Nations- FAO[2], and approximately 320,630 t according to the Aquaculture Business Association of Spain- APROMAR[4] (**Figure 1C**). This represents a 1.8% increase from 2021, with an overall value of approximately €1,574.80 million, which underscores the relevance of the species in the region[4].

Spanish marine teleost farming and the importance of gilthead seabream in Spain and the European Union-27

Spain's territory is bordered by the Mediterranean Sea to the east and southeast and the Atlantic Ocean to the southwest and northwest. Altogether, its coastline extends for approximately 8,000 kilometres.

In 2022, Spain's marine teleost aquaculture represented 78.39% of the country's aquaculture industry in terms of production (FAO), with the most relevant species being European seabass, Atlantic bluefin tuna and gilthead seabream, followed by turbot (Scophthalmidae; *Scophthalmus maximus*), meagre and Senegalese sole

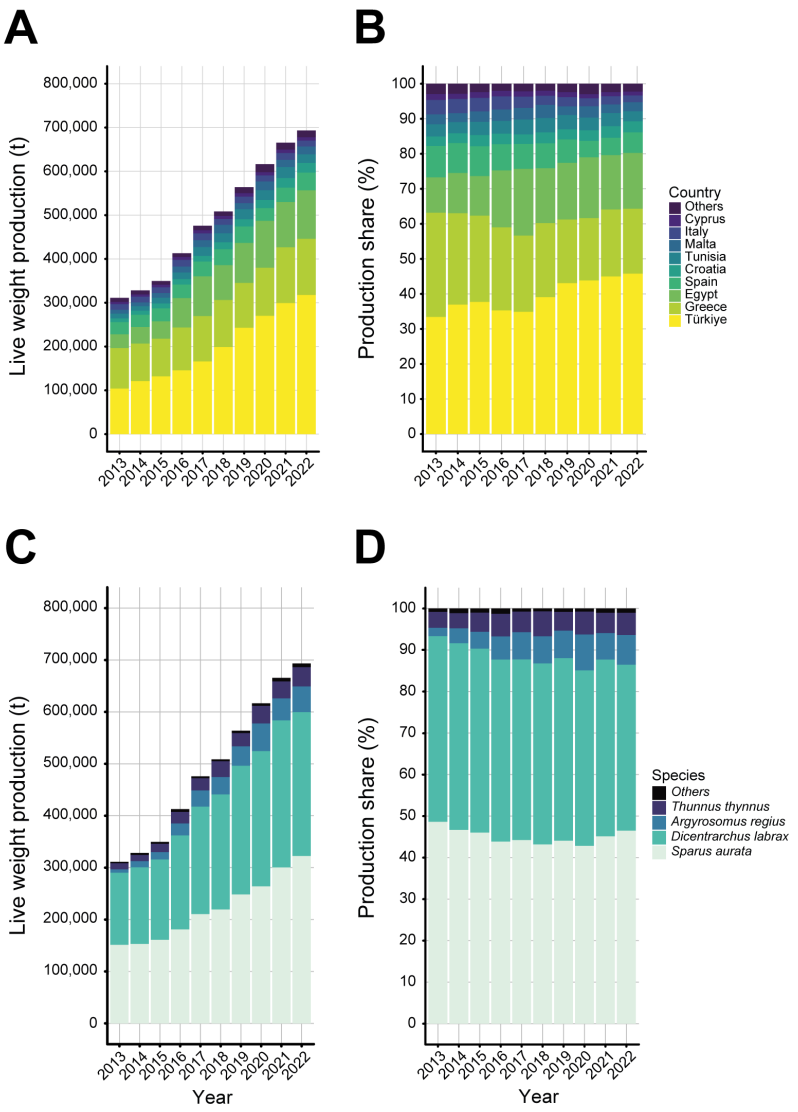

Figure 1. Mediterranean marine teleost aquaculture production data from 2013 to 2022. A: Evolution of live weight production of teleosts by country. **B**: Evolution of the production share of reared teleost by country. **C**: Evolution of live weight production by teleost species. D: Evolution of the production share by teleost species. **NOTE**: The data used was obtained from production values of FAO database FishStat[2].

(Soleidae; *Solea senegalensis*) (**Figure 2A**).

Gilthead seabream farming in Spain is shared between the Atlantic Ocean (1,574.25 t) and the Mediterranean Sea (7,463.70 t) (**Figure 2C**) and ranks fifth in its production within the Mediterranean basin (second within the EU-27), far behind the main producers (**Figure 2C**). Despite its position, gilthead seabream consumption in Spain was estimated at 34,462 t in 2022[4], and while approximately 4,600 t were exported, 29,500

t were imported, primarily from Türkiye and Greece[4], to satisfy the national demand, altogether underscoring the relevance of the species in the country.

Additionally, the EU-27 has experienced a negative trend in terms of production share over the last decade, dropping by 27.41% since 2012 and set to 31.71% in 2022 (**Figure 2B**)[2]. Nevertheless, in terms of production, gilthead seabream remains the second most relevant teleost species considering the entire finfish aquaculture industry within EU-27[2,5].

Gilthead seabream

Gilthead seabream belongs to the family Sparidae within the order Spariformes[6,7], and is characterised by the presence of molariform lateral teeth, the absence of incisiviform anterior teeth, an anterior set of maxillaries and a jaw with four to six strong canines, an anal fin with 11 or 12 soft rays, 11 to 13 branchispines in the first branchial arch, a general silvery grey colour, a large blackish spot on the upper part of the operculum and the beginning of the lateral line and a golden frontal band between the eyes[8] (**Figure 3**).

Gilthead seabream is a common resident of the Mediterranean Sea, also found in the western and southern Black Sea and in the eastern Atlantic Ocean from the British Isles to Cape Verde[9]. Even though the wild population requires a reassessment and update, since 2009 it has been classified as "Least Concern" according to the IUCN Red List of Threatened Species[10]. Like other sparids, gilthead seabream is a demersal neritic species found in coastal areas over seagrass beds, rocky and/ or sandy seafloors. Moreover, gilthead seabream is a euryhaline amphidromous species with a temperature preference ranging from 11 to 30 °C and can be found in depths of up to 150 m[8–11]. In terms of reproductive biology, gilthead seabream is a protandrous hermaphrodite, where juveniles develop first into males and continue as such or convert into females later on; however, once converted into females, gilthead seabream cannot revert back into males. Regarding the species' social behaviour, they are either solitary or aggregate in small to large schools, probably depending on the specimens' size, and juveniles establish linear dominance hierarchies[11].

Under farming conditions, gilthead seabream eggs are produced and fertilised in land-based hatcheries from selected broodstock. When fingerlings are about 10 g of body weight, they are then moved to either land ponds (extensive farming systems) or, more frequently, sea cages (intensive farming systems) for their grow-out phase with animal density ranging from 15 to 25 kg · m^{-3} [9]. It takes between 18 and 24 months for farmed gilthead seabream to reach 500 g of body weight; however, the commercial size ranges between 250 g and 1.5 kg[9]. In a single production cycle, once a batch reaches an average weight of 250 g, gilthead seabream is harvested periodically while stocks last, meaning

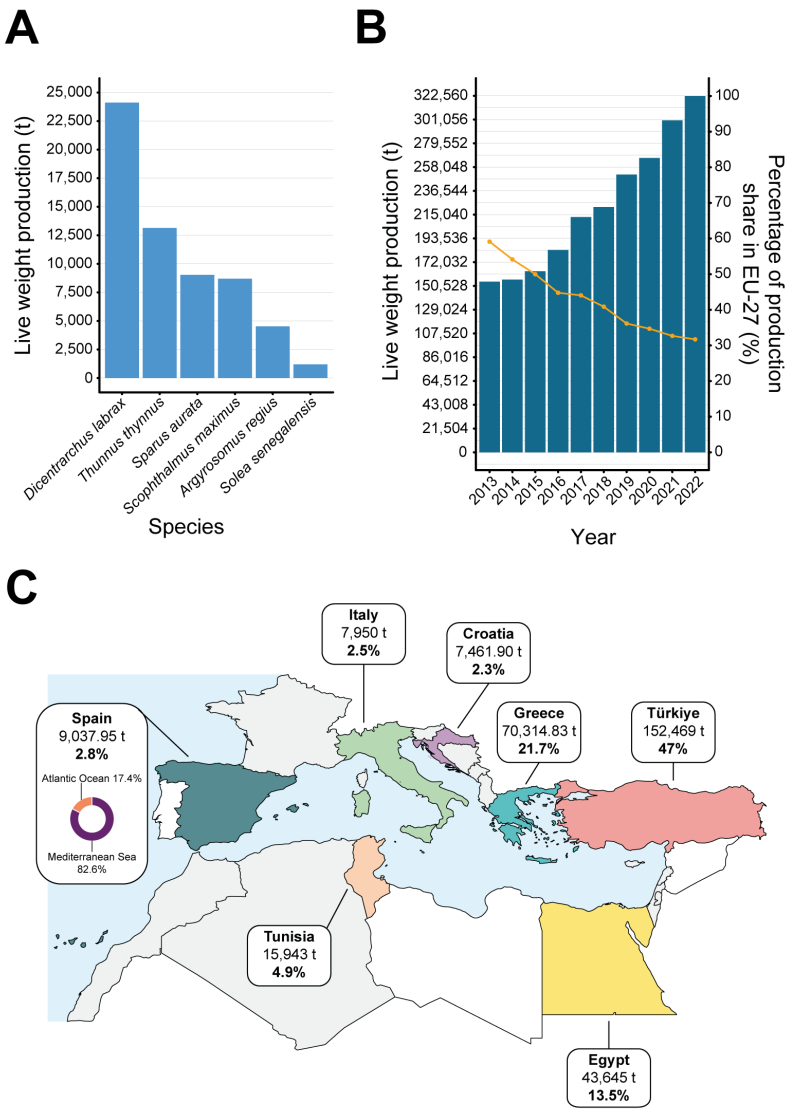

Figure 2. Spanish marine teleost aquaculture, gilthead seabream aquaculture production in the Mediterranean basin and the production share within the European Union-27. **A**: Main marine teleosts farmed in Spain in 2022 and the volume produced in tons. **B**: Evolution of the production of gilthead seabream within the Mediterranean basin and the evolution of the production share of the European Union-27. **C**: Live weight production of gilthead seabream in Mediterranean countries. Percentages in bold represent each country's production share. Countries with less than 2% production share were coloured in grey. Non-Mediterranean countries and countries without any data available were coloured in white. **NOTE**: The data used was obtained from production values of FAO database FishStat [2].

there is no all-in, all-out production strategy; hence, different year-class batches usually coexist in a specific time frame in the farming site.

Overall, teleost farming provides safe, high-quality fish meat to consumers, with full traceability of the products and consistent health surveillance and monitoring by field veterinarians and fish health technicians. Despite these advantages, the industry faces significant challenges. Offshore sea cage on-growing practices are particularly susceptible to disease outbreaks due high stocking densities, lack of fallowing strategies, and no year-class separation, together with the impossibility of animals to migrate. Furthermore, the global warming scenario poses additional threats. Environmental changes such as the increase in surface water temperatures and acidification may not only hinder the development of the sector, by restricting which species to rear and the optimal areas for on-growing practices, but also by the threat of novel and emerging pathogens[12].

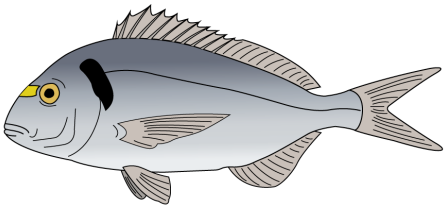

Figure 3. Gilthead seabream, *Sparus aurata* Linnaeus, 1758.

Health and welfare

Over the past decades, animal welfare has become a prominent issue, leading to a notable shift in the social perception regarding experimental and farming practices, both terrestrial and aquatic. Current EU legislation on fish farming includes Directive 98/58/EC[13], Regulations (EC) No 1099/2009[14], and (EU) 2016/429[15]. However, these are often overly broad, stating that further scientific knowledge and consensus are required. Others, such as the Regulation (EC) No 1/2005[16], completely disregard teleosts or fish.

Nonetheless, with the rise of aquaculture in mainstream discussions and the growing social concern on animal welfare, legislative efforts are being made to ensure better care and respect for animals. In 2017, the EU Commission established an expert group named the "Platform on Animal Welfare"[17]. In 2021, a report titled "Strategic guidelines for a more sustainable and competitive EU aquaculture for the period 2021 to 2030" was published, prioritising welfare[18]. By the end of 2023 the EU Commission adopted a legislative proposal to revise Regulation (EC) No 1/2005[19], and in early 2024, an EU reference centre for the welfare of aquatic animals was established[20].

Furthermore, organisations such as the Aquaculture Advisory Council (AAC), the

Federation of Aquaculture Producers (FEAP), the European Food Safety Authority (EFSA), and the World Organisation for Animal Health (WOAH), among others, actively serve as advisory institutions for the European Commission in this matter.

Animal welfare relies on three fundamental pillars: biological function, emotions (also referred to as affective states), and behaviour. Achieving an optimal biological function for animals in captivity involves ensuring they are well-nourished (optimal diet and feeding regime), healthy (optimal maintenance of the animals' homeostasis including the absence of disease), and provided with a comfortable living environment (mimicking the animal's natural habitat as far as possible). Emotions or affective states involve the absence of negative emotions like fear, distress and pain, and the presence of positive emotions, overall allowing animals to express their innate behaviours[21] (**Figure 4**). All these welfare factors are complexly interconnected, forming a delicate equilibrium wherein alterations in one element can significantly impact others, thereby influencing the overall welfare state (**Figure 4**).

Under current sea cage farming conditions, gilthead seabream exhibits a significantly diminished WelfareScore (previously known as FishEthoScore[22]), largely attributed to high stocking densities and absence of environmental enrichment resulting in elevated levels of aggression, deformities, and stress[11]. In this context, stress has been shown to be intimately related to disease and pain, ultimately resulting in observable behavioural alterations.

Stress, disease, pain and consciousness in Teleostei

Stress represents a general nonspecific physiological response within an organism, aimed at either resisting death or restoring homeostasis when encountering challenges. While mild stressful events may have adaptive benefits, prolonged exposure to severe stress (distress) can significantly compromise an animal's condition[23].

In aquaculture, several stressors impact teleost welfare, including inadequate water quality[24,25], handling during net captures (e.g., batch splitting and harvesting)[24,26,27], air exposure – hypoxia[25,28,29], noise[30–32], transportation[24], presence of predators[33], feeding regimes[24,34,35], sea transfer[36], cage net cleaning[36] and animal density (also referred to as stocking density or crowding), which also relates to the animal's spatial distribution within the tank, pond or cage[24,27,34,37]. However, the significance of these stressors varies according to the production stage and the specific aquaculture system, whether it be a recirculating aquaculture system (RAS), estuarine or pond environments, or open sea cage culture.

In general, these stressors can be more easily controlled in hatcheries and during the on-growing stages in RAS, with species-specific parameters established to ensure optimal

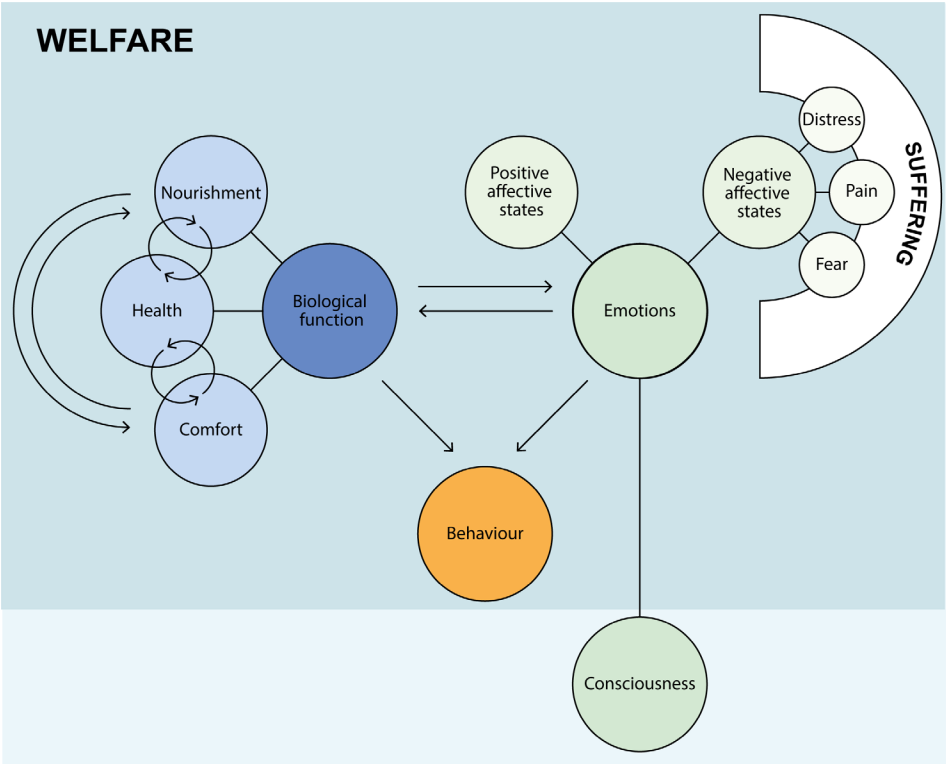

Figure 4. Schematic representation welfare, its associated concepts, and their interconnections. Welfare is characterised by a complex interconnected network based on a proper biological function, emotions in the absence of negative affective states, and the ability for animals to express innate behaviours. The concept of consciousness is closely linked to emotions and determines an organism's sentience and the ability for physical and mental experiences, but is not strictly integrated within the definition of welfare.

conditions. However, in estuarine or pond systems, these factors are less controllable, and they are even more challenging to manage in open sea cage culture.

The stress response in teleost can be categorised into three main stages. Initially, upon perceiving a stressor, there is a primary reaction characterised by a neuroendocrine response, leading to the synthesis and secretion of corticosteroids (mainly cortisol) and catecholamines (primarily adrenaline – epinephrine and noradrenaline – norepinephrine) into the bloodstream. This initial neuroendocrine response sets the stage for a secondary response, during which the animal manages the oxygen demand and redistributes the available energy to systems involved in fight, flight or coping through cardiovascular and respiratory adjustments. The secondary response also induces changes in the hydromineral balance due to adrenaline-mediated alterations in gill blood flow patterns and permeability, and although cortisol may restore the osmotic equilibrium, it also suppresses the immune system[23]. On a broader scale, stress exerts a detrimental impact on various aspects of the teleost's life, including development, behaviour, growth, reproduction and

health. These effects are observable and contribute to what is referred to as the tertiary response[23].

Stress can exacerbate physiological vulnerabilities, potentially leading to the onset or aggravation of diseases[27,38–40] given the immunosuppression. Diseases, on the other hand, trigger pathological processes that can result in both direct and indirect damage, ultimately leading to the experience of pain.

Pain can be defined as a sensation in response to intense stimuli, injury, or disease. Likewise, this sensation may manifest as nocioceptive, arising from stimulation of the somatosensory system, or neuropathic, originating from sensory receptors in conjunction with neurological damage, frequently observed in pathological processes. Pain in teleosts still remains a matter of controversy. While anthropic (anthropocentric and anthropomorphic) bias[41] denies the ability of teleost to feel pain arguing that they do not have a neocortex and hence they are unable to present any form of consciousness[42], on July 7, 2012, The Cambridge Declaration on Consciousness, stated that the absence of a neocortex does not hinder an organism's experience of affective states, challenging the notion that consciousness is exclusive to mammals[43]. Since then, it has been argued that trace and operant conditioning may serve as pertinent indicators of consciousness[44]. Furthermore, sleep-like behaviours have been identified in zebrafish (Cyprinidae; *Danio rerio*) [45,46], and self-awareness via the mirror test[47,48] and self-face recognition[49] was claimed in bluestreak cleaner wrasse (Labridae; *Labroides dimidiatus*). However, de Waal[50] argued that the bluestreak cleaner wrasse was able to make a connection between its reflection in a mirror and itself only upon a somatosensory stimulus, as opposed to the mirror test[48].

While teleosts have been acknowledged to possess some level of consciousness, the specific region within the cerebrum responsible for integrating pain signals remains undisclosed. Nonetheless, they do possess nociceptors, pathways to the central nervous system, and central processing in the brain. Furthermore, their reactions to potentially painful stimuli diverge notably from responses to innocuous stimuli and there is a discernible alteration in motivational behaviours following such potentially painful events[51].

In essence, stress renders animals susceptible to diseases, which can cause discomfort or pain, while simultaneously exacerbating stress in animals suffering from a pathological condition, becoming a vicious circle[23].

Immune response

The immune response is the defence mechanism animals use when facing injury or exposure to infectious agents. In vertebrates, it comprises both an innate immune response, which provides immediate, non-specific protection, and an adaptive immune response,

which offers a delayed but usually highly specific and long-lasting defence[52].

These responses are orchestrated and regulated by lymphoid organs, which in teleosts are mainly the thymus, the head kidney (pronephros), the spleen, and mucosal-associated lymphoid tissues such as the GALT (gut-associated lymphoid tissue), SALT (skin-associated lymphoid tissue), NALT (nasopharynx-associated lymphoid tissue) and the GIALT (gill-associated lymphoid tissue)[52].

When naïve animals encounter an infectious agent, the innate immunity is the first to respond, engaging both cellular and humoral effectors at mucosal and systemic levels. The innate immune response is triggered when organisms are exposed to either endogenous molecules released by damaged or stressed cells (danger-associated molecular patterns – DAMPs) or to exogenous antigens (pathogen-associated molecular patterns – PAMPs). These are recognised by various pattern recognition receptors (PRRs), such as Toll-like receptors (TLRs), nucleotide binding oligomerisation domain (NLRs) and C-type lectins (CLRs) among others[52].

Upon antigen recognition, the innate cellular response is activated, initiating local inflammation. This involves granulocytes (neutrophils or eosinophilic granular cells in gilthead seabream), circulating monocytes which develop into polarised macrophages, mast cells, dendritic cells, and non-specific cytotoxic cells (NCCs) (**Figure 5**)[52,53]. Additionally, further immunological roles have been attributed to other teleost cell types, such as rodlet cells[54], thrombocytes[55,56] and erythrocytes[57,58].

Simultaneously, the complement system, part of the innate humoral response and one of the crucial links between the innate and the adaptive (or acquired) immune responses is activated. The complement system can follow three different pathways: the classical, lectin or alternative pathway[59]. All pathways lead to the activation of C3, promoting opsonisation, inflammation and cell lysis[59]. M1 polarised macrophages will phagocytise opsonised antigens, synthesise cytokines (pro-inflammatory interleukins – Il1β, Il6 and Tnfα), and, along with other antigen-presenting cells, bind processed antigens to the major histocompatibility complex (MHC) class I and II[60]. These are then presented to immature T lymphocytes, activating the adaptive immune response (**Figure 5**)[60]. Prior to lymphocytic activation, lymphocytes already express membrane receptors for antigen recognition. T cells specialise in the thymus, differentiating into helper T cells and cytotoxic T cells. In B cells, somatic hypermutation increases the affinity of their antigen receptors, and when presented antigens are successfully recognised the B cells undergo clonal selection and expansion (**Figure 5**). Further maturation of B cells occurs in melanomacrophage centres, mainly located in the head kidney, spleen[61]. Ultimately, these cells produce immunoglobulins, key components of the adaptive humoral response (**Figure 5**).

Immunoglobulins (Igs), also known as antibodies in their secreted form, are highly diverse molecules at their antigen-binding domains. These molecules can be either expressed on the plasma membrane or secreted in soluble form. The basic structure of the Ig consists of two identical heavy chains and two identical light chains. Both heavy and light chains contain one N-terminal variable domain (VH and VL), constituting the variable region implicated in antigen recognition, and one or more C-terminal constant domains forming the constant region mediating effector functions (**Figure 5**)[62]. In teleosts, three different Ig heavy chain isotypes have been identified: IgM, IgD and IgT (known as IgZ in zebrafish and other cyprinids). While IgM and IgD have been described as systemic and IgT as a mucosal-dedicated immunoglobulin isotype, not all teleost species possess all these isotypes[62]. However, gilthead seabream does have all three[63].

Moreover, macrophages will change their phenotype from M1 to M2 in response to anti-inflammatory cytokines, typically during the transition from inflammation to tissue healing and remodelling[60]. A lymphocytic apoptotic process takes place, and surviving lymphocytes will become memory cells. Upon reexposure to the same antigen (secondary immune response), these memory cells initiate a more potent and faster immune response (**Figure 5**).

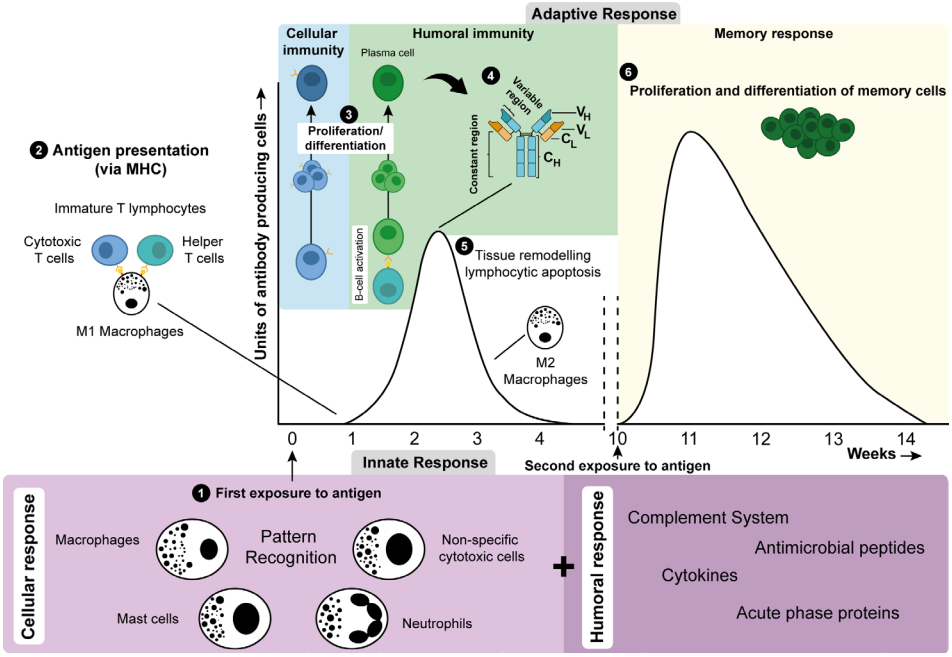

Figure 5. Immune system effectors. Schematic representation of the effectors involved in the innate and adaptive immune response upon first and second exposure to antigens over time. Chronologically, upon a **primary antigen exposure** (**1**), an innate immune response is triggered, involving humoral components and cellular effectors, including M1 macrophages with phagocytic capacity and pro-inflammatory activity. **Continued on the next page.**

Figure 5. (Continued). These cells, along with other effectors, process engulfed antigens and perform **antigen presentation via major histocompatibility complex** (**MHC**) (**2**) to T lymphocytes, activating the adaptive immune response. This triggers the **proliferation and differentiation of T and B lymphocytes** (**3**), with B cells producing **antibodies** (**4**) which consist of variable domains on the heavy ($\mathbf{V_H}$) and light ($\mathbf{V_L}$) chains responsible for antigen recognition, and constant domains on the heavy ($\mathbf{C_H}$) and light ($\mathbf{C_L}$) chains that mediate effector functions. After antigen clearance, M2 macrophages promote **tissue remodelling, and lymphocytic apoptosis** helps restore homeostasis (**5**), while **memory cells proliferate and differentiate**, ensuring long-term immunity (**6**).

Thus far, non-specific innate cellular and humoral immune responses have been observed in teleosts during ectoparasitic monogenean infections, particularly with skin monopisthocotylans. These responses include increased phagocytic activity[64,65], high expression of *il1β*, increased production of Tnfα[66,67], induction of TLR 3, 9, 21 and 22, enhanced anti-peptidase activity[68], modulation of the production and gene expression of complement system factors[69,70], and a systemic inflammatory response[71]. Furthermore, it has been widely evidenced that teleosts become less susceptible upon reexposure to monogenean infections[67,72–77], suggesting activation and development of an adaptive immune response with the subsequent production of memory B and T lymphocytes. However, studies specifically addressing the adaptive immune response in this context are still lacking, with a single study reporting an increase of IgM in rainbow trout (Salmonidae; *Oncorhyncus mykiss*) infected by *Discocotyle sagittata* (Polyopisthocotyla: Discocotylidae)[78].

Gill health

Placed within the opercular cavity, the gills of teleosts are arranged in two sets of four holobranchs, with one set positioned on the left side and the other on the right side. Each holobranch comprises two hemibranchs extending from the posterior edge of the C-shaped gill or branchial arch. Hemibranchs are elongated, slender cartilaginous projections, known as gill filaments or primary lamellae. Their surface area is further enhanced by folds present across their dorsal and ventral surfaces, known as lamellae or secondary lamellae[79–81] (**Figure 6**). These morphological structures are covered by a mucosal or gill epithelium, which includes pavement cells, ionocytes (mitochondrion-rich cells) and goblet cells[81] (**Figure 6**).

Gill health can be defined as the maintenance of the organ's physiological function within safe operational limits, or homeostasis, when exposed to stressors, whether biotic or abiotic[82]. The gills are a heavily vascularised organ with multiple functions, including respiration, osmoregulation, acid-base regulation and nitrogenous waste excretion, all of which are interconnected[83,84]. Due to their exposure, gills are a common target of many pathogens. The first protective barrier at the gills is the mucus layer over the mucosal epithelium, serving as a triple barrier – chemical, biological and physical – preventing direct contact between the environment and tissue. This mucus is mainly produced by

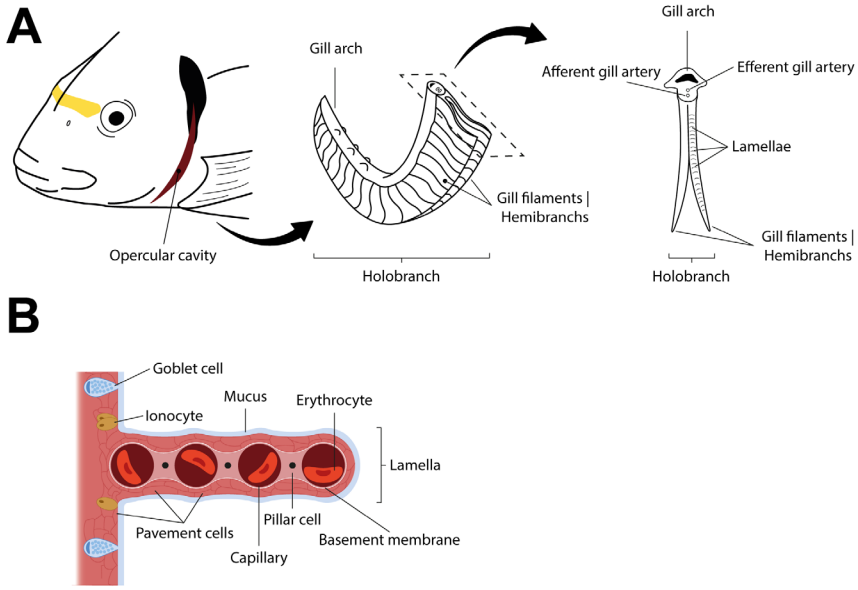

Figure 6. Teleost gill morphology. A: Illustrates the location of the opercular cavity containing the gills and their typical morphology. **B**: Detailed composition of the lamellar epithelium. Adapted from Wegner[81].

goblet cells in the mucosal epithelium, with its major constituents being mucins, which are high molecular weight hydrophilic glycoproteins. These glycoproteins form complex water-based matrices containing immunoglobulins, lysozymes, antibacterial peptides, and complement components. This makes them the core of the mucosal immune system at the gills and a critical component of the animals' innate immune system[85,86].

Associated with the mucus are microorganisms which, as a whole, are known as the microbiota. This microbiota is part of the gills' biological barrier, actively maintaining the hosts' homeostasis and health[87,88]. Disruption of the microbiota by pathogens (dysbiosis) leads to the increase in pathogenic bacteria, contributing to the worsening of disease and clinical signs[89,90].

Additionally, the physicochemical properties of the mucus (viscosity, pH and mucin glycosylation) can be adjusted in response to external stressors[91], though these changes must comply with proper gill performance. The mucosal epithelium, along with intercellular tight junction complexes, also act as a physical barrier, ensuring functional coherence and providing structural robustness to the secreted mucus layer [81,92].

While the immune barrier of teleost gills primarily relies on innate immune mechanisms, the overall health of the gills depends on both innate and adaptive immunity. Immunological mechanisms in teleost gills are closely related to the gill-associated lymphoid tissue (GIALT) and, also to the interbranchial lymphoid tissue (ILT), recently described in salmonids and cyprinids[93–95]. The GIALT comprises diffuse lymphoid tissue where leuko-

cytes are scattered across the gill filaments and lamellae[96], playing an active role in both the innate and adaptive immune response. Regarding the innate immune response, it has been observed an up-regulation of the complement system, pro- and anti-inflammatory genes[97–99], as well as pathways related to the cellular immune response, cytokine signalling, and tissue repair[100] upon parasitic and viral infections. With respect to the adaptive immune response, B cells (primarily IgT+ B cells upon parasitic or bacterial infections) and T cells have been identified as being dispersed throughout the mucosa within the epithelium[101–103]. The ILT, in turn, consists of lymphoepithelium containing lymphocytes embedded in stromal cells, with these lymphocytes predominantly being T cells[94,95].

Overall, when assessing gill health, morphological and histopathological alterations such as hypertrophy and hyperplasia of the epithelial cells, mucus oversecretion, and the presence of leukocytes among others, can serve as indicators of gill disease. However, accurate interpretation of gill health requires the integration of detailed information on clinical signs with analytical data on such gill disease indicators.

Infectious diseases in gilthead seabream aquaculture

Disease outbreaks are among the most concerning events in teleost farming due to their direct and indirect economic impact, the associated animal welfare implications, and the negative public perception of the aquaculture industry. Gilthead seabream, like any other animal, is susceptible to diseases of viral, bacterial, fungal, or parasitic aetiology. Furthermore, from a business model and health management perspective, it is critical to identify patterns in disease outbreaks not only in terms of seasonality but also of the production stage, rearing system and their impact, and altogether, taking into account the current global warming scenario.

Viral diseases

Within viral diseases, two viruses are the most concerning. On one hand, the lymphocystis disease virus genotypes I and VII (LCDV; family Iridoviridae, genus Lymphocystivirus) is an enveloped single linear double-stranded DNA virus[104,105]. While lymphocystis disease is self-limiting, the characteristic nodular lesions caused in the connective tissue in skin and fins due to hypertrophic fibroblasts[105] render diseased gilthead seabream unmarketable and prone to secondary infections. On the other hand, a nervous necrosis virus (NNV; family Nodaviridae, genus Betanodaviridae), consisting of a reassortant genotype of two non-enveloped single-stranded positive sense RNA molecules (RNA1, a red-spotted grouper NNV-like RNA strand, and RNA2, a stripped jack NNV-like RNA) (RGNNV/SJNNV). This betanodavirus reassortant RGNNV/SJNNV has been described to affect gilthead seabream larvae and juveniles in hatcheries, causing viral encephalo-

retinopathy and about 95% cumulative mortality in larvae during a 3-4 days period and 100% mortality in gilthead seabream juveniles surviving a first outbreak[106]. However, additional experimental infections have shown that gilthead seabream are able to become infected by RGNNV/SJNNV regardless of their age and persist infective for long periods of time, eventually becoming asymptomatic carriers[107] and a potential risk for other susceptible species such as European seabass during the on-growing phase.

Bacterial diseases

Regarding bacterial diseases, vibriosis is caused by bacteria within the *Vibrio* genus (family Vibronaceae). *Vibrio* spp. *Vibrio* spp. are short, curved to spiral-shaped Gram-negative, usually motile bacilli[108]. These bacteria are predominantly found in saltwater and brackish water habitats[108] and many species are facultative pathogens for teleosts[109] causing systemic haemorrhagic septicaemia[108]. In Mediterranean gilthead seabream aquaculture, *Vibrio* spp., such as *Vibrio alginolyticus*, *V. anguillarum*, and *V. harveyi*, are considered one of the most relevant pathogens, unlike *V. parahaemolyticus*, *V. vulnificus*, *V. splendidus*, *V. ordalii* and *V. tubiashii* [110–112].

Similarly, photobacteriosis is another relevant bacterial disease caused by Vibronaceae (genus *Photobacterium*), which was previously classified under the genus *Pasteurella* (family Pasteurellaceae). Two subspecies: *P. damselae* subsp. *piscicida* and *P. damselae* subsp. *damselae*, are known to cause disease in gilthead seabream, the former being the main pathogen[110]. This subspecies causes a peracute septicaemic condition characterised by splenomegaly and granulomatous-like bacterial foci in the spleen and kidney [109].

Tenacibaculum maritimum, the aetiological agent for tenacibaculosis, belongs to the family Flavobacteriaceae. These motile, long, thin Gram-negative bacilli, can cause lesions on the skin, fins, oral cavity, and occasionally in the gills, where co-infections with the ectoparasitic flatworm *Sparicotyle chrysophrii* (Polyopisthocotyla: Microcotylidae) are common during the on-growing stage[109]. However, tenacibaculosis rarely becomes systemic[108] and is more commonly reported in hatcheries[112], where rough handling during grading or other netting procedures in juvenile specimens can trigger the development of the disease[109].

Moreover, epitheliocystis and streptococcosis are currently considered emerging bacterial diseases in aquaculture-reared teleosts[113–115]. Epitheliocystis is a disease characterised by the presence of intracellular Gram-negative coccoid or bacilliform bacteria that cause hypertrophy of epithelial cells in gills and skin, forming spherical to ellipsoid cyst-like masses [108,109,115]. Causative agents in gilthead seabream include two β-proteobacteria, *Candidatus* Ichthyocystis sparus and *Candidatus* Ichthyocystis hellenicum, and one chlamydia, *Candidatus S*imilichlamydia sp.[116,117]. Interestingly, this disease is closely

associated with the presence of *S. chrysophrii*[118,119] with high parasite burdens favouring the proliferation of *Ca.* I. sparus in the gills[89].

Streptococcus spp., on the other hand, are Gram-positive cocci that may cause meningoencephalitis, panophthalmitis and often develops into septicaemia[108,109]. So far, *S. iniae* and β-haemolytic Group B *S. agalactiae* are the most commonly reported in teleosts, and have already been identified in gilthead seabream[120,121].

Although bacterial infections in gilthead seabream are generally less severe compared to other species [112], the zoonotic potential of some pathogens, including emerging *Streptococcus* spp., and *V. parahaemolyticus*, *V. vulnificus* and *P. damselae* subsp. *damselae*, remains a significant concern.

Parasitic diseases

Over the past years, it has been observed that most pathogens affecting gilthead seabream in aquaculture have a parasitic aetiology, including protozoan and metazoan ecto- and endoparasites (**Table 1**).

To date, about 42% of the parasitic species known to infect gilthead seabream in aquaculture settings across various locations, including the Mediterranean Sea, Red Sea and Atlantic Ocean belong to Neodermata (Trematoda: Digenea, Monopisthocotyla and Polyopisthocotyla) (**Table 1**). Among these, polyopisthocotylans, particularly *S. chrysophrii*, raise significant concern[122–125]. This concern stems from the observed anaemic condition[119] and systemic clinical manifestations, and the impacts of the infections in the industry[112].

Other relevant parasites infecting reared gilthead seabream include the ectoparasites *Cryptocaryon irritans* (Prostomatea: Holophryidae) and *Amyloodinium ocellatum* (Dinophyceae: Oodiniaceae), which cause pruritus, dyspnoea and characteristic white spots which correspond to trophonts in the case of *C. irritans*[123,126]. Additionally, the intracellular endoparasitic fungi *Ecytonucleospora nucleophila* (formerly *Enterospora nucleo phila*; Microsporidia: Enterocytozoonidae) and the endoparasite *Enteromyxum leei* (Myxosporea: Enteromyxidae), cause an emaciation syndrome by malabsorption[127,128].

Platyhelminthes: Neodermata

Most platyhelminth species inhabit moist, aqueous or aquatic environments. They exhibit a commonly bilateral symmetric morphology with dorsoventral flattening, absence of coelomic cavity and anus, low levels of cephalisation, and they are usually hermaphroditic[176].

Within the phylum Platyhelminthes, the superclass Neodermata stands as the most derived and diversified group[177]. Comprising primarily flatworms that adopted an obli-

Table 1. Reported parasites infecting gilthead seabream under farming conditions.

	Phylum	Class	Species	Site of infection	References
Ectoparasites	Arthropoda*	Copepoda (Family: Ergasilidae)	*Ergasilus lizae*	Gi	[129]
			Ergasilus sieboldi	Gi	[130]
			Ergasilus spp.	Gi	[131]
		(Family: Caligidae)	*Caligus minimus*	Sk	[132]
			Caligus spp.	Sk	[131]
		Isopoda (Family: Cymothoidae)	*Ceratothoa oestroides*	Bc, Oc, Sk	[133]
			Ceratothoa paralella	Bc, Oc, Sk	[134]
			Ceratothoa spp.	Bc, Oc, Sk	[131]
	Ciliophora	Phyllopharyngea	*Brooklynella hostilis*	Gi, Sk	[135]
		Prostomatea	*Cryptocaryon irritans* ▲	Gi, Sk, Ey	[109,136,137]
		Oligohymenophorea	*Porpostoma notatum*	Sk	[109]
			Trichodina spp.	Gi, Sk	[109,138]
	Euglenozoa	Kinetoplastea	*Cryptobia eilatica*	Gi	[139]
			Cryptobia spp.	Gi	[140]
			Ichthyobodo spp.	Gi, Sk	[138]
	Myzozoa	Dynophyceae	*Amyloodinium ocellatum* ▲	Gi	[131,141,142]
			Amyloodinium spp.	Gi	[138]
	Platyhelminthes*	Monopisthocotyla	*Encotyllabe vallei*	Gi	[143]
			Encotyllabe spari	Gi	[144]
			Gyrodactylus longipes	Gi	[145]
			Gyrodactylus orecchiae	Gi, Sk,Fn,Ey	[146]
			Lamellodiscus echeneis	Gi	[147,148]
			Lamellodiscus elegans	Gi	[149]
			Neobenedenia girellae	Sk	[150]
		Polyopisthocotyla	*Atrispinum salpae*	Gi	[151]
			Bivagina pagrosomi	Gi	[152]
			Choricotyle chrysophryi	Gi	[144]
			Polylabris tubicirrus	Gi	[153,154]
			Sparicotyle chrysophrii ▲	Gi	[125,155]
Endoparasites	Cnidaria*	Myxozoa (Family: Ceratomyxidae)	*Ceratomyxa sparusaurati*	Gb, In	[156]
			Ceratomyxa auratae	Gb	[157]
			Ceratomyxa spp.	Gb	[138]
		(Family: Enteromyxidae)	*Enteromyxum leei* ▲	In	[158]
		(Family: Myxobolidae)	*Henneguya* spp.	Gi, Ht	[159]
		(Family: Kudoidae)	*Kudoa iwatai*	In, Mu, Sb	[160]
		(Family: Ortholineidae)	*Ortholinea auratae*	Ub	[161]
		(Family: Sphaerosporidae)	*Sphaerospora sparidarum*	Kd	[162,163]
			Sphaerospora sparis	Kd	[164,165]
	Microsporidia	Microsporidia *incertae sedis*	*Ecytonucleospora nucleophila* ▲	In	[128,166]
		Microsporea	*Glugea* spp.	Mu, Sk	[167]
			Pleistophora spp.	Mu	[168]
	Myzozoa	Conoidasida (Family: Cryptosporidiidae)	*Cryptosporidium molnari*	In, St	[169]
		(Family: Eimeriidae)	*Eimeria sparis*	In	[170]
			Eimeria spp.	In	[138]
			Goussia sparis	In	[170]
	Nematoda*	Chromadorea	*Contracaecum* spp.	In	[171]
	Platyhelminthes*	Trematoda (Family: Opecoelidae)	*Allopodocotyle pedicellata*	In	[172]
			Macvicaria maillardi	In	[172]
			Macvicaria obovata	In	[172]
		(Family: Lepocreadiidae)	*Lepocreadium pegorchis*	In	[172]
		(Family: Aporocotylidae)	*Aporocotylidae* spp.	Ci	[131]
			Cardicola auratus	Ci	[173]
			Cardicola mediterraneus	Ci	[174]
		(Family: Monorchiidae)	*Monorchis monorchis*	Py	[172]

Abbreviations: Bc: buccal cavity; **Ci**: circulatory system; **Ey**: eye; **Fn**: fin; **Gb**: gallbladder; **Gi**: gills; **Ht**: heart; **In**: intestine; **Kd**: kidney; **Mu**: muscle; **Oc**: opercular cavity; **Py**: pyloric caeca; **Sb**: swim bladder; **Sk**: skin; **St**: stomach; **Ub**: urinary bladder. Asterisks (*****) indicate metazoan organisms; The symbol ▲ indicates the most relevant parasitosis. **NOTE:** The taxonomic classifications were obtained from the World Register of Marine Species – WoRMS [174].

gate parasitic lifestyle, albeit with free-living life stages, Neodermata presents a unique evolutionary strategy compared to fully free-living organisms[176]. Morphologically, organisms within this monophyletic group initially feature a multiciliated ectoderm limited to the larval stages[176,177]. This structure is later replaced by a syncytial neodermis or tegument, which dynamically interacts with their hosts[176–179]. Only a few specialised taxa deviate from this developmental pattern[176,177].

In the ever-evolving realm of taxonomy and systematics, Trematoda (flukes), Cestoda (tapeworms), and Monogenea comprised the superclass Neodermata until recently. Monogeneans, like numerous other organisms, have undergone multiple taxonomic revisions. Originally classified as a subclass of Trematoda, Monogenea later earned its status as a distinct class. The current-omics era has, however, facilitated the decision to divide Monogenea *sensu lato* into two classes: Monopisthocotyla and Polyopisthocotyla (formerly Monogenea taxonomic subclasses, Monopisthocotylea- Polyonchoinea and Polyopisthocotylea- Oligonchoinea, respectively) and therefore resolving Monogenea as a paraphyletic group[177,180] (**Figure 7)**. This taxonomic restructuring has also provided insights into the evolutionary relationships within Neodermata suggesting that two independent evolutionary events within the group led to a transition from ectoparasitism to endoparasitism, potentially originating within Monopisthocotyla and Polyopisthocotyla[177].

Moreover, neodermatans are believed to have originated during the history of the stem group Gnathostomata[176]. With the divergence of the class Chondrichthyes and superclass Osteichthyes, monopisthocotylans and polyopisthocotylans are thought to have radiated, while the trematode superclasses Digenea and Aspidogastrea diverged alongside the Gyrocotylidae order from other cestodes[176], denoting their close association

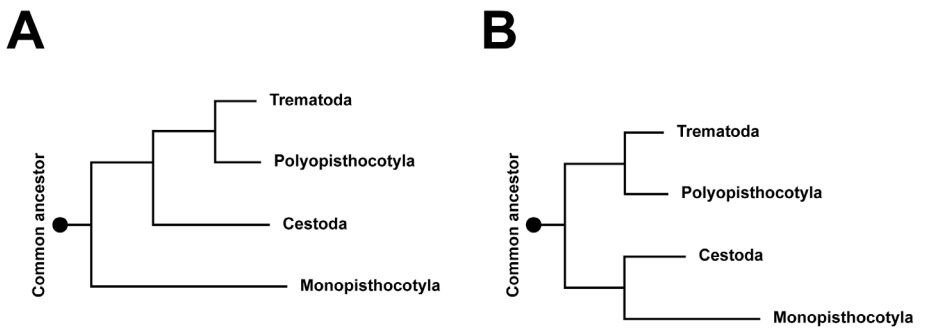

Figure 7. Schematic cladograms representing the current Neodermata monophyletic group taxonomic reclassification proposal. A: cladogram based on maximum likelihood phylogeny; B: cladogram based on a Bayesian inference phylogeny. Adapted from Brabec et al.[176].

with water and aquatic organisms since the Cambrian period, dated between 541 and 485.4 million years ago, and thus their high specialisation[176,181].

Polyopisthocotyla

Polyopisthocotylans are classified into four orders: Chimaericolidea, Diclybothriidea, Mazocraeidea (the major order), and Polystomatidea[182]. These ectoparasitic flatworms are obligate parasites infecting a range of hosts including Chondrichthyes, Osteichthyes, Amphibia, and rarely Reptilia and Mammalia. Although predominantly ectoparasitic, certain endoparasitic species have been identified, primarily within the Polystomatidea order[177].

Characterised by a posterior attachment organ known as the haptor or opisthaptor, these neodermatans exhibit sclerotised hooks during the post-larvae stages, which later metamorphose into haptoral clamps in juvenile and adult specimens. The anterior end features a group of glands and a subterminal mouth with one or two perioral suckers. Generally considered haematophagous, these parasites typically possess a bifurcated intestine or lateral diverticula, and they are oviparous and hermaphroditic[177]. Self-fertilisation is rare and would not be strictly feasible due to their morphology, but there is a chance it could take place by protandry and via the uterus[183].

Their life cycle is direct: ciliated free-swimming larvae (oncomiracidia) hatch from embryonated oval-shaped eggs with one to two polar filaments. These larvae primarily infect gills before metamorphosing into post-larvae and eventually maturing into adults, reaching lengths of over 3 cm long[177,184]. The prepatent period typically spans 4 to 7 weeks[184]. However, the duration of their life cycle, fecundity, embryonic development, infectivity and longevity are significantly influenced by abiotic factors, including water temperature, pH, photoperiod and salinity [184–187].

Sparicotyle chrysophrii

Sparicotyle chrysophrii is an oviparous and protandrous hermaphrodite polyopisthocotylan infecting the gills of gilthead seabream, currently classified in the order Mazocraeidea and the family Microcotylidae[188,189]. The primordial genital atrium is first observed 19 days post-infection (dpi), with testes primordia appearing between 19 to 21 dpi, and the germarium bearing developing oocytes between 21 and 26 dpi. Moreover, the first eggs in the uterus were seen at 26 dpi[189]. Released eggs (**Figure 8A**) are fusiform and have two polar filaments: one short filament ending in a hook, and one long filament. These filaments facilitate the eggs' entanglement with other eggs, gills of their hosts, and the nets of sea cages in aquaculture settings (**Figure 8B, C**). This entanglement significantly contributes to persistent and recurring infections by keeping the eggs close to the host environment, allowing continuous reinfection cycles.

The optimal temperature range for oncomiracidia is 14 to 22°C, coinciding with the

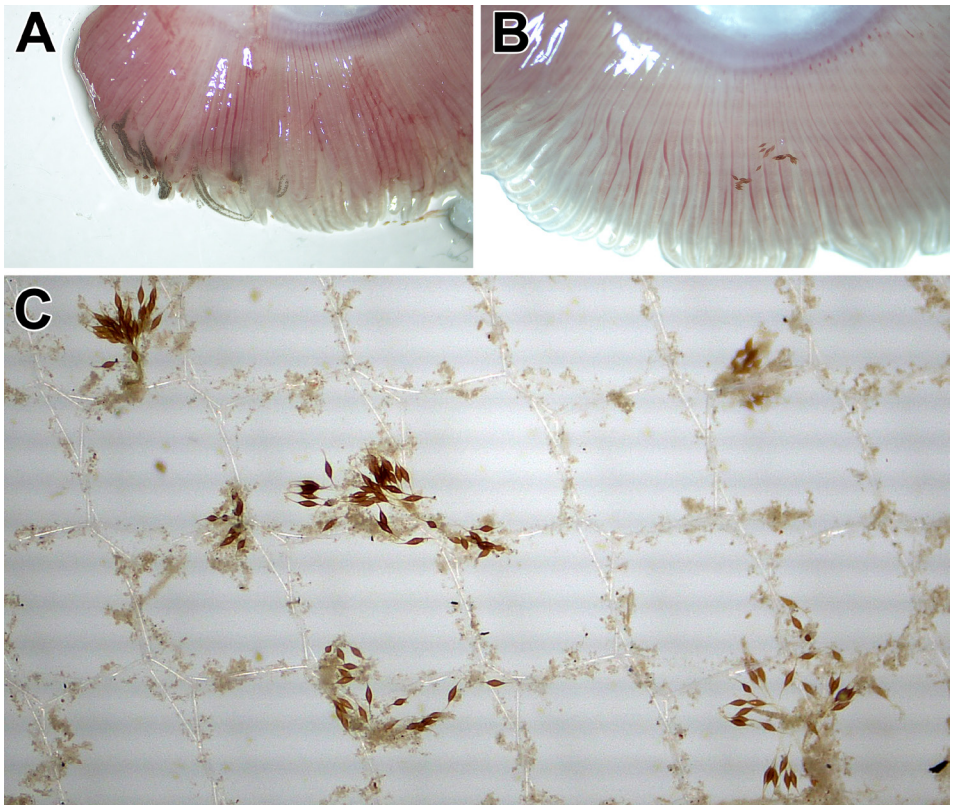

Figure 8. Adult *Sparicotyle chrysophrii* specimens and eggs. A: Gravid adult *S. chrysophrii* specimens in a gill arch from gilthead seabream. **B**: Entangled *S. chrysophrii* eggs in a gill arch from gilthead seabream. **C**: Entangled *S. chrysophrii* eggs in a polyester mesh.

usual water temperatures found in spring and autumn in the Mediterranean Sea[187]. As temperature rises from 22 to 26°C, the development rate of oncomiracidia accelerates, leading to shorter incubation and hatching periods, with 30°C defined as the upper thermal limit for their survival[187]. Additionally, fluctuations in the light intensity, transitioning from light to darkness or *vice versa*, minimally affect the embryonic development but do seem to trigger oncomiracidia hatching, with a higher frequency observed during transitions from light to darkness[186,187]. Furthermore, while low salinity negatively affects embryonic development, low pH levels do not; however, the latter negatively impacts hatching and hatching success rate[187].

This ectoparasitic flatworm has been found in sparid species other than gilthead seabream, including bogue (*Boops boops*)[143,190,191], sharpsnout seabream (*Diplodus puntazzo*)[149,153,172,192] annular seabream (*Diplodus annularis*), axillary seabream (*Pagellus acarne*), common pandora (*Pagellus erythrinus*) and blotched picarel (*Spicara maena*)[191]. Hence, it is described as specific to the Sparidae taxonomic family rather than being

species-specific, increasing the chances of parasite flow between wild and cultured sparids. Three genetic clusters of *S. chrysophrii* have been identified, with pronounced gene flow between *S. chrysophrii* from wild and reared gilthead seabream[191]. Although no transfer has been identified between wild bogue and reared gilthead seabream[143,190], possibly due to the existence of two different *S. chrysophrii* lineages[193], wild sparids should not be disregarded in this matter.

In the Mediterranean aquaculture industry, *S. chrysophrii* has been estimated to be responsible for up to 30% of the mortalities[112], resulting in significant direct and indirect economic losses. This parasite has a systemic impact on its host[89], causing lethargy, increased opercular movement rate, and gill paleness associated with generalised anaemia presumably due to the haematophagous nature of polyopisthocotylans [119,155].

Despite its impact, the primary treatment for this parasitosis remains formalin in its licensed formulation (Aquacen 380 mg · ml^{-1}; Cenavisa Animal Health and Aquaculture, Tarragona, Spain), which is used as a chemotherapeutic agent applied in bath treatments. However, formalin has a narrow therapeutic index and raises significant safety concerns for treatment operators, potentially limiting its use[194–196]. Alternatives that have been studied and tested include fenbendazole, benzimidazole[197], praziquantel[198,199], caprylic acid[197,200,201], two organosulfur compounds[202] and a microencapsulated feed additive containing garlic, carvacol and thymol essential oils [203], but none are in current use.

References

1. FAO. The state of world fisheries and aquaculture 2022. Towards blue transformation. The State of World Fisheries and Aquaculture 2022. Rome: FAO; 2022.

2. FAO. FishStat: global aquaculture production 1950-2022 [Internet]. 2024 [cited 2024 Mar 29]. Available from: www.fao.org/fishery/en/statistics/software/fishstatj

3. European Project Diversify: 7FP-KBBE-2013-GA 602131 [Internet]. [cited 2024 Apr 1]. Available from: http://www.diversifyfish.eu/

4. Aquaculture Business Association of Spain- APROMAR. Aquaculture in Spain 2023 [Internet]. 2023. Available from: https://apromar.es/informes/

5. Federation of European aquaculture producers- FEAP. European Aquaculture Production Report 2016-2022. 2024. [cited 2024 Mar 29] [Internet]. Available from: https://feap.info/index.php/data-home/data/

6. Betancur RR, Wiley EO, Arratia G, Acero A, Bailly N, Miya M, et al. Phylogenetic classification of bony fishes. BMC Evol Biol. BioMed Central Ltd.; 2017.

7. Nelson JS, Grande TC, Wilson MVH. Fishes of the World. 5th Edition. New Jersey: John Wiley & Sons, Inc.; 2016. p. 502–6.

8. Lloris D. Ictiofauna Marina. 1st Edition. Barcelona: OMEGA; 2015. p. 416–24.

9. Basurco B, Lovatelli A, García B. Current status of Sparidae aquaculture. In: Pavlidis MA, Mylonas CC, editors. Sparidae: Biology and aquaculture of gilthead sea bream and other species. 1st Edition. Chichester: John Wiley & Sons, Ltd.; 2011. p. 1–50.

10. Russell B, Carpenter KE, Pollard D. Sparus aurata. The IUCN Red List of Threatened Species 2014: e.T170253A1302459 [Internet]. [cited 2024 Mar 18]. Available from: https://dx.doi.org/10.2305/IUCN.UK.2014-3.RLTS.T170253A1302459.en

11. Volstorf J. Fair-Fish database: gilthead seabream. Sparus aurata [Internet]. 2022. [cited 2024 Mar 18]. Available from: https://fair-fish-database.net/db/species/sparus-aurata/

12. Klinger DH, Levin SA, Watson JR. The growth of finfish in global openocean aquaculture under climate change. Proc R Soc B. 2017;284:20170834.

13. Council Directive 98/58/EC. Concerning the protection of animals kept for farming purposes. Document 01998L0058-20191214 [Internet]. [cited 2024 May 31]. Available from: https://eur-lex.europa.eu/legal-content/EN/TXT/?uri=CELEX%3A01998L0058-20191214

14. Council Regulation (EC) No 1099/2009. On the protection of animals at the time of killing. Document 02009R1099-20191214 [Internet]. [cited 2024 May 31]. Available from: https://eur-lex.europa.eu/legal-content/EN/TXT/?uri=CELEX%3A02009R1099-20191214

15. Regulation (EU) 2016/429. On transmissible animal diseases and amending and repealing certain acts in the area of animal health ('Animal Health Law'). Document 02016R0429-20210421 [Internet]. [cited 2024 May 31]. Available from: https://eur-lex.europa.eu/eli/reg/2016/429/oj

16. Council Regulation (EC) No 1/2005. On the protection of animals during transport and related operations and amending Directives 64/432/EEC and 93/119/EC and Regulation (EC) No 1255/97. Document 02005R0001-20191214 [Internet]. [cited 2024 May 31]. Available from: https://eur-lex.europa.eu/legal-content/EN/

TXT/?uri=CELEX%3A02005R0001-20191214

17. Commission Decision (2017/C 31/12). Establishing the commission expert group 'Platform on Animal Welfare'. Document 32017D0131(01) [Internet]. Available from: https://eur-lex.europa.eu/legal-content/EN/TXT/?uri=CELEX:32017D0131(01)

18. European Commission. Strategic guidelines for a more sustainable and competitive EU aquaculture for the period 2021 to 2030. Document 52021DC0236 [Internet]. 2021. Available from: https://eur-lex.europa.eu/legal-content/EN/TXT/?uri=CELEX%3A52021DC0236

19. European Commission. Proposal for a regulation of the European Parliament and of the Council on the protection of animals during transport and related operations, amending Council Regulation (EC) No 1255/97 and repealing Council Regulation (EC) No 1/2005. Document 52023PC0770 [Internet]. 2023. Available from: https://eur-lex.europa.eu/legal-content/EN/TXT/?uri=COM%3A2023%3A770%3AFIN

20. Commission implementing decision 2024/266. Designating a European Union reference centre for the welfare of aquatic animals in accordance with Regulation (EU) 2017/625 of the European Parliament and of the Council (notified under document C(2024) 209). Document 32024D0266 [Internet]. Available from: https://eur-lex.europa.eu/eli/dec_impl/2024/266/oj

21. World Organisation for Animal Health - WOAH. Introduction to the recommendations for animal welfare. Terrestrial animal health code [Internet]. 2018 [cited 2024 Apr 28]. Available from: https://www.woah.org/fileadmin/Home/eng/Health_standards/tahc/2018/en_chapitre_aw_introduction.htm

22. Saraiva JL, Arechavala-Lopez P, Castanheira MF, Volstorf J, Studer BH. A global assessment of welfare in farmed fishes: the fishethobase. Fishes. 2019;4:30.

23. Schreck CB, Tort L. The Concept of Stress in Fish. In: Schreck CB, Tort L, Farrell AP, Brauner VJ, editors. Fish Physiology. 1st Edition. Elsevier Inc.; 2016. p. 1–34.

24. Ashley PJ. Fish welfare: current issues in aquaculture. Appl Anim Behav Sci. 2007;104:199–235.

25. Alfonso S, Sadoul B, Cousin X, Bégout ML. Spatial distribution and activity patterns as welfare indicators in response to water quality changes in European sea bass, *Dicentrarchus labrax*. Appl Anim Behav Sci. 2020;226:104974.

26. Brydges NM, Boulcott P, Ellis T, Braithwaite VA. Quantifying stress responses induced by different handling methods in three species of fish. Appl Anim Behav Sci. 2009;116:295–301.

27. Delfosse C, Pageat P, Lafont-Lecuelle C, Asproni P, Chabaud C, Cozzi A, et al. Effect of handling and crowding on the susceptibility of Atlantic salmon (*Salmo salar* L.) to *Lepeophtheirus salmonis* (Krøyer) copepodids. J Fish Dis. 2021;44:327–36.

28. Arends RJ, Mancera JM, Muñoz JL, Wendelaar Bonga SE, Flik G. The stress response of the gilthead sea bream (*Sparus aurata* L.) to air exposure and confinement. J Endocrinol. 1999;163:149–57

29. Segner H, Sundh H, Buchmann K, Douxfils J, Sundell KS, Mathieu C, et al. Health of farmed fish: its relation to fish welfare and its utility as welfare indicator. Fish Physiol Biochem. 2012;38:85–105.

30. Sierra-Flores R, Atack T, Migaud H, Davie A. Stress response to anthropogenic noise in Atlantic cod *Gadus morhua* L. Aquac Eng. 2015;67:67–76.

31. Filiciotto F, Giacalone VM, Fazio F, Buffa G, Piccione G, Maccarrone V, et al. Effect of acoustic environment on gilthead sea bream (*Sparus aurata*): sea and onshore aquaculture background noise. Aquaculture. 2013;414–

415:36–45.

32. Radford C, Slater M. Soundscapes in aquaculture systems. Aquac Environ Interact. 2019;11:53–62.

33. Breves JP, Specker JL. Cortisol stress response of juvenile winter flounder (*Pseudopleuronectes americanus*, Walbaum) to predators. J Exp Mar Biol Ecol. 2005;325:1–7.

34. López-Patiño MA, Skrzynska AK, Naderi F, Mancera JM, Míguez JM, Martos-Sitcha JA. High stocking density and food deprivation increase brain monoaminergic activity in gilthead sea bream (*Sparus aurata*). Animals. 2021;11:1503.

35. Hvas M, Kolarevic J, Noble C, Oppedal F, Stien LH. Fasting and its implications for fish welfare in Atlantic salmon aquaculture. Rev Aquac. John Wiley and Sons Inc; 2024. p. 1–25.

36. Hoem KS, Tveten AK. Sea transfer and net pen cleaning induce changes in stress-related gene expression in commercial Atlantic salmon (*Salmo salar*) gill tissue. Aquacult Int. 2023;31:2245–62.

37. Oliveira AR, Cabrera-Álvarez MJ, Soares F, Diáz-Gil C, Candeias-Mendes A, Saraiva JL, et al. Structural enrichment promotes natural behaviour and welfare of captive gilthead seabream broodstock. Appl Anim Behav Sci. 2024;275:106289.

38. Sarkodie EK, Zhou S, Baidoo SA, Chu W. Influences of stress hormones on microbial infections. Microb Pathog. 2019;131:270-6

39. Torabi Delshad S, Soltanian S, Sharifiyazdi H, Bossier P. Effect of catecholamine stress hormones (dopamine and norepinephrine) on growth, swimming motility, biofilm formation and virulence factors of *Yersinia ruckeri in vitro* and an *in vivo* evaluation in rainbow trout. J Fish Dis. 2019;42:477–87.

40. Pande GSJ, Suong NT, Bossier P, Defoirdt T. The catecholamine stress hormones norepinephrine and dopamine increase the virulence of pathogenic *Vibrio anguillarum* and *Vibrio campbellii*. FEMS Microbiol Ecol. 2014;90:761–9.

41. Suzuki DG. The Anthropic Principle for the Evolutionary Biology of Consciousness: beyond anthropocentrism and anthropomorphism. Biosemiotics. 2022;15:171–86.

42. Michel M. Fish and microchips: on fish pain and multiple realization. Philos Stud. 2019;176:2411–28.

43. Low P. The Cambridge Declaration on Consciousness. Cambridge; 2012 Jul.

44. Allen C. Fish cognition and consciousness. J Agric Environ Ethics. 2013;26:25–39.

45. Leung LC, Wang GX, Madelaine R, Skariah G, Kawakami K, Deisseroth K, et al. Neural signatures of sleep in zebrafish. Nature. 2019;571:198–204.

46. Singh R, Sharma D, Kumar A, Singh C, Singh A. Understanding zebrafish sleep and wakefulness physiology as an experimental model for biomedical research. Fish Physiol Biochem. 2024;50:827–42.

47. Kohda M, Hotta T, Takeyama T, Awata S, Tanaka H, Asai J, et al. If a fish can pass the mark tests, what are the implications for consciousness and self-awareness testing in animals? PLoS Biol. 2019;17:e3000021.

48. Kohda M, Sogawa S, Jordan AL, Kubo N, Awata S, Satoh S, et al. Further evidence for the capacity of mirror self-recognition in cleaner fish and the significance of ecologically relevant marks. PLoS Biol. 2022;20:e3001529.

49. Kohda M, Bshary R, Kubo N, Awata S, Sowersby W, Kawasaka K, et al. Cleaner fish recognize self in a mirror via self-face recognition like humans. Proc Natl Acad Sci USA. 2023;120: e2208420120.

50. de Waal FBM. Fish, mirrors, and a gradualist perspective on self-awareness. PLoS Biol. 2019;17:e3000112.

51. Sneddon LU, Elwood RW, Adamo SA, Leach MC. Defining and assessing animal pain. Anim Behav. 2014;97:201–12.

52. Secombes CJ, Wang T. The innate and adaptive immune system of fish. In: Austin B, editor. Infectious Disease in Aquaculture: prevention and control. First edition. Elsevier ; 2012. p. 3–68.

53. Wentzel AS, Janssen JJE, de Boer VCJ, van Veen WG, Forlenza M, Wiegertjes GF. Fish macrophages show distinct metabolic signatures upon polarization. Front Immunol. 2020;11:152.

54. Manera M, Dezfuli BS. Rodlet cells in teleosts: a new insight into their nature and functions. J Fish Biol. 2004;65:597–619.

55. Stosik M, Tokarz-Deptuła B, Deptuła W. Characterisation of thrombocytes in Osteichthyes. J Vet Res. 2019;63:123–31.

56. Passantino L, Cianciotta A, Patruno R, Ribaud MR, Jirillo E, Passantino GF. Do fish thrombocytes play an immunological role? Their cytoenzymatic profiles and function during an accidental piscine candidiasis in aquarium. Immunopharmacol Immunotoxicol. 2005;27:345–56.

57. Chan JTH, Picard-Sánchez A, Majstorović J, Rebl A, Koczan D, Dyčka F, et al. Red blood cells in proliferative kidney disease—rainbow trout (*Oncorhynchus mykiss*) infected by *Tetracapsuloides bryosalmonae* harbor IgM+ red blood cells. Front Immunol. 2023;14:1041325.

58. Morera D, Roher N, Ribas L, Balasch JC, Doñate C, Callol A, et al. Rna-seq reveals an integrated immune response in nucleated erythrocytes. PLoS One. 2011;6:e26998.

59. Nakao M, Tsujikura M, Ichiki S, Vo TK, Somamoto T. The complement system in teleost fish: progress of post-homolog-hunting researches. Dev Comp Immunol. 2011;35:1296–308.

60. Wiegertjes GF, Wentzel AS, Spaink HP, Elks PM, Fink IR. Polarization of immune responses in fish: the 'macrophages first' point of view. Mol Immunol. 2016;69:146–56.

61. Shibasaki Y, Afanasyev S, Fernández-Montero A, Ding Y, Watanabe S, Takizawa F, et al. Cold-blooded vertebrates evolved organized germinal center–like structures. Sci Immunol. 2023;8:eadf1627.

62. Mashoof S, Criscitiello MF. Fish immunoglobulins. Biology (Basel). 2016;5:45.

63. Piazzon MC, Galindo-Villegas J, Pereiro P, Estensoro I, Calduch-Giner JA, Gómez-Casado E, et al. Differential modulation of IgT and IgM upon parasitic, bacterial, viral, and dietary challenges in a perciform fish. Front Immunol. 2016;7:637.

64. Kumar S, Raman RP, Prasad KP, Srivastava PP, Kumar S, Rajendran K V. Modulation of innate immune responses and induction of oxidative stress biomarkers in *Pangasianodon hypophthalmus* following an experimental infection with dactylogyrid monogeneans. Fish Shellfish Immunol. 2017;63:334–43.

65. Chaves IS, Luvizotto-Santos R, Sampaio LAN, Bianchini A, Martínez PE. Immune adaptive response induced by *Bicotylophora trachinoti* (Monogenea: Diclidophoridae) infestation in pompano *Trachinotus marginatus* (Perciformes: Carangidae). Fish Shellfish Immunol. 2006;21:242–50.

66. Lindenstrøm T, Secombes CJ, Buchmann K. Expression of immune response genes in rainbow trout skin induced by *Gyrodactylus derjavini* infections. Vet Immunol Immunopathol. 2004;97:137–48.

67. Lindenstrøm T, Buchmann K, Secombes CJ. *Gyrodactylus derjavini* infection elicits IL-1β expression in rainbow

trout skin. Fish Shellfish Immunol. 2003;15:107–15.

68. Reyes-Becerril M, Alamillo E, Trasviña A, Hirono I, Kondo H, Jirapongpairoj W, et al. *In vivo* and *in vitro* studies using larval and adult antigens from *Neobenedenia melleni* on immune response in yellowtail (*Seriola lalandi*). J Fish Dis. 2017;40:1497–509.

69. Buchmann K. Immune mechanisms in fish skin against monogeneans-a model. Folia Parasitol (Praha). 1999;46:1–9.

70. Chen J, Zhi T, Xu X, Zhang S, Zheng Y, Yang T. Molecular characterization and dynamic expressions of three Nile tilapia (*Oreochromis niloticus*) complement genes after *Gyrodactylus cichlidarum* (Monogenea) infection. Aquaculture. 2019;502:176–88.

71. Faliex E, Da Silva C, Simon G, Sasal P. Dynamic expression of immune response genes in the sea bass, *Dicentrarchus labrax*, experimentally infected with the monogenean *Diplectanum aequans*. Fish Shellfish Immunol. 2008;24:759–67.

72. Ohno Y, Kawano F, Hirazawa N. Susceptibility by amberjack (*Seriola dumerili*), yellowtail (*S. quinqueradiata*) and Japanese flounder (*Paralichthys olivaceus*) to *Neobenedenia girellae* (Monogenea) infection and their acquired protection. Aquaculture. 2008;274:30–5.

73. Bondad-Reantaso, M. G., Ogawa, K., Yoshinaga, T., & Wakabayashi, H. Acquired protection against *Neobenedenia girellae* in Japanese flounder. Fish Pathol. 1995:30:233–8.

74. Cable J, Van Oosterhout C. The role of innate and acquired resistance in two natural populations of guppies (*Poecilia reticulata*) infected with the ectoparasite *Gyrodactylus turnbulli*. Biol J Linn Soc. 2007;90:647–55.

75. Hong Kim K, Jung Hwang Y, Bum Cho J. Immunization of cultured juvenile rockfish *Sebastes schlegeli* against *Microcotyle sebastis* (Monogenea). Dis Aquat Organ. 2000;40:29–32.

76. Nakane M, Ogawa K, Fujita T, Sameshima M, Wakabayashi H. Acquired protection of tiger puffer *Takifugu rubripes* against Infection with *Heterobothrium okamotoi* (Monogenea: Diclidophoridae). Fish Pathol. 2005;40:95–101.

77. Hirazawa N, Hagiwara H, Takano R, Noguchi M, Narita M. Assessment of acquired protection levels against the parasite *Neobenedenia girellae* (Monogenea) between body surface sites including fins of amberjack *Seriola dumerili* (Carangidae) and the skin in response to the parasite infection. Aquaculture. 2011;310:252–8.

78. Rubio-Godoy M, Sigh J, Buchmann K, Tinsley RC. Immunization of rainbow trout *Oncorhynchus mykiss* against *Discocotyle sagittata* (Monogenea). Dis Aquat Organ. 2003;2003:23–30.

79. Roberts RJ, Ellis AE. The anatomy and physiology of teleosts. In: Roberts RJ, editor. Fish Pathol. 4th Edition. Chichester: John Wiley & Sons, Ltd.; 2012. p. 17–61.

80. Nilsson GE. Ventilation and animal respiration. In: Farrell AP, editor. Encyclopedia of fish physiology: from genome to environment. London: Elsevier Inc; 2011. p. 796–802.

81. Wegner NC. Gill respiratory morphometrics. In: Farrell AP, editor. Encyclopedia of fish physiology: from genome to environment. London: Elsevier Inc; 2011. p. 803–11.

82. Foyle KL, Hess S, Powell MD, Herbert NA. What is gill health and what is its role in marine finfish aquaculture in the face of a changing climate? Front Mar Sci. 2020;7:400

83. Farrell AP. Gas exchange. In: Farrell AP, editor. Encyclopedia of fish physiology: from genome to environment. London: Elsevier Inc.; 2011. p. 791–972.

84. Farrell AP. The gut. In: Farrell AP, editor. Encyclopedia of fish physiology: from genome to environment. London: Elsevier Inc; 2011. p. 1229–449.

85. Chen J, Liu C, Yang T. Killing effect of fish serum and mucus on *Gyrodactylus cichlidarum* (Platyhelminthes, Monogenea) mediated by complement. Aquaculture. 2023;567:739248.

86. Valdenegro-Vega VA, Crosbie P, Bridle A, Leef M, Wilson R, Nowak BF. Differentially expressed proteins in gill and skin mucus of Atlantic salmon (*Salmo salar*) affected by amoebic gill disease. Fish Shellfish Immunol. 2014;40:69–77.

87. Sommer F, Bäckhed F. The gut microbiota-masters of host development and physiology. Nat Rev Microbiol. 2013;11:227–38.

88. Kamada N, Chen GY, Inohara N, Núñez G. Control of pathogens and pathobionts by the gut microbiota. Nat Immunol. 2013;14:685–90.

89. Toxqui-Rodríguez S, Riera-Ferrer E, Del Pozo R, Palenzuela O, Sitjà-Bobadilla A, Estensoro I, et al. Molecular interactions in an holobiont-pathogen model: integromics in gilthead seabream infected with *Sparicotyle chrysophrii*. Aquaculture. 2024;581:740365.

90. Llewellyn MS, Leadbeater S, Garcia C, Sylvain FE, Custodio M, Ang KP, et al. Parasitism perturbs the mucosal microbiome of Atlantic Salmon. Sci Rep. 2017;7:43465.

91. Gómez D, Sunyer JO, Salinas I. The mucosal immune system of fish: the evolution of tolerating commensals while fighting pathogens. Fish Shellfish Immunol. 2013;35:1729–39.

92. Chasiotis H, Kolosov D, Kelly SP. Permeability properties of the teleost gill epithelium under ion-poor conditions. Am J Physiol Regul Integr Comp Physiol. 2012;302:R727–39.

93. Rességuier J, Dalum AS, Du Pasquier L, Zhang Y, Koppang EO, Boudinot P, et al. Lymphoid tissue in teleost gills: variations on a theme. Biology (Basel). 2020;9:127.

94. Haugarvoll E, Bjerkås I, Nowak BF, Hordvik I, Koppang EO. Identification and characterization of a novel intraepithelial lymphoid tissue in the gills of Atlantic salmon. J Anat. 2008;213:202–9.

95. Koppang EO, Fischer U, Moore L, Tranulis MA, Dijkstra JM, Köllner B, et al. Salmonid T cells assemble in the thymus, spleen and in novel interbranchial lymphoid tissue. J Anat. 2010;217:728–39.

96. Salinas I, Miller RD. Comparative phylogeny of the mucosa-associated lymphoid tissue. In: Mestecky J, Strober W, Russell MW, Kelsall BL, Cheroutre H, Lambrecht BN, editors. Mucosal Immunol. 4th Edition. Kidlington: Elsevier Inc.; 2015.

97. Syahputra K, Kania PW, Al-Jubury A, Marnis H, Cahyo Setyawan A, Buchmann K. Differential immune gene response in gills, skin, and spleen of rainbow trout *Oncorhynchus mykiss* infected by *Ichthyophthirius multifiliis*. PLoS One. 2019;14:e0218630.

98. Valenzuela-Miranda D, Boltaña S, Cabrejos ME, Yáñez JM, Gallardo-Escárate C. High-throughput transcriptome analysis of ISAV-infected Atlantic salmon *Salmo salar* unravels divergent immune responses associated to head-kidney, liver and gills tissues. Fish Shellfish Immunol. 2015;45:367–77.

99. Austbø L, Aas IB, König M, Weli SC, Syed M, Falk K, et al. Transcriptional response of immune genes in gills and the interbranchial lymphoid tissue of Atlantic salmon challenged with infectious salmon anaemia virus. Dev Comp Immunol. 2014;45:107–14.

100. Król E, Noguera P, Shaw S, Costelloe E, Gajardo K, Valdenegro V, et al. Integration of transcriptome, gross morphology and histopathology in the gill of sea farmed Atlantic Salmon (*Salmo salar*): lessons from multi-site sampling. Front Genet. 2020;11:610.

101. Xu Z, Takizawa F, Parra D, Gómez D, Von Gersdorff Jørgensen L, Lapatra SE, et al. Mucosal immunoglobulins at respiratory surfaces mark an ancient association that predates the emergence of tetrapods. Nat Commun. 2016;7:10728.

102. Tongsri P, Meng K, Liu X, Wu Z, Yin G, Wang Q, et al. The predominant role of mucosal immunoglobulin IgT in the gills of rainbow trout (*Oncorhynchus mykiss*) after infection with *Flavobacterium columnare*. Fish Shellfish Immunol. 2020;99:654–62.

103. Salinas I. The mucosal immune system of teleost fish. Biology (Basel). 2015;4:525–39.

104. Shawky M, Taha E, Ahmed B, Mahmoud MA, Abdelaziz M, Faisal M, et al. Initial evidence that gilthead seabream (*Sparus aurata* L.) is a host for lymphocystis disease virus genotype I. 2021;11:3032.

105. Valverde EJ, Borrego JJ, Sarasquete MC, Ortiz-Delgado JB, Castro D. Target organs for lymphocystis disease virus replication in gilthead seabream (*Sparus aurata*). Vet Res. 2017;48.

106. Volpe E, Gustinelli A, Caffara M, Errani F, Quaglio F, Fioravanti ML, et al. Viral nervous necrosis outbreaks caused by the RGNNV/SJNNV reassortant betanodavirus in gilthead sea bream (*Sparus aurata*) and European sea bass (*Dicentrarchus labrax*). Aquaculture. 2020;523:735155.

107. Toffan A, Biasini L, Pretto T, Abbadi M, Buratin A, Franch R, et al. Age dependency of RGNNV/SJNNV viral encephalo-retinopathy in Gilthead Sea Bream (*Sparus aurata*). Aquaculture. 2021;539:736605.

108. Hadfield CA. Bacterial diseases. In: Hadfield CA, Clayton LA, editors. Clinical Guide to Fish Medicine. 1st Edition. Chichester: John Wiley & Sons, Inc.; 2021. p. 431–67.

109. Colorni A, Padrós F. Diseases and health management. In: Pavlidis MA, Mylonas CC, editors. Sparidae: Biology and aquaculture of gilthead sea bream and other species. 1st Edition. Chichester: John Wiley & Sons, Ltd.; 2011. p. 321–57.

110. Rigos G, Kogiannou D, Padrós F, Cristòfol C, Florio D, Fioravanti M, et al. Best therapeutic practices for the use of antibacterial agents in finfish aquaculture: a particular view on European seabass (*Dicentrarchus labrax*) and gilthead seabream (*Sparus aurata*) in Mediterranean aquaculture. Rev Aquac. John Wiley and Sons Inc; 2021. p. 1285–323.

111. Sanches-Fernandes GMM, Sá-Correia I, Costa R. Vibriosis outbreaks in aquaculture: addressing environmental and public health concerns and preventive therapies using gilthead seabream farming as a model system. Front Microbiol. Frontiers Media S.A.; 2022. p. 904815.

112. Muniesa A, Basurco B, Aguilera C, Furones D, Reverté C, Sanjuan-Vilaplana A, et al. Mapping the knowledge of the main diseases affecting sea bass and sea bream in Mediterranean. Transbound Emerg Dis. 2020;67:1089–100.

113. Romalde JL, Ravelo C, Valdés I, Magariños B, de la Fuente E, Martín CS, et al. *Streptococcus phocae*, an emerging pathogen for salmonid culture. Vet Microbiol. 2008;130:198–207.

114. Van Doan H, Soltani M, Leitão A, Shafiei S, Asadi S, Lymbery AJ, et al. Streptococcosis a re-emerging disease in aquaculture: significance and phytotherapy. Animals. 2022;12:2443.

115. Blandford MI, Taylor-Brown A, Schlacher TA, Nowak B, Polkinghorne A. Epitheliocystis in fish: an emerging

aquaculture disease with a global impact. Transbound Emerg Dis. 2018;65:1436–46.

116. Seth-Smith HMB, Dourala N, Fehr A, Qi W, Katharios P, Ruetten M, et al. Emerging pathogens of gilthead seabream: characterisation and genomic analysis of novel intracellular β-proteobacteria. ISME Journal. 2016;10:1791–803.

117. Seth-Smith HMB, Katharios P, Dourala N, Mateos JM, Fehr AGJ, Nufer L, et al. *Ca.* Similichlamydia in epitheliocystis co-infection of gilthead seabream gills: unique morphological features of a deep branching chlamydial family. Front Microbiol. 2017;8:508.

118. Padrós F, Crespo S. Proliferative epitheliocystis associated with monogenean infection in juvenile seabream *Sparus aurata* in the north east of Spain. Bull Eur Assoc Fish Pathol. 1995;15:42.

119. Sitjà-Bobadilla A, Álvarez-Pellitero P. Experimental transmission of *Sparicotyle chrysophrii* (Monogenea: Polyopisthocotylea) to gilthead seabream (*Sparus aurata*) and histopathology of the infection. Folia Parasitol (Praha). 2009;56:143–51.

120. Aamri F El, Caballero MJ, Real F, Acosta F, Déniz S, Román L, et al. *Streptococcus iniae* in gilthead seabream (*Sparus aurata*, L.) and red porgy (*Pagrus pagrus*, L.): ultrastructural analysis. Vet Pathol. 2015;52:209–12.

121. Evans JJ, Klesius PH, Gilbert PM, Shoemaker CA, Al Sarawi MA, Landsberg J, et al. Characterization of β-haemolytic Group B *Streptococcus agalactiae* in cultured seabream, *Sparus auratus* L., and wild mullet, *Liza klunzingeri* (Day), in Kuwait. J Fish Dis. 2002;25:505–13.

122. Ogawa K. Impacts of diclidophorid monogenean infections on fisheries in Japan. Int J Parasitol. 2002;32:373–80.

123. Fioravanti ML, Mladineo I, Palenzuela O, Beraldo P, Massimo M, Gustinelli A, et al. Guide 4 - Fish farmer's guide to combating parasitic infections in European sea bass and gilthead sea bream aquaculture. Available from: https://www.parafishcontrol.eu/images/PARAFISHCONTROL/Manuals/PFC-Manual4_Seabass_Seabream_vFINAL.pdf

124. Oidtmann BC, Mladineo I, Cook A, Beraldo P, Palenzuela O, Christofilogiannis P, et al. Main parasitic infections in gilthead seabream and European seabass aquaculture: risk factors from stakeholders' perspective. Aquacult Int. 2024;32:4275–302

125. Mladineo I, Volpatti D, Beraldo P, Rigos G, Katharios P, Padrós F. Monogenean *Sparicotyle chrysophrii*: the major pathogen of the Mediterranean gilthead seabream aquaculture. Rev Aquac. 2024;16:287–308.

126. Hadfield CA. Protozoal Diseases. In: Hadfield CA, Clayton LA, editors. Clinical Guide to Fish Medicine. 1st Edition. Chichester: John Wiley & Sons, Inc; 2021. p. 483–512.

127. Sitjà-Bobadilla A, Palenzuela O. *Enteromyxum* species. In: Woo PTK, Buchmann K, editors. Fish parasites: pathobiology and protection. Wallingford: CABI Publishing; 2012. p. 163–76.

128. Palenzuela O, Redondo MJ, Cali A, Takvorian PM, Alonso-Naveiro M, Álvarez-Pellitero P, et al. A new intranuclear microsporidium, *Enterospora nucleophila* n. sp., causing an emaciative syndrome in a piscine host (*Sparus aurata*), prompts the redescription of the family Enterocytozoonidae. Int J Parasitol. 2014;44:189–203.

129. Lui A, Manera M, Giari L, Mulero V, Dezfuli BS. Acidophilic granulocytes in the gills of gilthead seabream *Sparus aurata*: evidence for their responses to a natural infection by a copepod ectoparasite. Cell Tissue Res. 2013;353:465–72.

130. Abdel-Radi S, Rashad MM, Ali GE, Eissa AE, Abdelsalam M, Abou-Okada M. Molecular characterization and

phylogenetic analysis of parasitic copepoda; *Ergasilus sieboldi* isolated from cultured gilthead sea bream (*Sparus aurata*) in Egypt, associated with analysis of oxidative stress biomarkers. J Parasit Dis. 2022;46:1080–9.

131. Fioravanti ML, Caffara M, Florio D, Gustinelli A, Marcer F. A parasitological survey of European sea bass (*Dicentrarchus Labrax*) and gilthead sea bream (*Sparus aurata*) cultured in Italy. Vet Res Commun. 2006;30:249–52.

132. Paperna I. Review of diseases affecting cultured *Sparus aurata* and *Dicentrarchus labrax*. In: Bern, editor. L'aquaculture du bar et des sparidés. 1st Edition. Paris: INRA Publishing; 1980. p. 465–82.

133. Mladineo I. Life cycle of *Ceratothoa oestroides*, a cymothoid isopod parasite from sea bass *Dicentrarchus labrax* and sea bream *Sparus aurata*. Dis Aquat Organ. 2003;57:97–101.

134. Papapanagiotou EP, Trilles JP. Cymothoid parasite *Ceratothoa parallela* inflicts great losses on cultured gilthead sea bream *Sparus aurata* in Greece. Dis Aquat Organ. 2001;45:237–9.

135. Diamant A. *Brooklynella hostilis* (Hartmannulidae), a pathogenic ciliate from the gills of maricultured sea bream. Bull Eur Assoc Fish Pathol. 1998;18.

136. Colorni A. Aspects of the biology of *Cryptocaryon irritans*, and hyposalinity as a control measure in cultured gilt-head sea bream *Sparus aurata*. Dis Aquat Organ. 1985;1:19–22.

137. Cervera L, González-Fernández C, Arizcun M, Cuesta A, Chaves-Pozo E. Severe natural outbreak of *Cryptocaryon irritans* in gilthead seabream produces leukocyte mobilization and innate immunity at the gill tissue. Int J Mol Sci. 2022;23:937.

138. Álvarez-Pellitero P, Sitja-Bobadilla A, Franco-Sierra A. Protozoan parasites of gilthead sea bream, *Sparus aurata* L, from different culture systems in Spain. J Fish Dis. 1995;18:105–15.

139. Diamant A. Morphology and ultrastructure of *Cryptobia eilatica* n. sp. (Bodonidae: Kinetoplastida), an ectoparasite from the gills of marine fish. J Protozool. 1990;37:482–9.

140. Blanc E, Marques A, Bouix G, Brugerolle G, Breuil G. *Cryptobia* sp. from the gills of the gilthead sea bream *Sparus aurata*. Bull Eur Assoc Fish Pathol. 1989;9.

141. Paperna I, Steinitz Marine H. *Amyloodinium ocellatum* (Brown, 1931) (Dinoflagellida) infestations in cultured marine fish at Eilat, Red Sea: epizootiology and pathology. J Fish Dis. 1980;3:363–72.

142. Moreira M, Schrama D, Soares F, Wulff T, Pousão-Ferreira P, Rodrigues P. Physiological responses of reared sea bream (*Sparus aurata* Linnaeus, 1758) to an *Amyloodinium ocellatum* outbreak. J Fish Dis. 2017;40:1545–60.

143. Fernandez-Jover D, Faliex E, Sanchez-Jerez P, Sasal P, Bayle-Sempere JT. Coastal fish farming does not affect the total parasite communities of wild fish in SW Mediterranean. Aquaculture. 2010;300:10–6.

144. Mahmoud NE, Mahmoud AM, Fahmy MM. Parasitological and comparative pathological studies on monogenean infestation of cultured sea bream (*Sparus aurata*, Sparidae) in Egypt. J Oceanogr Mar Res. 2014;2: 1000129.

145. Paladini G, Hansen H, Fioravanti ML, Shinn AP. *Gyrodactylus longipes* n. sp. (Monogenea: Gyrodactylidae) from farmed gilthead seabream (*Sparus aurata* L.) from the Mediterranean. Parasitol Int. 2011;60:410–8.

146. Paladini G, Cable J, Fioravanti ML, Faria PJ, Cave D Di, Shinn AP. *Gyrodactylus orecchiae* sp. n. (Monogenea: Gyrodactylidae) from farmed populations of gilthead seabream (*Sparus aurata*) in the Adriatic Sea. Folia Parasitol (Praha). 2009;56:21–8.

147. Reversat J, Silan P, Maihard C. Structure of monogenean populations, ectoparasites of the gilthead sea bream Sparus aurata. Mar Biol. 1992;112:43–7.

148. Antonelli L, Quilichini Y, Marchand B. Biological study of Furnestinia echeneis Euzet and Audouin 1959 (Monogenea: Monopisthocotylea: Diplectanidae), parasite of cultured gilthead sea bream *Sparus aurata* (Linnaeus 1758) (Pisces: Teleostei) from Corsica. Aquaculture. 2010;307:179–86.

149. Mladineo I, Maršić-Lučić J. Host switch of *Lamellodiscus elegans* (Monogenea: Monopisthocotylea) and *Sparicotyle chrysophrii* (Monogenea: Polyopisthocotylea) between Cage-reared Sparids. Vet Res Commun. 2007;31:153–60.

150. Tedesco P, Caffara M, Miguel N, Moreira R, Gomes C, Gustinelli A, et al. Occurrence of *Neobenedenia girellae* (Monogenea: Capsalidae) in gilthead seabream *Sparus aurata* (Actinopterygii: Sparidae) cultured in Portugal. Pathogens. 2021;10:1269.

151. De Liberato C, Di Cave D, Berrilli F, Orecchia P. Fish parasites and related problems in Italian mariculture facilities. Parassitologia. 2000;42:166.

152. Dajem S Bin, Morsy K, Shati A, Ezzat A, El-Said F, Abdel-Gaber R. *Bivagina pagrosomi* Murray (1931) (Monogenea: Polyopisthocotylea), a microcotylid infecting the gills of the gilt-head sea bream *Sparus aurata* (Sparidae) from the Red Sea: morphology and phylogeny. J Vet Res. 2019;63:345–52.

153. Athanassopoulou F, Ragias V, Vagianou S, Di Cave D, Rigos G, Papathanasiou G, et al. Report of *Sparicotyle* (*Microcotyle*) *chrysophrii* Van Beneden and Hesse 1863, *Atrispinum seminalis* Euzet and Maillard 1973 and *Polylabris tubicirrus* Paperna and Kohn 1964 (Monogenea) on captive sea bream (*Sparus aurata*) and sharp snout sea bream (*Diplodus puntazzo*) in coastal Greece and Italy. Bull Eur Assoc Fish Pathol. 2005;25:256–61.

154. Silan P, Cabral P, Maillard C. Enlargement of the host range of *Polylabris tubicirrus* (Monogenea, Polyopisthocotylea) under fish-farming condition. Aquaculture. 1985;47:267–70.

155. Sitjà-Bobadilla A, Redondo MJ, Álvarez-Pellitero P. Occurrence of *Sparicotyle chrysophrii* (Monogenea: Polyopisthocotylea) in gilthead sea bream (*Sparus aurata* L.) from different mariculture systems in Spain. Aquac Res. 2010;41:939–44.

156. Palenzuela O, Sitjà - Bobadilla A, Álvarez-Pellitero P. *Ceratomyxa sparusaurati* (Protozoa: Myxosporea) infections in cultured gilthead sea bream *Sparus aurata* (Pisces: Teleostei) from Spain: aspects of the host-parasite relationship. Parasitol Res. 1997;83:539–48.

157. Rocha S, Casal G, Rangel L, Castro R, Severino R, Azevedo C, et al. Ultrastructure and phylogeny of *Ceratomyxa auratae* n. sp. (Myxosporea: Ceratomyxidae), a parasite infecting the gilthead seabream *Sparus aurata* (Teleostei: Sparidae). Parasitol Int. 2015;64:305–13.

158. Diamant A, Lom J, Dyková I. *Myxidium leei* n. sp., a pathogenic myxosporean of cultured sea bream *Sparus aurata*. Dis Aquat Organ. 1994;20:137–41.

159. Caffara M, Ml F. Heart infection due to *Henneguya* sp. (Myxozoa, Myxosporea) in gilthead sea bream (*Sparus aurata*) cultured in Italy. Bull Eur Assoc Fish Pathol. 2003;23:108.

160. Diamant A, Ucko M, Paperna I, Colorni A, Lipshitz A. *Kudoa iwatai* (Myxosporea: Multivalvulida) in wild and cultured fish in the red sea: redescription and molecular phylogeny. J Parasitol. 2005;91:1175–89.

161. Rangel LF, Rocha S, Borkhanuddin MH, Cech G, Castro R, Casal G, et al. *Ortholinea auratae* n. sp. (Myxozoa, Ortholineidae) infecting the urinary bladder of the gilthead seabream *Sparus aurata* (Teleostei, Sparidae), in a Portuguese fish farm. Parasitol Res. 2014;113:3427–37.

162. Sitjà-Bobadilla A, Álvarez-Pellitero P. *Leptotheca sparidarum* n. sp. (Myxosporea: Bivalvulida), a parasite from cultured common dentex (*Dentex dentex* L.) and gilthead sea bream (*Sparus aurata* L.) (Teleostei: Sparidae). J Eukaryot Microbiol. 2001;48:627–39.

163. Gunter N, Adlard R. The demise of *Leptotheca* Thélohan, 1895 (Myxozoa: Myxosporea: Ceratomyxidae) and assignment of its species to *Ceratomyxa* Thélohan, 1892 (Myxosporea: Ceratomyxidae), *Ellipsomyxa* Køie, 2003 (Myxosporea: Ceratomyxidae), *Myxobolus* Bütschli, 1882 and *Sphaerospora* Thélohan, 1892 (Myxosporea: Sphaerosporidae). Syst Parasitol. 2010;75:81–104.

164. Sitjà-Bobadilla A, Álvarez-Pellitero P. Light and electron microscopic description of *Polysporoplasma* n. g. (Myxosporea: Bivalvulida), *Polysporoplasma sparis* n. sp. from *Sparus aurata* (L.), and *Polysporoplasma mugilis* n. sp. from *Liza aurata* L. Eur J Protistol. 1995;31:77–89.

165. Bartošová P, Fiala I, Jirků M, Cinková M, Caffara M, Fioravanti ML, et al. *Sphaerospora sensu stricto*: Taxonomy, diversity and evolution of a unique lineage of myxosporeans (Myxozoa). Mol Phylogenet Evol. 2013;68:93–105.

166. Wang Y, Chen J, Na Y, Li X cang, Zhou J fang, Fang W hong, et al. *Ecytonucleospora hepatopenaei* n. gen. et comb. (Microsporidia: Enterocytozoonidae): a redescription of the *Enterocytozoon hepatopenaei* (Tourtip et al., 2009), a microsporidian infecting the widely cultivated shrimp Penaeus vannamei. J Invertebr Pathol. 2023;201:107988.

167. Mathieu-Daude F, Faye N, Coste F, Manier J-F, Marques A, Bouix G. Occurence of a microsporidiosis in marine cultured gilt-head sea bream from the Languedoc coast: a problem of specificity in the genus *Glugea* (Protozoa, Microspora). Bull Eur Assoc Fish Pathol. 1992;12:67–70.

168. Athanassopoulou F. A case report of *Pleistophora* sp. infection in cultured sea bream (*Sparus aurata* L.) in Greece. Bull Eur Assoc Fish Pathol. 1998;18:19–21.

169. Álvarez-Pellitero P, Sitjà-Bobadilla A. *Cryptosporidium molnari* n. sp. (Apicomplexa: Cryptosporidiidae) infecting two marine fish species, *Sparus aurata* L. and *Dicentrarchus labrax* L. Int J Parasitol. 2002;32:1007–21.

170. Sitjà-Bobadilla A, Palenzuela O, Álvarez-Pellitero P. Light microscopic description of *Eimeria sparis* sp. nov. and *Goussia sparis* sp. nov. (Protozoa:Apicomplexa) from *Sparus aurata* L. (Pisces: Teleostei). Parasitol Res. 1996;82:323–32.

171. Salati F, Meloni M, Cau M, Angelucci G. Presence of *Contracaecum* spp. in teleosts cultured and fished in Sardinia. Vet Parasitol. 2013;196:382–7.

172. Sánchez-García N, Raga JA, Montero FE. Risk assessment for parasites in cultures of *Diplodus puntazzo* (Sparidae) in the western Mediterranean: prospects of cross infection with *Sparus aurata*. Vet Parasitol. 2014;204:120–33.

173. Holzer AS, Montero FE, Repullés A, Nolan MJ, Sitja-Bobadilla A, Álvarez-Pellitero P, et al. *Cardicola aurata* sp. n. (Digenea: Sanguinicolidae) from Mediterranean *Sparus aurata* L. (Teleostei: Sparidae) and its unexpected phylogenetic relationship with *Paradeontacylix* McIntosh, 1934. Parasitol Int. 2008;57:472–82.

174. Palacios-Abella J, Montero FE, Merella P, Mele S, Raga JA, Repullés-Albelda A. *Cardicola mediterraneus* n. sp. (Trematoda, Aporocotylidae): a new species infecting the gilthead seabream, *Sparus aurata* L., from the western Mediterranean Sea. Parasitol Res. 2021;120:1949–63.

175. World Register of Marine Species- WoRMS [Internet]. [cited 2024 May 15]. Available from: https://www.marinespecies.org/index.php

176. Littlewood DTJ. The evolution of parasitism in flatworms. In: Maule AG, Marks NJ, editors. Parasitic flatworms molecular biology, biochemistry, immunology and physiology. Wallingford: CABI Publishing; 2006. p. 1–36.

177. Brabec J, Salomaki ED, Kolísko M, Scholz T, Kuchta R. The evolution of endoparasitism and complex life cycles in parasitic platyhelminths. Curr Biol. 2023;33:4269-4275.e3.

178. Mazanec H, Bušková N, Gardian Z, Kuchta R. Secretion of extracellular vesicles during ontogeny of the tapeworm *Schistocephalus solidus*. Folia Parasitol (Praha). 2023;70:003.

179. Marcilla A, Trelis M, Cortés A, Sotillo J, Cantalapiedra F, Minguez MT, et al. Extracellular vesicles from parasitic helminths contain specific excretory/secretory proteins and are internalized in intestinal host cells. PLoS One. 2012;7:e45974.

180. Caña-Bozada V, Robinson MW, Hernández-Mena DI, Morales-Serna FN. Exploring evolutionary relationships within neodermata using putative orthologous groups of proteins, with emphasis on peptidases. Trop Med Infect Dis. 2023;8:59.

181. Peng S, Babcock LE, Cooper RA. The cambrian period. The Geologic Time Scale . Elsevier B.V.; 2012. p. 437–88.

182. World Register of Marine Species - WoRMS. Polyopisthocotylea [Internet]. [cited 2024 May 20]. Available from: https://www.marinespecies.org/aphia.php?p=taxdetails&id=119220

183. Kearn G, Whittington I. Sperm transfer in monogenean (platyhelminth) parasites. Acta Parasitol. 2015;60:567–600.

184. Ogawa K. Diseases of cultured marine fishes caused by Platyhelminthes (Monogenea, Digenea, Cestoda). Parasitology. 2015;142:178–95.

185. Gannicott AM, Tinsley RC. Egg hatching in the monogenean gill parasite *Discocotyle sagittata* from the rainbow trout (*Oncorhynchus mykiss*). Parasitology. 1997;114:569–79.

186. Repullés-Albelda A, Holzer AS, Raga JA, Montero FE. Oncomiracidial development, survival and swimming behaviour of the monogenean *Sparicotyle chrysophrii* (Van Beneden and Hesse, 1863). Aquaculture. 2012;338–341:47–55.

187. Villar-Torres M, Montero FE, Raga JA, Repullés-Albelda A. Come rain or come shine: environmental effects on the infective stages of *Sparicotyle chrysophrii*, a key pathogen in Mediterranean aquaculture. Parasit Vectors. 2018;11:558.

188. World Register of Marine Species - WoRMS. Sparicotyle chrysophrii (Van Beneden & Hesse, 1863) Mamaev, 1984 [Internet]. [cited 2024 May 20]. Available from: https://www.marinespecies.org/aphia.php?p=taxdetails&id=119770

189. Repullés-Albelda A, Raga JA, Montero FE. Post-larval development of the microcotylid monogenean *Sparicotyle chrysophrii* (Van Beneden and Hesse, 1863): comparison with species of Microcotylidae and Heteraxinidae. Parasitol Int. 2011;60:512–20.

190. Mladineo I, Šegvić T, Grubišić L. Molecular evidence for the lack of transmission of the monogenean *Sparicotyle chrysophrii* (Monogenea, Polyopisthocotylea) and isopod *Ceratothoa oestroides* (Crustacea, Cymothoidae) between wild bogue (*Boops boops*) and cage-reared sea bream (*Sparus aurata*) and sea bass (*Dicentrarchus labrax*). Aquaculture. 2009;295:160–7.

191. Mladineo I, Hrabar J, Trumbić Ž, Rasouli-Dogaheh S, Rigos G, Palenzuela O, et al. Mediterranean-wide transfer of the polypisthocotylean *Sparicotyle chrysophrii* between 2 wild sparids and farmed gilthead seabream (*Sparus aurata*) inferred by ddRAD loci. [Internet]. Available from: https://ssrn.com/abstract=4754187

192. Sánchez-García N, Ahuir-Baraja AE, Raga JA, Montero FE. Morphometric, molecular and ecological analyses of the parasites of the sharpsnout seabream *Diplodus puntazzo* Cetti (Sparidae) from the Spanish Mediterranean : implications for aquaculture. J Helminthol. 2015;89:217–31.

193. Farjallah S, Amor N, Garippa G, Montero FE, Víllora-Montero M, Mohamed OB, et al. Genetic variation of *Sparicotyle chrysophrii* (Monogenea: Microcotylidae) from the gilthead sea bream *Sparus aurata* (Teleostei: Sparidae) in the Mediterranean Sea. Parasitol Res. 2023;122:157–65.

194. European Chemicals Agency- ECHA. Formaldehyde and formaldehyde releasers- Strategy for future work [Internet]. 2018. Available from: https://echa.europa.eu/documents/10162/17233/formaldehyde_review_report_en.pdf/551df4a2-28c4-2fa9-98ec-c8d53e2bf0fc?t=1516270136797

195. European Chemicals Agency- ECHA. Substance Evaluation Conclusion as require by REACH Article 48 and Evaluation Report for Formaldehyde [Internet]. 2019. Available from: https://echa.europa.eu/documents/10162/cc0acabf-6e82-f2ed-5dbe-8058f48ce6c4

196. Leal JF, Neves MGPMS, Santos EBH, Esteves VI. Use of formalin in intensive aquaculture: properties, application and effects on fish and water quality. Rev Aquac. 2018;10:281–95.

197. Merella P, Montero FE, Burreddu C, Garippa G. In-feed trials of fenbendazole and other chemical/natural compounds against *Sparicotyle chrysophrii* (Monogenea) infections in *Sparus aurata* (Osteichthyes). Aquac Res. 2021;52:5908–11.

198. Sitjà-Bobadilla A, de Felipe MC, Álvarez-Pellitero P. *In vivo* and *in vitro* treatments against *Sparicotyle chrysophrii* (Monogenea: Microcotylidae) parasitizing the gills of gilthead sea bream (*Sparus aurata* L.). Aquaculture. 2006;261:856–64.

199. Rigos G, Glaropoulos A, Tzokas K, Gourzioti E, Kogiannou D, Golomazou E. A field evaluation of orally administered praziquantel against the gill fluke *Sparicotyle chrysophrii* infecting gilthead seabream (*Sparus aurata*). J Fish Dis. 2023;46:1439–43.

200. Rigos G, Fountoulaki E, Cotou E, Dotsika E, Dourala N, Karacostas I. Tissue distribution and field evaluation of caprylic acid against natural infections of *Sparicotyle chrysophrii* in cage-reared gilthead sea bream *Sparus aurata*. Aquaculture. 2013;408–409:15–9.

201. Rigos G, Mladineo I, Nikoloudaki C, Vrbatovic A, Kogiannou D. Application of compound mixture of caprylic acid, iron and mannan oligosaccharide against *Sparicotyle chrysophrii* (Monogenea: Polyopisthocotylea) in gilthead sea bream, *Sparus aurata*. Folia Parasitol (Praha). 2016;63:027.

202. Cabello-Gómez JF, Aguinaga-Casañas MA, Falcón-Piñeiro A, González-Gragera E, Márquez-Martín R, Agraso M del M, et al. Antibacterial and antiparasitic activity of propyl-propane-thiosulfinate (PTS) and propyl-propane-thiosulfonate (PTSO) from *Allium cepa* against gilthead sea bream pathogens in *in vitro* and *in vivo* studies. Molecules. 2022;27:6900.

203. Firmino JP, Vallejos-Vidal E, Sarasquete C, Ortiz-Delgado JB, Balasch JC, Tort L, et al. Unveiling the effect of dietary essential oils supplementation in *Sparus aurata* gills and its efficiency against the infestation by *Sparicotyle chrysophrii*. Sci Rep. 2020;10:17764.

Chapter 2

Objectives

The gilthead seabream (*Sparus aurata* Linnaeus, 1758) plays a significant role in Mediterranean and European aquaculture. However, *Sparicotyle chrysophrii* (Van Beneden and Hesse, 1863) infections pose considerable challenges to the welfare of these farmed animals and the industry's performance. The main objective of this thesis is to enhance our understanding of the interactions between *S. chrysophrii* and its host, as well as the biology of the parasite itself.

To achieve these goals, the following specific objectives are defined:

- To establish and maintain an in vivo infection of *S. chrysophrii* under experimental conditions that replicate the effects observed in naturally infected farmed gilthead seabream.
- To study the changes in the blood plasma proteome and identify the main altered biological processes involved in the pathogenesis of diseased gilthead seabream.
- To analyse goblet cell distribution patterns and their transcriptional regulation, and examine mucin expression and glycosylation in the gills of gilthead seabream in response to *S. chrysophrii*.
- To explore the differential role of immunoglobulins at local and systemic levels upon a primary and secondary response against *S. chrysophrii* infections.
- To demonstrate the haematophagous nature of *S. chrysophrii*, its role in causing blood loss in gilthead seabream, and the subsequent impact on their health.
- To identify and isolate *S. chrysophrii* extracellular vesicles, characterise their protein composition and identify potential prophylactic and therapeutic target candidates.

Chapter 3

Sparicotyle chrysophrii experimental infection of gilthead seabream (*Sparus aurata*): Establishment of an *in vivo* model reproducing the pathological outcomes of sparicotylosis

Enrique Riera-Ferrer, Raquel Del Pozo, M. Carla Piazzon, Ariadna Sitjà-Bobadilla, Itziar Estensoro and Oswaldo Palenzuela

Fish Pathology Group, Institute of Aquaculture Torre de la Sal (IATS, CSIC), Consejo Superior de Investigaciones Científicas, Castellón, Spain

Aquaculture, 30 August 2023
https://doi.org/10.1016/j.aquaculture.2023.739588

Abstract

Sparicotyle chrysophrii (Microcotylidae) is considered the most threatening pathogen affecting the gilthead seabream (GSB; *Sparus aurata*) farming throughout the whole production cycle due to its economic impact. This study explores the best experimental conditions to set up an *in vivo* infection model capable of mimicking the sparicotylosis signs observed in farmed diseased fish. The experimental setup for parasite transmission consisted of a recipient (R) fish tank with naïve GSB receiving water from two *S. chrysophrii*-infected donor tanks in a recirculating aquaculture system (RAS). Egg collectors, consisting of a polyester mesh in a supporting plastic frame, were placed in the R tank in order to monitor the progression of the parasitosis. An additional tank with control unexposed naïve fish was maintained in parallel, with open water flow and disconnected from the RAS. After a preliminary trial, infective pressure in the R tank was increased by placing an additional egg collector already loaded with entangled parasite eggs, and by maintaining the fish number throughout the experiment.

Adult *S. chrysophrii* parasite load correlated with most of the evaluated biotic and abiotic factors. Haemoglobin and haematocrit significantly dropped around 40 days after exposing GSB to *S. chrysophrii*. Furthermore, the abundance of eosinophilic granular cells and goblet cells in gill filaments, and splenic melanomacrophagic centres increased. In contrast, hepatic fat was depleted in *S. chrysophrii*-infected GSB. This study provides an advancement not only for studying *S. chrysophrii*'s biology and its interaction with its host, but also for further studying the disease under experimental conditions in search of treatment alternatives and prophylactic measures.

Introduction

Mediterranean aquaculture has notably diversified in the past decade. However, the gilthead seabream (*Sparus aurata*; GSB) remains the most farmed species in the area and ranks second among marine farmed fish in Europe[1,2]. Parasitic infections are a growing concern in mariculture[3], more specifically, monogeneans are among the most threatening ectoparasites in aquaculture due to their impact on economically relevant finfish species, including GSB[4–10].

Sparicotylosis is caused by *Sparicotyle chrysophrii* (Microcotylidae), a polyopisthocotylean monogenean infecting the gills of GSB. Sparicotylosis represents the number one health concern in GSB livestock units under off-shore farming conditions across the Mediterranean Sea[11,12]. This disease has been associated with lethargy due to hypoxia, severe anaemia and emaciation, and histopathological findings such as lamellar synechiae, clubbing and shortening, epithelial hyperplasia resulting in secondary lamellae fusion, and proliferation of chloride cells have been described[13–15].

This parasite has a direct life cycle, which can be divided into a resistance, an infective and a pathogenic stage (**Figure 1**). Bundles of entangled eggs shed by gravid adults into the water column constitute the resistance stage. These eggs get hooked on biofouling and fibrous surfaces such as the net pen lines[14] or on fish gill filaments. Eggs with fully developed embryos hatch when the egg operculum opens, releasing the oncomiracidia into the water column[16]. The infective stage, the oncomiracidia, are free-swimming larvae propelled by cilia and able to swim in both vertical and horizontal planes. This stage has a short lifespan, and larvae die if they do not encounter their type host within hours[16]. When oncomiracidia come across their host, they attach to the gill filaments and develop into post-larvae, which will locate between gill filaments in a proximal plane close to the branchial arch. Then, they will undergo several growth phases in which the development of the parasite's haptor and other vital structures, such as the pharynx and gut, takes place[17]. Post-larvae develop into juveniles, which entail the pathogenic stages. This stage has a minimally pigmented gut, lacks post-larval hooklets and uses its clamps to attach to the gill filaments, inflicting mechanical trauma to the branchial tissue. Juveniles develop into adults with a more heavily pigmented gut, and their pathogenic effect becomes more evident. Finally, gravid adults shed the eggs into the water column, closing the cycle. Many authors have highlighted that the monogenean's development is temperature-dependent, where high temperature plays a key role in speeding egg development, embryonation rates, shedding and hatching, and therefore, timings in the parasite's development may differ throughout the year[15,16,18–24].

Many aspects still remain obscure despite the scientific and technical efforts to better understand *S. chrysophrii*'s biology, the effects on its host, and to find possible treatment

alternatives and husbandry strategies to mitigate and prevent this disease[14,25–28].

Thus far, several attempts to keep *S. chrysophrii* in an *in vivo* model have been performed[15,29,30]. However, these models were not standardised and plausible later improvements in the methodology have not been addressed in scientific literature. *In vivo* experimental models are not only convenient for having a constant source of parasites to study their biology, the host-pathogen interactions and the impact on the host, but also for testing alternative treatments under *in vitro* conditions that can then be scaled up to *in vivo* models. The success of *in vivo* models is hampered by obtaining an initial source of naturally infected fish, usually harbouring concomitant infections, and only available seasonally.

The current study aims to determine the best experimental conditions to maintain an *in vivo* infection of *S. chrysophrii* in GSB, capable of mimicking the natural sparicotylosis signs observed in farmed GSB in terms of biometry, haematology and histopathology.

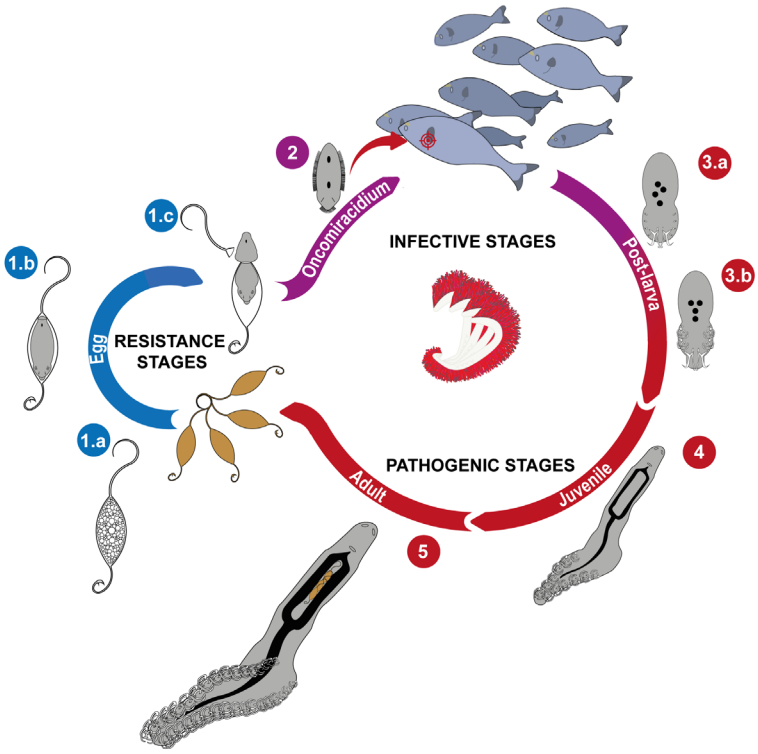

Figure 1. **Schematic representation of *Sparicotyle chrysophrii* life cycle. Resistance stage: 1.a:** Embryonated egg; **1.b:** Egg with a fully developed embryo and displaying a conspicuous operculum; **1.c:** Oncomiracidium hatching from the egg. **Infective stages: 2:** Free-swimming oncomiracidium searching for the gills of nearby gilthead seabream; **3.a:** Post-larval phase with haptoral posterior hooklets and hamuli and postero-lateral and lateral hooklets; **3.b:** Post-larval phase with hamuli, two pairs of clamps and anteriorly displaced hooklets; **4:** Juvenile stage (≤ 6 pairs of clamps and no hooks); **5:** Adult stage.

Materials and methods

Donor and recipient fish

In December 2019, GSB displaying growth arrestment and pale gills (n = 64) were harvested from commercial sea cages in the Western Mediterranean Sea and brought alive to the Fish Pathology facilities at the Institute of Aquaculture Torre de la Sal (IATS, CSIC). Upon arrival, a subsample of GSB (n = 10; 90 ± 14.4 g; mean weight ± SD) was euthanised by anaesthetic overexposure (MS-222, 0.1 $g \cdot L^{-1}$; Sigma-Aldrich, MO, USA), gill arches were dissected and checked under a stereomicroscope, and fresh smears were mounted and observed under a light microscope. Prevalence of infection in gills was 100 % for *S. chrysophrii*, 100 % for *Lamellodiscus echeneis*, 90 % for epitheliocystis and 80 % for lymphocystis. In the following months, these fish were allocated into two 500 L tanks (n = 32 each) with open water flow and parasite egg collectors (**Supplementary material: Figure S1**), consisting of a polyester mesh in a supporting plastic frame, placed in the tank. Donor (D) GSB were gradually euthanised, gill arches dissected, inspected under a stereomicroscope and *S. chrysophrii* adult specimens retrieved alive. The daily harvested worms were rinsed with filtered seawater and poured into two 200 L tanks with n = 20 healthy GSB each (82 ± 11.9 g; mean weight ± SD), held for up to three hours without water renewal. Additionally, *S. chrysophrii* eggs were retrieved from collectors, rinsed and poured into the same two tanks together with the *S. chrysophrii* harvest. GSB held in these tanks were subsequently used as D fish bearing the "purified" *S. chrysophrii* infection.

Naïve GSB juveniles used as unexposed control (C) and recipient (R) (details in **Table 1**), were purchased from a Mediterranean hatchery (Avramar, Burriana, Spain) and acclimatised to the indoor experimental facilities of IATS, CSIC under natural photoperiod and temperature conditions of the latitude (40°5′N; 0°10′E). Upon arrival, a subset of these animals was tested by microscopy, histology and molecular diagnosis for the absence of gill and intestinal parasites. Water parameters were monitored; oxygen saturation was kept above 85 %, and unionised ammonia below 0.02 $mg \cdot L^{-1}$ in all tanks.

All experiments were carried out according to current Spanish (Royal Decree 53/2013) and EU (Directive 2010/63/EU) legislation on the handling of experimental fish. All procedures were approved by the Ethics and Animal Welfare Committee of the Institute of Aquaculture Torre de la Sal (IATS, CSIC, Castellón, Spain), CSIC and "Generalitat Valenciana" (permit number 2018/VSC/PEA/0240).

Experimental set-up: Parasite transmission

Two experimental infection trials were conducted in a recirculating aquaculture system (RAS). The first trial (T1) was a preliminary approach, and in light of its infection outcome, modifications were carried out to standardise the experimental setup in the second trial

(T2). The core common experimental setup consisted of an R fish tank (200 L) with naïve GSB receiving water from two D tanks (200 L) in a closed recirculation water flow. An additional tank with C unexposed naïve fish, was maintained in parallel, with open water flow (i.e., disconnected from the RAS but under the same temperature and oxygen conditions). A clean and empty egg collector was placed in the R tank in T1 and T2 to register the egg production and drift in the RAS on a weekly basis, as described in detail in the following section- Egg shedding monitoring.

T1 was performed in winter 2020/21 (November- January) using R GSB receiving effluent water from D tanks. Fish were periodically sampled (**Table 1**) and after each sampling, euthanised R fish were not replaced; therefore, the biomass in the R tank decreased along the trial. T2 took place in spring 2021 (April-May) using smaller R GSB, individually tagged with passive integrated transponders (ID-100A/1.4 Mini transponder, Trovan, Spain) and receiving effluent water from D tanks. A collector, harbouring 388 *S. chrysophrii* eggs obtained from a D tank, was placed into the R tank to increase the infective pressure. In addition, after each sampling, removed R were replaced by adding the same number of D to the R tank. Consequently, in T2, as the GSB number in the R tank remained constant, biomass increased due to growth, and the infective pressure by tank cohabitation was maintained throughout the experiment. Details on both trials are included in **Table 1**.

Table 1. Details on *S. chrysophrii* experimental infections in gilthead seabream Trial 1 (T1) and Trial 2 (T2).

	T1			**T2**		
Period	Nov 2020-Jan 2021			April 2021-May 2021		
Water temperature range (°C; initial → final)	17.60 → 11.50			16.00 → 23.40		
Water temperature (°C; mean ± SD)	15.61 ± 2.66			20.42 ± 2.18		
Daily water temperature variation (°C; mean ± SD)	1.40 ± 0.90			1.05 ± 0.32		
Photoperiod (h; light : dark; initial → final)	10 : 14			13 : 11 →14: 10		
Initial weight (g; mean ± SD)	118.50 ± 11.90			20.22 ± 3.04		
Initial length (cm; mean ± SD)	16.30 ± 0.45			9.35 ± 0.44		
Final weight (g; mean ± SD)	157.30 ± 10.25			43.20 ± 5.28		
Final length (cm; mean ± SD)	18.20 ± 0.46			12.10 ± 0.56		
Samplings (dpe)	0, 11, 20, 32, 41, 61, 81			0, 14, 28, 42, 50, 58		
Fish groups	C	R	D	C	R	D
Fish number	23	28	40	20	28	52

Abbreviations: C: control; **R:** recipient; **D**: donor; **SD:** standard deviation; **dpe**: days post-exposure.

Egg shedding monitoring

In both trials, *S. chrysophrii* egg shedding from experimentally infected GSB and its successful drift through the RAS was monitored using a custom-made device modified from the egg quantifying method previously described by Buchmann[31] and Merella et al.[27] and named "egg collector". Clean 12 cm in diameter plastic frames holding a polyester mesh (pore size = 4 mm^2), a hook, and a sinker (**Supplementary material: Figure S1**) were submerged in R tanks. These collectors were temporarily removed and checked under a stereomicroscope every 7 days in both trials. Ten random fields at 2.5x magnification, corresponding to a total polyester-mesh surface of 18 cm^2, were checked, and the number of entangled eggs per cm^2 was determined.

Samplings and parasite diagnosis

Five C were sampled at 0 days post-exposure (dpe), whereas 3 C and 5 R were sampled during the following sampling points (**Table 1**), except at 81 dpe in T1, when only 3 R were sampled. In each sampling, GSB were euthanised by tricaine methanesulfonate (MS-222; Sigma-Aldrich, MO, USA) overexposure (0.1 $g{\cdot}L^{-1}$). Individual biometric data was registered, and GSB were bled from the caudal vein using heparinised syringes. Haemoglobin (Hb) values were immediately measured (HemoCue® Hb 201+ AB, Ängelholm, Sweden), and haematocrit (Hct) values were determined by standard microhematocrit capillary centrifugation in a haematocrit centrifuge (myLab HC-01, AHN®, Germany) at 10,000× *g* for 10 min.

The four right-sided gill arches of each R fish were dissected to carry out in situ juvenile, and adult *S. chrysophrii* counts under a stereomicroscope to determine the infection intensities. These counts were extrapolated for the 8-gill arches of each GSB according to Riera-Ferrer et al.[32]. The left gill arches, head kidney, spleen and liver samples were fixed in Bouin's solution and processed for routine paraffin histology.

Histopathology

Tissue sections (4 µm-thick) were stained with Giemsa, haematoxylin and eosin (H/E), or periodic acid-Schiff stain (PAS) and observed under a Leitz Dialux 22 light microscope (Leica, Hesse, Germany) connected to a digital Olympus DP70 camera (Olympus, Tokyo, Japan). Relevant histopathological findings determined in the preliminary T1 were analysed in depth in T2 and registered according to the following semiquantitative scoring criteria. The abundance of eosinophilic granular cells (EGCs) and goblet cells in gills was scored ranging from 0 (absence) to 3 (very abundant, meaning 25-30 cells/microscope field at 500× magnification). In liver sections, lipid and glycogen storage was scored from 0 (absence) to 3 (pervasive) by Giemsa or PAS staining, respectively. The abundance of

melanomacrophage centers (MMCs) was estimated in the spleen according to a semi-quantitative scale ranging from 0 (absence) to 3 (very abundant).

Statistical analysis

A Spearman's rank correlation coefficient test was run with the corrplot R package[33] to identify the experimental setup parameters significantly affecting parasite transmission in T2. The correlation analysis included infection intensity (total, juvenile and adult parasite load·fish^{-1}) and egg counts in collectors versus biotic and abiotic factors: weight, length, condition factor (CF) and biomass, haematological parameters (Hb, Hct), dpe and daily mean water temperature.

Mean data of haematological parameters, mean infection intensity, and histological scorings were compared among samplings within each experimental group (C or R) for each trial by One-way ANOVA, followed by Student-Newman-Keuls post-hoc test. Normality of the data was checked by Shapiro-Wilks test and homogeneity of variances by Brown-Forsythe test. When normality was not met, Kruskal-Wallis on ranks followed by Dunn's method was used instead. Differences between C and R groups were determined by Student's t-test or Mann-Whitney test when normality was not met. Differences were considered significant at a $p < 0.05$. These statistical analyses were carried out using SigmaPlot v14.5 software (Systat Software Inc., San Jose, CA, USA).

Results

Infection outcome

Sparicotyle chrysophrii infection was first confirmed after 11 and 14 dpe in T1 and T2, respectively. Initially, juvenile *S. chrysophrii* stages (≤ 6 pairs of clamps) were predominant and later on, at 32 dpe (T1) and 28 dpe (T2), adult *S. chrysophrii* stages appeared and became predominant over juveniles (**Figure 2**). Furthermore, the infection prevalence in both trials was 100 % for R fish in all sampling points. Juveniles were mostly found in a proximal plane, closer to the gill arch cartilage. In contrast, adults were located in a distal plane within the gill arches, closer to the gill filament apices (**Figure 3A**, **B**). In both trials, Hb values of R dropped dramatically compared to C around 40 dpe, (**Figure 4A**, **B**), after the increase of *S. chrysophrii* adult counts in gills. In both trials, the haemoglobin drop was sustained after 40 dpe, though more severe in T2, where significant differences were more robust. A concurrent drop of Hct at 42 dpe was observed only in T2, and became significant at 50 dpe. In T1, a non-significant decrease of haematocrit was found from 32 dpe onwards, and became significant only at 61 dpe (**Figure 4C**, **D**). Three mortalities were registered in T2 at 38, 42, 47 dpe, respectively.

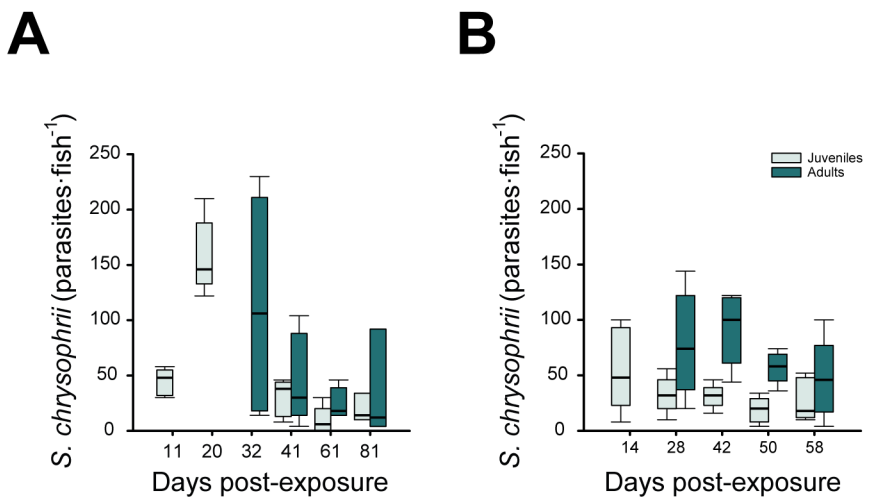

Figure 2. Boxplot representing *Sparicotyle chrysophrii* infection intensity. A: Trial 1, **B:** Trial 2. Infection intensity is represented for juveniles and adults separately.

Egg shedding monitoring

The egg collectors proved to be very convenient for the evaluation of *S. chrysophrii* eggs circulating in the RAS. The peak of *S. chrysophrii* egg counts was observed at 35 dpe in T2, 14 days before eggs peaked in T1 (**Figure 5**).

Correlation analysis

The correlation analysis showed that adult parasitic infection intensity and total parasite load significantly correlated with most biotic and abiotic factors. In particular, adult parasite load was positively correlated with exposure time (dpe), average water temperature, fish biometric parameters and biomass in tanks. It also negatively correlated with the haematological parameters (**Figure 6**). Juvenile parasitic infection intensity, on the other hand, presented fewer significant correlations with any of the examined variables.

Histopathological Response

In T2, from 28 dpe on, R gills showed a statistically significantly higher abundance of EGCs infiltrating the gill lamellae than C gills (**Figure 7C-H**; **Figure 8A**). These granulocytes were also observed along the gill filament, in/around blood vessels and sometimes degranulated. Occasionally, melanomacrophages were found in R gills (**Figure 7E**). Goblet cell abundance in R gills was also statistically significantly higher than in C from 42 dpe on (**Figure 7I-J**; **Figure 8B**). Some filaments of R gills presented signs of mucosal inflammation or lamellar clubbing and synechiae, as shown in **Figure 3C**, **E** and **Figure 7C**, **F**, **G**. Goblet cell and EGC presence, though statistically significantly increased upon infection, was dispersed throughout the gills and could not be specifically related with *S. chrysophrii*

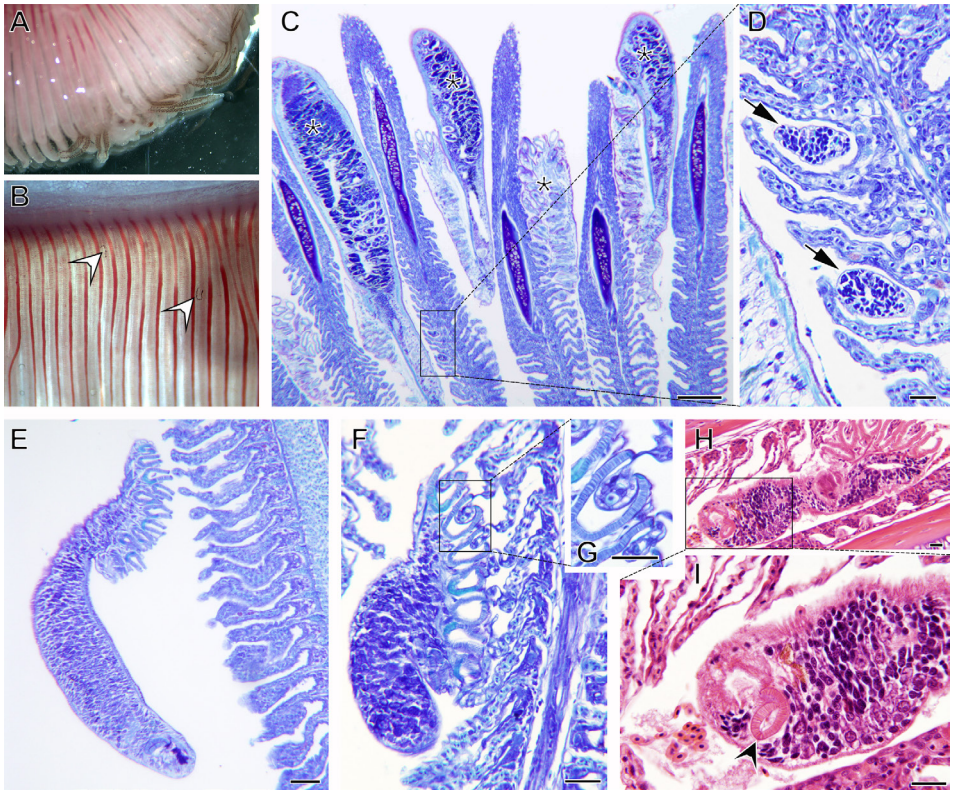

Figure 3. *Sparicotyle chrysophrii* microphotographs. A: Fresh gills under the stereomicroscope showing adult parasite stages close to the filament apices. **B:** post-larvae and juveniles close the arch cartilage (white arrow heads). **C:** Histological section of adult specimens (asterisks; *****) close to filament apices. **D:** Note the presence of two juveniles magnified in (black arrows). **E:** Adult specimen close to gill lamellae presenting some clubbing. **F:** Section of the parasite haptor attached to gill lamellae. **G:** Note how clamps pinch secondary lamellar tips, which appear abraded and weakened, magnified in. **H:** Longitudinal section of an adult specimen between gill filaments including its head segment. **I:** Note the maginified details of the oral suckers (black arrowhead) and the proximity of red blood cells. **C-G:** Giemsa-stained sections. **H-I:** H/E-stained sections. Scale bars = 20 µm, except in (**C**) = 200 µm.

attachment or *S. chrysophrii*-inflicted lesions (**Figure 3**). Epitheliocystis, a disease caused by secondary bacterial infections, appeared in R gills in both trials: from 61 dpe (T1) and from 42 dpe (T2) on (**Supplementary material: Figure S2**). The signs consisted of cysts in gill epithelia, some surrounded by epithelial proliferation with squamous metaplasia, which promoted the fusion of secondary lamellae. Besides the parasite's target organ, lipid storage in the liver statistically significantly decreased in R along the course of the trials, but was especially remarkable in T2 from 28 dpe on (**Figure 7K**, **M**; **Figure 8C**), whereas glycogen storage did not significantly vary (**Figure 7L**, **N**). Furthermore, abundance of splenic MMCs was statistically significantly higher in R (**Figure 7P**, **R**; **Figure 8D**). Details shown in **Figure 7O** and **7Q** evidence smaller and less dense splenic MMCs with dispersed melanin granules in C. When data from all samplings were grouped regardless

of the exposure time to the parasite, the summary histopathological differences between C and R GSB were: R presented statistically significantly more EGCs (R: 0.52 ± 0.08; C: 0.10 ± 0.05; mean ± SEM); more goblet cells (R: 1.54 ± 0.12; C: 0.76 ± 0.07; mean ± SEM); less fat depots in the liver (R: 2.40 ± 0.12; C: 1.14 ± 0.12; mean ± SEM); and more splenic MMCs (R: 1.98 ± 0.11; C: 1.55 ± 0.15; mean ± SEM) than C (**Supplementary material: Figure S3**). No significant alterations were found in the head kidney.

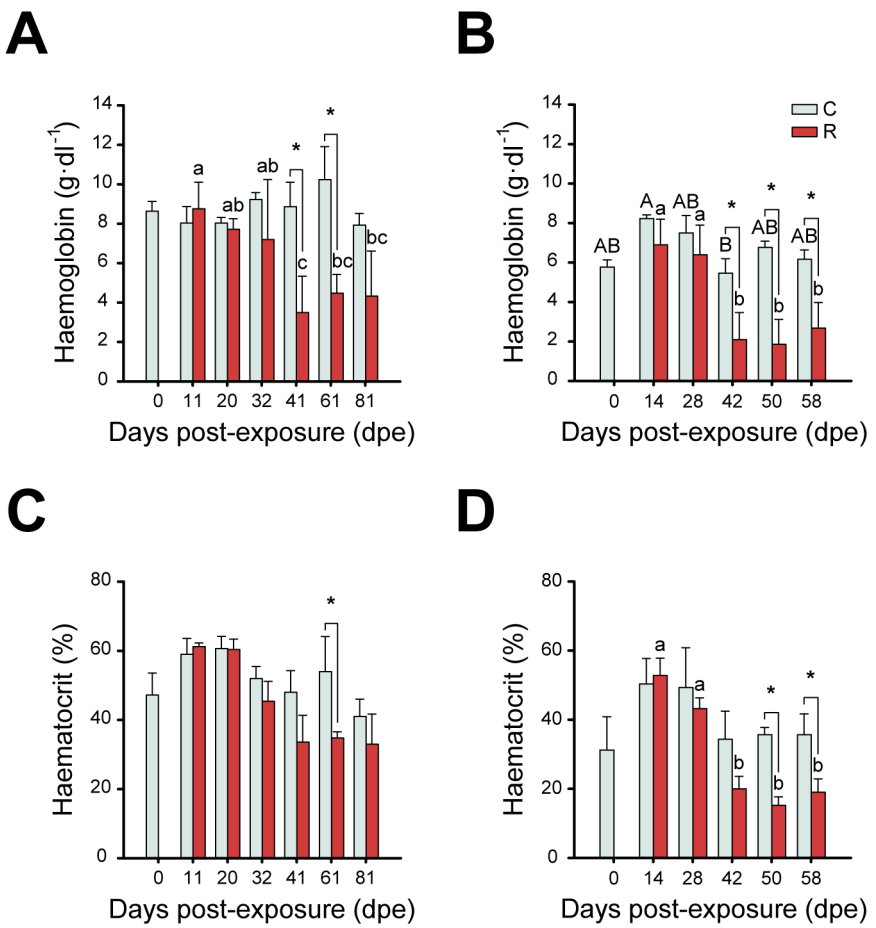

Figure 4. A, C: Haemoglobin and haematocrit (mean + SEM) in control (C) and recipient (R) gilthead seabream in Trial 1 throughout the experimental infection. **B, D:** Haemoglobin and haematocrit (mean + SEM) in control (C) and recipient (R) gilthead seabream in Trial 2 throughout the experimental infection. Different uppercase and lowercase letters stand for statistically significant differences within C or R groups, respectively. Asterisks (*) indicate statistically significant differences between C and R groups within each sampling point ($p < 0.05$).

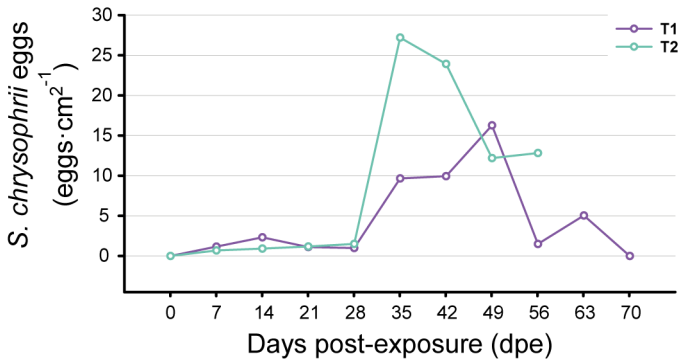

Figure 5. Monitoring of *Sparicotyle chrysophrii* eggs (eggs/cm^2) in the egg collector throughout experimental Trials 1 and 2.

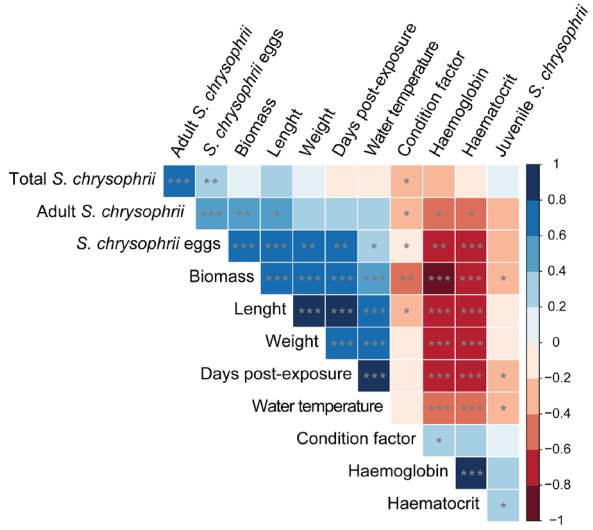

Figure 6. Correlation matrix of parameters affecting *Sparicotyle chrysophrii* experimental transmission in Trial 2. The colour gradient represents the correlation coefficient between variables. ***p*** values are shown by asterisks (*: $p < 0.05$, **: $p < 0.01$, ***: $p < 0.001$).

Discussion

The current study has shown the successful experimental *in vivo* infection model, replicating the signs associated with clinical sparicotylosis in farmed GSB in a RAS environment. Prevalence of infection in experimental fish was 100 % at all sampling times in both trials. Along the trials, several variables were monitored. The correlation analysis showed that one cluster of variables comprised of water temperature, exposure time, biomass, length and weight had a positive correlation with adult *S. chrysophrii* infection intensity, highlighting that the parasitic transmission was favoured by increasing temperature, higher biomass in R tanks and larger R fish (**Figure 2B**). A second cluster related to the

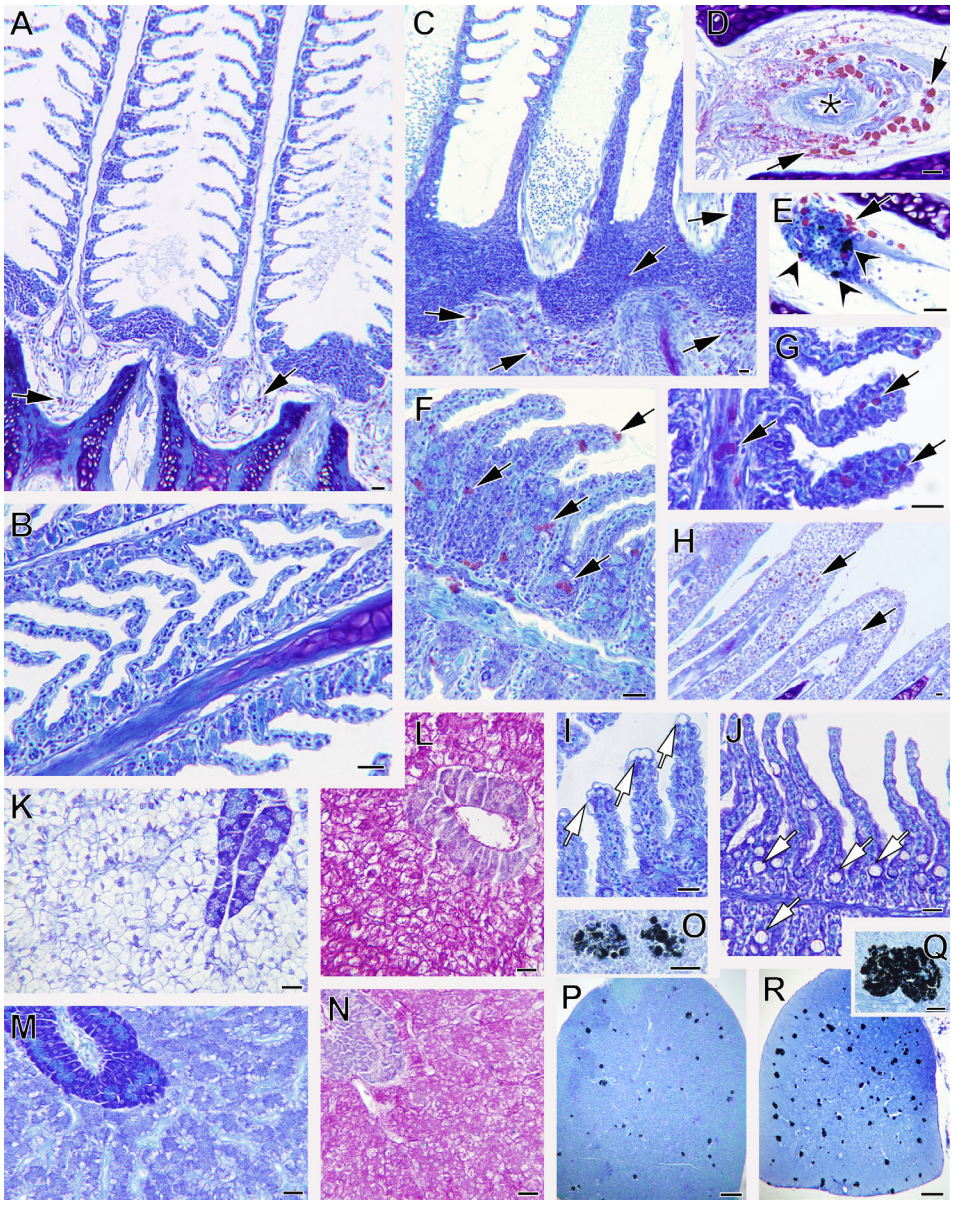

Figure 7. Histological alterations found in GSB experimentally exposed to *Sparicotyle chrysophrii* in Trial 1 and Trial 2. A, B: Control gill sections. **K, L:** Control liver sections. **O, P:** Control spleen sections. Control sections are shown for comparison. **C:** Higher abundance of eosinophilic granular cells-EGC (black arrows) is observed in infected gills, among inflammatory infiltrates at the base of the filaments. **D:** EGC (black arrows) infiltrated around efferent arteries (asterisk; *****) with apparent degranulation. **E:** EGC (black arrows) together with melanomacrophages (black arrowheads). **F, G:** EGC (black arrows) infiltrated in the epithelium of primary and secondary lamellae. **H:** EGC (black arrows) infiltrated in filament tips. **I:** Goblet cell (white arrows) hyperplasia was observed in the tips. **J:** Goblet cell (white arrows) at the base of secondary lamellae in infected fish. **K:** Liver sections of control fish present the usual fat in hepatocytes (colourless in the section). **L:** Liver sections of control fish present the usual glycogen deposits in hepatocytes (magenta). **Continued on the next page.**

Figure 7. (Continued). M: Note the severe lipid absence in hepatocytes of infected fish. **N:** Glycogen remains unchanged in infected fish. **O, P:** Spleen section of control fish presents small melanomacrophage centres (MMCs) with dispersed melanin granules. **Q, R:** Note the higher abundance of MMCs in the spleen of infected fish with densely packed melanin granules. All sections are stained with Giemsa, except (**L**) and (**N**) stained with PAS. All scale bars = 20 µm, except in (**O**) and (**Q**) scale bars = 200 µm.

pathogenic effect of the parasite, including the condition factor, and haemoglobin and haematocrit variables, had a negative correlation with adult *S. chrysophrii* infection intensity, reflecting the signs of sparicotylosis described for diseased farmed GSB, namely anaemia and emaciation[13–15].

The establishment of an *in vivo* model for parasite maintenance provides researchers with an unlimited source of parasites for further studies regarding the parasites' biology, opening possibilities to develop *in vitro* culture methods. Moreover, *in vivo* models permit not only the study of the pathogenesis of the disease but also host-parasite interactions, immune response and *in vivo* assays on the efficacy of therapeutic candidates, including functional feeds, under controlled conditions[34,35].

Constraint factors for sparicotylosis transmission

Salinity, pH and water temperature are abiotic factors with an impact on the development of monogenean parasites. However, the latter is the most influencing factor[18–24]. In the past years, specific optimal temperatures regarding the embryonic development, hatching rate, oncomiracidial swimming behaviour and survival, and the development of the infective stages, as well as its thermal limits for survival, have been set for *S. chrysophrii*[16,17,24].

S. chrysophrii prolificacy and egg viability studies are lacking. However, the current study gives some insights into the possible effects of temperature on the prolificacy of this parasite. Although neither the adult parasitic burdens nor the overall egg counts (**Figure 5**, **Figure 2**) statistically differ between T1 and T2, slight differences in egg shedding patterns were noticed. Egg counts in the colder T1 initially increased at 35 dpe and sustained until they peaked at 49 dpe, whereas this occurred around 14 dpe earlier in the warmer T2, with a unique peak at 35 dpe (**Figure 5**). We suspect that warmer water temperature hastening the monogeneans' metabolism and development, including *S. chrysophrii*'s reproductive maturity[20] could have had an impact on the egg counts. This hypothesis would be supported by the fact that the number of *S. chrysophrii* eggs in the collectors was significantly and positively correlated with water temperature. In addition, the significant positive correlation between egg counts and *S. chrysophrii* adults (**Figure 6**) showed that collector monitoring was an optimal non-lethal tool for the survey of the infection in GSB, besides the role of the collector as a way to retain eggs in the R tanks, favouring oncomiracidia-fish encounters.

Biomass (animal density) has been regarded as a key factor for parasite establishment in host communities[36]. In T2, as the population size was kept constant, fish grew up along the trial, and the biomass in the tanks increased. The current transmission model seems to be highly dependent on biomass in the system (**Figure 6**), as adult *S. chrysophrii* burden and the egg counts were highly and significantly correlated with the biomass (**Figure 6**). This effect could be explained by an increase in the chances of oncomiracidia-fish encounters, as available gill surface of fish increases. Similarly, longer exposure times correlated

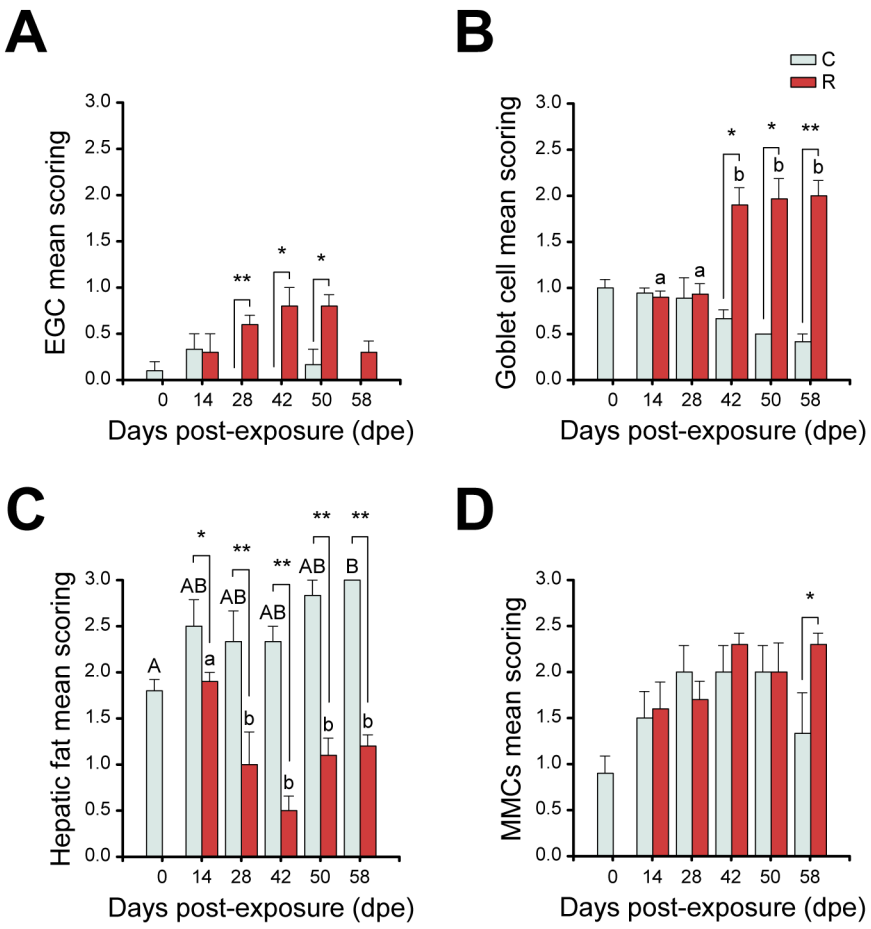

Figure 8. Scoring of histological alterations in control (C) and recipient (R) gilthead seabream through the experimental infection in Trial 2. A: Mean semiquantitative scoring (mean + SEM) from 0 (absence) to 3 (very abundant) is shown for eosinophilic granular cells (EGC) in gill filaments **B:** Mean semiquantitative scoring (mean + SEM) from 0 (absence) to 3 (very abundant) is shown for goblet cells in gill filaments. **C:** Mean semiquantitative scoring (mean + SEM) from 0 (absence) to 3 (very abundant) is shown for hepatic fat storage. **D:** Mean semiquantitative scoring (mean + SEM) from 0 (absence) to 3 (very abundant) is shown for melanomacrophage centres (MMCs) in spleen. Different uppercase o lowercase letters stand for statistically significant differences within C or R groups, respectively, $p < 0.05$. Asterisks indicate statistically significant differences between C and R groups within the same sampling point, (*****) $p < 0.05$ and (******) $p < 0.001$.

positively with egg counts as chances for reproduction and egg entangling increased over time, favouring parasite transmission.

Surprisingly, the correlation outcome of juvenile and adult counts vastly differed. In the current experiment, numbers of *S. chrysophrii* juveniles correlated negatively with both water temperature and biomass (**Figure 6**). Future experimental infections under same conditions will evidence if these findings, are in fact, a common trend. However, increasing temperature favours embryonic development and egg hatching rates and these observed negative correlations might be explained by the observations from Villar-Torres et al.[24], where a decrease in the swimming activity and survival rate in *S. chrysophrii* oncomiracidia was observed with increasing temperatures from 10°C to 26°C, resulting in a lesser ability to infect hosts. However, this negative correlation could also be explained by a type II error in the diagnosis procedure, due to excessive gill mucus discharge and the poor and friable conditions of gills from diseased GSB, which hampered their detection under the stereomicroscope and/or favoured their detachment, but further evidences are needed. In any case, the results of juvenile *S. chrysophrii* burden certainly altered the expected results for the total *S. chrysophrii* counts correlations. These results stress out the importance of adult and egg counts for the monitoring of this disease, with the current knowledge and available techniques.

Pathogenic effect of *Sparicotyle chrysophrii*

Polyopisthocoltylean monogeneans have been described as haematophagous parasites[37,38]. In the past years, a negative impact of *S. chrysophrii* on its hosts' haemostasis has been observed under experimental conditions[13,15,39], and it has been suggested that the parasite causes anaemia by branchial tissue disruption inflicted by the parasite's haptoral clamps[40]. Recently, the haematophagous nature of *S. chrysophrii* has been experimentally demonstrated[41], and it has been suggested that this parasite could cause an haemolytic anaemia in its host[13]. Either way, anaemia caused by haemorrhages and/ or by haemolytic events would group into regenerative anaemia, as supported by the findings in previous studies[15] where an increase in reticulocyte counts in diseased GSB was observed after 8 weeks of parasite exposure.

In the present study, Hb and Hct were significantly and negatively correlated with counts of *S. chrysophrii* adults (**Figure 6**). Regardless of the trial conditions, a significant drop in haemoglobin was registered in R at 41 and 42 dpe (**Figure 4A**, **B**), 9 to 14 days after the detection of adult *S. chrysophrii* stages (**Figure 2**), and a sustained significant drop in Hct was also registered in T2 (**Figure 4C**, **D**).

The head kidney is the main erythropoietic organ of teleost, while the spleen mainly acts as an erythrocytic reservoir[42,43] supplying erythrocytes to the circulation after a splenic

contraction when oxygen-deficient conditions take place[44–46]. Additionally, erythropoietic activity has been described as a physiological process strongly modulated by hypoxic events such as high-water temperature and low dissolved oxygen (strongly correlated parameters)[43,47]. Severe damage to the gills due to the parasite, such as lamellar synechia, clubbing, shortening and/or secondary lamellar fusion, as evidenced in this work and in previous studies[15] certainly compromise oxygen exchange and could, therefore, mask anaemia identification in diseased GSB when Hct is the only haematological parameter being monitored. Moreover, the impact of adult *S. chrysophrii* on the larger T1 fish was lower than on the smaller juveniles of T2 (**Figure 4**, **5**), which coincides with field observations in affected farms (authors' observations). The importance of fish size/age probably not only relies on the difference in total blood volume, being greater in adults, and on the potential erythrocytic reservoir held in the adult spleen, as well as on the ability to enable a faster erythropoietic response[45,46], but also on the higher susceptibility to hypoxia in smaller sized fish, worsening the clinical outcome[48].

Juvenile *S. chrysophrii* burden, contrary to adult burden, had a positive correlation trend with haematological parameters (**Figure 6**), evidencing that these stages have a minor impact on their host's haemostasis, if any. In any case, post-larval and juvenile histophagous feeding strategies proposed by other authors[40] cannot be disregarded.

The negative significant correlation of the CF with adults, eggs and even total parasite counts further evidenced the emaciative syndrome provoked by the disease and the poor health status of parasitised GSB under the anaemic condition previously described.

Histopathological findings

Eosinophilic granular cells (EGCs) are a cell type described to be involved, among others, in host defence against gill parasites[49,50] as part of the innate immune response in teleost fish, which is involved in inflammatory induction, vasodilation, neutrophil recruitment and macrophage activation[50]. Despite it has been suggested that GSB has a resident population of EGCs throughout the loose connective tissue of the gill arch and filaments[51], our study shows a significant increase of this cell type in R gills at 28 dpe (**Figure 8A**), when adult *S. chrysophrii* worms first appeared in R, and most probably induced by the gill tissue disruption provoked by the parasites' haptoral clamps (**Figure 3F**). Similar observations have been noted in GSB infected by other class gill parasites[52], and also in other monogenean infections affecting different host species[53]. Amongst EGC populations of GSB, the acidophilic granulocytes are considered functional equivalents of the mammalian neutrophils, being the predominant cell type recruited during immune responses[54,55] in accordance to our observations. The triggering of a local pro-inflammatory immune response arbitrated by acidophilic granulocyte degranulation during sparicotylosis was

previously highlighted by transcriptomic data[56].

Goblet cell hyperplasia was observed in the gills of infected fish from 42 dpe on, coinciding with the prevailing adult parasitic stages. The protective mucus layer of mucosal epithelia is synthesised by goblet cells. Gill mucus hypersecretion is common upon monopisthocotylean infections in maricultured fish[57], and goblet cell hyperplasia in response to gill parasitosis has been associated with an increased mucus secretion for preservation of the epithelial integrity, prevention of secondary infections and osmoregulatory failure after tissue damage[58]. Dietary immunostimulation against *Neobenedenia girellae* in greater amberjack (*Seriola dumerili*) and against *S. chrysophrii* in GSB demonstrated that more immunocompetent fish relied on up-regulation of mucin genes, the main components of the mucus secretion, and increase of goblet cell number with shift in the glycosylation profile of their mucins, respectively[56,59]. Involvement of goblet cell and mucin modulation in the local mucosal response of GSB against *S. chrysophrii* seems evident in the light of the current results, and could have worm-trapping and expulsion purposes as described for intestinal helminthiases in teleosts[53]. Interestingly, goblet cell hyperplasia became evident after the first month of parasite exposure, apparently triggered by the more pathogenic adult specimens.

Epitheliocystis, was found in the gills of R from 61 dpe on (T1) and from 42 dpe on (T2). This is a disease caused by pathogenic intracellular bacteria in a wide range of fish species, whose pathogenic agents are species-specific and opportunistic, and develops and progresses under environmental or pathological stress conditions[60]. Co-infection of *S. chrysophrii* and epitheliocystis has been previously reported[15,61], but attempts to characterise the causative agents point to complex bacterial associations of β-proteobacteria and chlamydial agents[62,63]. In the current study, epithelial cysts with and without a proliferative tissue response around them were found and lead to lamellar fusion (**Supplementary material: Figure S2**), in agreement to a previous description in GSB[64]. The effect of *S. chrysophrii* on the gill microbiota through clamp erosion and lesions on the mucosal surface or through the excretory/secretory products of the parasite is far from being understood, and further research efforts should focus on the interaction between this parasite and secondary infections, in particular, how the mucosal microbiota in GSB gills is modulated during sparicotylosis.

Melanomacrophage centres (MMCs) correspond to melanomacrophage (MMs) aggregations, phagocytes with high melanin, haemosiderin and lipofuscin content located in the stroma of haematopoietic and lymphoid tissues, mainly in the kidney and spleen of teleost fish[65–69]. Multiple non-immunological and immune roles have been ascribed to MMCs[67]. The primary functions of MMs have been suggested to be phagocytosis, detoxification/ debris clearance (catabolism of erythrocytes), iron recycling, and long-

term storage of either endogenous or exogenous highly indigestible or toxic material[66,67,70–72]. Recently, MMCs have been suggested to be the evolutionary precursors of mammalian germinal centres, key in the differentiation and clonal expansion of memory B cells[67,73,74]. In this study, MMCs abundance was significantly higher in R than in C (**Supplementary material: Figure S3 D**), especially at 58 dpe (**Figure 8D**). Furthermore, MMCs in R appeared to be larger in size and more dense (**Figure 7O-R**), results which are in line with those obtained by De Vico et al.[75] . Moreover, the high catabolism of erythrocytes damaged by haemolytic anaemia, as previously suggested by Riera-Ferrer et al.[13] would explain the higher haemosiderin-iron content in splenic MMCs reported by De Vico et al.[75] during sparicotylosis. Even more interesting is the suggested role of MMCs in the onset of adaptive immune responses[76], which would explain the increase in MMCs abundance observed in this study in R. In this context, *S. chrysophrii* triggered activation of B cells upon infection in a previous study[77] suggesting a specific immune response with a probable shift of the immunoglobulin repertoire described by Riera-Ferrer et al.[13].

The emaciation provoked by sparicotylosis was evidenced by a reduction of lipid deposits in the liver (**Figure 7K-N**; **Figure 8C**; **Supplementary material: Figure 3S C**), and likely reflects compensation for the disease's high energy costs with depletion of hepatic lipid storage as an energy source. Similar observations were previously registered during the course of a parasite-induced enteritis in GSB, which impaired nutrient absorption[78]. Thus, lipid storage in the liver of GSB seems a good indicator of health condition. In addition, *S. chrysophrii* feeding on its host's lipid reservoir is plausible, as suggested by the hypocholesterolaemia and plasmatic depletion of very low-density and low-density lipoproteins[13] and by the fact that platyhelminths are unable to synthesise fatty acids de novo[79]. Other studies have reported dependence on the host lipid content for immune evasion by the digenean trematode *Schistosoma mansoni*[80] or for modulation of the host's immune system by the monogenean *Eudiplozoon nippocum*[81,82]. Hepatic fat depletion has been related with deriving low-density and high-density lipoproteins for the maintenance of erythrocytic membrane stability[83], which might also be affected in *S. chrysophrii*-infected GSB. The normal presence of hepatic glycogen in our samples (**Figure 7M-N**) suggests that *S. chrysophrii* is not reliant on glycogen as a source of energy, as previously suggested for the monogenean *Diclidophora merlangi*, which would obtain its energy from aerobic respiration rather than from glycogen reservoirs from their hosts[84].

S. chrysophrii's demand for oxygen would, in turn, explain the location of adult *S. chrysophrii* specimens within the gills, close to the gill filament apex and downstream in the ventilating water flow (**Figure 3A**, **C**), and could additionally be supplemented by oxygen in the ingested blood meal, as suggested by Houlihan and Macdonald[85] in *D. merlangi*. Post-larval and juvenile *S. chrysophrii* specimens are, however, placed close to

the branchial arches in the secondary interlamellar spaces (**Figure 3B**, **D**), most probably due to an underdeveloped opisthaptor or lower numbers of clamps as this location may provide better shelter from water currents and detachment.

Conclusions

The proposed in vivo transmission model enables the maintenance of *S. chrysophrii* under experimental conditions, being temperature and biomass the most critical parameters. This model allows to achieve those pathological effects and parasite loads described in farmed GSB, and therefore opens the door to test treatment alternatives under experimental conditions. In addition, the use of egg collectors proved to be a reliable non-lethal tool to monitor the progression of the parasitosis without the need of handling or euthanising fish, therefore contributing to the 3R strategy in experimental animal procedures.

Funding

This work has been financed by the Spanish Ministry of Science and Innovation and Universities to the project SpariControl (RTI2018-098664-B-I00, AEI/FEDER, UE) and by the Spanish Ministry of Science and Innovation with funding from European Union NextGenerationEU project (ThinkInAzul, PRTR-C17·I1) and from Generalitat Valenciana to the project REMEDISA-PARASITE (GVA-THINKINAZUL/2021/022). ERF was supported by an FPI contract PRE2019-087409 (MCIN/AEI/10.13039/501100011033). MCP was funded by a Ramón y Cajal Postdoctoral Research Fellowship (RYC2018-024049-I & ACOND/2022 Generalitat Valenciana). RDP was contracted under the PTA Programme from the Spanish Ministry of Science, Innovation and Universities (PTA2018-015315-I). IE was funded by contracts from the Ministerio de Ciencia e Innovaci´on and Generalitat Valenciana, Spain. ERF, MCP and RDP contracts were co-funded by the European Social Fund (ESF). We acknowledge support of the publication fee by the CSIC Open Access Publication Support Initiative through its Unit of Information Resources for Research (URICI).

Acknowledgements

The authors thank Dr. P. Merella for the suggestions provided for the construction of ***S. chrysophrii*** egg collectors. Further thanks to J. Monfort and L. Rodríguez for their technical assistance on the histological processing and I. Vicente for the technical assistance with fish husbandry and samplings at IATS.

Supplementary material

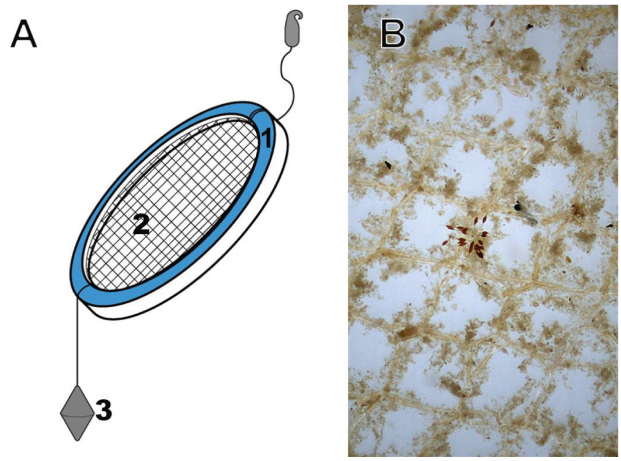

Figure S1. A: *Sparicotyle chrysophrii* egg collector consisting of a supporting plastic frame (1), polyester mesh (2) and sinker (3). **B:** Polyester mesh under the stereomicroscope with entangled *S. chrysophrii eggs*.

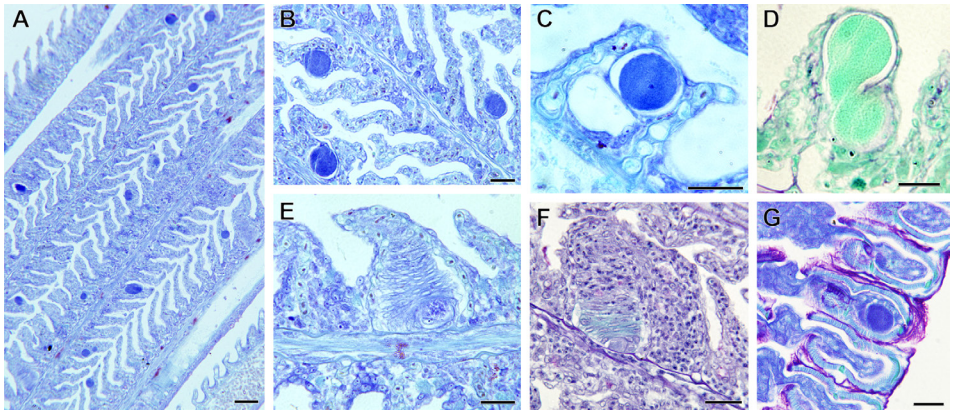

Figure S2. Epitheliocystis secondary infection in gills of gilthead seabream experimentally exposed to *Sparicotyle chrysophrii* for 42 days. A: Gill overview with severe epitheliocystis infection. **B-D:** Epithelial cysts with absence of tissue response. **C:** Beginning of lamellar fusion. **D:** Membrane surrounding cyst with PAS+ (magenta) reactivity. **E, F:** Proliferative epithelial response with squamous metaplasia around cysts. Note the coarser granular cyst content in (**E**). Note the slight acidophilia in the squamous region and intense epithelial proliferation leading to lamellar fusion (**F**). **G:** Detail of *S. chrysophrii* clamps pinching a cyst. **A-C, E, G:** Giemsa staining; **D:** PAS staining; **F:** Alcian blue/PAS staining. All scale bars = 20 µm, except in **A** = 50 µm.

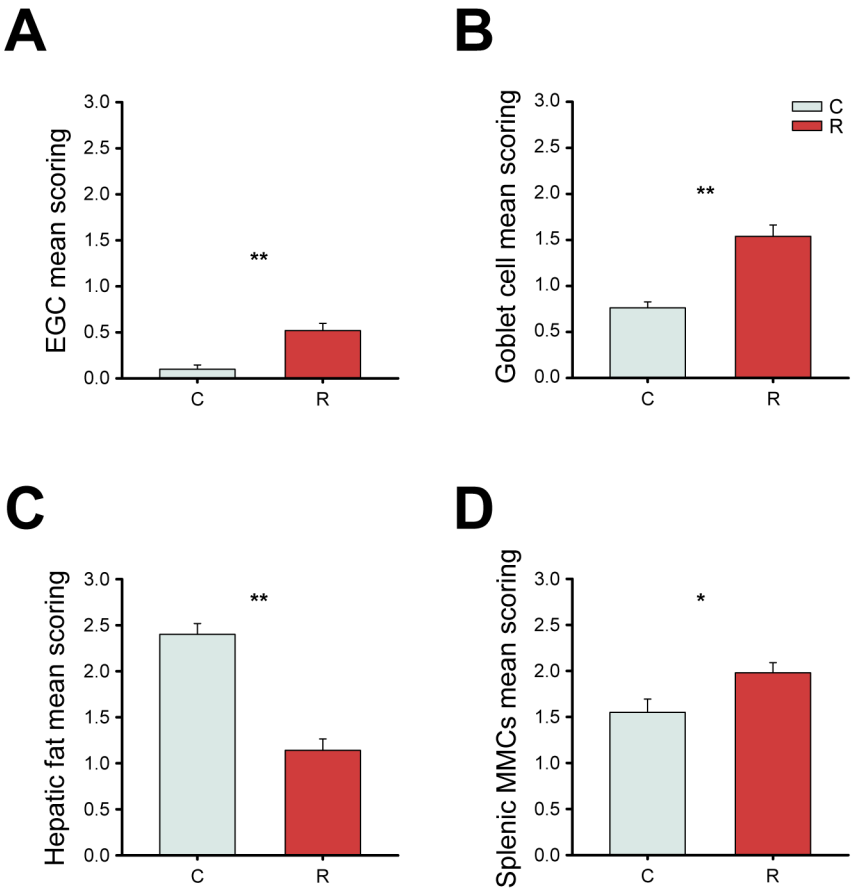

Figure S3. Scoring of histological alterations grouping all sampling times of control (C) and recipient (R) gilthead seabream in Trial 2. Mean semiquantitative scoring (mean + SEM) from 0 (absence) to 3 (very abundant). **A:** eosinophilic granular cells in gill filaments. **B:** goblet cells in gill filaments. **C:** hepatic fat storage. **D:** melanomacrophage centers in spleen. Asterisks represent statistically significant differences, (*****) $p < 0.05$ and (******) $p < 0.001$.

References

1. Federation of European aquaculture producers- FEAP. European Aquaculture Production Report- 2014-2020. 2021 [cited 2022 Apr 4]. Available from: https://feap.info/wp-content/uploads/2022/03/production-report-v1.1.pdf

2. FAO. FishStat: global aquaculture production 1950-2020 [Internet]. 2022 [cited 2022 Apr 4]. Available from: www.fao.org/fishery/en/statistics/software/fishstatj

3. Shinn AP, Pratoomyot J, Bron JE, Paladini G, Brooker EE, Brooker AJ. Economic costs of protistan and metazoan parasites to global mariculture. Parasitology. 2015;142:196–270.

4. Grau A, Crespo S, Pastor E, González P, Carbonell E. High infection by *Zeuxapta seriolae* (Monogenea: Heteraxinidae) associated with mass mortalities of amberjack *Seriola dumerili* Risso reared in sea cages in the Balearic Islands (western Mediterranean). Bull Eur Assoc Fish Pathol. 2003;23:139–42.

5. Ternengo S, Agostini S, Quilichini Y, Euzet L, Marchand B. Intensive infestations of *sciaenocotyle pancerii* (Monogenea, Microcotylidae) on *Argyrosomus regius* (Asso) under fish-farming conditions. J Fish Dis. 2010;33:89–92.

6. Sitjà-Bobadilla A, Redondo MJ, Álvarez-Pellitero P. Occurrence of *Sparicotyle chrysophrii* (Monogenea: Polyopisthocotylea) in gilthead sea bream (*Sparus aurata* L.) from different mariculture systems in Spain. Aquac Res. 2010;41:939–44.

7. Ogawa K, Bondad-Reantaso MG, Fukudome M, Wakabayashi H. *Neobenedenia girellae* (Hargis , 1955) Yamaguti, 1963 (Monogenea : Capsalidae) from Cultured Marine Fishes of Japan. American Society of Parasitologists. 1995;81:223–7.

8. Tu X, Ling F, Huang A, Wang G. An infection of *Gyrodactylus kobayashii* Hukuda, 1940 (Monogenea) associated with the mortality of goldfish (*Carassius auratus*) from central China. Parasitol Res. 2015;114:737–45.

9. Merella P, Cherchi S, Garippa G, Fioravanti ML, Gustinelli A, Salati F. Outbreak of *Sciaenacotyle panceri* (Monogenea) on cage-reared meagre *Argyrosomus regius* (Osteichthyes) from the western Mediterranean Sea. Dis Aquat Organ. 2009;86:169–73.

10. Jahangiri L, MacKinnon B, St-Hilaire S. Infectious diseases reported in warm-water marine fish cage culture in East and Southeast Asia—A systematic review. Aquac Res. 2022;53:2081–108.

11. Vendramin N, Zrncic S, Padrós F, Oraic D, Le Breton A, Zarza C, et al. Fish health in Mediterranean Aquaculture, past mistakes and future challenges. Bull Eur Assoc Fish Pathol. 2016;36:38–45.

12. Muniesa A, Basurco B, Aguilera C, Furones D, Reverté C, Sanjuan-Vilaplana A, et al. Mapping the knowledge of the main diseases affecting sea bass and sea bream in Mediterranean. Transbound Emerg Dis. 2020;67:1089–100.

13. Riera-Ferrer E, Piazzon MC, Del Pozo R, Palenzuela O, Estensoro I, Sitjà-Bobadilla A. A bloody interaction: plasma proteomics reveals gilthead sea bream (*Sparus aurata*) impairment caused by *Sparicotyle chrysophrii*. Parasit Vectors. 2022;15:322.

14. Sitjà-Bobadilla A, de Felipe MC, Álvarez-Pellitero P. *In vivo* and *in vitro* treatments against *Sparicotyle chrysophrii* (Monogenea: Microcotylidae) parasitizing the gills of gilthead sea bream (*Sparus aurata* L.). Aquaculture. 2006;261:856–64.

15. Sitjà-Bobadilla A, Álvarez-Pellitero P. Experimental transmission of *Sparicotyle chrysophrii* (Monogenea: Polyopisthocotylea) to gilthead seabream (*Sparus aurata*) and histopathology of the infection. Folia Parasitol (Praha). 2009;56:143–51.

16. Repullés-Albelda A, Holzer AS, Raga JA, Montero FE. Oncomiracidial development, survival and swimming behaviour of the monogenean *Sparicotyle chrysophrii* (Van Beneden and Hesse, 1863). Aquaculture. 2012;338–341:47–55.

17. Repullés-Albelda A, Raga JA, Montero FE. Post-larval development of the microcotylid monogenean *Sparicotyle chrysophrii* (Van Beneden and Hesse, 1863): comparison with species of Microcotylidae and Heteraxinidae. Parasitol Int. 2011;60:512–20.

18. Ernst I, Whittington ID, Corneillie S, Talbot C. Effects of temperature, salinity, desiccation and chemical treatments on egg embryonation and hatching success of *Benedenia seriolae* (Monogenea: Capsalidae), a parasite of farmed *Seriola* spp. J Fish Dis. 2005;28:157–64.

19. Hoai TD. Reproductive strategies of parasitic flatworms (Platyhelminthes, Monogenea): the impact on parasite management in aquaculture. Aquaculture International. 2020;28:421–47.

20. Lackenby JA, Chambers CB, Ernst I, Whittington ID. Effect of water temperature on reproductive development of *Benedenia seriolae* (Monogenea: Capsalidae) from *Seriola lalandi* in Australia. Dis Aquat Organ. 2007;74:235–42.

21. Repullés-Albelda A, Kostadinova A, Raga JA, Montero FE. Seasonal population dynamics of *Zeuxapta seriolae* (Monogenea: Heteraxinidae) parasitising *Seriola dumerili* (Carangidae) in the western Mediterranean. Vet Parasitol. 2013;193:163–71.

22. Valles-Vega I, Ascencio F, Sicard-González T, Angulo C, Fajer-Avila EJ, Inohuye-Rivera RB, et al. Effects of temperature on the life cycle of *Neobenedenia* sp. (Monogenea: Capsalidae) from *Seriola rivoliana* (Almaco jack) in Bahía de La Paz, BCS Mexico. Parasitol Res. 2019;118:3267–77.

23. Zhang X, Shang B, Cheng Y, Wang G, Stojanovski S, Li W. Effects of different regimes of low temperature on egg hatching of *Dactylogyrus vastator* (Monogenea: Dactylogyridae). Exp Parasitol. 2022;240:13–6.

24. Villar-Torres M, Montero FE, Raga JA, Repullés-Albelda A. Come rain or come shine: environmental effects on the infective stages of *Sparicotyle chrysophrii*, a key pathogen in Mediterranean aquaculture. Parasit Vectors. 2018;11:558.

25. Aguado-Giménez F, Ballester-Moltó M, García-García B. Influence of production strategy on gross waste output and temporal pattern of gilthead seabream (*Sparus aurata*) farming: implications for environmental management. Water (Basel). 2022;14.

26. Fioravanti ML, Mladineo I, Palenzuela O, Beraldo P, Massimo M, Gustinelli A, et al. Fish farmer's guide to combating parasitic infections in european sea bass and gilthead sea bream aquaculture [Internet]. ParaFishControl. 2020 [cited 2022 Mar 3]. p. 29. Available from: https://www.parafishcontrol.eu/images/PARAFISHCONTROL/Manuals/PFC-Manual4_Seabass_Seabream_vFINAL.pdf

27. Merella P, Montero FE, Burreddu C, Garippa G. In-feed trials of fenbendazole and other chemical/natural compounds against *Sparicotyle chrysophrii* (Monogenea) infections in *Sparus aurata* (Osteichthyes). Aquac Res. 2021;52:5908–11.

28. Mladineo I, Trumbić Ž, Ormad-García A, Palenzuela O, Sitjà-Bobadilla A, Manuguerra S, et al. *In vitro* testing of alternative synthetic and natural antiparasitic compounds against the monogenean *Sparicotyle chrysophrii*. Pathogens. 2021;10.

29. Ormad-García A. Transmission and maintenance of *Sparicotyle chrysophrii* infection in gilthead sea bream (*Sparus aurata*) using a recirculating aquatic system [Internet]. Polytechnic University of Valencia; 2018. Available from: https://m.riunet.upv.es/bitstream/handle/10251/114952/Ormad%20-%20Transmisi%C3%B3n%20y%20mantenimiento%20de%20la%20infecci%C3%B3n%20por%20Sparicotyle%20chrysophrii%20en%20la%20dorada%20en%20s....pdf?sequence=1&isAllowe d=y

30. Rigos G, Henry M, Tsigenopoulos C. *Sparicotyle chrysophrii* and gilthead sea bream- potential experimental infection model. Bull Eur Assoc Fish Pathol. 2015;35:50–4.

31. Buchmann K. Temperature-dependent reproduction and survival of *Pseudodactylogyrus bini* (Monogenea) on the European eel (*Anguilla anguilla*). Parasitol Res. 1988;75:162–4.

32. Riera-Ferrer E, Estensoro I, Del Pozo R, Piazzon MC, Moreno-Estruch P, Sitjà-Bobadilla A, et al. A non-lethal approach upon *Sparicotyle chrysophrii* burden prediction in gilthead sea bream (*Sparus aurata*). Aquaculture Europe 2021. 2021.

33. Wei T, Simko V. Corrplot: Visualization of a correlation matrix. R package version 0.94.2021

34. Ahmed NH. Cultivation of parasites. Trop Parasitol. 2014;4:80–9.

35. Hutson KS, Brazenor AK, Vaughan DB, Trujillo-González A. Monogenean parasite cultures: current techniques and recent advances. Adv Parasitol. 2018;99:61–91.

36. Hechinger RF, Lafferty KD. Host diversity begets parasite diversity: bird final hosts and trematodes in snail intermediate hosts. Proceedings of the Royal Society B: Biological Sciences. 2005;272:1059–66.

37. Halton DW, Jennings JB. Observations on the nutrition of monogenetic trematodes. Biol Bull. 1965;129:257–72.

38. Llewellyn J. Observations on the food and the gut pigment of the polyopisthocotylea (Trematoda: Monogenea). Parasitology. 1954;44:428–37.

39. Henry MA, Nikoloudaki C, Tsigenopoulos C, Rigos G. Strong effect of long-term *Sparicotyle chrysophrii* infection on the cellular and innate immune responses of gilthead sea bream, *Sparus aurata*. Dev Comp Immunol. 2015;51:185–93.

40. Antonelli L, Quilichini Y, Marchand B. *Sparicotyle chrysophrii* (Van Beneden and Hesse 1863) (Monogenea: Polyopisthocotylea) parasite of cultured gilthead sea bream *Sparus aurata* (Linnaeus 1758) (Pisces: Teleostei) from Corsica: ecological and morphological study. Parasitol Res. 2010;107:389–98.

41. Riera-Ferrer E, Estensoro I, Piazzon MC, Del Pozo R, Palenzuela O, Sitjà-Bobadilla A. Unveiling the blood-feeding behaviour of the gill parasite *Sparicotyle chrysophrii*. 20th International Conference on Diseases of Fish and Shellfish. 2021. p. 35.

42. Verde C, Giordano D, Russo R, di Prisco G. Erythropoiesis in Fishes. In: Farrell AP, editor. Encyclopedia of fish physiology: from genome to environment. Lodon: Academic Press; 2011. p. 992–7.

43. Witeska M. Erythrocytes in teleost fishes: A review. Zoology and Ecology. 2013;23:275–81.

44. Valenzuela A, Silva V, Tarifeño E, Klempau A. Effect of acute hypoxia in trout (*Oncorhynchus mykiss*) on immature erythrocyte release and production of oxidative radicals. Fish Physiol Biochem. 2005;31:65–72.

45. Yamamoto K. Contraction of spleen in exercised freshwater teleost. Comp Biochem Physiol A Physiol. 1988;89:65–6.

46. Yamamoto K, Itazawa Y, Kobayashi H. Supply of erythrocytes into the circulating blood from the spleen of exercised fish. Comp Biochem Physiol A Physiol. 1980;65A:5–11.

47. Boyd CE. Water quality: an introduction. Third Edit. Springer Nature Switzerland AG; 2020.

48. Verberk WCEP, Sandker JF, van de Pol ILE, Urbina MA, Wilson RW, McKenzie DJ, et al. Body mass and cell size shape the tolerance of fishes to low oxygen in a temperature-dependent manner. Glob Chang Biol. 2022;28:5695–707.

49. Dezfuli BS, Giari L. Mast cells in the gills and intestines of naturally infected fish: evidence of migration and degranulation. J Fish Dis. 2008;31:845–52.

50. Reite OB, Evensen Ø. Inflammatory cells of teleostean fish: a review focusing on mast cells/eosinophilic granule cells and rodlet cells. Fish Shellfish Immunol. 2006;20:192–208.

51. Noya M, Lamas J. Response of eosinophilic granule cells of gilthead seabream (*Sparus aurata*, Teleostei) to bacteria and bacterial products. Cell Tissue Res. 1996;287:223–30.

52. Dezfuli BS, Giari L, Lui A, Lorenzoni M, Noga EJ. Mast cell responses to *Ergasilus* (Copepoda), a gill ectoparasite of sea bream. Fish Shellfish Immunol. 2011;30:1087–94.

53. Dezfuli BS, Pironi F, Giari L, Noga EJ. Immunocytochemical localization of piscidin in mast cells of infected seabass gill. Fish Shellfish Immunol. 2010;28:476–82.

54. Mulero I, Chaves-Pozo E, García-Alcázar A, Meseguer J, Mulero V, García Ayala A. Distribution of the professional phagocytic granulocytes of the bony fish gilthead seabream (*Sparus aurata* L.) during the ontogeny of lymphomyeloid organs and pathogen entry sites. Dev Comp Immunol. 2007;31:1024–33.

55. Sepulcre M, Pelegrín P, Mulero V, Meseguer J. Characterisation of gilthead seabream acidophilic granulocytes by a monoclonal antibody unequivocally points to their involvement in fish phagocytic response. Cell Tissue Res. 2002;308:97–102.

56. Firmino JP, Vallejos-Vidal E, Sarasquete C, Ortiz-Delgado JB, Balasch JC, Tort L, et al. Unveiling the effect of dietary essential oils supplementation in *Sparus aurata* gills and its efficiency against the infestation by *Sparicotyle chrysophrii*. Sci Rep. 2020;10:17764.

57. Ogawa K. Diseases of cultured marine fishes caused by Platyhelminthes (Monogenea, Digenea, Cestoda). Parasitology. 2015;142:178–95.

58. Castrillo PA, Varela-Dopico C, Bermúdez R, Ondina P, Quiroga MI. Morphopathology and gill recovery of Atlantic salmon during the parasitic detachment of *Margaritifera margaritifera*. J Fish Dis. 2021;44:1101–15.

59. Fernández-Montero Á, Torrecillas S, Izquierdo M, Caballero MJ, Milne DJ, Secombes CJ, et al. Increased parasite resistance of greater amberjack (*Seriola dumerili* Risso 1810) juveniles fed a cMOS supplemented diet is associated with upregulation of a discrete set of immune genes in mucosal tissues. Fish Shellfish Immunol. 2019;86:35–45.

60. Blandford MI, Taylor-Brown A, Schlacher TA, Nowak B, Polkinghorne A. Epitheliocystis in fish: an emerging aquaculture disease with a global impact. Transbound Emerg Dis. 2018;65:1436–46.

61. Padrós F, Crespo S. Proliferative epitheliocystis associated with monogenean infection in juvenile seabream *Sparus aurata* in the north east of Spain. Bull Eur Assoc Fish Pathol. 1995;15:42.

62. Seth-Smith HMB, Dourala N, Fehr A, Qi W, Katharios P, Ruetten M, et al. Emerging pathogens of gilthead seabream: characterisation and genomic analysis of novel intracellular β-proteobacteria. ISME Journal. 2016;10:1791–803.

63. Seth-Smith HMB, Katharios P, Dourala N, Mateos JM, Fehr AGJ, Nufer L, et al. Ca. Similichlamydia in epitheliocystis co-infection of gilthead seabream gills: unique morphological features of a deep branching chlamydial family. Front Microbiol. 2017;8:508.

64. Crespo S, Zarza C, Padrós F, Marín De Mateo M. Epitheliocystis agents in sea bream *Sparus aurata*: Morphological evidence for two distinct chlamydia-like developmental cycles. Dis Aquat Organ. 1999;37:61–72.

65. Agius C. Preliminary studies on the ontogeny of the melano-macrophages of teleost haemopoietic tissues and age-related changes. Dev Comp Immunol. 1981;5:597–606.

66. Agius C, Roberts RJ. Melano-macrophage centres and their role in fish pathology. J Fish Dis. 2003;26:499–509.

67. Steinel NC, Bolnick DI. Melanomacrophage centers as a histological indicator of immune function in fish and other poikilotherms. Front Immunol. 2017;8:1–8.

68. Uribe C, Folch H, Enriquez R, Moran G. Innate and adaptive immunity in teleost fish: a review. Vet Med (Praha). 2011;56:486–503.

69. Wolke RE. Piscine macrophage aggregates: a review. Annu Rev Fish Dis. 1992;2:91–108.

70. Agius C. The role of melano-macrophage centres in iron storage in normal and diseased fish. J Fish Dis. 1979;2:337–43.

71. Agius C, Agbede SA. An electron microscopical study on the genesis of lipofuscin, melanin and haemosiderin in the haemopoietic tissues of fish. J Fish Biol. 1984;24:471–88.

72. Fulop GMI, McMillan DB. Phagocytosis in the spleen of the sunfish *Lepomis* spp. J Morphol. 1984;179:175–95.

73. Buchmann K. Mucosal Immunity in Fish. In: Buchmann K, Secombes CJ, editors. Principles of fish immunology: from cells and molecules to host protection. 1st ed. 2022. p. 387–443.

74. Stosik MP, Tokarz-Deptuła B, Deptuła W. Melanomacrophages and melanomacrophage centres in Osteichthyes. Central European Journal of Immunology. 2019;44:201–5.

75. De Vico G, Cataldi M, Carella F, Marino F, Passantino A. Histological, histochemical and morphometric changes of splenic melanomacrophage centers (Smmcs) in sparicotyle-infected cultured sea breams (*Sparus aurata*). Immunopharmacol Immunotoxicol. 2008;30:27–35.

76. Vigliano FA, Bermúdez R, Quiroga MI, Nieto JM. Evidence for melano-macrophage centres of teleost as evolutionary precursors of germinal centres of higher vertebrates: An immunohistochemical study. Fish Shellfish Immunol. 2006;21:467–71.

77. Piazzon MC, Mladineo I, Naya-Català F, Dirks RP, Jong-Raadsen S, Vrbatović A, et al. Acting locally- Affecting globally: RNA sequencing of gilthead sea bream with a mild *Sparicotyle chrysophrii* infection reveals effects on apoptosis, immune and hypoxia related genes. BMC Genomics. 2019;20:1–16.

78. Picard-Sánchez A, Estensoro I, Perdiguero P, del Pozo R, Tafalla C, Piazzon MC, et al. Passive immunization delays disease outcome in gilthead sea bream infected with *Enteromyxum leei* (Myxozoa), despite the moderate changes in IgM and IgT repertoire. Front Immunol. 2020;11:1–14.

79. Barrett J. Nutrition and Biosynthesis. Biochemistry of Parasitic Helminths. 1st ed. London and Basingstoke: Macmillan Publishers Ltd; 1981. p. 149–244.

80. Bennett MW, Caulfield JP. Specific binding of human low-density lipoprotein to the surface of schistosomula of *Schistosoma mansoni* and ingestion by the parasite. American Journal of Pathology. 1991;138:1173–82.

81. Lombardo JF, Pórfido JL, Sisti MS, Giorello AN, Rodríguez S, Córsico B, et al. Function of lipid binding proteins of parasitic helminths: still a long road. Parasitol Res. 2022;121:1117–29.

82. Vorel J, Cwiklinski K, Roudnický P, Ilgová J, Jedličková L, Dalton JP, et al. *Eudiplozoon nipponicum* (Monogenea, Diplozoidae) and its adaptation to haematophagy as revealed by transcriptome and secretome profiling. BMC Genomics. 2021;22:1–17.

83. Van Der Stoep M, Korporaal SJA, Van Eck M. High-density lipoprotein as a modulator of platelet and coagulation responses. Cardiovasc Res. 2014;103:362–71.

84. Arme C, Fox MG. Oxygen uptake by *Diclidophora merlangi* (Monogenea). Parasitology. 1974;69:201–5.

85. Houlihan DF, Macdonald S. *Diclidophora merlangi* and *Entobdella soleae*: egg production and oxygen consumption at different oxygen partial pressures. Exp Parasitol. 1979;48:109–17.

Chapter 4

A bloody interaction: Plasma proteomics reveals gilthead sea bream (*Sparus aurata*) impairment caused by *Sparicotyle chrysophrii*

Enrique Riera-Ferrer, M. Carla Piazzon, Raquel Del Pozo, Oswaldo Palenzuela, Itziar Estensoro and Ariadna Sitjà-Bobadilla

Fish Pathology Group, Institute of Aquaculture Torre de la Sal (IATS, CSIC), Consejo Superior de Investigaciones Científicas, Castellón, Spain

Parasites & Vectors, 10 September 2022
https://doi.org/10.1186/s13071-022-05441-1

Abstract

Sparicotylosis is an enzootic parasitic disease that is well established across the Mediterranean Sea. It is caused by the polyopisthocotylean monogenean *Sparicotyle chrysophrii* and affects the gills of gilthead sea bream (GSB; *Sparus aurata*). Current disease management, mitigation and treatment strategies are limited against sparicotylosis. To successfully develop more efficient therapeutic strategies against this disease, understanding which molecular mechanisms and metabolic pathways are altered in the host is critical. This study aims to elucidate how *S. chrysophrii* infection modulates the plasma proteome of GSB and to identify the main altered biological processes involved.

Experimental infections were conducted in a recirculating aquaculture system (RAS) in which naïve recipient GSB (R; 70 g; n = 50) were exposed to effluent water from *S. chrysophrii*-infected GSB (98 g; n = 50). An additional tank containing unexposed naïve control fish (C; 70 g; n = 50) was maintained in parallel, but with the open water flow disconnected from the RAS. Haematological and infection parameters from sampled C and R fish were recorded for 10 weeks. Plasma samples from R fish were categorised into three different groups according to their infection intensity, which was based on the number of worms·fish^{-1}: low (L: 1–50), medium (51–100) and high (H: > 100). Five plasma samples from each category and five C samples were selected and subjected to a SWATH-MS proteome analysis. Additional assays on haemoglobin, cholesterol and the lytic activity of the alternative complement pathway were performed to validate the proteome analysis findings.

The discriminant analysis of plasma protein abundance revealed a clear separation into three groups (H, M/L and C). A pathway analysis was performed with the differentially quantified proteins, indicating that the parasitic infection mainly affected pathways related to haemostasis, the immune system and lipid metabolism and transport. Twenty-two proteins were significantly correlated with infection intensity, highlighting the importance of apolipoproteins, globins and complement component 3. Validation assays of blood and plasma (haemoglobin, cholesterol and lytic activity of alternative complement pathway) confirmed these correlations.

Sparicotylosis profoundly alters the haemostasis, the innate immune system and the lipid metabolism and transport in GSB. This study gives a crucial global overview of the pathogenesis of sparicotylosis and highlights new targets for further research.

Introduction

Sparicotylosis is a gill infection caused by the polyopisthocotylean monogenean parasite *Sparicotyle chrysophrii* (formerly *Microcotyle chrysophrii*; Microcotylidae). This parasite has a direct life-cycle in which gravid adult specimens shed embryonated eggs into the water column from which motile ciliated larvae hatch after 5–10 days. If any hosts are nearby, the larvae will attach to their gill filaments, giving rise first to post-larvae and subsequently to juveniles and adults[1,2]. This disease is enzootic in the Mediterranean Sea, affecting several fish species of the Sparidae family[3–7], amongst which gilthead seabream (GSB; *Sparus aurata*) stands out as the type host and its commercial relevance in the Mediterranean aquaculture industry[8].

Sparicotylosis is associated with lethargy due to hypoxia, severe anaemia and emaciation. Gill histopathological findings, such as lamellar synechiae, clubbing and shortening, epithelial hyperplasia resulting in secondary lamellae fusion and proliferation of chloride cells, have been described[9,10].

Disease management in on-growing offshore net pens is a complex process. The high stocking densities, the proximity of the cages, the marine currents and the seeding of fingerlings without year-class separation or fallowing strategies create a perfect niche for amplification and dissemination of any pathogen. Current methods to control sparicotylosis rely on disinfectant bath treatments, net changing or cleaning[11] and nutraceutical formulation feedings[12].

For more than two decades, efforts have been made to widen the chemotherapeutic alternatives against *S. chysophrii*[9,12,13], but only hydrogen peroxide and formalin baths, which present a narrow therapeutic index and several concerns[12,14–17], remain as treatment options against sparicotylosis. The successful development of more efficient therapeutic strategies to control sparicotylosis critically relies on knowledge of both the host's and parasite's molecular mechanisms and metabolic pathways, which are relevant in the host-parasite relationship. Thus far, few studies dealing with *S. chrysophrii*-GSB interactions have been published. Henry et al.[18] described the inhibition of the humoral response and activation of cellular components in GSB-*S. chrysophrii* long-term infections. A subsequent tissue-level transcriptomic analysis of mild *S. chrysophrii* infections revealed that apoptosis, inflammation and cell proliferation played leading roles in the gills, whereas a hypometabolic response was detected in the spleen[19].

In recent years, proteomic analyses have transformed how host-parasite interactions are studied and understood. These interactions can be studied either by determining the expression of the parasite proteome throughout the infection process (i.e. tegumental and secreted proteins and extracellular vesicles), by detecting parasite proteins in its host, or by defining the infection effects on the host's proteome. Thus far, significant progress

has been achieved in understanding critical high-impact zoonotic and animal parasitic diseases through this technology[20–29].

The aim of the study reported here is to elucidate how *S. chrysophrii* infection modulates the plasma proteome of GSB and to identify the main altered biological processes involved.

Materials and methods

Animals, experimental infections and sampling

Healthy GSB juveniles were purchased from a Mediterranean-based hatchery (Piscimar, Burriana, Spain) and maintained at the indoor experimental facilities of the Institute of Aquaculture Torre de La Sal, Consejo Superior de Investigaciones Científicas (IATS, CSIC; 40°5′N, 0°10′E) under natural photoperiod and temperature conditions. Water parameters were monitored; oxygen saturation was kept > 85% and unionised ammonia was kept < 0.02 mg·L^{-1} in all tanks. All animals used in this experiment were fed twice daily, 5 days per week, until visual satiety, with a commercial dry pellet diet of the adequate size.

The experimental infection was conducted in a recirculation aquaculture system (RAS) from April to June, with water temperatures ranging from 15.23 °C to 23.85 °C. The experimental design consisted of a recipient (R) tank (200 L) holding naïve GSB (70 g; n = 50) receiving water from a donor (D) tank (200 L) with *S. chrysophrii*-infected GSB (98 g; n = 50). The infective status of D fish was confirmed by observation of *S. chrysophrii* eggs on egg collectors placed in the D tank. In parallel, an additional tank with control (C); n = 50) unexposed naïve fish from the same stock was maintained with the open water flow disconnected from RAS but the same temperature and oxygen conditions maintained.

After the beginning of the exposure to *S. chrysophrii*, one sampling was performed every 2 weeks for 10 weeks. Three mortalities were registered in the R group, one at day 44 and two at day 49 post exposure. In each sampling, 20 fish (10 R, 10 C) were euthanised by tricaine methanesulfonate (MS-222) overexposure (0.1 g·L^{-1}), and blood was collected from the caudal vein using heparinised syringes, taking special care to avoid haemolysis; the collected blood samples were constantly maintained on ice. Details on fish numbers, sampling times and the downstream use of individual samples are indicated in **Table 1** and **Supplementary material: Figure S1**. Following blood collection, haemoglobin (Hb) values were immediately recorded (HemoCue® 201+ Hb System; HemoCue AB, Ängelholm, Sweden). The remaining blood was centrifuged at 3000× *g* for 30 min, and plasma was stored at − 80 °C until processing. The right-side gill arches of each R specimen were dissected and *S. chrysophrii* counts of adult and juvenile specimens were carried out *in situ* under a stereomicroscope to determine the infection intensity. Infection intensities were extrapolated for the eight gill arches of each fish after Riera-Ferrer et al. [30].

Table 1. Experimental setup and sampling details.

Sampling	Days post exposure (dpe)	Mean temperature (°C)	Sampled Fish	Mean infection intensity in R fish ($\bar{x}$ ±SEM)
S1	14	17.88	10C; 10R	50.4 ± 15.32
S2	28	20.58	10C; 10R	134.4 ± 22.77
S3	42	20.48	10C; 10R	117 ± 32.89
S4	57	22.02	10C; 10R	76.8 ± 15.30
S5	68	23.35	10C; 7R	53.8 ± 16.32

Abbreviations: C: control (unexposed) fish; **R**: recipient (naïve) fish; **SEM**: standard error of the mean. **NOTE:** The mean ($\bar{x}$) infection intensity for the eight gill arches are determined based on the number of worms·fish^{-1}.

Ethics statement

All experiments were carried out according to current Spanish (Royal Decree 53/2013) and EU (Directive 2010/63/EU) legislation on the handling of experimental fish. All procedures were approved by the Ethics and Animal Welfare Committee of the Institute of Aquaculture Torre de la Sal (IATS, CSIC, Castellón, Spain), CSIC and "Generalitat Valenciana" (permit number 2018/VSC/PEA/0240).

Plasma proteome analysis

Candidate selection

A total of 20 different plasma samples were processed for proteomic analysis by the Central Service for Experimental Research (SCSIE) proteomics facility at the University of Valencia, Spain, which is a member of the Spanish network of proteomic research facilities (ProteoRed). All R fish were categorised into three groups according to their infection intensity recorded as worms·fish^{-1}: low, medium and high (L: 1–50; M: 51–100; H: > 100 worms·fish^{-1},respectively). Five plasma samples of each category and five C samples were selected for testing of infection intensity. The remaining plasma samples were stored until used in the validation assays (alternative complement pathway activity, cholesterol and biotin concentration).

Sample preparation

For the albumin depletion assay, 12 µL of each individual sample was precipitated with cold ethanol at a final concentration of 40% (*v/v*). The precipitation was incubated overnight at 5 °C and then centrifuged at 15,000× *g* for 1 h. The albumin-containing supernatant was then removed, and the pellets air-dried. The pellets were then dissolved in

	Application			
Proteome analysis	**Haemoglobin analysis**	**Cholesterol assay**	**Alternative complement pathway**	**Biotin assay**
4R	10C; 10R	10C; 10R	10C; 10R	10C; 10R
1R	10C; 10R	10C; 10R	10C; 10R	10C; 10R
6R	10C; 10R	10C; 10R	10C; 10R	10C; 10R
2C; 3R	10C; 10R	10C; 10R	10C; 10R	10C; 10R
3C; 1R	10C; 7R	10C; 7R	10C; 7R	10C; 7R

50 µL of 0.5% sodium dodecyl sulfate (SDS) in 50 mM ammonium bicarbonate. The proteins were quantified with a protein quantification assay kit (Macherey–Nagel GmbH & Co. KG, Düren, Germany) according to the manufacturer's instructions.

Due to the presence of lipids in the samples, 7 µg of protein was loaded in a one-dimensional (1D) polyacrylamide gel electrophoresis (PAGE) system without resolving and in-gel digested. The gel slices of each sample were cut into small cubes and sequentially dehydrated with 50% acetonitrile in 50 mM ammonium bicarbonate and 100% acetonitrile. Cysteine residues were reduced by 10 mM dithiothreitol in 50 mM ammonium bicarbonate buffer at 60 °C for 20 min, and sulfhydryl groups were alkylated with 5.5 mM iodoacetamide in 50 mM ammonium bicarbonate, in the dark, at room temperature, for 30 min. Gel cubes were incubated overnight at 37 °C in 100 µL of 50 mM ammonium bicarbonate solution with 400 ng of trypsin. The digestions were quenched with trifluoroacetic acid (final concentration: 1%). The supernatants were then removed, and the gel plugs were dehydrated with neat acetonitrile. The acetonitrile peptide solutions were recombined with the previous supernatants. The digestion mixture was dried in a vacuum centrifuge and resuspended in 20 µL of 2% acetonitrile, 0.1% trifluoroacetic acid.

Sequential window acquisition of all theoretical-mass spectra (SWATH-MS) analysis

For every mixture of digested peptide, 2 µL of peptide mixture sample was loaded in a NanoLC 425 HPLC system (Eksigent Technologies, Redwood, CA, US) onto a trap column (C18-CL 3 µm, 300 Å; internal diameter (id): 350 µm × 0.5 mm) and desalted with 0.1% trifluoroacetic acid at a flow rate of 5 $\mu L \cdot min^{-1}$ for 5 min. The peptides were then loaded onto an analytical column (C18-CL 3 µm, 120 Å; id: 75 µm × 150 mm; Eksigent Technologies) equilibrated in 5% acetonitrile, 0.1% formic acid. Peptide elution was carried out with a linear gradient of 7–40% acetonitrile with 0.1% formic acid at a flow rate of 300 $nL \cdot min^{-1}$. Peptides were analysed in a nanoESI qQTOF mass spectrometer (TripleTOF

6600+ System; AB Sciex, Framingham, MA, USA). The samples were ionised in a Source Type: Optiflow < 1 µL Nano applying 3.0 kV to the spray emitter at 200 °C. The TripleTOF mass spectrometer was operated in swath mode, in which a 0.050-s time-offlight mass spectrometry (TOF–MS) scan from 350 to 1250 $m \cdot z^{-1}$ was performed. Thereafter, 0.080-s product ion scans were acquired in 100 variable windows from 400 to 1250 $m \cdot z^{-1}$. The total cycle time was 2.79 s. The individual sequential window acquisition of all theoretical mass spectra (SWATH-MS) injections were randomised to avoid bias in the analysis. Prior to running the individual samples, a pooled sample was injected to determine the best gradient and sample amount.

Spectral library building

Plasma aliquots of all samples were pooled to build the spectral library by in-gel digestion and liquid chromatography-tandem mass spectrometry (LC–MS/MS) with data-dependent acquisition (DDA) in order to separate and identify the proteins present in the samples. After resolving the 1D SDS-PAGE, the gel lane corresponding to the library was cut into pieces, and each piece was digested with trypsin, extracted with acetonitrile, dried and resuspended as described above. Exactly as described before, each library sample was first loaded into a trap column and then into an analytical column, before loading the eluted peptides in the nanoESI qTOF mass spectrometer for analysis in DDA mode. Survey MS1 scans were acquired from 350 to 1400 $m \cdot z^{-1}$ for 250 ms. The quadrupole resolution was set to 'low' for MS2 experiments, which were acquired at 100–1500 $m \cdot z^{-1}$ for 25 ms in 'high sensitivity' mode. The following switch criteria were used: charge: 2+ to 4+; minimum intensity; 100 counts per second (cps). Up to 100 ions were selected for fragmentation after each survey scan. Dynamic exclusion was set to 15 s. The obtained DDA data files were processed using the ProteinPilot v5.0 (AB Sciex, Framingham, MA, USA) search engine, and a single list of peaks was generated using the default parameters and combining the acquired information of all gel fragments. The Paragon algorithm (ProteinPilot software; AB Sciex, Framingham, MA, USA) was used to search against 279,921 sequences available in GSB protein databases (NCBI, UniProt and transcriptome from the genome assembly[31]). A false discovery rate (FDR) correction was applied for the validation of the data. The identified proteins were grouped based on MS/MS spectra by the ProteinPilot Pro Group algorithm to avoid using the same spectral evidence for more than one protein. The protein within each group that could explain more spectral data with a 95% confidence threshold was depicted as the primary protein of the group. To increase the spectral data with data-independent acquisition (DIA) information, the data from the pooled samples were analysed by DIA Umpire as previously published[32].

Protein quantification

The SCIEX.wiff data-files obtained from SWATH runs of the 20 individual plasma samples were loaded into PeakView v2.1 (AB Sciex, Framingham, MA, USA) with the generated spectral library consisting of a combination of data-dependent and independent acquisition information, obtained from the pooled sample interrogated in the available protein databases at a peptide confidence threshold of 95% and an FDR < 1. The extracted ion chromatograms were integrated, and peak areas were used to calculate the total protein quantity of each individual sample.

Validation assays

In order to corroborate some of the findings of the proteomic analysis, three assays were performed in plasma samples from all sampled fish, including the ones used in the proteomics study.

Plasma complement assay

The lytic activity of the alternative complement pathway (ACP) was determined using sheep red blood cells (RBCs; Thermo Fisher Scientific, Waltham, MA, USA) as targets, and the dilution corresponding to 50% haemolysis per mL was expressed as alternative complement activity (ACH50). This assay was performed following the procedure described in[33], in sample duplicates using 2.85×10^8 sheep RBCs·mL^{-1}.

Plasma cholesterol assay

Plasma cholesterol was measured using the Infinity Cholesterol Liquid Stable Reagent (Thermo Fisher Scientific, Waltham, MA, USA), following the manufacturer's instructions. A calibration curve was performed using serial dilutions of Cholesterol (0–780 mg·dL^{-1}; Sigma-Aldrich, St. Louis, MO, USA). The amount of plasma per reaction was 4 µL. Reactions were performed in duplicate.

Plasma biotin detection

Plasma biotin was measured using the Biotin Quantitation Kit (Abcam, Cambridge, UK) following the manufacturer's instructions, using 30 µL of plasma, in duplicate. Biotinylated bovine serum albumin was used as a positive control. A standard curve was prepared using biotin concentrations ranging between 20 and 1000 µM.

Data and statistical analysis

The protein areas obtained with PeakView® v2.1 software (AB Sciex) were normalised by the total sum of the areas of all the quantified proteins. Normalised data were used to

build a partial least squares-discriminant analysis (PLSDA) model using the Bioconductor R package 'ropls'[34]. The quality of th ePLS-DA model was evaluated with the fit [R2Y(cum)] and prediction [Q2 (cum)] indicators. A validation test consisting of 500 random permutations was performed to discard overfitting of the PLS-DA model. The contribution of the different proteins to the group separation was determined by variable importance in projection (VIP) values. A VIP value > 1 was considered to be the threshold to determine discriminant proteins in the PLSDA model[35–37]. Hierarchical clustering, heatmap representation and K-means analyses were performed with the normalised area values of all discriminant proteins (VIP > 1) using iDEP.95 web application[38].

To perform a pathway analysis, the discriminant protein identifiers were converted to their human equivalents, when possible, and analysed with the Bioconductor 'Reactome-PA' R package[39].

The R package corrplot was used to calculate correlations between the different proteins and the infection intensity applying the cor.test function to compute significant correlation coefficients with a confidence level of 0.95.

All data were checked for normality prior to any statistical analysis. Statistical differences between C and R (L, M, H) Hb, ACP, cholesterol and biotin values were calculated using a one-way analysis of variance and a post-hoc multiple comparisons Holm-Šídák test. Differences were considered significant at $p < 0.05$, and a power analysis was performed in every test. All statistical analyses were performed using SigmaPlot v.14.0 (Systat Software, Inc., San Jose, CA USA).

Results

Plasma proteome analysis

A total of 291 GSB proteins were identified and quantified in the whole set of plasma samples. The normalised abundance values of each individual sample were used to construct a PLS-DA model to determine differences amongst groups. The PLS-DA model was based on five components (**Supplementary material: Figure S2**) which explained 98.8% (R2Y) and predicted 70% (Q2Y) of the total variance (**Figure 1A**). The model was validated using a permutation test (**Supplementary material: Figure S2**), and no outliers were detected during this analysis (**Supplementary material: Figure S2**). The PLS-DA model clearly separated the C group from fish in the R group. The dispersion of the C samples in the plot showed great individual variability in this group (**Figure 1A**). Highly infected fish (H) formed a separate group, whereas fish with medium and low levels of infection (M/L) were not significantly separated by the model and constituted a single set. Recipient fish (H and M/L groups) showed lower variability in their proteomic profiles than the C group. A PLS-DA model using the sampling point as variable, instead of infection intensity, was

constructed to determine whether differences could be due to the sampling time. As this model failed, we proceeded with the results showing differences by infection intensity.

The PLS-DA model yielded 129 proteins with VIP values > 1 which are responsible for the separation of the proteomic profiles among the three groups (**Supplementary material: Table S1**). These differentially abundant proteins driving the separation of the different groups were further explored in a heatmap. Hierarchical clustering once again showed a clear separation into three groups: C, M/L and H, validating the results obtained from the PLS-DA (**Figure 1B**). K-means analysis, conducted to visualise patterns among the differentially abundant proteins, revealed four clear clusters (**Figure 2**). Cluster A consisted of 20 proteins that were more abundant in the C samples than in R samples, among which immunoglobulin proteins prevailed. Cluster B grouped 46 proteins that were more abundant in the highly infected samples (H) than in the other two groups. Cluster C contained 41 proteins with a high abundance in the M/L group, a low abundance in the H group and intermediate values in the C group. Cluster D comprised 22 proteins with a low presence in C samples and increased presence in R fish.

Pathway analysis

In an attempt to clarify the biological significance of the changes observed in the plasma proteome of the different groups, pathway analysis was performed with the differentially abundant proteins classified in the four K-means clusters. Enriched pathways (p adj. < 0.05) in R GSB were coherent with functions expected to be found in plasma, highlighting an enrichment in pathways related to haemostasis, immune system, metabolism of vitamins and proteins, and transport of lipoproteins or O_2/ CO_2 (**Figure 3**). Among the pathways associated with the immune system, the complement system was highly represented. Overall, the most represented function was related to lipid (cholesterol) transport. Only 15 of the 129 proteins (11.63%) could not be converted into human equivalents and were not considered for the pathway analysis.

Proteins correlated with infection intensity

Correlation analysis revealed that 22 proteins were significantly correlated with the infection degree (**Table 2**). Fourteen proteins, including three apolipoproteins, two globins, complement component 3 (C3), ceruloplasmin and biotinidase, were negatively correlated with the infection intensity. Conversely, eight proteins exhibited a positive correlation with the disease.

Validation assays

Haemoglobin values (**Figure 4**), plasma cholesterol concentrations (**Figure 5**) and ACP (**Figure 6**) showed a gradual and significant decrease with increasing infection intensity.

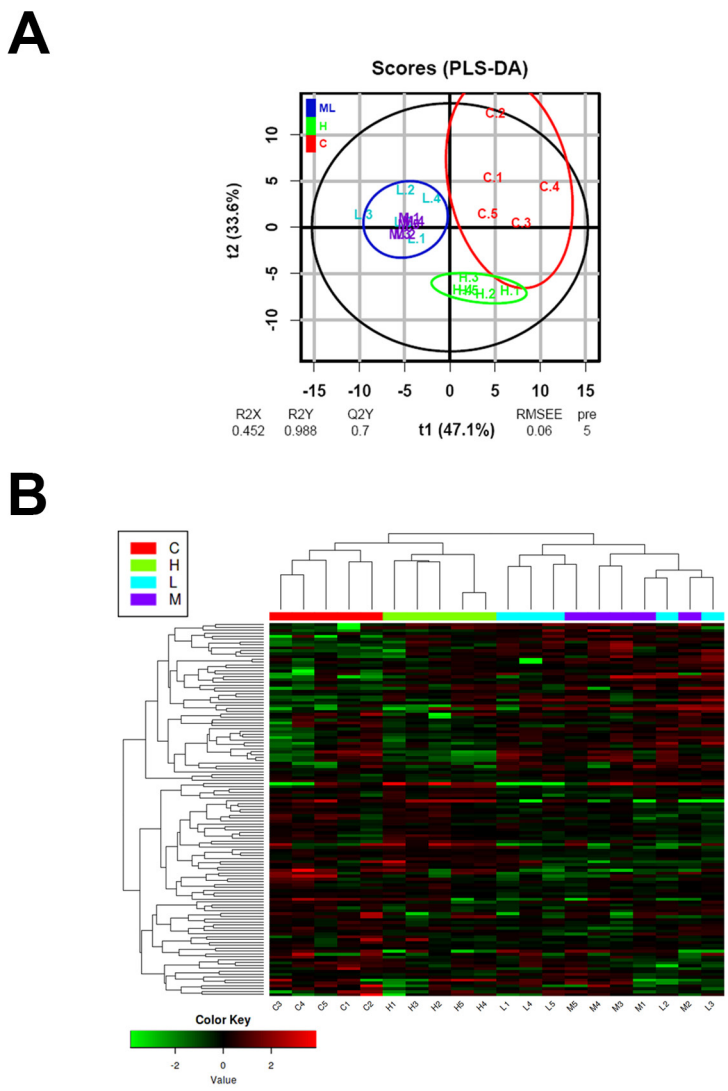

Figure 1. A: Two-dimensional PLS-DA score plot representing the distribution of the samples between the first two components of the model (t1 & t2). Uninfected fish (Control (C); n = 5) are represented in red; *Sparicotyle chrysophrii*-infected fish are represented in different colours according to level of infection (worms·fish^{-1}), with green indicating a high level of infection (H; n = 5), violet indicating a medium level of infection (M; n = 5) and blue indicating a low level of infection (L; n = 5). Ellipses represent the Mahalanobis distance. R2X and R2Y represent the fraction of the variance of the X and Y matrix, respectively (explained variance). Q2Y represents the predictive accuracy of the model. Values that approximate 1 indicate an effective model. RMSEE represents the square root of the mean error between the actual and the predicted responses. The model was constructed using five components (pre = 5). **B:** Heatmap representing the abundance distribution (Z-score) of the 129 proteins identified to be driving the separation among groups in a). Dendrograms represent hierarchical clustering of proteins (rows) and samples (columns). Samples are colour coded following the same criteria as in **A** PLS-DA, Partial least squares-discriminant analysis.

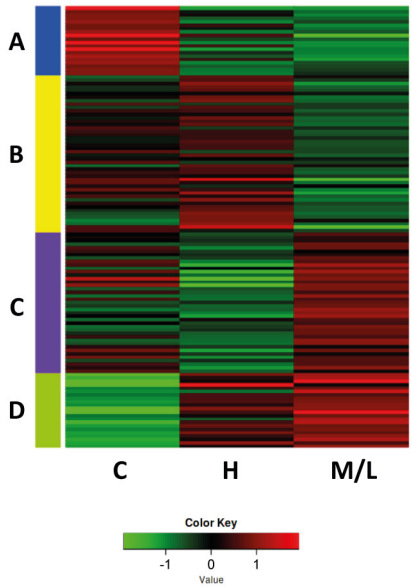

Figure 2. K-means analysis separating the 129 discriminant proteins into four clusters based on expression level in the different groups (Z-score). Different colours indicate different clusters, with blue indicating cluster A (n = 20), yellow indicating cluster B (n = 46), violet indicating cluster C (n = 41) and green indicating cluster D (n = 22). Group means are represented for clarity. **Abbreviations: C**: control (unexposed) fish; **H**: fish with high degree of infection; **M/L**: fish with medium/low degree of infection.

These results validated the detected gradual decline in plasma alpha-2 and beta globins, apolipoproteins B-100, H and A-II and C3 at the protein level. On the other hand, no significant differences were detected in plasma biotin levels, and the measured values were very close to the lower detection threshold of the technique (**Supplementary material: Figure S3**). It is to be noted that biotinidase levels were also in the low range, preventing us from drawing firm conclusions about the detected differences.

Discussion

Despite the impact of *S. chrysophrii* on infection on animal welfare and the economic repercussions, little is known about the effect of *S. chrysophrii* in GSB. The results of the present study on plasma proteomics of *S. chrysophrii* infected GSB provide information that will enable a better understanding of the pathogenesis of sparicotylosis, providing evidence on the metabolic pathways affected by the disease under different infection intensities. Furthermore, these results may shed some light upon which host resources are required by this monogenean species to ensure its survival as a first approach to elucidate the unknown pathogenicity mechanisms of the parasite and ultimately suggest immune-evasion strategies.

The discriminant analysis of the abundance of all detected proteins formed three dif-

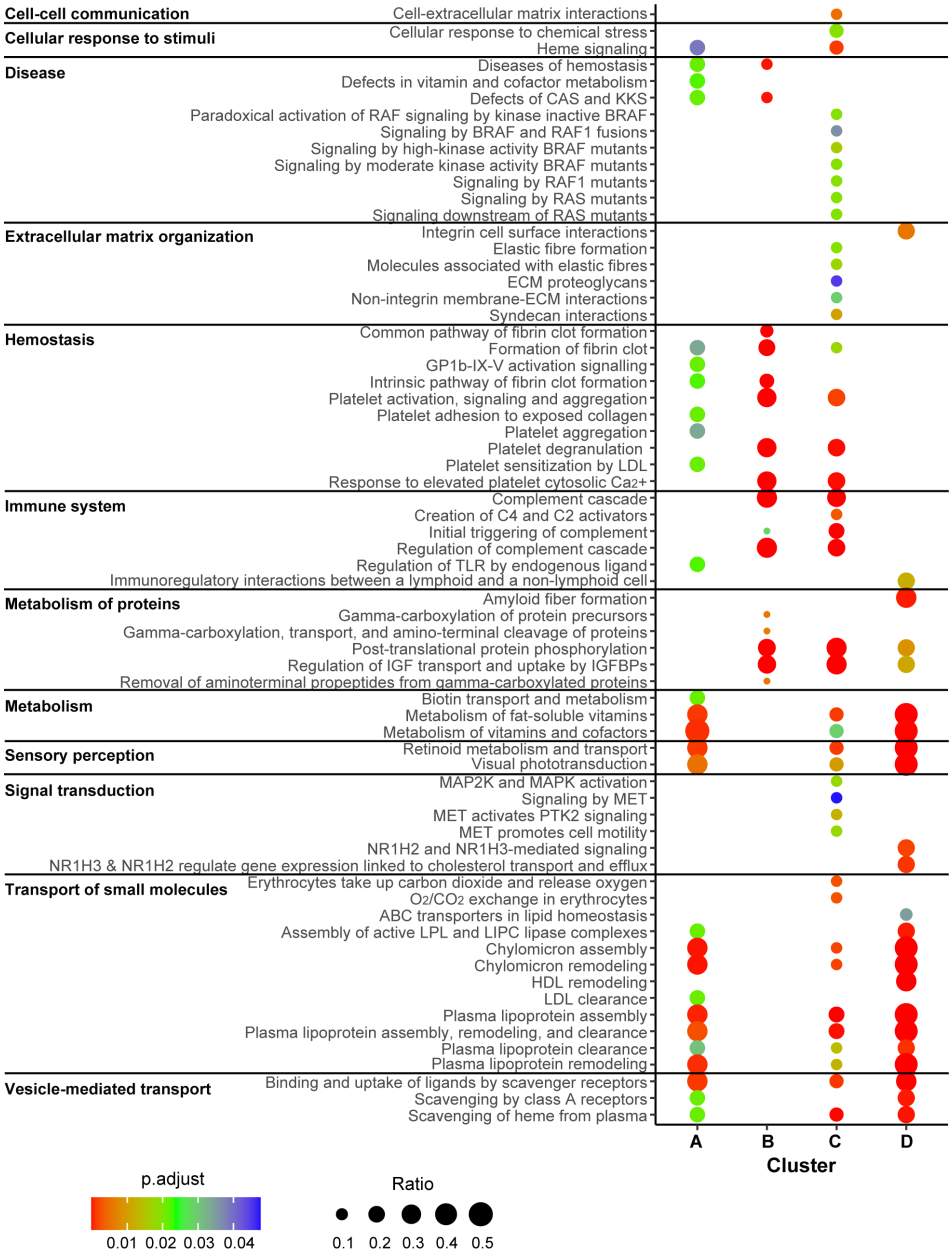

Figure 3. Dot plot pathway enrichment map showing significantly overrepresented pathways (left) (*p* adj. < 0.05) in the lists of proteins obtained for the different clusters in the K-means analysis (right) represented in **Figure 2**. The colour of the dots represents the *p* adj. value, and the size of the dots represents the proportion of proteins relative to the total amount of proteins for each pathway.

Table 2. Plasma proteins whose abundance was significantly correlated with *Sparicotyle chrysophrii* infection degree.

Protein	Correlation coefficient[a]	*p* value[b]
Saxitoxin and tetrodotoxin-binding protein 1-like	-0.65	0.002
Alpha-2 globin	-0.62	0.003
Immunoglobulin light chain, partial	-0.61	0.005
Biotinidase	-0.58	0.007
Apolipoprotein B-100	-0.56	0.010
Ectonucleotide pyrophosphatase/phosphodiesterase family member 2	-0.54	0.014
Complement C3-like	-0.51	0.020
Apolipoprotein H	-0.50	0.024
Carboxypeptidase N subunit 2	-0.49	0.030
Beta globin	-0.48	0.033
Apolipoprotein A-II	-0.48	0.033
Ceruloplasmin	-0.47	0.037
Serpin family G member 1	-0.45	0.048
Ladderlectin-like	-0.45	0.048
Immunoglobulin lambda chain C region	0.57	0.009
Hibernation-specific plasma protein HP-55	0.56	0.010
L-rhamnose-binding lectin CSL2	0.53	0.016
Alpha-1-microglobulin	0.52	0.018
Cyclin dependent kinase like 1	0.47	0.036
Serotransferrin	0.46	0.039
Coagulation factor X-like	0.46	0.040
Estrogen-regulated protein	0.45	0.048

[a] Negative and positive correlations and the strength of each correlation are shown by the sign and value of the correlation coefficient.

[b] Significant correlations were assumed at p value < 0.05.

ferent groups (C, M/L and H). The dispersal of these proteins among the healthy GSB (C) group was clearly greater than that among diseased fish (M/L and H groups) (**Figure 1A**). However, differentially abundant proteins in the M/L group showed a greater disparity than those in the H group, which in turn seemed closer to the C group phenotype in both the PLSDA model and heatmap (**Figure 1**). Large variability is always an expected feature in control samples; in our study, the fish were obtained from a commercial farm and were not clonal lines or even from a single family. Although they came from the same production batch, they probably had very different genetic backgrounds, which would provide variable results. The observed decrease in variability during infection is interesting, as it points towards a homogeneous response elicited by/against the parasite, with all fish responding with the same trend. These observations suggest that the hosts suffer a profound imbalance with mild (M/L) *S. chrysophrii*-infection intensities, as observed by

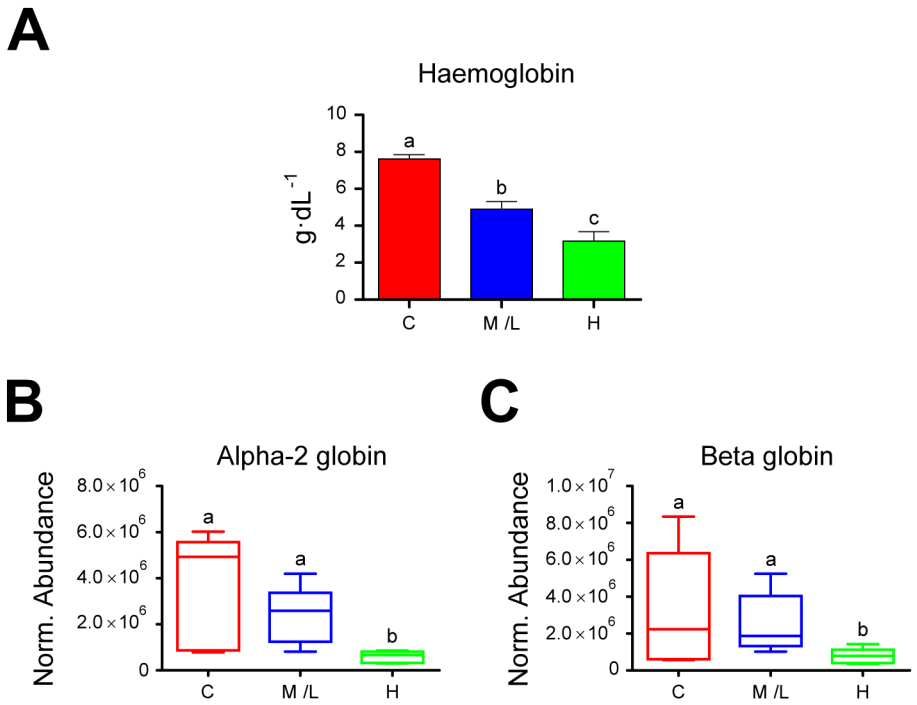

Figure 4. A: Haemoglobin values measured in control fish (C, n = 50) and in *Sparicotyle chrysophrii*-infected fish with a medium/low (M/L, n = 31) and high (H, n = 16) infection degree. **B**, **C:** Normalised protein abundance values of alpha-2 globin (**B**) and beta-globin (**C**) measured by proteomics in plasma samples of C fish (n = 5) and in M/L (n = 10) and H (n = 5) infection groups. Values are presented as the mean ± SEM (standard error of the mean). Statistical differences among groups at $p < 0.05$ are noted with different letters (Kruskall-Wallis test).

Piazzon et al.[19]. In GSB that survived to high parasitic burdens (H), the plasma proteomic profile closely resembled that of C fish, possibly reflecting the onset of compensation mechanisms to restore homeostasis, such as haemostatic events. During the progress of sparicotylosis under experimental conditions, this apparent recovery of the plasma's proteomic profile might be the result of the monogeneans' intimate coevolution with their hosts. Monogenean evolution is associated with strict host specificity and coevolution between worm and host[40,41], which, in light of the results of the present study, might include attenuation of the worm's pathogenicity in order to assure the host's survival and parasite's persistence. Under farming conditions, however, which include high stocking densities, exposure to environmental stressors and multiple pathogen offenders, high infection pressures and recurrent sparicotylosis infections once the disease is established, high mortality is reported, even after the fish has received treatment. Apparently, under these harsh farming conditions, fish would be unable to recover homeostasis, resulting in the combined pathogenic effect of the parasite with the biotic and abiotic stressors, including secondary opportunistic infections, being more devastating. Hence, future pro-

teomic plasma studies of moribund GSB from sea cages suffering sparicotylosis would shed some light on this issue. However, the current results were obtained under experimental conditions, in a time-limited exposure (10 weeks) to a single purified pathogen offender, in contrast to an enzootic farm. The potential therapeutic importance of such a natural attempt of homeostatic restitution in highly infected fish under experimental conditions is paramount, since a strategy based on an earlier stimulation of these mechanisms by dietary or health interventions would open the path to mitigation of the effects of the disease. *Sparicotyle chrysophrii*-modulated proteins are involved in several biological processes in GSB. Among these, the levels of various proteins increased while those of others decreased in a complex network of interactions. The main pathways severely modulated by *S. chrysophrii* were those related to haemostasis, lipid metabolism and transport and the immune system (**Figure 3**).

Haemostasis

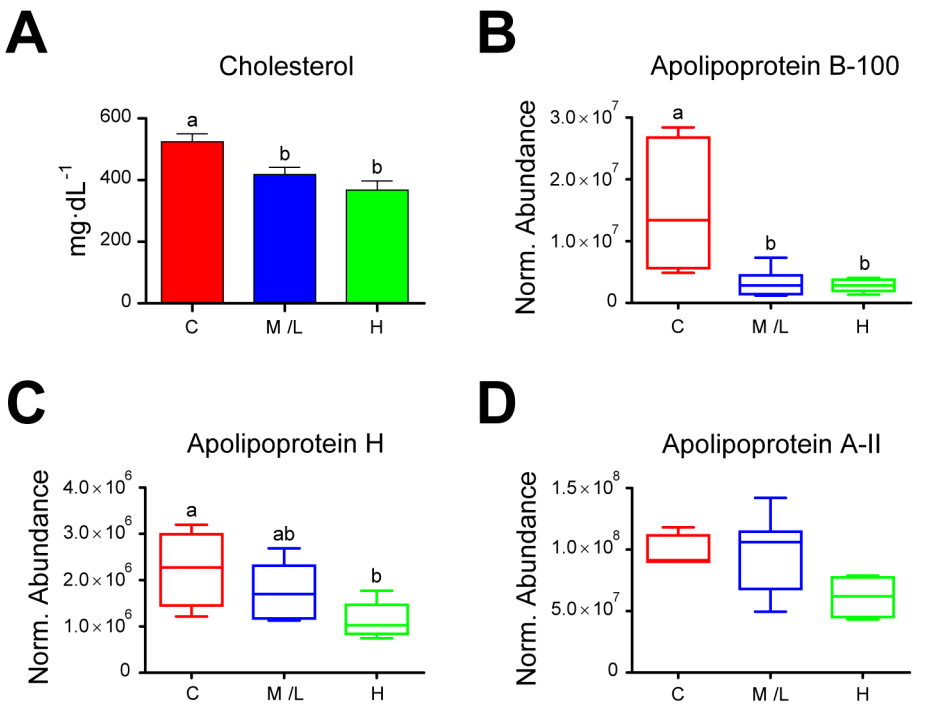

Figure 5. A: Plasma cholesterol values measured in control fish (n = 50) and in *Sparicotyle chrysophrii*-infected fish with a medium/low (M/L, n = 31) and high (H, n = 16) infection degree. **B–D**: Normalised protein abundance values of apolipoprotein B-100 (**B**), apolipoprotein H (**C**) and apolipoprotein A-II (**D**) measured by proteomics in plasma samples of C fish (n = 5) and in the M/L (n = 10) and H (n = 5) infection groups. Values are presented as the mean ± SEM. Statistical differences among groups at $p < 0.05$ are noted with different letters (one-way analysis of variance (**A**, **C**, **D**) or Kruskall-Wallis test (**B**)).

Polyopisthocotylean monogeneans have been described as haematophagous parasites[42,43], but it has not been until recently that the haematophagous nature of *S. chrysophrii* has been experimentally demonstrated[44]. From the current study, we can discern a clear negative impact on haemostasis in GSB. Blood Hb levels significantly dropped as the parasite burden increased (**Figure 4**). These low Hb values mirrored the plasma proteomic results, which showed that the main Hb constituents, alpha-2 and beta globins, negatively and significantly correlated with the infection intensity (**Table 2**; **Figure 4**). In addition, alpha-1-microglobulin, a radical scavenger associated with haem toxicity and erythroprotective anti-haemolytic effects in humans[45], presented a positive and significant correlation (**Table 2**). This suggests that *S. chrysophrii*-infected GSB suffer from haemolytic anaemia, as an increase in alpha-1-microglobulin occurs in hosts facing a haemolytic insult, which leads to the release of Hb and free haem groups from erythrocytes, increasing the oxidative stress[45]. Overall, these results would imply anaemia and oxygen transport impairment, explaining the hypoxia and lethargy signs observed in parasitised fish. Furthermore, the specific mechanisms this parasite uses for blood-feeding are still unknown, but our preliminary results on the matter suggest that *S. chrysophrii* is able to feed on blood meals resulting from GSB RBC lysate. The exact mechanism remains to be elucidated.

The coagulation cascade also seems to be triggered by sparicotylosis. In mammalian[46,47] and fish[48] blood, the extrinsic pathway is initiated following tissue damage and subsequent exposure of subendothelial tissue factor (TF) to coagulation factor VII, whereas the intrinsic pathway is triggered by the exposure of a foreign negatively charged sur-

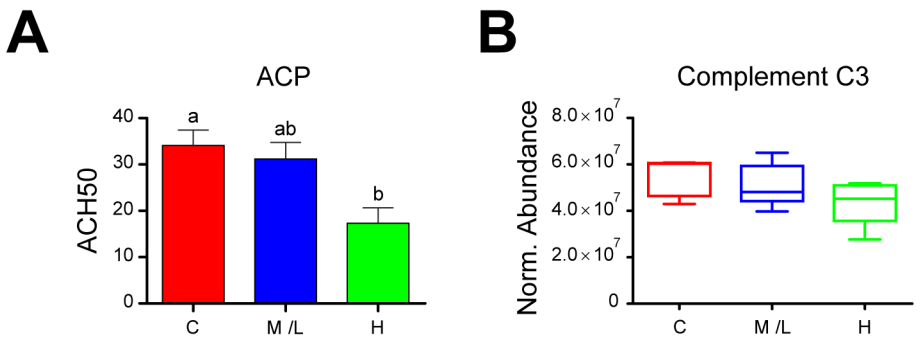

Figure 6. A: Activity of plasma alternative complement pathway (ACP) measured in control fish (n = 50) and in *Sparicotyle chrysophrii*-infected fish with a medium/low (M/L, n = 31) and high (H, n = 16) infection degree. b Normalised protein abundance values of complement component 3 (C3) protein measured by proteomics in plasma samples of C fish (n = 5) and in the M/L (n = 10) and H (n = 5) infection groups. Values are presented as the mean ± SEM. Statistical differences among groups at $p < 0.05$ are noted with different letters (one-way analysis of variance).

face to coagulation factor XII. Both pathways converge in coagulation factor X, after which the common pathway of the coagulation cascade follows, resulting in the production of thrombin and leading to clot formation and final restoration of haemostasis[46,47]. In the current study, most proteins involved in the coagulation cascade were represented in cluster B of the K-means analysis (**Figure 2**). In GSB suffering sparicotylosis, both intrinsic (coagulation factor IX) and extrinsic (factor VII) pathways of the coagulation cascade as well as the common pathway of the coagulation cascade (factors X and V) were modulated (**Supplementary material: Table S1**). It is noteworthy that all coagulation factors in cluster B were upregulated in the H group, but not in the M/L group (**Figure 2**), which is in agreement with the significantly positive correlation of factor X with the infection intensity (**Table 2**). Thus, the coagulation capacity of GSB apparently increased when high parasitic burdens were reached. Similarly, in several tick species, different proteins with anticoagulant properties affecting the intrinsic, extrinsic and common coagulation pathways[49–51] have been described and characterised, suggesting that these haematophagous parasites can modulate their host's haemostasis at different levels.

Since *S. chrysophrii* is an ectoparasite and not an intravascular parasite, we suspect that the intrinsic pathway could be, in part, triggered by remnants of RBCs[52] resulting from haemolysis. In contrast, the activation of the extrinsic pathway may be due to tissue disruption induced by the parasite's haptor and feeding mechanisms.

Lipid metabolism and transport

Different parasitic species, ranging from Protozoa to Metazoa, have been described as being able to alter the lipidic profile of their host species, both in fish[53] as well as in higher vertebrates[54–63]. In particular, Platyhelminthes are unable to synthesise fatty acids *de novo*[64], thus relying on the host's lipid reservoir to ensure their survival. Several fatty acid-binding proteins (FABPs) have been identified in trematode species, such as *Schistosoma* spp., *Fasciola* spp. and, most recently, in the diplozoid monogenean *Eudiplozoon nipponicum*[65,66]. Although FABPs have been described to play a role in fatty acid uptake by *Fasciola hepatica* from host blood and in immunomodulation, their function in monogeneans remains unknown[65]. Our results show that apolipoprotein B-100 (ApoB-100) and apolipoprotein A-II (ApoA-II) levels were negatively and significantly correlated with the infection intensity (**Table 2**; **Figure 5**). In agreement with this observation, the expression of apolipoproteins was found downregulated in the liver and spleen of GSB with a mild *S. chrysophrii* infection[19]. In addition, cholesterolaemia values in plasma samples of *S. chrysophrii*-infected GSB were significantly lower than those in the C group, supporting our proteomic results (**Figure 5**). The reduction in plasma cholesterol levels in GSB was also triggered by environmental stressors[67,68]) and dietary intervention involving

the replacement of fish meal and oil by vegetable ingredients[33,69]. The latter provoked a simultaneous drop in plasma cholesterol and blood Hb, which was reversed by a butyrate additive in the diet. This finding could open a path for the use of butyrate as a mitigation strategy for the effects of sparicotylosis.

ApoB-100 is a crucial structural component in very-lowdensity lipoproteins (VLDL) and low-density lipoproteins (LDL), which are predominantly composed of triglycerides and cholesteryl esters, respectively. ApoA-II, on the other hand, is associated with high-density lipoproteins (HDL2 and HDL3) that are predominantly composed of cholesteryl esters[70,71]. Our results suggest a dependency of *S. chrysophrii* on its host's lipid reservoir, but the function of these lipids is intriguing. In the case of the previously mentioned trematode species *Schistosoma* spp. and *Fasciola* spp. and the diplozoid monogenean *E. nipponicum*, it has been suggested that the host's incorporated lipids may play important roles in maintaining different cellular structures after their distribution and storage in the parasite's body or they may also be found in excretion/ secretion products, which are involved in the modulation of the host's immune system[66,67]. The human trematode *Schistosoma mansoni* has been described to bind part of the host's LDL to their surface, which might be an immune evasion strategy, in addition to ingesting LDL, breaking it down and distributing lipids throughout the worm[72]. *Sparicotyle chrysophrii* might be using similar strategies since it seems to preferentially rely on the easier digestible and transportable smaller sized VLDLs and LDLs of the host, but there is still no evidence for the worm feeding or displacing GSB's lipoproteins.

Plasma lipoproteins (LDLs and HDLs) play an essential role in host defence as a component of the immune system[73–75] and against bacterial, viral and parasitological infections[73] in mammals. Hence, in our fish-parasite model, an alteration in lipoprotein levels could render the host more susceptible to secondary infections. Moreover, other roles in haemostasis have been granted to LDLs and HDLs, thus somewhat contributing to the control of haematological parameters, such as RBC membrane stability[76].

Immune system

Differences in the host's immune response have been observed between monopisthocotylean and polyopisthocotylean monogenean parasites[77]. These differences have been suggested to lie in the different feeding strategies[77] since polyopisthocotylean monogeneans are generally considered to be haematophagous and, therefore, need to evade the host's immune response to ensure their feeding and survival. Our study shows how *S. chrysophrii* infection changes the abundance of several complement proteins (factor H, factor B, factor I, C1q, C3, C4, C5, C6, C7, C8; **Supplementary material: Table S1**), inducing an inhibition of the alternative pathway as the infection intensity increases (**Figure 6**).

Along the same line, other studies with the same host and parasite species have revealed that this parasite downregulated c3 splenic expression, upregulated complement factor H (complement inhibitor) in spleen and gills[19] and lowered complement levels in serum[18]. A local downregulation of c3 expression has also been described in other monogenean infections[78,79]. We observed that the depletion of complement effectors in GSB plasma worsened during the infection, compromising the fish immunocompetence. It is also noteworthy that the presence of immunoglobulin chains, mostly variable regions of the light chains, among the proteins were significantly less abundant in R fish, regardless of their infection intensity (cluster A). This result indicates that B cells are being modulated upon parasite infection, with a probable shift of the immunoglobulin (Ig) repertoire. Modulation of Ig transcripts, including light chains and variable genes, have also found at a transcriptomic level in gills (local) and spleen (systemic) in mild *S. chrysophrii* infections[19]. Further studies elucidating Ig titres and the Ig repertoire at systemic and local levels are needed to determine if this is due to an inhibition of antibody production or a shift towards a focused and specific response. Our results point to a complex network regulating the innate immune response, including SERPINs and ceruloplasmin, which may indirectly modulate the complement system, resulting in neutrophil activation and inflammation.

Proteins linking haemostasis and the immune system

Serine-protease inhibitor

Serine proteases are enzymes that have been highly conserved during evolution which play crucial roles in several physiological processes, including blood coagulation, fibrinolysis, inflammation and immune response. Serineprotease inhibitors (SERPINs) obtain their name from serine protease inhibitors. They are a superfamily of proteins that primarily regulate the proteolytic pathways of serine and cysteine proteases[80–83]. It has been described that protease inhibitors may have a leading role in host-parasite interactions and, more specifically, in evasion mechanisms and survival on the parasite's behalf[84–86].

In the current study, three SERPINs were differentially expressed following infection; SERPINA1 (α1–antitrypsin), SERPIND1 (heparin coagulation factor II) and SERPING1 (C1-inhibitor; C1INH) (**Supplementary material: Table S1**). SERPINA1 was grouped in cluster C (more abundant in the M/L group), whereas both SERPIND1 and SERPING1 were grouped in cluster B (more abundant in the H group) (**Figure 2**).

SERPINA1 inhibits neutrophil elastase, a serine protease with microbiocidal effects that is involved in the acute phase of the inflammation process and tissue remodelling[87]. We relate this observation to an early impairment of an inflammatory response elicited by neutrophils. This event could be driven by either a GSB response towards a trau-

matic event involving tissue disruption or by deliberate modulation of SERPINA1 by *S. chrysophrii* as an evasion mechanism, with the ultimate aim to enable attachment to gill filaments. It has recently been suggested that some digenean trematode parasites could have the ability to modulate the host's SERPINs[25], but no published data are are available on SERPINA family members being modulated by fish parasites.

Both SERPIND1 and SERPING1 play key roles in coagulation; however, SERPING1 also affects the immune system. SERPIND1 is known to, directly and indirectly, inhibit thrombin in the common pathway of the coagulation cascade[80,81,88], thus preventing fibrinogen and platelet activation and ultimately preventing clot formation and haemostasis restoration. At the haemostatic level, SERPING1 inhibits several components within the intrinsic coagulation pathway [plasma kallikrein, activated factors XII (FXIIa) and XI (FXIa)] as well as fibrinolytic proteases (plasmin, tPA and uPA). Further SERPING1 inhibitory abilities extend to both C1s and C1r, modular proteases responsible for the activation and proteolytic activity of the C1 complex of the classic complement pathway[46,47,80,81,83,89–91].

Thus, the significantly higher abundance of SERPIND1 and SERPING1 in GSB with high parasitic burdens could imply an anticoagulant and innate immunosuppressor effect in these hosts (**Figure 2**). However, within cluster B, SERPING1 shows a significant negative correlation with the infection intensity (**Table 2**). SERPINs operate within a complex physiological modulation network, and further SERPIN-targeted studies are needed to unravel this paradox, as well as the opposing coagulant and anticoagulant actions of serpins and the coagulation cascade. Counterregulation evidenced by our results might be the effect of the host response aiming for homeostatic balance or a host versus parasite modulation.

Ceruloplasmin

Ceruloplasmin is an acute-phase protein that has been associated with inflammation, severe infection and tissue damage in mammals and fish. Ceruloplasmin has also been described as a copper-carrying protein, ultimately playing a role in hypoxic vasodilation and ischaemia–reperfusion cytoprotection[92–94] and having the ability to oxidise toxic plasma ferrous iron into its ferric form to be transported by transferrin[93]. Moreover, under hyperammonaemia conditions, the intrinsic pathway of the coagulation cascade is triggered, and the functional activity of platelets decreases. However, ceruloplasmin can prevent haemostatic disorders by restoring platelet functionality and preventing hypercoagulation[95].

Henry et al.[18] previously described no significant differences in ceruloplasmin activity in GSB after a 10 weeklong *S. chrysophrii* infection. Our results suggest an initial increase in plasma ceruloplasmin levels in M/L fish followed by a later decrease during the course

of infection in the H group. Thus, we hypothesise that fish with lower infection intensities were in an acute phase of the disease, while H GSB restored their ceruloplasmin to control levels later during the progress of infection. However, comparison of our results with previously published findings[18] is however complicated since experimental designs and the infection outcome were very different.

Conclusions

Understanding how GSB responds to *S. chrysophrii* is critical for developing new treatments and health management strategies in the aquaculture industry. The present plasma proteomic study of *S. chrysophrii*-infected GSB provides a crucial global overview of the pathogenesis of sparicotylosis, representing a valuable contribution to the understanding of the disease and highlighting new targets for further research. However, our results are based on the disease progression of a pure *S. chrysophrii* experimental infection, which does not totally depict farming conditions. Sparicotylosis profoundly alters the haemostasis, the innate immune system and the lipid metabolism and transport in GSB. However, in high-intensity experimental infections, GSB seems to attempt to restore some of the alterations suffered during the acute phase of the disease. This could be either due to the close evolutionary ties between *S. chrysophrii* and GSB, or to a host protection mechanism against the damage caused by the activation of acute mechanisms.

Funding

This work has been financed by the Spanish Ministry of Science and Innovation and Universities project (SpariControl, RTI2018-098664-B-I00, AEI/ FEDER, UE). ERF was supported by an FPI contract PRE2019-087409 (MCIN/ AEI/10.13039/501100011033). MCP was funded by a Ramón y Cajal Postdoctoral Research Fellowship (RYC2018-024049-I & ACOND/2022 Generalitat Valenciana). RDP was contracted under the PTA Programme from the Spanish Ministry of Science, Innovation and Universities (PTA2018-015315-I). ERF, MCP and RDP contracts were co-funded by the European Social Fund (ESF). We acknowledge support of the publication fee by the CSIC Open Access Publication Support Initiative through its Unit of Information Resources for Research (URICI).

Acknowledgements

The authors thank Prof. J. Pérez-Sánchez from the Nutrigenomics and Fish Growth Endocrinology group (IATS, CSIC) for providing access to genomic database of GSB, M. Luz Valero from SCSIE proteomics facility (University of Valencia, Spain) for the proteomics analyses and support and I. Vicente for technical assistance with fish husbandry and samplings at IATS.

Supplementary material

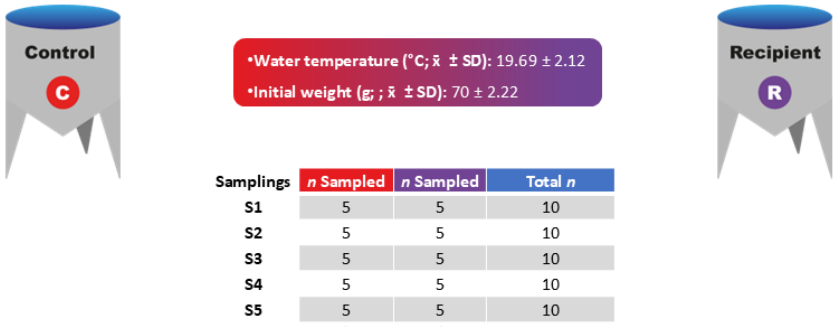

Samplings	*n* Sampled	*n* Sampled	Total *n*
S1	5	5	10
S2	5	5	10
S3	5	5	10
S4	5	5	10
S5	5	5	10

Samplings	*Sparus aurata* used for analyses (*n*)				
	Proteome Analysis	Validation Assays			
		Haemoglobin	Cholesterol	Alternative Complement Activity	Biotin
S1	0	10	10	10	10
S2	0	10	10	10	10
S3	0	10	10	10	10
S4	2	10	10	10	10
S5	3	10	10	10	10

Samplings	*Sparus aurata* used for analyses (*n*)						
	Proteome Analysis			Validation Assays			
	L	M	H	Haemoglobin	Cholesterol	Alternative Complement Activity	Biotin
S1	3	1	0	10	10	10	10
S2	0	1	0	10	10	10	10
S3	2	1	3	10	10	10	10
S4	0	1	2	10	10	10	10
S5	0	1	0	7	7	7	7

Figure S1. Schematic representation of the samples taken in each samping and their downstream use.

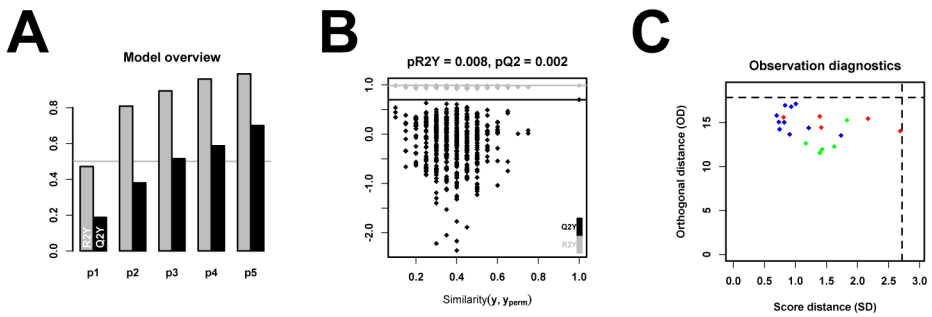

Figure S2. Partial least squares discriminant analysis model overview depicting the optimal number of components used to build the model (p1-p5). **A:** The Y axis represents the cumulative fit (R2Y) and prediction (Q2Y) coefficients for each of the components. **B, C:** Validation of the model (permutation test, 500 permutations) to estimate R2Y and Q2Y significance. **B:** pR2Y and pQ2 are considered significant at < 0.05. **C:** Observation diagnostics was performed to detect outliers by plotting the score and orthogonal distances of each sample (red = control fish; blue = fish with low/medium infection degree; green = fish with high infection degree). No outliers were detected in this model.

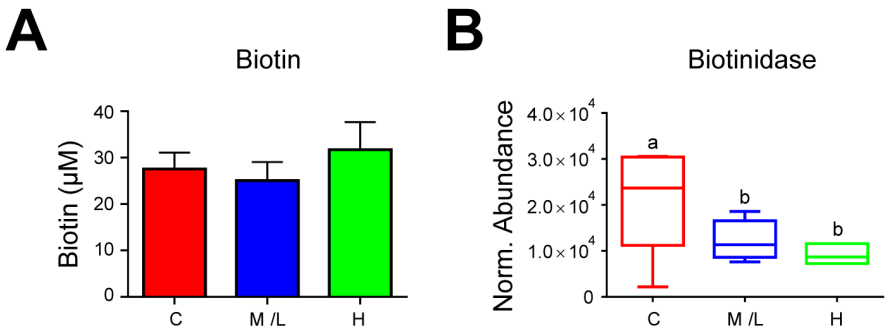

Figure S3. A: Plasma biotin values measured in control (C, n = 50) and *Sparicotyle chrysophrii* infected fish with a medium/low (M/L, n = 27) and high (H, n = 10) infection degree. **B:** Normalised protein abundance values of biotinidase measured by proteomics in plasma samples of control (C, n = 5), medium/low (M/L, n = 10), and high (H, n = 5) infection groups. Values are represented as mean ± SEM and statistical differences among groups are noted with different letters (Kruskall-Wallis test, $p < 0.05$).

Table S1. List of proteins with VIP value > 1 responsible for the separation of groups in the PLS-DA model presented in **Figure 1** ordered by the corresponding cluster from the k-means analysis (**Figure 2**). The group mean normalised abundance values are shown on the right.

VIP value	Cluster	Protein	C	H	ML
1.749	A	Apolipoprotein B-100	15650721	2853649	3106166
1.600	A	Immunoglobulin light chain, partial	705514.3	255963.8	351235.7
1.577	A	Platelet glycoprotein Ib alpha chain-like	612497.3	418105.2	271711.3
1.485	A	Killer cell immunoglobulin-like receptor 2DL4	101704.1	41156.09	32261.75
1.408	A	Biotinidase	21384.02	9260.471	12168.53
1.373	A	Apolipoprotein A-IV-like	2377271	1436581	982063.9
1.319	A	Immunoglobulin heavy chain V region 186-1	514391.6	315670	258341.9
1.306	A	Hemopexin	21644096	13427939	11241985
1.264	A	Immunoglobulin kappa light chain-like	199527.9	72001.2	21649.43
1.256	A	Peptidyl-prolyl cis-trans isomerase	38122.49	20402.39	22906.58
1.255	A	Immunoglobulin kappa chain V-IV region JI	93082.68	53880.41	30955.65
1.218	A	Immunoglobulin lambda-1 light chain-like	114112.6	25295.57	31873.79
1.173	A	Immunoglobulin heavy chain V region 23	353691.1	206261.8	199232.3
1.172	A	Immunoglobulin kappa chain V-V region	268800.8	98838.61	121181.8
1.111	A	Immunoglobulin kappa chain V region 3315	1069890	537224.6	526468
1.110	A	Immunoglobulin kappa chain V region	158039.7	40964.35	41309.85
1.087	A	Immunoglobulin light chain precursor	213977.7	146501.5	89777.41
1.073	A	Immunoglobulin lambda chain V-I region NIG-64	154849.5	85707.69	67089.98
1.054	A	Immunoglobulin kappa chain V-III region SIE	66487.71	23077.73	30993.59
1.003	A	Protein phosphatase 1 regulatory subunit 37	14991.03	6387.5	8672.204
1.824	B	2,3-bisphosphoglycerate 3-phosphatase	153762.6	217354	41436.1
1.706	B	Complement factor H-like	3578049	3668095	2406683
1.571	B	Acidic mammalian chitinase-like	270862	193523	133958.3
1.549	B	Complement component C7-like	4583971	4078644	3183155
1.527	B	Immunoglobulin lambda chain C region	51555.9	88978.28	47795.84
1.462	B	Complement C8 alpha chain	2908566	2678801	2215124
1.445	B	Complement component 8 subunit beta	4036038	4080879	3217344
1.419	B	Complement component C6	359952.8	259580	193489.2
1.417	B	Immunoglobulin kappa chain V region 3315	33896	49399.85	11407.88
1.411	B	Complement component C8 gamma chain	1205956	1153823	904403.1
1.359	B	Insulin like growth factor binding protein acid labile subunit	4267582	3683416	3015556
1.355	B	Basement membrane-specific heparan sulfate proteoglycan core protein-like	1434326	1576110	1096872
1.348	B	Complement factor I-like	192779.6	263356.7	141555
1.287	B	Phospholipase A2	257120.7	284190.8	208180.9
1.286	B	Complement factor B-like	1197943	813517.4	841825
1.275	B	Cyclin dependent kinase like 1	100613.6	139448.8	79973.81
1.271	B	Sushi domain-containing protein 1	3798636	4329887	2828029
1.255	B	Prostaglandin D2 synthase a	314562.8	323528.2	239822.4
1.253	B	Inter-alpha-trypsin inhibitor heavy chain H3-like	16862232	18944199	12948488
1.243	B	Complement C5	18840283	20327820	15177107
1.242	B	Complement factor H-like	5322873	4609994	3583831
1.234	B	Inter-alpha-trypsin inhibitor heavy chain 2	7163381	6068062	5689793
1.232	B	Immunoglobulin lambda-like polypeptide 5	359731.7	283724.7	232056.7
1.231	B	Galactose-specific lectin nattectin-like	113821.3	153919.6	100149.1
1.209	B	Christmas factor	5087223	7040451	4262606
1.195	B	Coagulation factor X-like	72864.8	122185.2	93096.52
1.182	B	Carboxylic ester hydrolase	680037.9	607526.1	452275.9

Table S1. (continued).

VIP value	Cluster	Protein	C	H	ML
1.180	B	Complement C3-like	4126098	2872202	3022169
1.156	B	Myosin-1-like	7330906	7888413	4829019
1.138	B	Serotransferrin	4.71E+08	5.89E+08	5.37E+08
1.135	B	Inter-alpha-trypsin inhibitor heavy chain H3-like	42881682	47900243	39309501
1.118	B	Serpin family G member 1	7255642	4870776	5057112
1.117	B	Cholesteryl ester transfer protein	2943214	2822766	2348301
1.111	B	Complement factor B-like	3861740	3320922	2774434
1.110	B	Sulfhydryl oxidase	515034.8	441054	396821.7
1.110	B	Ectonucleotide pyrophosphatase/phosphodiesterase family member 2	646801.4	500087.9	543631.5
1.101	B	Ovostatin	26765033	23112233	23044901
1.097	B	Coagulation factor V	2560959	2111352	2173467
1.077	B	Alpha-2-macroglobulin-like	10411204	11025940	9234581
1.074	B	Alpha-2-HS-glycoprotein-like	55584.39	39950.23	37957.38
1.056	B	Serpin family D member 1	7397831	7160459	6456337
1.039	B	Hepatocyte growth factor-like protein	1151480	1516996	1325491
1.034	B	Immunoglobulin kappa variable 4-1	145983	208288.7	73136.23
1.033	B	Apolipoprotein H	953985.2	797190.9	747958.3
1.014	B	Uncharacterized protein LOC108889753	1276167	801556.4	845196.8
1.000	B	Fibrinopeptide A	8923972	11272343	4764393
1.698	C	Saxitoxin and tetrodotoxin-binding protein 1-like	9998238	4924539	8607888
1.670	C	Apolipoprotein C-I-like	1338215	1147903	2407684
1.505	C	Protein LEG1 homolog	183581.4	133910.2	274659.2
1.493	C	Coagulation factor VII	398683.4	387651.1	553589.3
1.450	C	Alpha-2 globin	3561864	592452.5	2417036
1.442	C	Uncharacterized protein LOC115583141	1156159	863145.7	1463174
1.433	C	Alpha-1 globin	4142623	1589915	5687422
1.424	C	Hemoglobin subunit beta-like	3394669	1133597	4143733
1.283	C	Apolipoprotein H	2002979	1129237	1778221
1.274	C	Carboxypeptidase N subunit 2	317178.9	235677.6	279535.4
1.263	C	Apolipoprotein M	254037.1	226413.6	288220.6
1.261	C	Immunoglobulin kappa chain V-III region	105746	40991.93	79304.14
1.257	C	Calcium/calmodulin-dependent protein kinase	544540	352144.6	770038.8
1.235	C	Ladderlectin-like	94082.61	54334.81	89147.1
1.234	C	Hyaluronan binding protein 2	3374656	2948974	4898173
1.229	C	Pentaxin	15583403	13984587	19428874
1.224	C	Alpha-1-antiproteinase-like	752086.7	573835.9	750395.3
1.206	C	Complement C3-like	30778454	24860259	28505545
1.186	C	Uncharacterized protein LOC108874211	433479.1	269948.1	399954.2
1.183	C	Complement C3-like	9512726	9716328	12539872
1.178	C	Alpha-2-macroglobulin-P-like	28300909	20289060	23020769
1.160	C	Apolipoprotein A-I-like	482404.9	450823	944918.4
1.159	C	Complement C1q subcomponent subunit A	167280.1	63589.21	143693.9
1.154	C	Ceruloplasmin	7134971	4456076	6925239
1.133	C	Uncharacterized protein LOC102308728	230092.9	112486.7	346737.9
1.132	C	Complement C5	50442.95	25131.46	64959.86
1.125	C	Beta globin	3239509	769684.5	2615011
1.120	C	Ceruloplasmin	294468.5	294120.5	458973.9
1.119	C	Glutathione peroxidase	723473.2	776164.8	931343.7
1.109	C	Catechol O-methyltransferase domain-containing protein 1-like	384420.9	287203.7	465685.4

Table S1. (continued)

VIP value	Cluster	Protein	C	H	ML
1.105	C	Complement C3-like	54825324	43696304	50855239
1.104	C	Complement C3-like	5942156	4003954	7055740
1.104	C	Apolipoprotein A-II	91473117	67653090	95688137
1.097	C	Uncharacterized protein LOC100691126	38499.15	23304.7	30577.6
1.077	C	Integrin beta-1-like	549273.7	412130.3	478066.2
1.063	C	Hyaluronan-binding protein 2-like	71458474	54203754	65973105
1.059	C	Apolipoprotein M	2301506	2105953	2898012
1.055	C	Actin beta	188369	155499.3	313216.6
1.032	C	Fetuin-B-like	21570963	19432646	29567175
1.021	C	Complement C4-like	5528011	3591302	4960030
1.019	C	Fibronectin-like	15871918	8058888	15700710
1.633	D	Leukocyte cell-derived chemotaxin-2	365018	501245.7	749523.9
1.620	D	Estrogen-regulated protein	162535.9	451225.4	482598.8
1.459	D	Apolipoprotein A-IV-like	3237784	5667434	10081092
1.387	D	Eukaryotic translation initiation factor 3 subunit J	72767.47	171827	365856.7
1.373	D	L-rhamnose-binding lectin CSL2	20689.91	46556.79	36153.55
1.342	D	Pentraxin fusion protein-like	6525636	18378878	23681835
1.336	D	Apolipoprotein Eb	793071.8	1165132	1461142
1.310	D	Uncharacterized protein LOC115590787	1743951	2286005	2429043
1.302	D	Cephalotoxin-like protein	45697.47	89813.68	159024.5
1.299	D	Alpha-1-microglobulin	43310.22	85237.14	79460.37
1.283	D	Hibernation-specific plasma protein HP-55	595725.7	3257283	1387781
1.268	D	Uncharacterized protein LOC115567382	544909.1	529826.4	1472558
1.251	D	Intercellular adhesion molecule 5	119908.3	130199.4	287460.9
1.203	D	Uncharacterized protein LOC109958385	320757.6	377113.2	509328.7
1.143	D	Immunoglobulin heavy chain V-III region VH26	14189.97	22889.11	43284.68
1.128	D	Apolipoprotein A-I	597464.4	1336229	3260891
1.124	D	Intercellular adhesion molecule 1	85630.28	117256.4	153803.9
1.104	D	Complement C6	71660.89	128460	140574.2
1.075	D	Saxitoxin and tetrodotoxin-binding protein 1 Precursor	2126130	2750834	3386555
1.069	D	Fetuin B	34011.1	53064.51	77467.53
1.031	D	Apolipoprotein C-II	441958.2	728909.3	929008.3
1.007	D	Si:ch1073-126c3.2	14124.34	20664.46	33547.54

The proteomics data has been deposited in the PRIDE repository, with the dataset identifier PXD034541.

References

1. Repullés-Albelda A, Raga JA, Montero FE. Post-larval development of the microcotylid monogenean *Sparicotyle chrysophrii* (Van Beneden and Hesse, 1863): comparison with species of Microcotylidae and Heteraxinidae. Parasitol Int. 2011;60:512–20.

2. Repullés-Albelda A, Holzer AS, Raga JA, Montero FE. Oncomiracidial development, survival and swimming behaviour of the monogenean *Sparicotyle chrysophrii* (Van Beneden and Hesse, 1863). Aquaculture. 2012;338–341:47–55.

3. Mladineo I. Parasite communities of Adriatic cage-reared fish. Dis Aquat Organ. 2005;64:77–83.

4. Sánchez-García N, Raga JA, Montero FE. Risk assessment for parasites in cultures of *Diplodus puntazzo* (Sparidae) in the Western Mediterranean: prospects of cross infection with *Sparus aurata*. Vet Parasitol. 2014;204:120–33.

5. Mladineo I, Maršić-Lučić J. Host switch of *Lamellodiscus elegans* (Monogenea: Monopisthocotylea) and *Sparicotyle chrysophrii* (Monogenea: Polyopisthocotylea) between cage-reared sparids. Vet Res Commun. 2007;31:153–60.

6. Mladineo I, Šegvić T, Grubišić L. Molecular evidence for the lack of transmission of the monogenean *Sparicotyle chrysophrii* (Monogenea, Polyopisthocotylea) and isopod *Ceratothoa oestroides* (Crustacea, Cymothoidae) between wild bogue (*Boops boops*) and cage-reared seabream (*Sparus aurata*) and sea bass (*Dicentrarchus labrax*). Aquaculture. 2009;295:160–7.

7. Katharios P, Papandroulakis N, Divanach P. Treatment of *Microcotyle* sp. (Monogenea) on the gills of cage-cultured red porgy, *Pagrus pagrus* following baths with formalin and mebendazole. Aquac Eng. 2006;251:167–71.

8. Federation of European aquaculture producers- FEAP. European Aquaculture Production Report- 2014-2019. 2020 [cited 2022 Mar 7]. Available from: https://feap.info/wp-content/uploads/2020/10/20201007_feap-production-report-2020.pdf.

9. Sitjà-Bobadilla A, de Felipe MC, Álvarez-Pellitero P. *In vivo* and *in vitro* treatments against *Sparicotyle chrysophrii* (Monogenea: Microcotylidae) parasitizing the gills of gilthead sea bream (*Sparus aurata* L.). Aquaculture. 2006;261:856–64.

10. Sitjà-Bobadilla A, Álvarez-Pellitero P. Experimental transmission of *Sparicotyle chrysophrii* (Monogenea: Polyopisthocotylea) to gilthead seabream (*Sparus aurata*) and histopathology of the infection. Folia Parasitol. 2009;56:143–51.

11. Fioravanti ML, Mladineo I, Palenzuela O, Beraldo P, Massimo M, Gustinelli A, et al. Fish farmer's guide to combating parasitic infections in European sea bass and gilthead sea bream aquaculture. ParaFishControl. 2020 [cited 2022 Mar 3]. Available from: https://www.parafishcontrol.eu/parafishcontrol-results/parafishcontrol-deliverables.

12. Mladineo I, Trumbić Ž, Ormad-García A, Palenzuela O, Sitjà-Bobadilla A, Manuguerra S, et al. *In vitro* testing of alternative synthetic and natural antiparasitic compounds against the monogenean *Sparicotyle chrysophrii*. Pathogens. 2021;10:980.

13. Merella P, Montero FE, Burreddu C, Garippa G. In-feed trials of fenbendazole and other chemical/natural compounds against *Sparicotyle chrysophrii* (Monogenea) infections in *Sparus aurata* (Osteichthyes). Aquac Res. 2021;52:5908–11.

14. Bögner D, Bögner M, Schmachtl F, Bill N, Halfer J, Slater MJ. Hydrogen peroxide oxygenation and disinfection capacity in recirculating aquaculture systems. Aquac Eng. 2021;92:102140.

15. European Chemicals Agency- ECHA. Formaldehyde and formaldehyde releasers- Strategy for future work. 2018 [cited 2022 Mar 15]. Available from: https://echa.europa.eu/documents/10162/17233/formaldehyde_review_report_en.pdf/551df4a2-28c4-2fa9-98ec-c8d53e2bf0fc?t=1516170136797.

16. European Chemicals Agency - ECHA. Substance evaluation conclusion as require by REACH article 48 and evaluation report for formaldehyde. 2019 [cited 2022 Mar 15]. Available from: https://echa.europa.eu/documents/10162/cc0acabf-6e82-f2ed-5dbe-8058f48ce6c4.

17. Leal JF, Neves MGPMS, Santos EBH, Esteves VI. Use of formalin in intensive aquaculture: properties, application and effects on fish and water quality. Rev Aquac. 2018;10:281–95.

18. Henry MA, Nikoloudaki C, Tsigenopoulos C, Rigos G. Strong effect of long-term *Sparicotyle chrysophrii* infection on the cellular and innate immune responses of gilthead sea bream, *Sparus aurata*. Dev Comp Immunol. 2015;51:185–93.

19. Piazzon MC, Mladineo I, Naya-Català F, Dirks RP, Jong-Raadsen S, Vrbatović A, et al. Acting locally- Affecting globally: RNA sequencing of gilthead sea bream with a mild *Sparicotyle chrysophrii* infection reveals effects on apoptosis, immune and hypoxia related genes. BMC Genomics. 2019;20:1–16.

20. Liu RD, Cui J, Liu XL, Jiang P, Sun GG, Zhang X, et al. Comparative proteomic analysis of surface proteins of *Trichinella spiralis* muscle larvae and intestinal infective larvae. Acta Trop. 2015;150:79–86.

21. Suttiprapa S, Sotillo J, Smout M, Suyapoh W, Chaiyadet S, Tripathi T. *Opisthorchis viverrini* proteome and host - parasite interactions. Adv Parasitol. 2018;102:45-72.

22. Cui S, Xu L, Zhang T, Xu M, Yao J, Fang C, et al. Proteomic characterization of larval and adult developmental stages in *Echinococcus granulosus* reveals novel insight into host – parasite interactions. J Proteomics. 2013;84:158–75.

23. Tu V, Mayoral J, Sugi T, Tomita T, Han B, Weiss LM. Enrichment and proteomic characterization of the cyst wall from *in vitro* T*oxoplasma gondii* cysts. MBio. 2019;10:1–15.

24. Marzano V, Pane S, Foglietta G, Mortera SL, Vernocchi P, Muda AO, et al. Mass spectrometry based-proteomic analysis of *Anisakis* spp.: a preliminary study towards a new diagnostic tool. Genes. 2020;11:1–18.

25. Zhang FK, Hu RS, Elsheikha HM, Sheng ZA, Zhang WY, Zheng W bin, et al. Global serum proteomic changes in water buffaloes infected with *Fasciola gigantica*. Parasite Vector. 2019;12:281.

26. Zhou C, Xie S, Li M, Huang C, Zhou H, Cong H. Analysis of the serum peptidome associated with *Toxoplasma gondii* infection. J Proteomics. 2020;222:1–9.

27. Gillis-Germitsch N, Kockmann T, Kapel CMO, Thamsborg SM, Webster P, Tritten L, et al. Fox serum proteomics analysis suggests host-specific responses to *Angiostrongylus vasorum* infection in canids. Pathogens. 2021;10:1–16.

28. Raza A, Schulz BL, Nouwens A, Jackson LA, Piper EK, James P, et al. Serum proteomes of Santa Gertrudis cattle before and after infestation with *Rhipicephalus australis* ticks. Parasite Immunol. 2021;43:1–13.

29. Kuleš J, Lovrić L, Gelemanović A, Ljubić BB, Rubić I, Bujanić M, et al. Complementary liver and serum protein profile in wild boars infected by the giant liver fluke *Fascioloides magna* using tandem mass tags quantitative approach. J Proteomics. 2021;247:104332.

30. Riera-Ferrer E, Estensoro I, Del Pozo R, Piazzon MC, Moreno-Estruch P, Sitjà-Bobadilla A, et al. A non-lethal approach upon *Sparicotyle chrysophrii* burden prediction in gilthead sea bream (*Sparus aurata*), Aquaculture Europe 2021, Madeira, Portugal, Book of abstracts 2021 p. 1093.

31. Pérez-Sánchez J, Naya-Català F, Soriano B, Piazzon MC, Hafez A, Gabaldón T, et al. Genome sequencing and transcriptome analysis reveal recent species-specific gene duplications in the plastic gilthead sea bream (*Sparus aurata*). Front Mar Sci. 2019;6:1–18.

32. Tsou CC, Avtonomov D, Larsen B, Tucholska M, Choi H, Gingras AC, et al. DIA-Umpire: comprehensive computational framework for data-independent acquisition proteomics. Nat Methods. 2015;12:258–64.

33. Sitjà-Bobadilla A, Peña-Llopis S, Gómez-Requeni P, Médale F, Kaushik S, Pérez-Sánchez J. Effect of fish meal replacement by plant protein sources on non-specific defence mechanisms and oxidative stress in gilthead sea bream (*Sparus aurata*). Aquaculture. 2005;249:387–400.

34. Thévenot EA, Roux A, Xu Y, Ezan E, Junot C. Analysis of the human adult urinary metabolome variations with age, body mass index, and gender by implementing a comprehensive workflow for univariate and OPLS statistical analyses. J Proteome Res. 2015;14:3322–35.

35. Wold S, Sjöström M, Eriksson L. PLS-regression: a basic tool of chemometrics. Chemom Intell Lab Syst. 2001;58:109–30.

36. Kieffer DA, Piccolo BD, Vaziri ND, Liu S, Lau WL, Khazaeli M, et al. Resistant starch alters gut microbiome and metabolomic profiles concurrent with amelioration of chronic kidney disease in rats. Am J Physiol- Ren Physiol. 2016;310:F857–71.

37. Li H, Ma ML, Luo S, Zhang RM, Han P, Hu W. Metabolic responses to ethanol in *Saccharomyces cerevisiae* using a gas chromatography tandem mass spectrometry-based metabolomics approach. Int J Biochem Cell Biol. 2012;44:1087–96.

38. Ge SX, Son EW, Yao R. iDEP: An integrated web application for differential expression and pathway analysis of RNA-Seq data. BMC Bioinformatics. 2018;19:1–24.

39. Yu G, He QY. ReactomePA: An R/Bioconductor package for reactome pathway analysis and visualization. Mol Biosyst. 2016;12:477–9.

40. Kearn GC. Evolutionary expansion of the Monogenea. Int J Parasitol. 1994;24:1227–71.

41. Poulin R. The evolution of monogenean diversity. Int J Parasitol. 2002;32:245–54.

42. Llewellyn J. Observations on the food and the gut pigment of the polyopisthocotylea (Trematoda: Monogenea). Parasitology. 1954;44:428–37.

43. Halton DW, Jennings JB. Observations on the nutrition of monogenetic trematodes. Biol Bull. 1965;129:257–72.

44. Riera-Ferrer E, Estensoro I, Piazzon MC, del Pozo R, Palenzuela O, Sitjà-Bobadilla A. Unveiling the blood-feeding behaviour of the gill parasite *Sparicotyle chrysophrii*. 20th International Conference on Diseases of Fish and Shellfish. Book of abstracts 2021. p. 35.

45. Kristiansson A, Gram M, Flygare J, Hansson SR, Åkerström B, Storry JR. The role of α1-microglobulin (A1M) in erythropoiesis and erythrocyte homeostasis— Therapeutic opportunities in hemolytic conditions. Int J Mol Sci. 2020;21:1–22.

46. Smith SA, Travers RJ, Morrissey JH. How it all starts: initiation of the clotting cascade. Crit Rev Biochem Mol Biol. 2015;50:326–36.

47. He S, Cao H, Thålin C, Svensson J, Blombäck M, Wallén H. The clotting trigger is an important determinant for the coagulation pathway *in vivo* or *in vitro*-inference from data review. Semin Thromb Hemost. 2021;47:63–73.

48. Tavares-Dias M, Oliveira SR. A review of the blood coagulation system of fish. Brazilian J Biosci. 2009;7:205–24.

49. Parizi LF, Ali A, Tirloni L, Oldiges DP, Sabadin GA, Coutinho ML, et al. Peptidase inhibitors in tick physiology. Med Vet Entomol. 2018;32:129–44.

50. Kotál J, Polderdijk SGI, Langhansová H, Ederová M, Martins LA, Beránková Z, et al. *Ixodes ricinus* salivary serpin iripin-8 inhibits the intrinsic pathway of coagulation and complement. Int J Mol Sci. 2021;22:9480.

51. Ehebauer MT, Mans BJ, Gaspar ARM, Neitz AWH. Identification of extrinsic blood coagulation pathway inhibitors from the tick *Ornithodoros savignyi* (Acari: Argasidae). Exp Parasitol. 2002;101:138–48.

52. Cappellini MD. Coagulation in the pathophysiology of hemolytic anemias. Am Soc Hematol. 2007;74–8.

53. Yuskiv LL, Yuskiv ID. The lipid metabolism in carp during invasion by the tapeworm *Bothriocephalus acheilognathi*. Regul Mech Biosyst. 2020;11:214–9.

54. Luján HD, Mowatr MR, Byrd LG, Nash TE. Cholesterol starvation induces differentiation of the intestinal parasite *Giardia lamblia*. Proc Natl Acad Sci USA. 1996;93:7628–33.

55. Coppens I, Sinai AP, Joiner KA. *Toxoplasma gondii* exploits host low-density lipoprotein receptor- mediated endocytosis for cholesterol acquisition. J Cell Biol. 2000;149:167–80.

56. Sonda S, Ting LM, Novak S, Kim K, Maher JJ, Farese R v., et al. Cholesterol esterification by host and parasite is essential for optimal proliferation of *Toxoplasma gondii*. J Biol Chem. 2001;276:34434–40.

57. Pucadyil TJ, Tewary P, Madhubala R, Chattopadhyay A. Cholesterol is required for *Leishmania donovani* infection: implications in leishmaniasis. Mol Biochem Parasitol. 2004;133:145–52.

58. Bansal D, Bhatti HS, Sehgal R. Role of cholesterol in parasitic infections. Lipids Health Dis. 2005;4:1–7.

59. Stanley RG, Jackson CL, Griffiths K, Doenhoff MJ. Effects of *Schistosoma mansoni* worms and eggs on circulating cholesterol and liver lipids in mice. Atherosclerosis. 2009;207:131–8.

60. Rivero MR, Miras SL, Quiroga R, Rópolo AS, Touz MC. *Giardia lamblia* low-density lipoprotein receptor-related protein is involved in selective lipoprotein endocytosis and parasite replication. Mol Microbiol. 2011;79:1204–19.

61. Magen E, Bychkov V, Ginovker A, Kashuba E. Chronic *Opisthorchis felineus* infection attenuates atherosclerosis - an autopsy study. Int J Parasitol. 2013;43:819–24.

62. O'neal AJ, Butler LR, Rolandelli A, Gilk SD, Pedra JHF. Lipid hijacking: a unifying theme in vector-borne diseases. eLife. 2020;9:1–31.

63. Tokumasu F, Hayakawa EH, Fukumoto J, Tokuoka SM, Miyazaki S. Creative interior design by *Plasmodium falciparum*: lipid metabolism and the parasite's secret chamber. Parasitol Int. 2021;83:102369.

64. Barrett J. Nutrition and Biosynthesis. In: Biochemistry of Parasitic Helminths. 1st ed. London and Basingstoke: Macmillan Publishers Ltd; 1981. p. 149–244.

65. Vorel J, Cwiklinski K, Roudnický P, Ilgová J, Jedličková L, Dalton JP, et al. *Eudiplozoon nipponicum* (Monogenea, Diplozoidae) and its adaptation to haematophagy as revealed by transcriptome and secretome profiling. BMC Genomics. 2021;22:274.

66. Lombardo JF, Pórfido JL, Sisti MS, Giorello AN, Rodríguez S, Córsico B, et al. Function of lipid binding proteins of parasitic helminths: still a long road. Parasitol Res. 2022;121:1117–29.

67. Schrama D, Richard N, Silva TS, Figueiredo FA, Conceição LEC, Burchmore R, et al. Enhanced dietary formulation to mitigate winter thermal stress in gilthead sea bream (*Sparus aurata*): a 2D-DIGE plasma proteome study. Fish Physiol Biochem. 2017;43:603–17.

68. Diógenes AF, Teixeira C, Almeida E, Skrzynska A, Costas B, Oliva-Teles A, et al. Effects of dietary tryptophan and chronic stress in gilthead seabream (*Sparus aurata*) juveniles fed corn distillers dried grains with solubles (DDGS) based diets. Aquaculture. 2019;498:396–404.

69. Benedito-Palos L, Ballester-Lozano GF, Simó P, Karalazos V, Ortiz Á, Calduch-Giner J, et al. Lasting effects of butyrate and low FM/FO diets on growth performance, blood haematology/biochemistry and molecular growth-related markers in gilthead sea bream (*Sparus aurata*). Aquaculture. 2016;454:8–18.

70. Bayly GR. Lipids and disorders of lipoprotein metabolism. In: Marshall WJ, Lapsley M, Day AP, Ayling RM, editors. Clinical Biochemistry: Metabolic and Clinical Aspects. 3rd ed. London: Churchill Livingstone; 2014. p. 702–36.

71. Nelson DL, Cox MM. Lipid Biosynthesis. In: Lehninger Principles of Biochemistry. 7th ed. New York: Macmillan Learning; 2017.

72. Bennett MW, Caulfield JP. Specific binding of human low-density lipoprotein to the surface of schistosomula of *Schistosoma mansoni* and ingestion by the parasite. Am J Pathol. 1991;138:1173–82.

73. Han R. Plasma lipoproteins are important components of the immune system. Microbiol Immunol. 2010;54:246–53.

74. Norata GD, Pirillo A, Ammirati E, Catapano AL. Emerging role of high density lipoproteins as a player in the immune system. Atherosclerosis. 2012;220:11–21.

75. Grao-Cruces E, Lopez-Enriquez S, Martin ME, Montserrat-de la Paz S. High-density lipoproteins and immune response: a review. Int J Biol Macromol. 2022;195:117–23.

76. Van der Stoep M, Korporaal SJA, van Eck M. High-density lipoprotein as a modulator of platelet and coagulation responses. Cardiovasc Res. 2014;103:362–71.

77. Buchmann K. Antiparasitic immune responses. In: Buchmann K, Secombes CJ, editors. Principles of fish immunology: from cells and molecules to host protection. 1st ed. Gewerbestrasse: Springer Nature Switzerland AG. 2022. p. 535–63.

78. Zhou S, Li WX, Zou H, Zhang J, Wu SG, Li M, et al. Expression analysis of immune genes in goldfish (*Carassius auratus*) infected with the monogenean parasite *Gyrodactylus kobayashii*. Fish Shellfish Immunol. 2018;77:40–5.

79. Zhang C, Li DL, Chi C, Ling F, Wang GX. *Dactylogyrus intermedius* parasitism enhances *Flavobacterium columnare* invasion and alters immune-related gene expression in *Carassius auratus*. Dis Aquat Organ. 2015;116:11–21.

80. Gettins PGW. Serpin structure, mechanism, and function. Chem Rev. 2002;102:4751–803.

81. Law RHP, Zhang Q, McGowan S, Buckle AM, Silverman GA, Wong W, et al. An overview of the serpin superfamily. Genome Biol. 2006;7:1–11.

82. Huntington JA. Serpin structure, function and dysfunction. J Thromb Haemost. 2011;9:26–34.

83. Sanrattana W, Maas C, de Maat S. SERPINs-From trap to treatment. Front Med. 2019;6:1–8.

84. Knox DP. Proteinase inhibitors and helminth parasite infection. Parasite Immunol. 2007;29:57–71.

85. Molehin AJ, Gobert GN, McManus DP. Serine protease inhibitors of parasitic helminths. Parasitology. 2012;139:681–95.

86. Bao J, Pan G, Poncz M, Wei J, Ran M, Zhou Z. Serpin functions in host-pathogen interactions. PeerJ. 2018;2018:1–16.

87. Pham CTN. Neutrophil serine proteases: specific regulators of inflammation. Nat Rev Immunol. 2006;6:541–50.

88. Rau JC, Mitchell JW, Fortenberry YM, Church FC. Heparin cofactor II: discovery, properties, and role in controlling vascular homeostasis. Semin Thromb Hemost. 2011;37:339–48.

89. Beinrohr L, Murray-Rust TA, Dyksterhuis L, Závodszky P, Gál P, Pike RN, et al. Serpins and the complement system. Methods Enzymol. 2011;499:55–75.

90. Rossi V, Bally I, Lacroix M, Arlaud GJ, Thielens NM. Classical complement pathway components C1r and C1s: Purification from human serum and in recombinant form and functional characterization. Methods Mol Biol. 2014;1100:43–60.

91. Mutch NJ. Regulation of fibrinolysis by platelets. In: Michelson AD, Cattaneo M, Frelinger AL, Newman PJ, editors. Platelets. 4th ed. Cambridge: Academic Press; 2019. p. 417–31.

92. Yamamoto K, Yoshida K, Miyagoe Y, Ishikawa A, Hanaoka K, Nomoto S, et al. Quantitative evaluation of expression of iron-metabolism genes in ceruloplasmin-deficient mice. Biochim Biophys Acta. 2002;1588:195–202.

93. Das S, Sahoo PK. Ceruloplasmin, a moonlighting protein in fish. Fish Shellfish Immunol. 2018;82:460–8.

94. Orzheshkovskyi VV, Trishchynska MA. Ceruloplasmin: its role in the physiological and pathological processes. Neurophysiology. 2019;51:141–9.

95. Osikov MV, Makarov EV, Krivokhizhina LV. Ceruloplasmin prevents hemostatic disorders during experimental hyperammonemia. Bull Exp Biol Med. 2006;142:416–8.

Chapter 5

Mucosal affairs: Glycosylation and expression changes of gill goblet cells and mucins in a fish–polyopisthocotylan interaction

Enrique Riera-Ferrer, Raquel Del Pozo, Uxue Muñoz-Berruezo, Oswaldo Palenzuela, Ariadna Sitjà-Bobadilla, Itziar Estensoro and M. Carla Piazzon

Fish Pathology Group, Institute of Aquaculture Torre de la Sal (IATS, CSIC), Consejo Superior de Investigaciones Científicas, Castellón, Spain

Frontiers in Veterinary Science, 09 April 2024
https://doi.org/10.3389/fvets.2024.1347707

Abstract

Secreted mucins are highly O-glycosylated glycoproteins produced by goblet cells in mucosal epithelia. They constitute the protective viscous gel layer overlying the epithelia and are involved in pathogen recognition, adhesion and expulsion. The gill polyopisthocotylan ectoparasite *Sparicotyle chrysophrii*, feeds on gilthead seabream (*Sparus aurata*) blood eliciting severe anaemia.

Control unexposed and recipient (R) gill samples of gilthead seabream experimentally infected with *S. chrysophrii* were obtained at six consecutive times (0, 11, 20, 32, 41, and 61 days post-exposure (dpe)). In histological samples, goblet cell numbers and their intensity of lectin labelling was registered. Expression of nine mucin genes (*muc2*, *muc2a*, *muc2b*, *muc5a/c*, *muc4*, *muc13*, *muc18*, *muc19*, *imuc*) and three regulatory factors involved in goblet cell differentiation (*hes1*, *elf3*, *agr2*) was studied by qPCR. In addition, differential expression of glycosyltransferases and glycosidases was analysed *in silico* from previously obtained RNAseq datasets of *S. chrysophrii*-infected gilthead seabream gills with two different infection intensities.

Increased goblet cell differentiation (up-regulated *elf3* and *agr2*) leading to neutral goblet cell hyperplasia on gill lamellae of R fish gills was found from 32 dpe on, when adult parasite stages were first detected. At this time point, acute increased expression of both secreted (*muc2a*, *muc2b*, *muc5a/c*) and membrane-bound mucins (*imuc*, *muc4*, *muc18*) occurred in R gills. Mucins did not acidify during the course of infection, but their glycosylation pattern varied towards more complex glycoconjugates with sialylated, fucosylated and branched structures, according to lectin labelling and the shift of glycosyltransferase expression patterns. Gilthead seabream gill mucosal response against *S. chrysophrii* involved neutral mucus hypersecretion, which could contribute to worm expulsion and facilitate gas exchange to counterbalance parasite-induced hypoxia. Stress induced by the sparicotylosis condition seems to lead to changes in glycosylation characteristic of more structurally complex mucins.

Introduction

The barrier function of mucosal epithelia is structurally supported by the epithelial cell lining and in a more dynamic manner by the overlying mucus secretion, which is constantly flowing through renewal and off-sloughing. In fish, all exposed body surfaces, including skin, gills, nostrils, and digestive tract, are covered by mucosal epithelia, which constitute first line of defence against external offenders, friction, and dehydration and also participate in disease resistance, respiration, and ionic and osmotic regulation[1,2]. Thus, the role of mucosal health and mucous modulation should not be underestimated in the context of intensive aquaculture rearing systems in a global warming scenario, in which finfish health is under constant threat of imbalance.

The regulation of the mucus-secreting cells and mucus composition upon disease and infection[3–6], including parasitosis[7,8], is an appealing study topic in human medicine for its diagnostic and therapeutic value[9]. Mucus responses in fish skin, gills, and gut have also gathered research interest[10–16]. More specifically, gill parasites often provoked mucus over-secretion, as a host mucosal response intended to expel the parasite invader[17–21], but the fish host may have to deal with several drawbacks such as ion and gas exchange imbalance or microbiota dysbiosis.

The flatworm gill ectoparasite *Sparicotyle chrysophrii*, formerly classified in the Monogenea class and recently reclassified into the Polyopisthocotyla class[22], is currently considered the most distressing pathogen for gilthead seabream (*Sparus aurata*) Mediterranean aquaculture[23]. The high stocking densities, the lack of fallowing strategies, and the enzootic locations of the off-shore cage farms are favouring parasite outbreaks and transmission. The growing concern in regard to the production losses has directed recent research efforts toward studies on the parasites' biology[24–28], the host response[29–32], and the search for treatments[33–38]. However, a closer look at the modulation of the mucous secretion and the goblet cells in the gills of gilthead seabream during the course of this parasitosis has not been thoroughly taken.

Mucus is mainly produced by goblet cells, secretory cells present in the epithelial cell lining, which synthesise and expel secreted mucins, the main component of the adherent mucus gel. Mucins are high-molecular weight hydrophilic glycoproteins forming a complex matrix, in which water and a cocktail of bioactive molecules are retained, avoiding direct contact between the environment and tissue. By modulating the mucus layer physically (viscosity), biologically (immunoglobulin, lysozyme, antimicrobial peptide contents), and chemically (pH, mucin glycosylation), organisms are able to cope dynamically with the changing external stressors, including their own mucosal microbiota.

The mechanisms that orchestrate goblet cell proliferation, differentiation and distribution patterns, and mucin expression and glycosylation in fish upon parasite challenge are

still obscure. This study intends to integrate the study of goblet cell distribution patterns with their transcriptional regulation, together with mucin expression and glycosylation in the gills of gilthead seabream during the course of sparicotylosis using histochemical, lectin-binding, transcriptional, and transcriptomic approaches.

Materials and methods

Experimental setup and sample collection

Parasite-free, clinically healthy, gilthead seabream juveniles were purchased from a local fish farm and adapted to the indoor experimental facilities of IATS, CSIC under natural photoperiod and temperature conditions (40°5'N; 0°10'E). Along the whole experiment, sea water was 5 µm-filtered and UV-irradiated, salinity was 37.5‰, oxygen saturation was kept above 85%, and unionized ammonia below 0.02 mg·L^{-1}. *Sparicotyle chrysophrii* experimental infection was carried out as previously described by Riera-Ferrer et al.[39]. In brief, randomly selected recipient fish (R; n = 25; initial mean weight 138.40 g ± 22,84 SD) were allocated in a 200 L tank in a recirculating aquaculture system (RAS) connected to a tank with *S. chrysophrii*-infected donor fish. Control unexposed gilthead seabream (C; n = 20; initial mean weight 132.30 g ± 11.67 SD) were kept in a separate tank with open water flow, which was disconnected from RAS. The trial lasted for 61 days, and fish were lethally sampled six successive times: 0 days post exposure (dpe) (n = 5 C fish); 11 dpe, 20 dpe, 32 dpe, 41 dpe, and 61 dpe (n = 3 C fish and n = 5 R fish, in each sampling). Fish were culled by tricaine methanesulfonate (MS-222) overexposure (0.1 g·L^{-1}) and bled from the caudal vessels and tissue samples obtained for different purposes. The right gill arches of R fish were immediately examined under a stereomicroscope, and intensity and prevalence of *S. chrysophrii* infection were registered. A piece of the left gill arches was fixed in Bouin solution for histological processing, and parallel samples were taken in RNA later for gene expression analysis.

Mucin histochemistry and lecting labelling

Bouin-fixed gills were routinely dehydrated and paraffin-embedded. Sections of 4 µm thickness were stained with periodic acid Schiff (PAS)-alcian blue (pH 2.5), to identify neutral mucins (glycoproteins with oxidisable vicinal diols stained magenta) and acidic mucins (glycoproteins with carboxyl groups and *O*-sulfate esters stained blue) in all fish samples. Terminal glycoconjugates were analysed in selected gill sections of 4 C and 4 R fish with medium-high infection intensity (50-115 worms·fish^{-1}) on 32 dpe. To do so, paraffin sections collected on Superfrost™ Plus slides (Menzel-Gläser, Braunschweig, Germany) were deparaffinised and hydrated; endogenous peroxidase activity quenched in 0.3% hydrogen peroxide for 30 min and incubated for 1 h with six different biotinylated lectins. Following

incubation with the avidin–biotin–peroxidase complex (Vector Laboratories, CA, USA) for 30 min, bound peroxidase was finally developed upon a 5-min incubation with 3,3′-diaminobenzidine tetrahydrochloride chromogen (Sigma–Aldrich, MO, USA). The reaction was stopped with deionised water, and the sections were counterstained with Gill's haematoxylin, dehydrated, and mounted in di-N-butyl-phthalate in xylene. Washing steps between incubations consisted of immersions of 5 min in Tris-buffered saline (TBS, 20 mM Tris–HCl, 0.5 M NaCl, pH 7.2) with and without 0.05% Tween20. Binding specificity of the controls was evaluated by incubating each lectin with its corresponding blocking sugar (0.2 M) for 1 h before the application to the gill sections. Major lectin specificities, lectin sources, blocking sugars and used concentrations are shown in **Table 1**.

Microscopic evaluation

Histological staining was performed and analysed in gill sections of all C and R fish samples. The presence of goblet cell was estimated for the different types of staining with a semiquantitative scoring scale ranging from 0 (absence) to 3 (very abundant, meaning 25–30 cells/microscope field at 500× magnification) at four different gill locations: filament tip, interlamellar pockets, lamellar epithelium, and cartilage-covering epithelium. The intensity of each lectin labelling in these goblet cells was registered according to a semiquantitative scale ranging from 0 (no label) to 3 (very intense label). In addition, the presence and staining of discharged extracellular mucus were registered. Slides were observed under a Leitz Dialux22 (Leica, Hesse, Germany) light microscope, and representative images were taken with an Olympus DP70 Camera (Olympus, Tokyo, Japan).

Mucin gene analyses

The available gilthead seabream genomes (Pérez-Sánchez et al.[40] and fSpaAur1.1; www.

Table 1. Lectin sources, specificities, blocking sugars and concentrations used for labelling.

Acronym	Lectin Source	Specificities
Con A	*Concanavalina ensiformis*	Manα-1 > Glcα-1 > GlcAcα-1
UEA	*Ulex europaeus*	L-Fucα1,2Galβ1,4
WGA	*Triticum vulgaris*	GlcNAc(β1,4GlcNAc)1-2 > β1,4GlcNAc > NeuNAc
SBA	*Glycine max*	terminal αβGalNac > αβGal
BSL I	*Griffonia simplicifolia*	D-Gal > D-GalNAc
SNA	*Sambucus nigra*	NeuAc-α2,6Gal > NeuAcα2,6GalNAc

ensembl.org) and gilthead seabream sequences in the NCBI database were screened for mucin genes. The obtained sequences that were not previously described in this species[15] were checked by BLAST for verification. The previously available sequences were compared with other sequences in NCBI to further complete partial sequences. The obtained sequences (protein coding regions) were then searched by BLAST against the Ensembl gilthead seabream genome, and the genome location and intron/exon structure were retrieved and represented using online tools (wormweb.org/exonintron). Protein sequences were analysed in InterPro (www.ebi.ac.uk/interpro/) and SMART (smart.embl-heidelberg.de/), to define protein domains and locations. Primers for new sequences were designed using Primer3[41]. Primer specificity was checked by BLAST against the gilthead seabream genomes, and their efficiency was calculated by serial dilutions (only efficiencies of >90 were considered acceptable).

The sequences of transcription factors relevant to epithelial cell differentiation (goblet cell regulatory factors) were obtained from the NCBI nucleotide database. Primers were designed as described above. Transcript accession numbers and primer sequences used in this study are shown in **Table 2**.

RNA isolation, cDNA synthesis, and gene expression analyses

RNA from RNAlater® (Thermo Scientific, MA, USA)-fixed gills on 11, 32, and 61 dpe sampling points (3 C and 5 R per sampling) was extracted using MagMAX™-96 total RNA isolation kit (Invitrogen™, CA, USA). RNA concentration and quality were determined using a NanoDrop 2000c (Thermo Scientific, MA, USA), and 500 ng of which was treated with DNase I amplification grade (Invitrogen™, CA, USA). Reverse transcription was performed for 500 ng of input RNA using the High-Capacity cDNA Archive Kit (Applied Biosystems®, MA, USA). All procedures were performed following the manufacturer's instructions.

Real-time quantitative PCR was performed in a CFX96 Connect™ Real-Time PCR Detec-

Lectin concentration ($\mu g \cdot mL^{-1}$)	**Blocking sugar**
2	Methyl-α-D-Man + methyl-α-D-Glc
20	L-Fucα
10	GlcNAcα
5	GlcNAcα
5	Gal+GalNAcα
20	NeuNAc

Table 2. Primer sequences used in this study.

Gene name	Symbol
Mucin 2a	*muc2a*
Mucin 2b	*muc2b*
Mucin 5 a/c	*muc5ac*
Mucin 4	*muc4*
Intestinal mucin	*imuc*
Mucin 18	*muc18*
Anterior gradient protein 2	*agr2*
Transcription factor HES-1-B	*hes1b*
ETS-related transcription factor Elf-3	*elf3*
β actin	*βact*

	Accession Number		Sequence (5'-3')
	XM_030425503	F	ACGCTTCAGCAATCGCACCAT
		R	CCACAACCACACTCCTCCACAT
	XM_030414678	F	CCTGTTCAGTGCCCATCCAT
		R	TAAAGCCCAGACTGCAGGTG
	XM_030414679	F	TGGCAATAACACCTGGGGAC
		R	TGTTGTTTGCATGCCACTCG
	XM_030442219	F	GGTGAAGAAGCTGAGGGGTC
		R	TCATTGTACCCAGCCAGCAG
	XM_030418634	F	GTGTGACCTCTTCCGTTA
		R	GCAATGACAGCAATGACA
	XM_030399104	F	ATGGAGGACAGAGTGGAGG
		R	CGACACCTTCAGCCGATG
	XM_030410519	F	CGACGTTGAGATCCAGAGGG
		R	TCCGGGGAACATACTGTCCA
	KF857344	F	GAAGCATCTCCGGAACCTCC
		R	GCGGGTGACTTCATTCATGC
	XM_030424933	F	CGAGAAACTAAGTCGGGCGA
		R	TAAACCAGTCTGCGTCCGTC
	X89920	F	TCCTGCGGAATCCATGAGA
		R	GACGTCGCACTTCATGATGCT

tion System (Bio-Rad CA, USA). Overall, 20 µL reactions contained 3.3 ng of input cDNA, 5X PyroTaq EvaGreen qPCR Mix Plus (Cultek, Madrid, Spain), and specific primers at a final concentration of 0.45 µM. PCR conditions consisted of an initial denaturation step at 95°C for 3 min, followed by 40 cycles of denaturation for 15 s at 95°C and annealing/extension for 60 s at 60°C. The specificity of the reactions was verified by analysis of melting curves for each reaction. Fluorescence data acquired during the PCR extension phase were normalised by the delta–delta Ct method[42] using *β-actin* as housekeeping gene for normalisation, the most stable reference gene in this tissue when compared with other housekeeping genes (*elongation factor 1α*, *α-tubulin,* and 18S rRNA).

In silico analysis of glycosylation enzyme expression

Enzymes regulating glycosylation were screened *in silico*. The gilthead seabream genome[40] was mined for sequences annotated as sialilidases, mannosidases, fucosyltransferases, acetylglucosaminyltransferases, sialyltransferases, mannosyltransferases, glucosyltransferases, and phosphomannomutases. Identified sequences were used to mine RNA sequencing results from two previous studies of gilthead seabream infected with *S. chrysophrii*: a study on fish with a mild natural infection (Piazzon et al.[31]; SRA accession PRJNA507368; n = 4 control and n = 4 infected fish, mean intensity of infection 2.73 parasites·fish^{-1}] and other on fish with high intensity of infection during an experimental challenge (Toxqui-Rodríguez et al.[43]; SRA accession PRJNA992062; n = 5 control and n = 5 infected fish, mean intensity of infection 121.2 parasites·fish^{-1}). Gill-normalised expression values (FPKM) for each identified enzyme were retrieved from the count tables, and differential expression was checked for the DESeq results obtained from each of the studies.

Statistics

Semiquantitative histological scoring on goblet cells and lectin labelling was analysed among the different infection timings by one-way ANOVA followed by Student–New-

Table 3. Infection outcome in recipient (R) gilthead seabream experimentally exposed to *Sparicotyle chrysophrii*.

	11 dpe		20 dpe	
	Juvenile	**Adult**	**Juvenile**	**Adult**
R (n=5)	44.4 ±5.34	0	157.6 ±14.84	0
T (°C)	17.96 ± 0.13		17.78 ± 0.34	

Mean parasite load of juvenile and adult stages per fish ± SEM and mean temperature (T) ± SEM per each period are given. dpe, days post exposure. **Abbreviations: dpe**: days post-exposure.

man–Keuls using SigmaPlot v14.5 software (Systat Software Inc., CA, USA). When normality or equal-variance failed, the non-parametric Kruskal–Wallis test, followed by Dunn's post-hoc test for the multiple comparisons, was applied. For all data sets, differences between C and R fish were analysed by Student's t-test, and when normality failed, the Mann–Whitney U sum test was used. Gene expression data were log-transformed (LN) for statistical analyses. For normally distributed data, differences were evaluated using Student's t-test and one-way ANOVA followed by Tukey's post-hoc test for multiple comparisons. When conditions were not met, non-parametric tests (Mann–Whitney–Wilcoxon or Kruskal–Wallis followed by Dunn's test) were used. The significance level was set at $p < 0.05$ unless otherwise stated.

Results

Infection outcome

The prevalence of infection by *S. chrysophrii* was 100%, and detailed data on infection outcome are shown in **Table 3**. In addition, epitheliocystis, a disease (often secondary) caused by pathogenic intracellular bacteria, was observed in the gills of R fish from 61 dpe on. This bacterial infection provoked the characteristic nodular intracellular inclusions in the gill epithelia.

Mucin histochemistry and lectin labelling

A significant increase in neutral goblet cells was found at the interlamellar pockets, the tips of the gill filaments, and the epithelia of the lamellae, of R fish from 31 dpe on (**Figure 1**). Neutral goblet cells increased significantly at the epithelium covering the proximal cartilage later, at 41 and 61 dpe, and scoring for acidic and mixed neutral-acidic goblet cells at this gill site was slightly higher in R fish than in C fish along the whole experiment though not significant (**Supplementary material: Figure S1**). Goblet cells bearing neutral mucins were ubiquitous in all gill locations, whereas acidic and mixed neutral-acidic goblet cells were only observed at the epithelium covering the proximal cartilage and adipose

32 dpe		41 dpe		61 dpe	
Juvenile	**Adult**	**Juvenile**	**Adult**	**Juvenile**	**Adult**
0	112.8 ±43.62	30.40 ±7.39	46.80 ±18.08	9.20 ±5.54	24.80 ±6.25
16.03 ± 0.22		14.75 ± 0.07		13.59 ± 0.29	

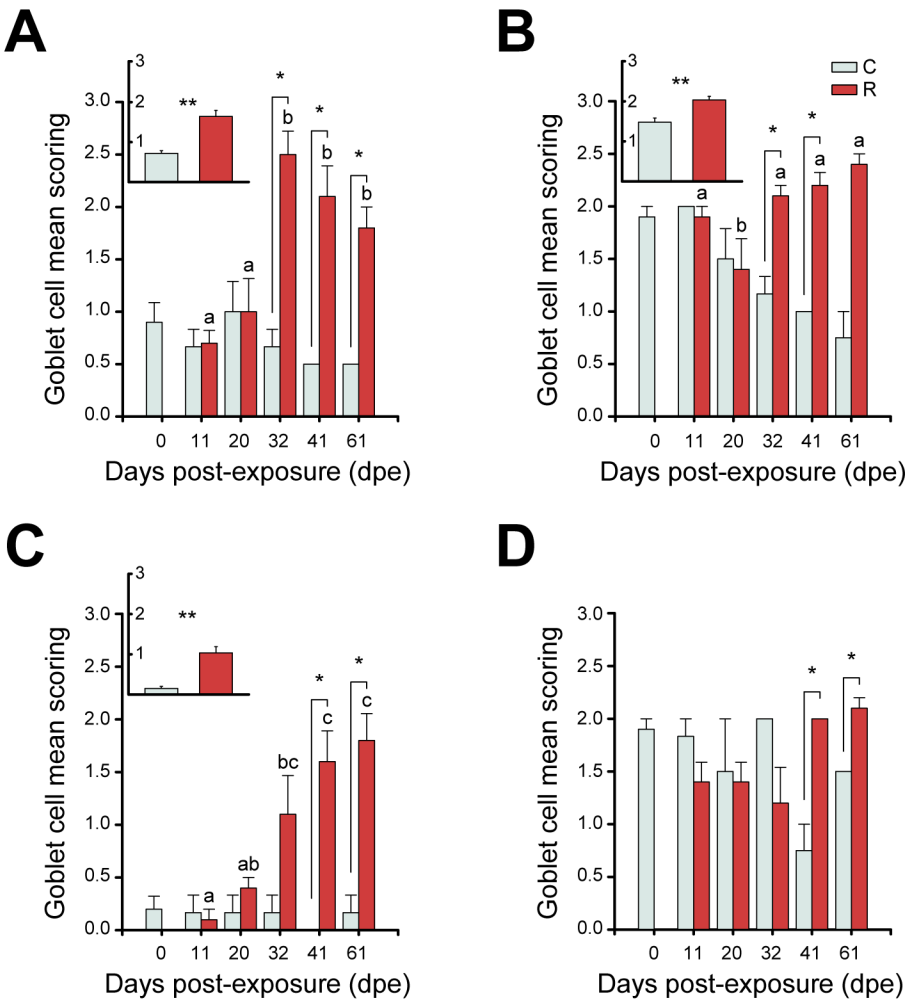

Figure 1. Goblet cell scoring (mean + SEM) with neutral mucins at different locations in gilthead seabream gills upon *Sparicotyle chrysophrii* infection. **A:** interlamellar pocket. **B:** filament tip. **C:** lamellar epithelium. **D:** epithelium covering the proximal cartilage and adipose tissue. Inserts represent pooled data of C or R fish, regardless of the infection timing (*****$p < 0.05$ and ******$p < 0.001$). Different letters stand for statistically significant differences within the R group, $p < 0.05$. Asterisks represent statistically significant differences within the same sampling point ($p < 0.05$). **Abbreviations: C**: control (unexposed) fish (n = 18); **R**: recipient (naïve) parasitised fish (n = 25); **dpe**: days post exposure.

tissue (**Figure 2**). Additionally, secreted mucus was often observed in the interlamellar spaces of R fish.

Differences in lectin label intensity among goblet cells of C and R fish were not significant. Nevertheless, some interesting observations were made (**Table 4**; **Figure 2**). Lectin label intensity of goblet cells located at the tips of the gill filaments showed an overall decrease, except for BSL I specifically binding to Gal (**Figures 2C**, **D**). This terminal sugar was the only one whose staining intensity increased in the goblet cells at all gill locations of R fish. Terminal GalNac residues labelled by SBA also presented an increase in R fish, especially in goblet cells of the lamellae epithelia (**Figures 2K**, **L**), but also in the extracellular mucus secretion. Label intensity of terminal GlcNac/sialic acids (WGA) was only higher in goblet cells at the interlamellar pockets of R fish (**Figures 2G**, **H**). Fucose sugars evidenced by UEA increased in the goblet cells at all the gill locations of R fish (**Figures 2R**, **S**), except at the filament tips. In general, ConA and SNA labels for Man/Glc and NeuNac/sialic acids, respectively, presented the least changes upon parasite infection and mostly decreased in all goblet cells of R fish. However, Man/Glc label was more intense in the interlamellar mucus secretion of R fish.

Identification of gilthead seabream mucins

Nine mucin sequences were identified in the gilthead seabream genome, among them five sequences were secreted and four sequences were membrane-bound. The intron–exon structure of the sequences and genomic locations are shown in **Supplementary material: Table S1**. Five of these sequences appear complete, beginning with a signal peptide and ending in a stop codon. The structure of the three soluble mucins that do not present a signal peptide seems to indicate that not a large stretch of the sequence is missing. However, the sequence of the membrane-bound *imuc* is clearly incomplete, and although long stretches of repeated mucin domains can be found encoded upstream in the chromosome, the complete structure could not be fully elucidated and will require further sequencing.

Regarding soluble mucins, in chromosome 4, a sequence annotated as mucin 2 (*muc2*) and another one annotated as mucin 5 ac (*muc5a/c*) were identified in tandem, whereas in chromosome 8, two sequences annotated as mucin 2 appeared also in tandem (*muc2a* and *muc2b*). All these sequences showed a similar structure, with three VWD domains and three C8 domains, with a variable number of intercalated TIL domains in the N terminus. The middle of the sequences was characterised by the presence of repeat regions and low complexity or disorder domains that correspond to PTS domains with variable numbers of WxxW domains intercalated. In the C terminus, one VWD and one C8 domain were found in all sequences followed by two VWC domains. All four sequences pre-

sented a C terminus cysteine knot domain. A sequence annotated as mucin 19 (*muc19*) was found in chromosome 14, with a very similar structure as the other secreted mucins (**Figure 3**).

As expected, the structure of the membrane-bound mucins was more variable. The sequence annotated as intestinal mucin (*imuc*), found in chromosome 6, presented a series of repeat domains, followed by an EGF and a transmembrane domain. Mucin 4 (*muc4*), encoded in chromosome 15, showed the characteristic NIDO, AMOP, and VWD domains, followed by several EGF domains before the transmembrane region[44]. Mucin 18 (*muc18*), encoded in chromosome 2, showed the typical structure with five immunoglobulin-like domains, a transmembrane region, and a short cytoplasmic tail[45]. Finally, a sequence annotated as mucin 13 (*muc13*) was found in chromosome 20, which was characterised by a repeat region followed by a SEA domain surrounded by EGF domains[46] (**Figure 3**).

Table 4. Lectin label intensity at the different gill sites in goblet cells (GCs) and in the mucus secretion (Muc sec).

Gill site	Experimental group	Intensity of lectin label	
		ConA	SBA
Tip GC	C	3.0 ± 0	2.5 ± 0.5
	R	2.13 ± 0.72	2.33 ± 0.38
ILP GC	C	0.5 ± 0.29	0.5 ± 0.2
	R	0.38 ± 0.38	0.5 ± 0.29
Epi GC	C	0.38 ± 0.24	0.17 ± 0.14
	R	0.25 ± 0.14	1.5 ± 0.2
Prox GC	C	0 ± 0	2 ± 0.2
	R	0 ± 0	2 ± 0.2
Muc sec	C	0.25 ± 0.14	1.25 ± 0.66
	R	1 ± 0.29	1.88 ± 0.24

For each site and lectin, the mean staining intensity ± SEM in control unexposed fish (C, n = 4) and recipient parasitised fish (R, n = 4) from fish with medium-high infection intensity (50–115 worms in right gill arches) at 32 days post exposure are given. **Abbreviations: Tip:** filament tips. **ILP:** interlamellar pockets. **Epi:** lamellar epithelium. **Prox**: epithelium covering proximal cartilage and adipose tissue. No significant differences were found when comparing C and R groups.

Gene expression of mucins and goblet cell regulatory factors

After testing several sets of primers, only six of the nine mucins were found to be expressed in gilthead seabream gills. The two soluble mucins encoded in chromosome 4 (*muc2* and *muc5a/c*), *muc2a* from chromosome 8, and the membrane-bound *muc4*, *imuc*, and *muc18*.

Transcription of mucin genes was robustly upregulated for all detected mucin genes at 32 dpe (**Figure 4A**). Interestingly, expression of *muc5a/c* was upregulated at all the analysed timings, and fold changes of the secreted *muc2* and *muc2a* were the highest. The regulatory factors responsible for epithelial cell differentiation *elf* and *agr2* were also significantly upregulated at 32 dpe (**Figure 4B**).

Genome search for glycosylation enzymes and their differential expression

Enzymes involved in glycosylation were studied *in silico*. A total of 273 sequences annotated as silialidases, mannosidases, fucosyltransferases, acetylglucosaminyltransferases,

UEA	WGA	BSL I	SNA
2.3 ± 0.14	1.5 ± 0	0.0 ± 0	0.1 ± 0.13
1 ± 0.87	0.83 ± 0.14	1.5 ± 1.06	0 ± 0
0.13 ± 0.13	0.63 ± 0.13	0 ± 0	0 ± 0
0.25 ± 0.25	0.75 ± 0.14	0.13 ± 0.13	0 ± 0
0.13 ± 0.13	1.25 ± 0.14	0.38 ± 0.13	0.1 ± 0.13
0.38 ± 0.24	1 ± 0	0.63 ± 0.24	0 ± 0
0.25 ± 0.14	1.63 ± 0.38	0.63 ± 0.13	0 ± 0
0.63 ± 0.47	1.5 ± 0.2	1 ± 0.2	0.4 ± 0.38
0.63 ± 0.24	1.63 ± 0.8	0.63 ± 0.38	0 ± 0
0.5 ± 0.2	2.5 ± 0.35	1.33 ± 0.29	0 ± 0

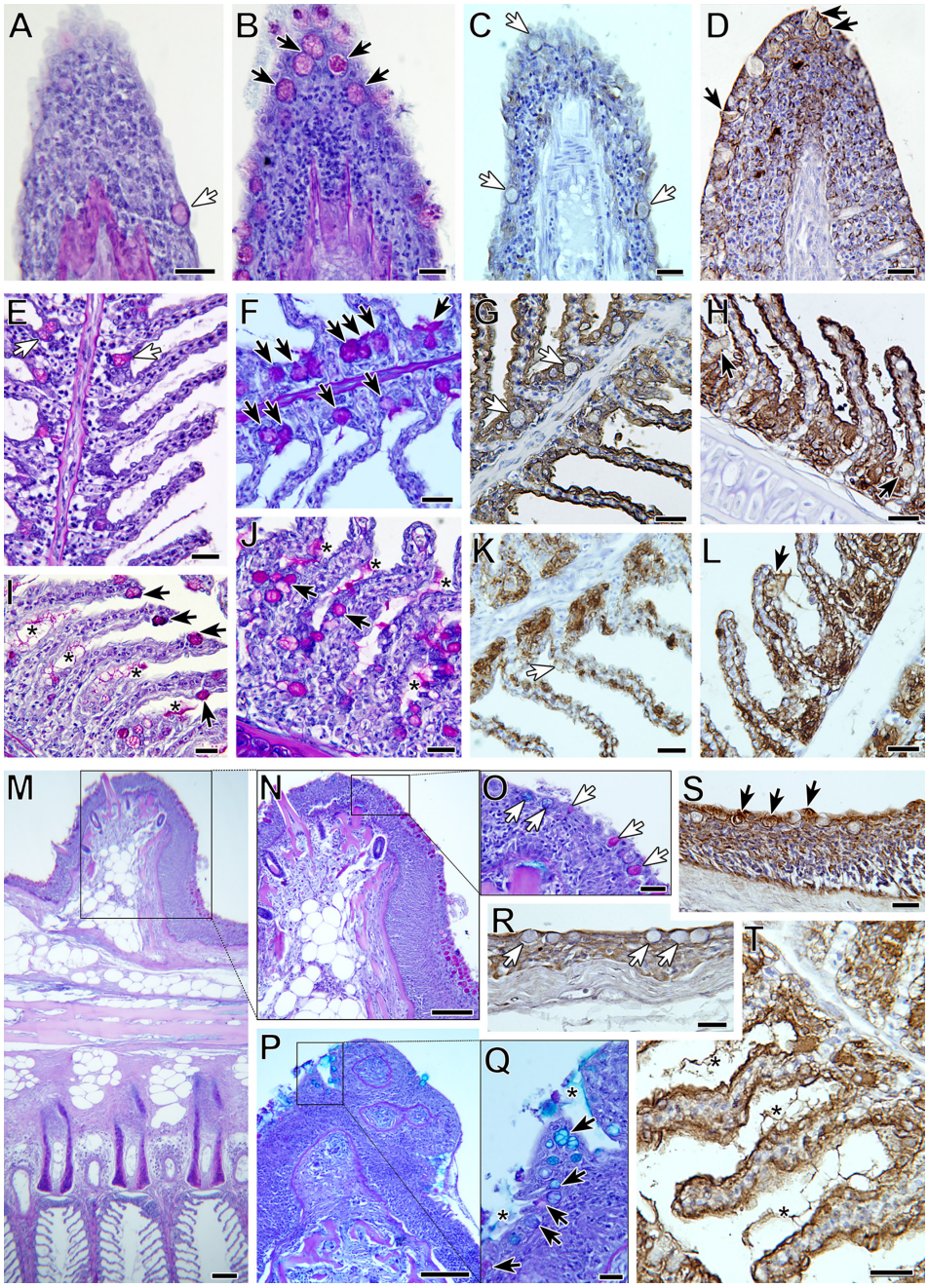

Figure 2. Goblet cell distribution and terminal mucin glycosylation in gilthead seabream gills upon *Sparicotyle chrysophrii* experimental infection (**B**, **D**, **F**, **H**, **I**, **J**, **L**, **P**, **Q**, **S**, **T**) compared with control gills (**A**, **C**, **E**, **G**, **K**, **M**, **N**, **O**, **R**). Black arrows indicate goblet cells in control gills and white arrows in infected ones. Neutral goblet cell (magenta) hyperplasia was observed in the gills of infected fish at different locations: filament tips (**A**, **B**), with increased BSL-I label for Gal (**C**, **D**); interlamellar pockets (**E**, **F**), with increased WGA label for GlcNac/sialic acid (**G**, **H**); along the lamellar epithelium (**I**, **J**), with increased SBA label for GalNac (**K**, **L**). **Continued on the next page.**

Figure 2. (Continued). The epithelium covering the proximal cartilage and adipose tissue (**M**) was the only location with neutral and acidic goblet cells (**N–Q**), with increased UEA label for Fuc (**R**, **S**). Note the presence of interlamellar secreted mucus in infected gills (asterisks; *****), with intense WGA label (**T**). PAS-alcian blue staining was used in (**A**, **B**, **E**, **F**, **I**, **J**, **M–Q**) and lectin labeling with hematoxylin counterstain in (**C**, **D**, **G**, **H**, **K**, **L**, **R–T**). All scale bars = 20 µm.

sialyltransferases, mannosyltransferases glucosyltransferases, and phosphomannomutases were found in the gilthead seabream genome (**Supplementary material: Table S2A**). Examination of the differential expression results from the RNA sequencing experiments by Piazzon et al.[31] and Toxqui-Rodríguez et al.[43] revealed that 29 of these sequences were differentially expressed in at least one of the experiments when comparing control and *S. chrysophrii*-infected fish (**Supplementary material: Table S2B**). Marked whereas fish with high infection intensities[43] presented both significant upregulation and downregulation (**Figure 5**). Half of these modulated genes responded with opposite trends depending on the infection intensity of the fish, except for the five sialyltransferase genes, which had the same regulation patterns regardless of the parasite load. Higher numbers of significantly regulated genes occurred in low infection-intensity fish than in high infection-intensity fish.

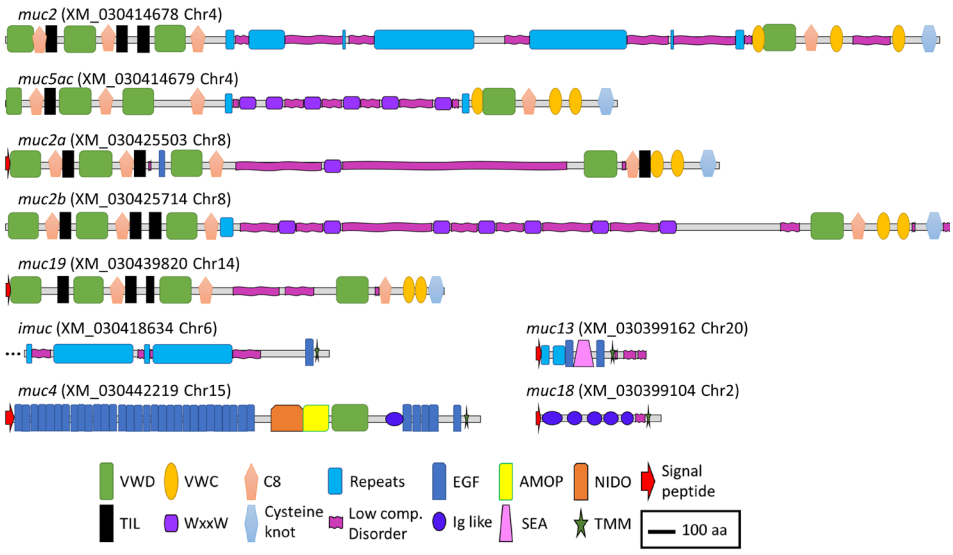

Figure 3. Schematic representation of the deduced amino acid sequences from the mucin genes annotated in the gilthead seabream genome. Abbreviations: VWD: Von Willebrand factor type D domain. **VWC:** Von Willebrand factor type C domain. **C8:** conserved cysteine-rich domain. **Repeats:** mucin-like tandem repeats domains. **EGF:** epidermal growth factor domain. **AMOP:**adhesion-associated domain in MUC4 and other proteins. **NIDO:** nidogen-like domain. **TIL:** trypsin inhibitor-like cysteine-rich domain. **WxxW:** WxxW domain. **Low comp Disorder:** low complexity or disorder domains containing regions rich in the amino acids serine, threonine, and proline (PTS domains). **Ig like:** immunoglobulin like domains. **SEA:** sperm protein, enterokinase, and agrin domain. **TMM:** transmembrane domain. Scale bar: 100 amino acids.

Discussion

Sparicotyle chrysophrii infections in gilthead seabream farms have become a major issue for aquaculture. In the current study, we unveil some aspects of the local mucosal response triggered by this gill ectoparasite, providing valuable data on mucin and goblet cell distribution and regulation. Studies focusing on mucosal immune responses in fish have traditionally focused on the mucosa-associated lymphoid tissues (MALT), their cell effectors, and their molecular signaling. Thereby, the importance of the strictly mucus-related compartment, i.e., the mucus secretion itself, its mucin components, and the responsible goblet cells and goblet cell glycosidases, have been mostly neglected. Never-

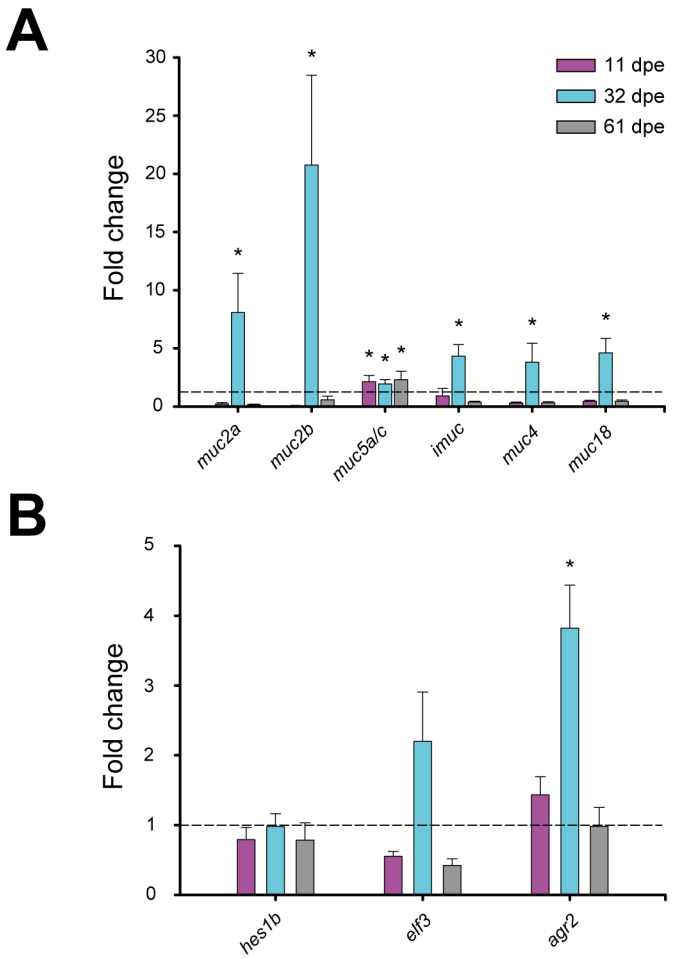

Figure 4. A: Normalised expression of mucin genes in gilthead seabream gills upon *Sparicotyle chrysophrii* experimental infection. **B:** Normalised expression of regulatory factors of goblet cell differentiation in gilthead seabream gills upon *S. chrysophrii* experimental infection. (*****; $p < 0.05$). Mean fold changes were calculated *versus* control samples of non-exposed fish + SEM of n = 5. **Abbreviations: dpe:** days post-exposure.

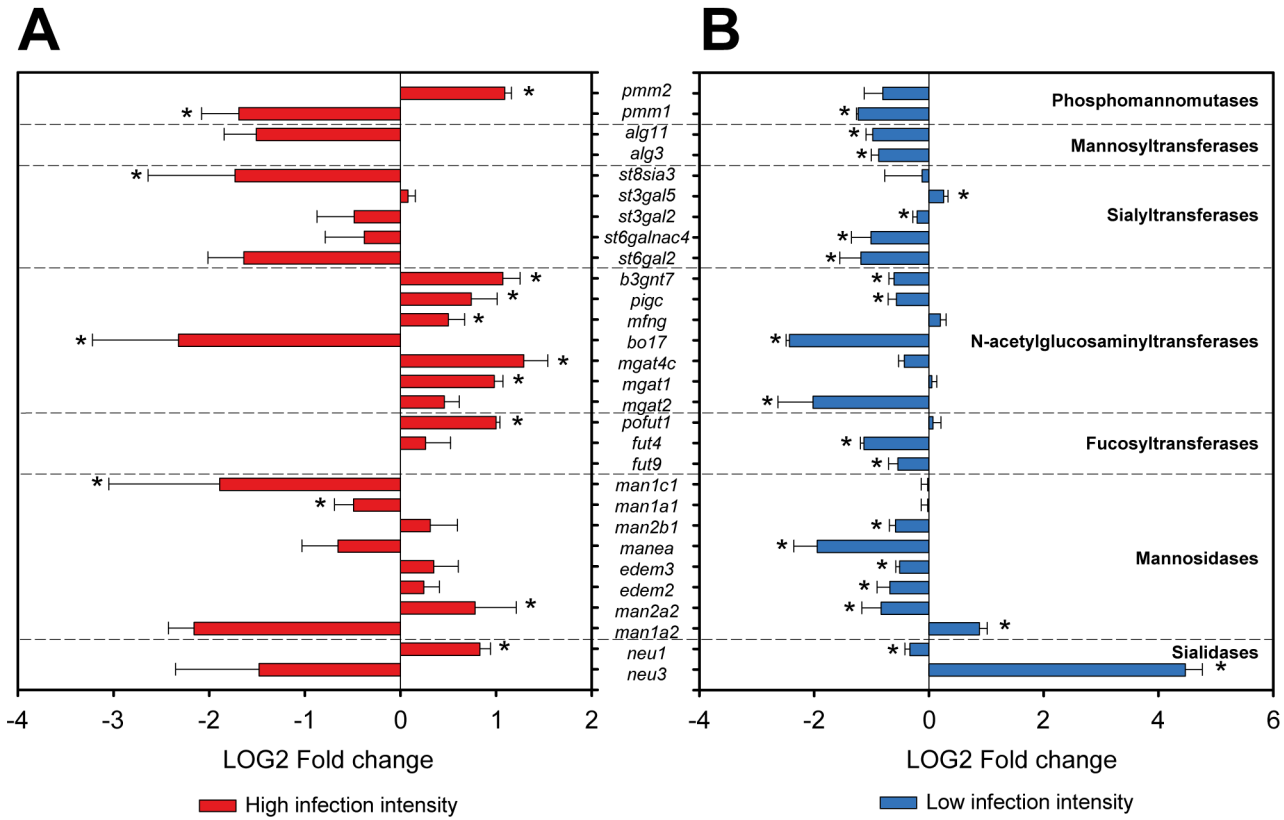

Figure 5. A: RNAseq normalised gene expression of glycosyltransferases and glycosydases in gilthead seabream gills upon *Sparicotyle chrysophrii* high-intensity experimental infection. B: RNAseq normalised gene expression of glycosyltransferases and glycosydases in gilthead seabream gills upon *Sparicotyle chrysophrii* low-intensity sea cage infection. (*; $p < 0.05$). Log2 mean fold changes were calculated relative to the control samples of non-infected fish ± SEM of n = 5 in **A** and n = 4 in **B**.

theless, in the current-omics era, recent advances in glycomics granted mucus secretion its position as key mediator between epithelial cells, MALT, and microbiota and their joint interactions with external factors such as pathogens[47–49].

The main clinical sign during sparicotylosis is anaemia, which is caused by the haematophagous nature of a parasite[32,39,50]. Furthermore, the parasite's attaching mechanism to the gill filament through specialised clamps in its opisthaptor region[51] inflicts evident histopathological lesions such as lamellar synechiae and clubbing, resulting in disruption of the epithelium and marginal blood vessels[50]. Gill haemorrhages and an increased mucoid exudate are among the recognised pathogenic effects and host response elicited by gill monogeneans, as reviewed by Ogawa[52]. Regarding goblet cells, histological scoring of experimentally infected gilthead seabream showed an overall hyperplasia of neutral goblet cells in gill filaments in R fish compared to C fish at some points during the parasite challenge (**Figures 1**, **2**). This hyperplasia was especially notable and significant over the course of parasite exposure in the interlamellar pockets and the lamellar epithelium from 32 dpe on. A shift in the position of goblet cell distribution toward interlamellar cavities upon infection with the larval parasitic stage of the freshwater mussel *Margaritifera margaritifera* in Atlantic salmon (*Salmo salar*) was attributed to their role in gill clearance and remodeling[18]. Similarly, the present rearrangement of goblet cell distribution is probably helping, by an increased mucus secretion between lamellae, to lubricate the surface of hyperplasic epithelia avoiding lamellar fusion. Thus, goblet cell hyperplasia was not evident at the other locations away from the lamellae, i.e., filament tips and the epithelium covering the proximal cartilage.

Meaningfully, goblet cell hyperplasia occurred after the first month of parasite challenge once infective oncomiracidia, post-larvae, and juveniles of *S. chrysophrii* turned into the more pathogenic adult worm stages, which was in agreement with the previous observations[39]. At 32 dpe, the highest adult stage infection intensity reached 112.8 ± 43.62, with each adult worm bearing 2 rows of up to 72 clamps (personal observation). These, pinch on the lamellae eroding the mucosal surface and disrupting the gill tissue, probably triggering the increased mucus secretion to protect the nude or damaged gill epithelium. Mucosal and waterborne bacteria infecting such wounds also contribute to an inflammatory response in the parasitised gills[53]. In fact, the current *S. chrysophii*-infected fish had developed epitheliocystis at the later sampling point. *Sparicotyle chrysophrii* and epitheliocystis co-infection in gilthead seabream are common under farm and experimental conditions[39,50,54], and its specific bacterial aetiology was a matter of discussion until recently[43,55,56].

In the context of intestinal helminth infections, hyperplasia and hypertrophy of the mucous cells were described at the site of parasite attachment, especially for the ones

with acid glycoconjugates[57]. Hypertrophy of mucus cells with an increase in carboxylated glycoproteins containing sialic acid was observed in gills of gilthead seabream fed with an essential oil-supplemented diet and exposed to *S. chrysophrii*, but no change occurred in cell numbers[34]. In the present study, gilthead seabream responded to parasite infection with an increase in goblet cells with neutral glycoconjugates. In healthy gills, the abundant secretion of neutral mucus characterised by glycoproteins with oxidisable vicinal diols is associated with pH regulation for acidity buffering of acidic mucins, with the maintenance of homeostasis and lubrication[58–60]. The shift toward mucin acidification upon infection, related to viscosity increase in the mucus secretion and trapping of offending microorganisms due to higher amount of O-sulfate esters[60, 61], was not detected by histochemistry in the gills of *S. chrysophrii*-infected gilthead seabream. Conversely, the predominantly neutral mucin production found from 32 dpe on involves a less viscous mucus layer which facilitates laminar water flow and gas exchange in the gill lamellae[61,62]. Lethargy, as a sign of respiratory distress, is common upon sparicotylosis[38], and even a mild *S. chrysophrii* infection elicited the downregulation of hypoxia-related oxygen homeostasis genes not only locally but also in the spleen of gilthead seabream[31]. Thus, the reduced oxygen availability induced by the direct parasitic damage on the gills and blood consumption resulting in anaemia provokes severe hypometabolic effects at systemic level during mild infections. Our current results point to a local mucosal response by the fish aiming to counterbalance parasite-induced hypoxia by secreting less viscous mucus on the lamellar surface that facilitates gas exchange.

Goblet cells bearing acidic, carboxylated mucins were found only in the epithelium covering the proximal cartilage of the arches, away from the gill respiratory epithelium, both in C and R fish (**Figure 2**; **Supplementary material: Figure S1**). Rakers and gill arches lubricated with highly viscous and sticky mucus, predominantly containing glycoproteins with O-sulfate esters and sialic acids, were reported from diverse teleost species in order to protect the epithelium of the pharyngeal cavity against mechanical injuries during food ingestion and transport food particles[62]. Moreover, glycoproteins in such secretions cross-link sulfate and sialic acid groups resulting in a more resistant barrier against bacterial enzymatic degradation and thus, more difficult to breach by bacteria and more efficient in containing microbial infections[61].

At the transcriptional level, goblet cell hyperplasia was supported by the overexpression of mucin genes and regulatory factors involved in goblet cell differentiation (**Figure 4**). Apomucin, the linear polypeptide backbone of the mucin, is encoded by specific Muc genes in goblet cells. Assembly, automatic annotation, and *in silico* identification of mucins in non-mammalian species are challenging mainly due to their very long repetitive sequences and the poorly conserved sequence of mucin domains[63]. Only a few studies

have been conducted on teleost mucin gene expression with mucin transcription data that are barely available for Atlantic salmon[64,65], zebrafish (*Danio rerio*)[66–68], and common carp (*Cyprinus carpio*)[69,70], and one previous record exists for gilthead seabream[15]. In the later study, partial sequences and structure of some mucins were described for gilthead seabream from transcriptomic data. In the current study, we integrated this previously defined information with the newly available genome data from two different genome assemblies for this species (fSpaAur1.1 in ensembl.org, NCBI and Pérez-Sánchez et al.[40]) and identified nine mucin sequences. Our analysis of the automatic annotation of the sequences showed a coherent complete mucin structure for the membrane-bound mucins (*muc4*, *muc13*, and *muc18*), except for *imuc*, whose C terminus part was the only partially identified. However, upstream of the *imuc* sequence in chromosome 6, several large repetitive PST domains can be identified that probably encode a part of the N terminus sequence of this protein, or belong to a different mucin sequence encoded in tandem, as typically found in gel-forming mucin gene organisation[71]. Long-read sequence analyses should be conducted to unravel the complete sequence of this mucin. Similarly, although *muc2* and *muc5* sequences appear almost complete from N to C terminus, the predicted coding sequences in the middle repeat part are not very consistent, with atypical intron–exon boundary sequences (**Supplementary material: Table S1**). In addition, the similarities between *muc2* and *muc5* sequences, and the poor conservation of mucin domains, are challenging for mucin classification and nomenclature in teleosts and other non-mammalian species. In this line, zebrafish *muc5* sequences have been termed *muc5.1–3* instead of using the mammalian nomenclature *MUC5AC/MUC5B*[67]. Therefore, the nomenclature used in the current study is somewhat arbitrary, and a more accurate annotation of fish mucins should be performed integrating mammalian and non-mammalian sequences, since up to 133 Muc2-type and 263 Muc5-type proteins have been identified from vertebrate genomes[68]. Muc2, Muc19, and Muc5 are very large, secreted, gel-forming mucins, whereas I-Muc, Muc4, Muc13, and Muc18 are membrane-bound mucins[15,72,73]. Pérez-Sánchez et al.[15] found that Muc18, the most abundant gill mucin, and I-Muc constitutively expressed in the gills of gilthead seabream. These authors annotated the *imuc* sequence, which had no clear orthologous genes in mammals and was found highly expressed in the posterior intestine, where it revealed itself as a biomarker of intestinal health changing its expression upon parasite infections. Additionally, expression of *muc2*, *muc13*, and *muc19* was found restricted to the gastrointestinal tract, in agreement with our current results which found no detectable expression in gills. Our results further reveal that I-Muc has an additional role in gill protection and mucosal response[15].

Expression and a robust upregulation of *muc2* genes, *muc5*, *imuc*, *muc4*, and *muc18*

were found in the parasitised gills of gilthead seabream at 32 dpe, recovering their initial levels at 61 dpe for all mucin genes except for *muc5a/c*, which remained upregulated along the course of the entire experiment. Apparently, the secreted *muc2* sequences and the membrane-bound *imuc*, *muc4*, and *muc18* responded acutely once the highly pathogenic adult worms were established, with fold changes up to >20. The highest fold changes among them corresponded to the secreted *muc2a* and *muc2b*, while upregulation of the membrane-bound mucins *imuc*, *muc4*, and *muc18* was not as high. Mucin upregulation in response to a gill parasite was described in Atlantic salmon, displaying clinical amoebic gill disease at 21 dpe, when a 30-fold *muc5* upregulation was found[64]. In addition, in gills, those authors found downregulation of the membrane-bound *muc18* and very low and variable expression of a *muc2* sequence, which they considered to have a major role in the intestine of Atlantic salmon. Sveen et al.[65] found three different *muc5a/c* genes, two *muc2* genes, and one *muc5b* gene expressed in the gills of Atlantic salmon, from which two *muc5a/c* and two *muc2* genes were significantly upregulated only 3 h after handling stress. In common carp, different pathogenic viruses provoked severe mucosal distress in gills by downregulating *muc2-like* and *muc18* gene expression at the time that clinical signs of the disease appeared and susceptibility to secondary infections increased[69]. In contrast, the expression of three different *muc5* genes was upregulated in the whole body of zebrafish larvae in response to bacterial challenges upon pectin administration, which was considered an innate antimicrobial immune response[66]. Therefore, it seems evident that mucin expression is involved in protective responses upon exposure to different pathogens and stressors, but there are large differences in mucin expression patterns among different fish species.

Regulatory mediators are responsible for the tuning of the goblet cell differentiation, leading to their hyperplasia and consequent mucus hypersecretion[74,75]. Accordingly, *elf3* and *agr2*, both involved in goblet cell differentiation, were synchronically upregulated with the observed mucin upregulation in R gills. In the intestines of Elf3-deficient mice, poor differentiation of goblet cells occurred[76]. In addition, gene homologs of *agr2* in humans and mice are strongly expressed in mucus-secreting cells of the digestive and respiratory epithelia, and in zebrafish, *agr2* gene expression was found in mucus cells from all mucosal tissues including gills[77]. Such regulatory mediators are, however, also responsible for avoiding a chronic inflammatory/repair response, which would worsen respiratory distress and hypoxia[74], and consequently, their expression levels were restored after the second month of parasite exposure. The transcriptional response of *hes1b* was slightly different, presenting a minor downregulation in the gills of R fish along the entire parasite challenge. Nevertheless, in fish as in mammals, the Notch-Hes1 pathway drives intestinal differentiation, and its inhibition results in goblet cell differentiation[78,79], which

is in line with our results. Accordingly, downregulation of *hes1* was described before as an intestinal helminth defense in order to increase mucin secretion and prevent worm attachment or promote detachment[80].

Regarding terminal glycosylation of the mucins contained in gill goblet cells, we found moderate changes including an overall increase in Gal, GalNac, and Fuc in R fish (**Table 4**). In addition, GlcNac/sialic acid terminal residues also increased slightly in the goblet cells of the interlamellar pockets of R fish. Glycosylation of the apomucin is carried out post-transcriptionally by glycotransferases and glycosidases in the Golgi apparatus during the secretory pathway. The resulting glycan oligomerisation and branching and defining of the terminal sugar moieties produce the structural diversity of the glycome. Terminal sugar residues determine the charge and antigens of the mucins and are the molecular basis for interspecies recognition being capable of activating immune responses. In fact, chemical modifications of glycans have been proposed as diagnostic and therapeutic strategies against diseases[81]. Firmino et al.[34] suggested that diet supplementation with essential oils during sparicotylosis enhanced the mucosal defense mechanism, in part by an increase in sialic acid-containing mucins, which helped parasite trapping and shedding and led to a significant reduction in parasite abundance and prevalence. Here, in the absence of any particular dietary treatment, WGA binding to almost all sialylated glycans and GlcNAc showed a moderate increase in the goblet cells of the interlamellar pockets and the interlamellar mucus secretion of R fish at 32 dpe. In contrast, SNA, binding only to sialic acid attached to terminal α2, 6Gal, gave the weakest of all lectin labels, being almost negligible. Thus, overall sialylated and Glc-N-acetylated glycans seem to be increasingly secreted in the gills of gilthead seabream as a response to the establishment of adult *S. chrysophrii* stages. The increase in sialic acid and GlcNAc together with goblet cell hyperplasia is recognised as part of the expulsion response against helminth infections, since sialic acids serve for pathogen binding and dumping[8]. In agreement, six N-acetylglucosaminyltransferases were upregulated in the RNAseq dataset of gilthead seabream gills with severe sparicotylosis (**Figure 5**). The addition of GlcNAc to the oligosaccharide chain can generate core 2 and 4 structures, allowing branching and providing the substrate for the further addition of sugar by other glycosyltransferases. This is a regulatory turning point of glycosylation, since many biologically important oligosaccharide structures involved in recognition and adhesion are constructed on this branch, and improper N-acetylglucosaminyltransferase expression in mammals is related to pathological conditions[82]. In addition, the expression profile of sialyltransferases was clearly downregulated in the RNAseq dataset of fish with low infection intensity, whereas in highly infected fish, only one sialyltransferase of the five we identified was significantly downregulated, and sialidases presented opposite expression profiles, depending on the infection inten-

sity of the fish.

While sialic acids confer a negative charge to the glycoconjugate, terminal fucose residues confer hydrophobicity, but both are associated with mucosal protection and their alteration may result in disease[72,75]. Thus, human fucosyltransferases and their expression have been studied for their importance in inflammation, mucosal colonisation, and host immune response modulation[83,84], and more recently, their importance for the maintenance of healthy gut microbiota profiles has been stressed out[85,86]. In R gills, a moderate increase in Fuc terminal residues was observed in the lamellar goblet cells and those of the epithelium covering the proximal cartilage, and fucosyltransferase expression appeared upregulated in fish with high infection intensity (**Figures 2**, **5**). Such results may also point to a protective host response through modulation of mucin glycosylation. Conversely, the only previous study including glycosylation of gilthead seabream gills mucus found scarce Fuc residues after feeding with an essential oil-supplemented diet and challenging fish with the polyopisthocotylan[34]. However, those fish had a mean infection intensity of 2.7 parasites·fish^{-1}, much lower than the current one of 112.8 ± 43.62, and very similar to the 2.73 parasites·fish^{-1} of the low-intensity RNAseq dataset[31], in which fucosyltransferases were downregulated. Thus, some protective mechanisms of mucosal modulation in the gills of gilthead seabream may only be triggered upon severe polyopisthocotylan infection. Through a glycomic approach, the presence of complex fucosylated mucin structures was found in Atlantic salmon gills, which would lead to increased structure diversity of glycan epitopes to diversify its repertoire as a possible defensive immune strategy[87]. Similarly, the skin mucin structure of Atlantic salmon subjected to chronic stress carried increased Fuc, sialic acid, and core 1 glycans[47].

In addition, GalNAc, which is incorporated by N-acetylgalactosaminyltransferases to the apomucin initiating the oligosaccharide sidechains, seemed to increase in the goblet cells of the R fish lamellar epithelium and the mucus secretion. The detection of this sugar moiety at the terminal position in secreted mucins was considered a sign of immature mucin secretion in gilthead seabream upon intestinal parasite infection[88] and also in vertebrates, in general[89]. Secretion of not fully mature mucins seems to contradict the previous observations of mucins with increased GlcNAc, sialic acid, and Fuc, indicators of complex glycans. Future glycomic work will be conducted to validate or reject if the mucosal gill secretion of gilthead seabream contains immature, not fully glycosylated mucins upon sparicotylosis.

Phosphomannomutase isozymes, as known from mammals, are required for the process of N-glycosylation. They provide Man-1-P, the substrate needed by mannosyltransferases, to incorporate Man into glycoconjugates[90]. Identified mannosyltransferase sequences participate in this early N-linked glycosylation, from which derived glycan struc-

tures are key for functions such as cell recognition, host-defense, and protein secretion in many organisms[91]. The downregulation of mannosyltransferase observed in the gills of fish with low infection intensity was not detected in fish with high intensity, as also happened for one phosphomannomutase and most mannosidases identified (**Figure 5**). Mannosidases and sialidases are both relevant glycosidases for the release of mucin glycans and would play their role in sloughing mucus with the retained parasites off, as previously suggested for an endopeptidase by Firmino et al.[34]. Overall, enzyme gene expression from the RNAseq analyses performed herein pointed to a hyporegulative profile in the gills of the fish with low infection intensity, which was mostly reverted or even inverted for many glycosyltransferases and glycosidases in fish with high infection intensity. This would correspond to a defence response in gills involving higher mucin biosynthesis and release, which is in line with the observed goblet cell hyperplasia and mucus hypersecretion upon severe *S. chrysophrii* infection, once the adult parasite stages are established.

Many aspects beyond our current scope, such as glycosyltransferase competition and their intracellular location, epigenetics, health status, or microbiome/pathobiome signaling, can influence the final O-glycosylation profile, which compromises mucin secretion, conformation, involvement in adhesion and recognition events, and microbiome niches. Furthermore, each glycosyltransferase accounts for the proper arrangement of the individual monosaccharides in each unique oligosaccharide structure, and their gene expression serves as fine tuning of the glycosylation process. Future transcriptomic and glycomic approaches will help us understand the scope of the detected mucin modulation in this host–microbiome–parasite interaction by integrating the transcriptional, glycosylation, and microbiome viewpoints. We are still far from understanding the entire interplay occurring between host mediators and effectors, microbiota and microbiota-derived factors, and parasites and their excretory–secretory products. However, this study helps to understand how the gill mucosal microhabitat responds to the *S. chrysophrii* offender and consequent microbiota shift[43] by increased goblet cell differentiation leading to neutral goblet cell hyperplasia on gill lamellae, acutely increased mucin expression, and a probable increase in more complex glycoconjugates with sialylated, fucosylated, and branched structures.

Funding

The author(s) declare that financial support was received for the research, authorship, and/or publication of this article. This study was supported by the Spanish Ministry of Science and Innovation (MCIN/AEI/10.13039/501100011033) through the projects SpariControl (RTI2018-098664-B-I00), with AEI/FEDER, UE funding, and Mucosal Frontier (PID2020-115070RA-I00); the ThinkInAzul Programme supported by MICIN with funding from Nex-

tGeneration EU (PRTR-C17.I1), the Generalitat Valenciana (THINKINAZUL/2021/022), and the Generatitat Valenciana AICO2023 funding (CIAICO/2022/144). ER-F was supported by the FPI contract PRE2019-087409. MP was supported by the Ramón y Cajal fellowship (RYC2018-024049-I and ACOND/2022 Generalitat Valenciana), both funded by MICIN (MCIN/AEI/10.13039/501100011033) and co-funded by the European Social Fund (ESF), and UM-B was supported by the JAE Intro ICU grant from CSIC (JAEICU-21-IATS-07).

Acknowledgements

The authors thank the collaboration of J. Monfort and L. Rodríguez for the technical assistance on the histological processing, I. Vicente for the technical assistance with fish husbandry and samplings at IATS and J. Pérez-Sánchez from the Nutrigenomics and Fish Growth Endocrinology Group (IATS, CSIC) for access to genomic databases.

Supplementary material

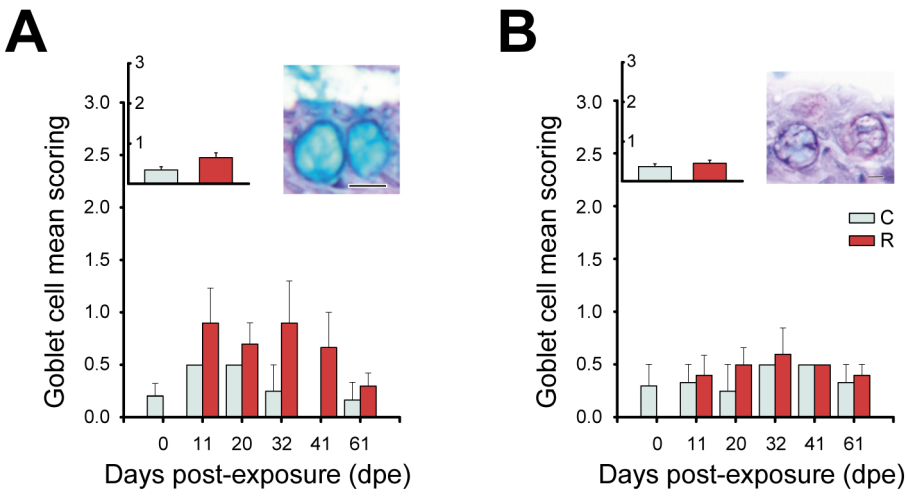

Figure S1. A: Goblet cell scoring with acidic mucins in the epithelium covering the proximal gill cartilage of gilthead seabream upon *Sparicotyle chrysophrii* infection. **B:** Goblet cell scoring with mixed neutral-acidic mucins in the epithelium covering the proximal gill cartilage of gilthead seabream upon *Sparicotyle chrysophrii* infection. Graph inserts represent pooled data of C or R fish, regardless of the infection timing; image inserts show the differential staining with PAS-alcian blue. C = control, unexposed fish (n=18); R = recipient, parasitised fish (n=25). **Abbreviations: dpe:** days post exposure. Scale bars = 5 µm.

The following supplementary material is freely available at https://www.frontiersin.org/articles/10.3389/fvets.2024.1347707/full#supplementary-material

- **Supplementary material: Table S1.** Genomic organization of the coding sequence of the nine mucin genes identified in the fSpaAur1.1 assembly. Numeric and sequence details ar shown in **a)** and the schematic representations are shown in **b)**.

- **Supplementary material: Table S2A.** Results from the *in silico* search of enzymes related to glycosylation in the gilthead seabream genome (Pérez-Sánchez et al.[40]). The query was conducted by term search within the genome annotation targeting silialidases, mannosidases, fucosyltransferases, acetylglucosaminyltransferases, sialyltransferases, mannosyltransferases glucosyltransferases, and phosphomannomutases. Gene symbols were retrieved from UniProt as the best matching for the annotation.

- **Supplementary material: Table S2B.** Sequences identified in **A)** were located in the DESeq2 result tables from previous RNA sequencing experiments of gilthead seabream gills during *Sparicotyle chrysophrii* infections. Differentially expressed (*p* adj < 0.05) sequences in at least one of the experiments are shown, together with the mean expression value of each group (in FPKM), the log2 fold change of the infected group versus the control (log2FC), the standard error of the fold change (lfcSE) and the *p* adj value. HIGH: Toxqui-Rodríguez et al.[43] SRA accession PRJNA992062; n=5 control (C) and n=5 infected (R) fish, mean intensity of infection 121.2 parasites/fish. LOW: Piazzon et al.[31]; SRA accession PRJNA507368; n=4 control (C) and n=4 infected (R) fish, mean intensity of infection 2.73 parasites·fish^{-1}.

References

1. Dash S, Das SK, Samal J, Thatoi HN. Epidermal mucus, a major determinant in fish health: a review. Iran J Vet Res. 2018;19:72.

2. Shephard KL. Functions for fish mucus. Rev Fish Biol Fish. 1994;4:401–29.

3. Kim YS, Ho SB. Intestinal goblet cells and mucins in health and disease: recent insights and progress. Curr Gastroenterol Rep. (2010) 12:319–30.

4. McGuckin MA, Lindén SK, Sutton P, Florin TH. Mucin dynamics and enteric pathogens. Nat Rev Microbiol. (2011) 9:265–78.

5. Sheng YH, Hasnain SZ, Florin THJ, McGuckin MA. Mucins in inflammatory bowel diseases and colorectal cancer. J Gastroenterol Hepatol. 2012;27:28–38.

6. Yang S, Yu M. Role of goblet cells in intestinal barrier and mucosal immunity. J Inflamm Res. 2021;14:3171–83.

7. Hicks SJ, Theodoropoulos G, Carrington SD, Corfield AP. The role of mucins in host-parasite interactions. Part I- protozoan parasites. Parasitol Today. 2000;16:476–81.

8. Theodoropoulos G, Hicks SJ, Corfield AP, Miller BG, Carrington SD. The role of mucins in host-parasite interactions: part II- helminth parasites. Trends Parasitol. 2001;17:130–5.

9. Hollingsworth MA, Swanson BJ. Mucins in cancer: protection and control of the cell surface. Nat Rev Cancer. 2004;4:45–60.

10. Bosi G, Giari L, DePasquale JA, Carosi A, Lorenzoni M, Dezfuli BS. Protective responses of intestinal mucous cells in a range of fish–helminth systems. J Fish Dis. 2017;40:1001–14.

11. Djordjevic B, Morales-Lange B, Øverland M, Mercado L, Lagos L. Immune and proteomic responses to the soybean meal diet in skin and intestine mucus of Atlantic salmon (*Salmo salar* L.). Aquac Nutr. 2021;27:929–40.

12. Koshio S. Immunotherapies targeting fish mucosal immunity- current knowledge and future perspectives. Front Immunol. 2016;6:153304.

13. Leknes IL. Histochemical study on the intestine goblet cells in cichlid and poecilid species (Teleostei). Tissue Cell. 2010;42:61–4.

14. Marcos-López M, Rodger HD, O'Connor I, Braceland M, Burchmore RJS, Eckersall PD, et al. A proteomic approach to assess the host response in gills of farmed Atlantic salmon *Salmo salar* L. affected by amoebic gill disease. Aquaculture. 2017;470:1–10.

15. Pérez-Sánchez J, Estensoro I, Redondo MJ, Calduch-Giner JA, Kaushik S, Sitjà-Bobadilla A. Mucins as diagnostic and prognostic biomarkers in a fish-parasite model: transcriptional and functional analysis. PLoS One. 2013;8:e65457.

16. Dezfuli BS, Lorenzoni M, Carosi A, Giari L, Bosi G. Teleost innate immunity, an intricate game between immune cells and parasites of fish organs: who wins, who loses. Front Immunol. 2023;14:1250835.

17. Battazza A, da Silva Brasileiro FC, Machado EF, de Matos MG, dos Santos CBT, Rodrigues MV, et al. Identification and characterization of *Sinuolinea niloticus* from Nile tilapia (*Oreochromis niloticus*) farmed in Botucatu, Brazil. Aquac Int. 2020; 28:1899–906.

18. Castrillo PA, Varela-Dopico C, Bermúdez R, Ondina P, Quiroga MI. Morphopathology and gill recovery of Atlantic salmon during the parasitic detachment of *Margaritifera margaritifera*. J Fish Dis. 2021;44:1101–15.

19. McAllister CT, Cloutman DG, Leis EM, Camus AC, Robison HW. A new *Myxobolus* (Cnidaria: Myxosporea: Myxobolidae) from the gills of the southern striped shiner, *Luxilus chrysocephalus isolepis* (Cypriniformes: Leuciscidae), from southwestern Arkansas, USA. Syst Parasitol. 2023;100:215–29.

20. Pleić IL, Bušelić I, Trumbić Ž, Bočina I, Šprung M, Mladineo I. Expression analysis of the Atlantic bluefin tuna (*Thunnus thynnus*) pro-inflammatory cytokines, IL-1β, TNFα1 and TNFα2 in response to parasites *Pseudocycnus appendiculatus* (Copepoda) and *Didymosulcus katsuwonicola* (Digenea). Fish Shellfish Immunol. 2015;45:946–54.

21. Roberts SD, Powell MD. The viscosity and glycoprotein biochemistry of salmonid mucus varies with species, salinity and the presence of amoebic gill disease. J Comp Physiol B. 2005;175:1–11.

22. Brabec J, Salomaki ED, Kolísko M, Scholz T, Kuchta R. The evolution of endoparasitism and complex life cycles in parasitic platyhelminths. Curr Biol. 2023;33:4269–4275.e3.

23. Muniesa A, Basurco B, Aguilera C, Furones D, Reverté C, Sanjuan-Vilaplana A, et al. Mapping the knowledge of the main diseases affecting sea bass and sea bream in Mediterranean. Transbound Emerg Dis. 2020;67:1089–100.

24. Repullés-Albelda A, Holzer AS, Raga JA, Montero FE. Oncomiracidial development, survival and swimming behaviour of the monogenean *Sparicotyle chrysophrii* (Van Beneden and Hesse, 1863). Aquaculture. 2012;338-341:47–55.

25. Repullés-Albelda A, Raga JA, Montero FE. Post-larval development of the microcotylid monogenean *Sparicotyle chrysophrii* (Van Beneden and Hesse, 1863): comparison with species of Microcotylidae and Heteraxinidae. Parasitol Int. 2011;60:512–20.

26. Villar-Torres M, Montero FE, Raga JA, Repullés-Albelda A. The influence of water temperature on the life-cycle of *Sparicotyle chrysophrii* (Monogenea: Microcotylidae), a common parasite in gilthead seabream aquaculture. Aquaculture. 2023;565:739103.

27. Villar-Torres M, Montero FE, Raga JA, Repullés-Albelda A. Effects of temperature and age on the swimming behaviour of a fish parasite, *Sparicotyle chrysophrii*. Anim Behav. 2023;200:159–66.

28. Villar-Torres M, Montero FE, Raga JA, Repullés-Albelda A. Come rain or come shine: environmental effects on the infective stages of *Sparicotyle chrysophrii*, a key pathogen in Mediterranean aquaculture. Parasit Vectors. 2018;11:558.

29. Aslam ML, Carraro R, Sonesson AK, Meuwissen T, Tsigenopoulos CS, Rigos G, et al. Genetic variation, GWAS and accuracy of prediction for host resistance to *Sparicotyle chrysophrii* in farmed gilthead sea bream (*Sparus aurata*). Front Genet. 2020;11:594770.

30. Henry MA, Nikoloudaki C, Tsigenopoulos C, Rigos G. Strong effect of long-term *Sparicotyle chrysophrii* infection on the cellular and innate immune responses of gilthead sea bream, *Sparus aurata*. Dev Comp Immunol. 2015;51:185–93.

31. Piazzon MC, Mladineo I, Naya-Català F, Dirks RP, Jong-Raadsen S, Vrbatović A, et al. Acting locally- affecting globally: RNA sequencing of gilthead sea bream with a mild *Sparicotyle chrysophrii* infection reveals effects on apoptosis, immune and hypoxia related genes. BMC Genomics. 2019;20:200.

32. Riera-Ferrer E, Piazzon MC, Del Pozo R, Palenzuela O, Estensoro I, Sitjà-Bobadilla A. A bloody interaction: plasma proteomics reveals gilthead sea bream (*Sparus aurata*) impairment caused by *Sparicotyle chrysophrii*. Parasit Vectors. 2022;15:322.

33. Cabello-Gómez JF, Aguinaga-Casañas MA, Falcón-Piñeiro A, González-Gragera E, Márquez-Martín R, Agraso MDM, et al. Antibacterial and antiparasitic activity of propyl-propane-thiosulfinate (PTS) and propyl-propane-thiosulfonate (PTSO) from *Allium cepa* against gilthead sea bream pathogens in *in vitro* and *in vivo* studies. Molecules. 2022;27:6900.

34. Firmino JP, Vallejos-Vidal E, Sarasquete C, Ortiz-Delgado JB, Balasch JC, Tort L, et al. Unveiling the effect of dietary essential oils supplementation in *Sparus aurata* gills and its efficiency against the infestation by *Sparicotyle chrysophrii*. Sci Rep. 2020;10:17764.

35. Mladineo I, Trumbić Ž, Ormad-García A, Palenzuela O, Sitjà-Bobadilla A, Manuguerra S, et al. *In vitro* testing of alternative synthetic and natural antiparasitic compounds against the monogenean *Sparicotyle chrysophrii*. Pathogens. 2021;10:980.

36. Rigos G, Fountoulaki E, Cotou E, Dotsika E, Dourala N, Karacostas I. Tissue distribution and field evaluation of caprylic acid against natural infections of *Sparicotyle chrysophrii* in cage-reared gilthead sea bream *Sparus aurata*. Aquaculture. 2013;408-409:15–9.

37. Rigos G, Mladineo I, Nikoloudaki C, Vrbatovic A, Kogiannou D. Application of compound mixture of caprylic acid, iron and mannan oligosaccharide against *Sparicotyle chrysophrii* (Monogenea: Polyopisthocotylea) in gilthead sea bream, *Sparus aurata*. Folia Parasit. 2016;63:1–6.

38. Sitjà-Bobadilla A, de Felipe MC, Alvarez-Pellitero P. *In vivo* and *in vitro* treatments against *Sparicotyle chrysophrii* (Monogenea: Microcotylidae) parasitizing the gills of gilthead sea bream (*Sparus aurata* L.). Aquaculture. 2006;261:856–64.

39. Riera-Ferrer E, Del Pozo R, Piazzon MC, Sitjà-Bobadilla A, Estensoro I, Palenzuela O. *Sparicotyle chrysophrii* experimental infection of gilthead seabream (*Sparus aurata*): establishment of an *in vivo* model reproducing the pathological outcomes of sparicotylosis. Aquaculture. 2023;573:739588.

40. Pérez-Sánchez J, Naya-Català F, Soriano B, Piazzon MC, Hafez A, Gabaldón T, et al. Genome sequencing and transcriptome analysis reveal recent species-specific gene duplications in the plastic gilthead sea bream (*Sparus aurata*). Front Mar Sci. 2019;6:498471.

41. Untergasser A, Cutcutache I, Koressaar T, Ye J, Faircloth BC, Remm M, et al. Primer3—new capabilities and interfaces. Nucleic Acids Res. 2012;40:e115.

42. Livak KJ, Schmittgen TD. Analysis of relative gene expression data using real-time quantitative PCR and the 2-ΔΔCT method. Methods. 2001;25:402–8.

43. Toxqui-Rodríguez S, Riera-Ferrer E, Del Pozo R, Palenzuela O, Sitjà-Bobadilla A, Estensoro I, et al. Molecular interactions in a holobiont-pathogen model: integromics in gilthead seabream infected with *Sparicotyle chrysophrii*. Aquaculture. 2023;581:740365.

44. Chaturvedi P, Singh AP, Batra SK. Structure, evolution, and biology of the MUC4 mucin. FASEB J. 2008;22:966–81.

45. Lehmann JM, Riethmuller G, Johnson JP. MUC18, a marker of tumor progression in human melanoma, shows sequence similarity to the neural cell adhesion molecules of the immunoglobulin superfamily. Proc Natl Acad Sci USA. 1989;86:9891–5.

46. Williams SJ, Wreschner DH, Tran M, Eyre HJ, Sutherland GR, McGuckin MA. MUC13, a novel human cell surface mucin expressed by epithelial and hemopoietic cells. J Biol Chem. 2001;276:18327–36.

47. Benktander J, Sundh H, Sundell K, Murugan AVM, Venkatakrishnan V, Padra JT, et al. Stress impairs skin barrier function and induces α2-3 linked N-acetylneuraminic acid and core 1 O-glycans on skin mucins in Atlantic salmon, *Salmo salar*. Int J Mol Sci. 2021;22:1488.

48. Jin C, Padra JT, Sundell K, Sundh H, Karlsson NG, Lindén SK. Atlantic salmon carries a range of novel O-glycan structures differentially localized on skin and intestinal mucins. J Proteome Res. 2015;14:3239–51.

49. Venkatakrishnan V, Padra JT, Sundh H, Sundell K, Jin C, Langeland M, et al. Exploring the Arctic charr intestinal glycome: evidence of increased N-glycolylneuraminic acid levels and changed host-pathogen interactions in response to inflammation. J Proteome Res. 2019;18:1760–73.

50. Sitjà-Bobadilla A, Alvarez-Pellitero P. Experimental transmission of *Sparicotyle chrysophrii* (Monogenea: Polyopisthocotylea) to gilthead seabream (*Sparus aurata*) and histopathology of the infection. Folia Parasit. 2009;56:143–51.

51. Antonelli L, Quilichini Y, Marchand B. *Sparicotyle chrysophrii* (Van Beneden and Hesse 1863) (Monogenea: Polyopisthocotylea) parasite of cultured gilthead sea bream *Sparus aurata* (Linnaeus 1758) (Pisces: Teleostei) from Corsica: ecological and morphological study. Parasitol Res. 2010;107:389–98.

52. Ogawa K. Diseases of cultured marine fishes caused by Platyhelminthes (Monogenea, Digenea, Cestoda). Parasitology. 2015;142:178–95.

53. Colorni A, Padrós F. Diseases and health management, Sparidae: biology and aquaculture of gilthead sea bream and other species. Chichester: Wiley-Blackwell (2011).

54. Padrós F, Crespo S. Proliferative epitheliocystis associated with monogenean infection in juvenile seabream *Sparus aurata* in the north east of Spain. Bull Eur Assoc Fish Pathol. 1995;15:42.

55. Blandford MI, Taylor-Brown A, Schlacher TA, Nowak B, Polkinghorne A. Epitheliocystis in fish: an emerging aquaculture disease with a global impact. Transbound Emerg Dis. 2018;65:1436–46.

56. Seth-Smith HMB, Dourala N, Fehr A, Qi W, Katharios P, Ruetten M, et al. Emerging pathogens of gilthead seabream: characterisation and genomic analysis of novel intracellular β-proteobacteria. ISME J. 2016;10:1791–803.

57. Dezfuli BS, Pironi F, Campisi M, Shinn AP, Giari L. The response of intestinal mucous cells to the presence of enteric helminths: their distribution, histochemistry and fine structure. J Fish Dis. 2010;33:481–8.

58. Díaz AO, García AM, Escalante AH, Goldemberg AL. Glycoproteins histochemistry of the gills of *Odontesthes bonariensis* (Teleostei, Atherinopsidae). J Fish Biol. 2010;77:1665–73.

59. Mistri A, Kumari U, Mittal S, Mittal AK. Gill epithelium of an angler catfish, *Chaca chaca* (Siluriformes, Chacidae): enzyme and glycoprotein histochemistry. Anat Histol Embryol. 2020;49:67–79.

60. Srivastava N, Kumari U, Rai AK, Mittal S, Mittal AK. Histochemical analysis of glycoproteins in the gill epithelium of an Indian major carp, *Cirrhinus mrigala*. Acta Histochem. 2012;114:626–35.

61. Chieng CCY, Daud HM, Yusoff FM, Thompson KD, Abdullah M. Mucosal responses of brown-marbled grouper *Epinephelus fuscoguttatus* (Forsskål, 1775) following intraperitoneal infection with *Vibrio harveyi*. J Fish Dis. 2020;43:1249–58.

62. Kumari U, Yashpal M, Mittal S, Mittal AK. Histochemical analysis of glycoproteins in the secretory cells in the gill epithelium of a catfish, *Rita rita* (Siluriformes, Bagridae). Tissue Cell. 2009;41:271–80.

63. Lang T, Alexandersson M, Hansson GC, Samuelsson T. Bioinformatic identification of polymerizing and transmembrane mucins in the puffer fish *Fugu rubripes*. Glycobiology. 2004;14:521–7.

64. Marcos-López M, Calduch-Giner JA, Mirimin L, MacCarthy E, Rodger HD, O'Connor I, et al. Gene expression analysis of Atlantic salmon gills reveals mucin 5 and interleukin 4/13 as key molecules during amoebic gill disease. Sci Rep. 2018;8:13689.

65. Sveen LR, Grammes FT, Ytteborg E, Takle H, Jørgensen SM. Genome-wide analysis of Atlantic salmon (*Salmo salar*) mucin genes and their role as biomarkers. PLoS One. 2017;12:e0189103.

66. Edirisinghe SL, Dananjaya SHS, Nikapitiya C, Liyanage TD, Lee KA, Oh C, et al. Novel pectin isolated from *Spirulina maxima* enhances the disease resistance and immune responses in zebrafish against *Edwardsiella piscicida* and *Aeromonas hydrophila*. Fish Shellfish Immunol. 2019;94:558–65.

67. Jevtov I, Samuelsson T, Yao G, Amsterdam A, Ribbeck K. Zebrafish as a model to study live mucus physiology. Sci. Rep. 2014;4:6653.

68. Lang T, Klasson S, Larsson E, Johansson MEV, Hansson GC, Samuelsson T. Searching the evolutionary origin of epithelial mucus protein components—mucins and FCGBP. Mol Biol Evol. 2016;33:1921–36.

69. Adamek M, Hazerli D, Matras M, Teitge F, Reichert M, Steinhagen D. Viral infections in common carp lead to a disturbance of mucin expression in mucosal tissues. Fish Shellfish Immunol. 2017;71:353–8.

70. Baloch AA, Steinhagen D, Gela D, Kocour M, Piačková V, Adamek M. Immune responses in carp strains with different susceptibility to carp edema virus disease. PeerJ. 2023;11:e15614.

71. Moniaux N, Escande F, Porchet N, Aubert JP, Batra SK. Structural organization and classification of the human mucin genes. Front Biosci. 2001;6:d1192–206.

72. Corfield AP. Mucins: a biologically relevant glycan barrier in mucosal protection. Biochim Biophys Acta Gen Subj. 2015;1850:236–52.

73. Roussel P, Delmotte P. The diversity of epithelial secreted mucins. Curr Org Chem. 2004;8:413–37.

74. Rogers DF. Physiology of airway mucus secretion and pathophysiology of hypersecretion. Respir Care. 2007;52:1134–49.

75. Rose MC, Voynow JA. Respiratory tract mucin genes and mucin glycoproteins in health and disease. Physiol Rev. 2006;86:245–78.

76. Ng AYN, Waring P, Ristevski S, Wang C, Wilson T, Pritchard M, et al. Inactivation of the transcription factor Elf3 in mice results in dysmorphogenesis and altered differentiation of intestinal epithelium. Gastroenterology. 2002;122:1455–66.

77. Shih LJ, Lu YF, Chen YH, Lin CC, Chen JA, Hwang SPL. Characterization of the *agr2* gene, a homologue of *X. laevis anterior gradient 2*, from the zebrafish, *Danio rerio*. Gene Expr Patterns. 2007;7:452–60.

78. Crosnier C, Vargesson N, Gschmeissner S, Ariza-McNaughton L, Morrison A, Lewis J. Delta-notch signalling controls commitment to a secretory fate in the zebrafish intestine. Development. 2005;132:1093–104.

79. Wang Q, He G, Mai K, Xu W, Zhou H, Wang X, et al. Chronic rapamycin treatment on the nutrient utilization and metabolism of juvenile turbot (*Psetta maxima*). Sci Rep. 2016;6:28068.

80. Drurey C, Lindholm HT, Coakley G, Poveda MC, Löser S, Doolan R, et al. Intestinal epithelial tuft cell induction is negated by a murine helminth and its secreted products. J Exp Med. 2021;219:e20211140.

81. Ohtsubo K, Marth JD. Glycosylation in cellular mechanisms of health and disease. Cell. 2006;126:855–67.

82. Falkenberg VR, Alvarez K, Roman C, Fregien N. Multiple transcription initiation and alternative splicing in the 5′ untranslated region of the core 2 β1-6 N-acetylglucosaminyltransferase I gene. Glycobiology. 2003;13:411–8.

83. Holmén JM, Olson FJ, Karlsson H, Hansson GC. Two glycosylation alterations of mouse intestinal mucins due to infection caused by the parasite *Nippostrongylus brasiliensis*. Glycoconj J. 2003;19:67–75.

84. Ma B, Simala-Grant JL, Taylor DE. Fucosylation in prokaryotes and eukaryotes. Glycobiology. 2006;16:158R–84R.

85. Kononova S, Litvinova E, Vakhitov T, Skalinskaya M, Sitkin S. Acceptive immunity: the role of fucosylated glycans in human host–microbiome interactions. Int J Mol Sci. 2021;22:3854.

86. Kononova SV. How fucose of blood group glycotypes programs human gut microbiota. Biochem Mosc. 2017;82:973–89.

87. Benktander J, Padra JT, Maynard B, Birchenough G, Botwright NA, McCulloch R, et al. Gill mucus and gill mucin O-glycosylation in healthy and amebic gill disease-affected Atlantic salmon. Microorganisms. 2020;8:1871.

88. Estensoro I, Jung-Schroers V, Álvarez-Pellitero P, Steinhagen D, Sitjà-Bobadilla A. Effects of *Enteromyxum leei* (Myxozoa) infection on gilthead sea bream (*Sparus aurata*) (Teleostei) intestinal mucus: glycoprotein profile and bacterial adhesion. Parasitol Res. 2013;112:567–76.

89. Álvarez-Pellitero P. Mucosal intestinal immunity and response to parasite infections in ectothermic vertebrates, immunology and immune system disorders. New York, NY: Nova Science Publishers, Inc (2011).

90. Cano M, Ilundain AA. Ontogeny of D-mannose transport and metabolism in rat small intestine. J Membr Biol. 2010;235:101–8.

91. Dai Z, Aryal UK, Shukla A, Qian WJ, Smith RD, Magnuson JK, et al. Impact of *alg3* gene deletion on growth, development, pigment production, protein secretion, and functions of recombinant *Trichoderma reesei* cellobiohydrolases in *Aspergillus niger*. Fungal Genet Biol. 2013;61:120–32.

Chapter 6

Immunoprotective role of fish mucus against the ectoparasitic flatworm *Sparicotyle chrysophrii*

Enrique Riera-Ferrer, M. Carla Piazzon, Raquel Del Pozo, Elena Gimeno-Bañón, Oswaldo Palenzuela, Ariadna Sitjà-Bobadilla and Itziar Estensoro

Fish Pathology Group, Institute of Aquaculture Torre de la Sal (IATS, CSIC), Consejo Superior de Investigaciones Científicas, Castellón, Spain

***Submitted to: Fish and Shellfish Immunology**

Abstract

The gill ectoparasitic flatworm, *Sparicotyle chrysophrii*, has a significant impact on gilthead seabream farming in the Mediterranean. Yet, it remains unclear whether gilthead seabream develops immunological memory and protection following exposure to the parasite, which causes severe anaemia by feeding on the host's blood.

This study compared recovered gilthead seabream (RE; n=25), which had previously overcome sparicotylosis after 10.5 months of exposure to *S. chrysophrii*, and naïve fish (NAI; n=25), that had no prior exposure to the parasite. Both groups were exposed to *S. chrysophrii* eggs, and parasitic burdens, biometric and haematological parameters were monitored over 62 days post-exposure (dpe). Total and specific IgM and IgT titers were measured in plasma and gill mucus by ELISA, binding specificity of specific immunoglobulins were determined by immunohistochemistry, and immunoglobulin-expressing cells were quantified in spleens and gills of RE and NAI fish.

Results showed a strong mucosal immune response in RE gills, with high local secretion of parasite-specific immunoglobulins, particularly IgT, which were absent in NAI and undetectable in plasma of all recipient fish. Five months after the initial exposure, RE gill mucus still had significantly higher specific IgM and IgT titers than NAI. However, after the secondary exposure, these titres gradually decreased in RE, eventually becoming significantly lower than in NAI by the end of the trial. Immunohistochemistry confirmed the binding specificity of anti-*S. chrysophrii* IgT in RE gill mucus and IgM in plasma. Additionally, RE showed a higher number of IgT-expressing cells in the gills and IgM-expressing cells in the spleen.

Introduction

Monogeneans, formerly considered a platyhelminth class (Monogenea) within Neodermata and recently reclassified into two independent classes, Monopisthocotyla and Polyopisthocotyla[1,2], are mainly ectoparasites of aquatic organisms. They predominantly infect the external surfaces of fish, including the gills, skin, and fins. These parasites pose significant challenges to aquaculture and wild fish populations by causing severe damage and increasing susceptibility to secondary infections, ultimately affecting their growth, survival, and overall fitness[3,4]. In Mediterranean aquaculture farms rearing gilthead seabream (*Sparus aurata*), *Sparicotyle chrysophrii* (Polyopisthocotyla: Microcotylidae) is considered the most devastating pathogen, responsible for up to 30% of mortality during the on-growing stage in some sea cages[5,6]. Field data from fish farmers' observations indicate that juvenile specimens are more susceptible to sparicotylosis, exhibiting more severe clinical signs and higher mortality rates than adults. These observations may be driven by two primary factors: the greater impact of parasites' blood feeding on smaller fish due to their lower blood volume[7], and the possibility that adult gilthead seabream could develop some kind of resistance against this flatworm over their lifespan in sea cages.

The immune response of fish to parasitic infections has been a focal point of recent research due to its significant implications for aquaculture health and productivity[3,8–16]. The fish immune system comprises both innate and adaptive components, with the latter involving the production of specific immunoglobulins (Igs) that play a vital role in pathogen recognition and neutralisation. Notably, immunoglobulin M (IgM) and immunoglobulin T (IgT) are pivotal in the adaptive immune response of fish against parasitic infections[17–19]. These Igs facilitate the immune system's ability to recognise, target, and eliminate parasitic invaders, thereby contributing to the overall health and resilience of fish populations. Research on immune responses to helminths has primarily focused on the identification of key immune components involved in recognising and combating these parasites. Natural and experimental infections have provided insights into the interactions between worms and the fish immune system, highlighting the importance of both innate and adaptive components against different types of worms[20,21]. In monogenean infections, significant roles are played by pro-inflammatory cytokines, humoral factors such as complement and mucins, and different cellular actors[22–30]. All these findings suggest that an effective immune response against these parasites involves a coordinated action of both local and systemic immune components.

In gilthead seabream, infections by *S. chrysophrii* seem to trigger a cellular immune response while inhibiting its humoral components[31,32]. A plasma proteomics study revealed that sparicotylosis profoundly alters haemostasis, the innate immune system, and

lipid metabolism and transport in gilthead seabream with high infection intensity[33]. In cases of mild infection intensities, there is a general upregulation of Igs, complement, and genes related to inflammation, cytotoxicity, and both innate and adaptive immunity in gills[34]. Upon high infection intensities, key pathways regulated in the gills, liver and spleen include immune response, stress response, starvation, hypoxia, apoptosis, and haemostasis[35]. Additionally, the gill mucosal response in gilthead seabream involves goblet cell hyperplasia and neutral mucus hypersecretion[32,36].

A key aspect of the adaptive immune response is the development of immunological memory, which enables fish to mount a more robust and rapid response upon subsequent exposures to the same parasite. This phenomenon, characterised by the accelerated production of specific Igs, highlights the importance of prior exposure and recovery in enhancing the immune capabilities of teleost fish in parasitic infections[37–40]. A number of investigations have shown that fish are capable of producing specific antibodies to monogenean parasites, e.g. in the Japanese pufferfish (*Takifugu rubripes*), common carp (*Cyprinus carpio*), and European eel (*Anguilla anguilla*), but not in spot croacker (*Leiostomus xanthurus*), rainbow trout (*Onchorhynchus mykiss*), or Japanese flounder (*Paralichthys olivaceus*)[26,41]. Interestingly, Japanese pufferfish produced specific antibodies to *Heterobothrium okamotoi* (Polyopisthocotyla: Diclidophoridae) after parasites had finished feeding on the gills and the inflammatory response was triggered[42].

Other subsequent experiments showed that *Bicotylophora trachinoti* (Polyopisthocotyla: Discocotylidae) infection levels were higher in fish naturally infected for the first time than in re-infected[43]. Moreover, Cable and Vann Oosterhout[44] indicated that acquired immunity may significantly contribute to the resistance of guppies (*Poecilia reticulata*) against *Gyrodactylus turnbulli* (Monopisthocotyla: Gyrodactylidae). Nevertheless, the involvement of specific antibodies was not studied in any of these cases. Furthermore, active immunisation of rainbow trout with *Discocotyle sagittata* (Polyopisthocotyla: Discocotylidae) extracts conferred partial protection against infection[45], and the injection of *Cichlidogyrus* spp. (Monopisthocotyla: Ancyrocephalidae) antigenic extract in Nile tilapia (*Oreochromis niloticus*) induced a characteristic pattern of primary and secondary immune responses[46]. The adaptive immune response in Nile tilapia participated in the resistance against *Gyrodactylus cichlidarum* (Monopisthocotyla: Gyrodactylidae) infection, underscoring the involvement of mucosal immunity[47]. Moreover, studies on related neodermatans, such as trematodes belonging to the family Aporocotylidae, have emphasised the potential for developing vaccines based on specific antigens to provide long-term protection against these parasites[48].

In this study, we aim to explore the mechanisms underlying gilthead seabream immune response to *S. chrysophrii*, with a particular focus on the role of Igs at local and

systemic levels, and the implications for the recovery from past infections and resistance to further infections. Understanding the immune response is crucial for developing effective management and prophylactic strategies to mitigate the impacts of these infections in aquaculture settings.

Materials and methods

Experimental fish groups

A stock of healthy gilthead seabream juveniles, purchased from a local hatchery, was maintained at the indoor experimental facilities of the Institute of Aquaculture Torre la Sal (IATS) and used as control and recipient fish. Photoperiod, salinity and temperature conditions were maintained according to the geographic coordinates 40°5´N, 0°10´E, with oxygen saturation above 85% and unionised ammonia levels below 0.02 $mg \cdot L^{-1}$. Fish were fed *ad libitum* with a commercial dry pellet diet (BioMar, Aarhus, Denmark) twice daily, five days per week.

Gilthead seabream (103.4 ± 14.2 g; mean ± SD; n = 30) were experimentally infected in a primary challenge following the procedure described in Riera-Ferrer et al.[32], by exposure to a *S. chrysophrii*-contaminated water effluent in a recirculation aquaculture system (RAS) between October 2020 and March 2021 at 14.50 ± 2.12 °C (mean ± SD; minimum temperature: 10.1 °C; maximum temperature: 18.5 °C). Thereafter, these fish were transferred to clean tanks and kept with parasite-free open water flow. Clean parasite egg collectors (after Riera-Ferrer et al.[32]) were placed in these tanks and were checked and replaced on a weekly basis. After 4.5 months of monitoring, when the absence of parasite eggs in collectors was sustained during two weeks, it was considered that these fish had naturally overcome sparicotylosis and they were used as the reexposed (RE) experimental fish group (328.2 ± 29.6 g; mean ± SD; n = 24). Unexposed gilthead seabream of the same age from the healthy fish stock were used as the naïve (NAI) experimental fish group (484.9 ± 60.1 g; mean ± SD; n = 25).

Secondary parasite challenge and samplings

Both RE and NAI fish were individually tagged with passive integrated transponders (PIT) and homogenously distributed into two replicate 500 L tanks, where the two groups (RE and NAI) cohabited, and were kept in parasite-free open water flow. The secondary *S. chrysophrii* challenge took place by exposure to egg collectors loaded with 320 parasite eggs, placed in each tank between September to November 2021 at 22.33 ± 2.28 °C (mean ± SD; minimum temperature: 17.40 °C; maximum temperature: 26 °C). During the trial, three samplings took place (S0, S1 and S2). At S0, before parasite eggs were introduced into the cohabitation tanks, n = 4 RE and n = 5 NAI fish were sampled. At S1 (30 days post

exposure to the parasite (dpe)) and S2 (62 dpe), n = 10 RE and n = 10 NAI fish were sampled, respectively. In all samplings, fish were euthanised by tricaine methanesulfonate (MS-222; Sigma-Aldrich, MO, USA) overexposure (0.1 $g \cdot L^{-1}$). Individual biometric values were recorded, blood was collected from the caudal vessels with heparinised syringes, haemoglobin levels were immediately registered (HemoCue®201+Hb System; HemoCue-AB, Ängelholm, Sweden), and haematocrit values were determined using standard microhaematocrit capillary centrifugation in a haematocrit centrifuge (myLab HC-01, AHN®, Germany) at 10,000× *g* for 10 min. The remaining blood was centrifuged at 3,000× *g* for 30 min, and individual plasma samples were stored at -20 °C until further processing. Gill mucus of the four left-side gill arches was collected by repeatedly flushing the dissected gills with 1 mL of cold Hank's balanced salt solution (HBSS), which was then centrifuged at 10,000× *g* for 10 min, and the supernatant stored at -20 °C until further processing.

Two right-side gill arches were dissected, and parasite infection intensity was determined by manual count of juvenile and adult *S. chrysophrii* under the stereomicroscope. Total parasite load per fish was then extrapolated for the eight gill arches of each fish, according to Riera-Ferrer et al.[49]. Tissue samples of the remaining right-side gills and spleen were fixed in 10% neutral buffered formalin and processed for routine paraffin histology.

Ethics statement

All experiments were carried out according to current Spanish (Royal Decree 53/2013) and EU legislation on the handling of experimental fish (Directive 2010/63/EU). All procedures were approved by the Ethics and Animal Welfare Committee of the Institute of Aquaculture Torre de la Sal (IATS, CSIC, Castellón, Spain), CSIC and "Generalitat Valenciana" (permit number 2018/VSC/PEA/0240).

Humoral IgM and IgT detection

Total and specific IgM and IgT in all RE and NAI plasma and gill mucus samples were measured in duplicates by ELISA (details on antigen and antibodies concentrations are shown in **Table 1**). For total Ig detection, 96-flat-bottomed well microplates (Maxisorp; Thermo Scientific™ Nunc™, Thermo Fisher Scientific, MA, USA) were coated with fish plasma or gill mucus diluted in coating buffer (carbonate-bicarbonate buffer, pH 9.6) overnight at 4 °C. Between incubation steps, three successive washings with TTBS (20 mM Tris-HCl, 0.5 M NaCl, pH 7.2 (TBS) with 0.05% Tween 20) and one with TBS were performed. Thereafter, wells were blocked with 5% skimmed milk in TBS for 2 h at 37 °C, before incubating with custom-made rabbit polyclonal antibodies (Ab) against gilthead seabream IgM[50] or IgT[51] for two further hours at 37 °C. Incubation with goat anti-rabbit IgG horseradish peroxidase conjugate (Sigma-Aldrich, MO, USA) diluted in TBS for 1 h at 37 °C followed, and

Table 1. Antigen and antibody concentrations and dilutions used for the different ELISA protocols.

ELISA	Parasite antigen ($\mu g \cdot mL^{-1}$)	Gilthead seabream plasma/mucus
Plasma total IgM	-	1:3,000
Plasma total IgT	-	1:5
Gill mucus total IgM	-	1:3,000
Gill mucus total IgT	-	1:2
Plasma specific IgM	20	1:25
Plasma specific IgT	20	1:25
Gill mucus specific IgM	20	1:25
Gill mucus specific IgT	20	1:25

the last washing step was performed. TMB peroxidase substrate (3,3′,5,5′-tetramethylbenzidine solution + H2O2; BioRad, CA, USA) was added, incubated in the dark with gentle shaking at room temperature for 30 min, and finally the reaction was stopped by the addition of 1 N H_2SO_4. The plates were then read at 450 nm with an automatic plate reader (Tecan Group Ltd., Männedorf, Switzerland).

In order to detect specific anti-*S. chrysophrii* Igs, a parasite antigen was first prepared for specific ELISAs. Adult *S. chrysophrii* specimens were retrieved from the gill filaments during routine parasite diagnosis under the stereomicroscope and kept frozen at -80 °C until a total of 50 parasites were harvested. These were then pooled in 250 µL of sterile PBS and homogenised in a lysing tube with ceramic beads at 6 $m \cdot s^{-1}$ for 30 s in a FastPrep™ homogeniser (MP Biomedicals, CA, USA). The parasite homogenate was centrifuged at 12,000× *g* 30 min at 4 °C, the supernatant collected and its total protein content was quantified with NanoDrop™ 2000c spectrophotometer (Thermo Fisher Scientific, MA, USA) and then aliquoted and frozen at -20 °C. For specific ELISAs, 96-flat-bottomed well microplates were coated with parasite homogenate diluted in coating buffer overnight at 4 °C, washed, blocked as above stated, and then incubated with the diluted fish plasma or gill mucus overnight at 4 °C. Fish Igs were then bound with the custom-made anti-*S. aurata* IgM and IgT rabbit polyclonal antibodies (Abs), incubated with goat anti-rabbit IgG horseradish peroxidase conjugate, washed, incubated with the peroxidase substrate, and the reaction stopped as above stated before absorbance at 450 nm was read.

In addition, total protein content was measured in all gill mucus samples with the

Primary Ab (rabbit anti-gilthead seabream)	**Conjugated secondary Ab** (goat anti-rabbit)
1:40,000	1:1,000
1:1,000	1:1,000
1:10,000	1:1,000
1:1,000	1:1,000
1:13,000	1:1,000
1:100	1:1,000
1:10,000	1:1,000
1:100	1:1,000

Bradford protein assay (Bio-Rad Laboratories Inc., CA, USA) using bovine serum albumin (Sigma-Aldrich, MO, USA) dilutions as a standard curve (ranging from 0 to 22,000 $\mu g \cdot mL^{-1}$). Absorbance was measured at 595 nm following manufacturer's instructions. In order to avoid bias in the concentration of mucus samples due to differences in flushing intensity by operators, optical density (OD) measurements obtained from gill mucus ELISAs were corrected by total protein content.

Immunohistochemical IgM and IgT specificity

Based on the results of the specific ELISAs, plasma and gill mucus samples with the highest specific Ig titres were selected and applied in an immunohistochemical protocol in order to localise the specific IgM and IgT immunoreactivity on parasite sections. Adult *S. chrysophrii* were again retrieved from gill filaments during routine parasite diagnosis under the stereomicroscope, fixed in 10% neutral buffered formalin and processed for routine paraffin histology as a pellet.

Briefly, sections of the parasite pellet were deparaffinised and hydrated, endogenous peroxidase activity was quenched by incubation for 30 min in 3% H_2O_2 and slides were blocked with 1.5% normal goat serum (Vector Laboratories, CA, USA) for 30 min. The standard washing procedure consisted of 5 min successive immersions in TTBS and TBS between incubation steps, which were performed in a humid chamber at room temperature. Tissue sections were then incubated for 1 h with each individual plasma (1:30) diluted in TBS 1% bovine serum albumin (Sigma-Aldrich, MO, USA) or mucus (undiluted), and

for one further hour with the rabbit polyclonal antibody against gilthead IgM (1:13,000) or a mouse monoclonal antibody against gilthead seabream IgT (1:10). Thereafter, tissues were incubated with a biotinilated goat anti-rabbit or horse anti-mouse antibody (Vector Laboratories, CA, USA) for 1 h, respectively, and the avidin-biotin-peroxidase complex (ABC; Vector Laboratories, CA, USA) was applied for one hour. Bound peroxidase was visualised by adding 3,3'-diaminobezidine tetrahydrochloride chromogen (DAB; Sigma-Aldrich, MO, USA) and the reaction was stopped after 2 min with deionised water. Tissue sections were subsequently counterstained with Gill's haematoxylin, dehydrated and mounted in di-N-butyl-phthalate in xylene. Each plasma sample was tested in duplicate. Negative controls omitted the fish plasma or mucus, the primary and secondary Abs or the ABC. Immunoreactivity of fish plasma or mucus against the parasite was observed by microscopic examination with a Leitz Dialux22 (Leica, Hesse, Germany) light microscope. The images were taken with an Olympus DP70 Camera (Olympus, Tokyo, Japan).

mRNA IgM and IgT *in situ* hybridisation

IgM and IgT transcripts were detected by RNA-*in situ* hybridisation (RNA-ISH) in the spleen and gill sections of 5 RE and 4 NAI at 62 dpe using the ViewRNA™ ISH Tissue 2-plex Assay kit (Affymetrix, Ca, USA). This method uses a proprietary DNA signal amplification technology allowing simultaneous detection of two target mRNAs in tissue sections with single-copy sensitivity. The probe sets were designed using the sequences of gilthead seabream IgM (GenBank Accession Numbers: JQ811851 and KX599199) and IgT (GenBank Accession Numbers: KX599200 and KX599201) heavy chains, in regions 20-903 and 2-901, respectively. To allow the detection of all Ig transcripts regardless of their soluble or membrane-bound form, variable domains and regions not expressed in both forms were excluded. The ISH procedure was performed on 4-µm-thick paraffin sections following the manufacturer's instructions, using a 10 min heat pretreatment at 90 to 95 °C and a 30 min protease step at 40 °C. After probe hybridisation and development with Fast Blue and Fast Red substrates, the slides were counterstained with 25% Gill's haematoxylin for 3 min, washed, and mounted in aqueous mounting medium (Fluoromount-G™, Thermo Fisher Scientific, MA, USA). Labelled cells in each tissue section of each fish were quantified in 10 random microscope fields at 625×.

(See figure on next page.)

Figure 1. Evolution of biometry (A-C), parasite outcome (D) and haematological (E-F) variables throughout two months of exposure to *Sparicotyle chrysophrii*. A: Weight (mean ± SD). **B:** length (mean ± SD). **C:** Fulton's condition factor (mean ± SD). **D:** Boxplot representing the infection intensity of *S. chrysophrii* throughout the trial (whiskers represent maximum and minimum values). **E:** haemoglobin concentration (mean ± SD). **F:** concentration (mean ± SD). Different uppercase and lowercase letters stand for statistically significant differences within NAI or RE groups along the trial, respectively (One-way ANOVA). Asterisks (*) indicate statistically significant differences between NAI and RE within each sampling point (t-test, *:$p < 0.05$; **: $p < 0.01$).

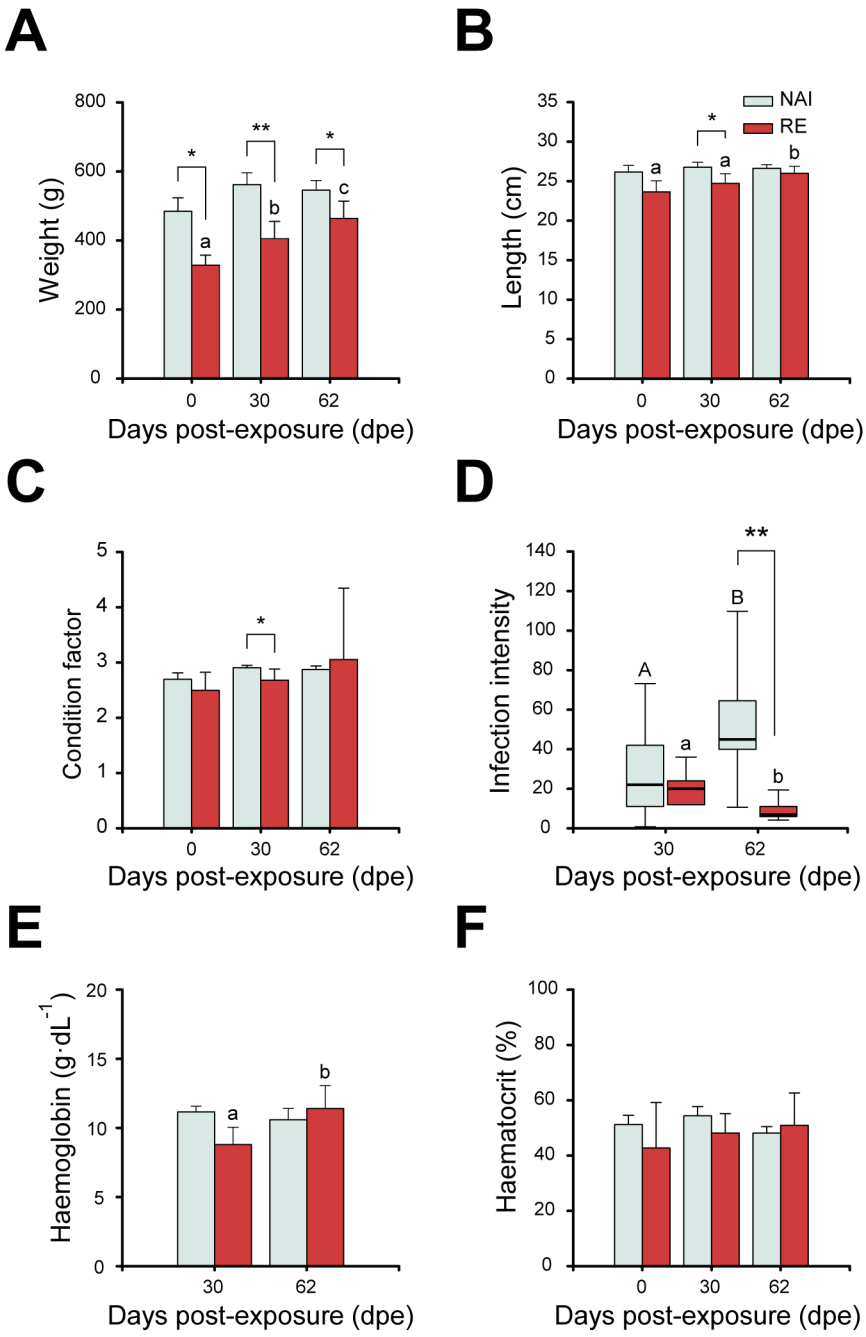

Figure 1. (See legend on previous page).

Statistics

Biometric, haematology, infection outcome,, and ELISA data, and counts of IgM or IgT expressing cells were analysed for statistically significant differences within RE and NAI among sampling points by one-way analyses of variance (ANOVA-I) followed by Student–Newman–Keuls test. Data which failed the normality or equal variance test were analysed with Kruskal–Wallis ANOVA-I on ranks followed by Dunn's post-hoc test. Within a sampling points, significant differences between RE and NAI were detected by the Student's t-test. The significance level was set at $p < 0.05$.

Results

Infection outcome

The infection prevalence at 30 dpe was 90% and 100% in NAI and RE, respectively, and reached 100% in both NAI and RE groups by 62 dpe. Initially, no statistically significant differences were observed between NAI and RE regarding their infection intensity ($p = 0.339$) (**Figure 1D**); however, at 62 dpe, the infection intensity in RE fish significantly dropped ($p = 0.003$), whereas that of NAI significantly increased ($p = 0.031$), resulting in a significantly higher infection intensity in NAI than in RE ($p < 0.001$). RE fish fitness was not affected by parasite exposure and their condition factor slightly increased, unlike in NAI fish, which showed no weight or length increase and whose condition factor did not increase and was lower than in RE by the end of the experiment (**Figure 1A**, **B**, **C**). Interestingly, RE haemoglobin levels increased over time (**Figure 1E**), whereas those of NAI remained stable, as well as haematocrit levels for both RE and NAI throughout the experiment (**Figure 1F**).

Circulating and mucosal antibodies

No statistically significant differences were observed in total and specific IgM and IgT levels in plasma between NAI and RE fish, which remained relatively stable. Over time, only an increasing trend of plasmatic Ig levels in RE fish was observed. In contrast, major differences in NAI and RE Ig levels were found in the gill mucus. Total IgM levels in RE gill mucus increased throughout the experimental infection more than in NAI and, by 30 dpe, they were significantly higher. By contrast, RE specific IgM levels were initially significantly higher than those of NAI prior to the challenge, but this pattern reversed by the end of the challenge, two months later. Similarly, total and specific IgT levels in gill mucus were significantly higher in RE than in NAI at the beginning of the challenge, but lower by 62 dpe (**Figure 2**).

Plasma and gill mucus immunoreactivity against *Sparicotyle chrysophrii*

The immunoreactivity was indicated by a brown DAB precipitate, where the specific Igs of

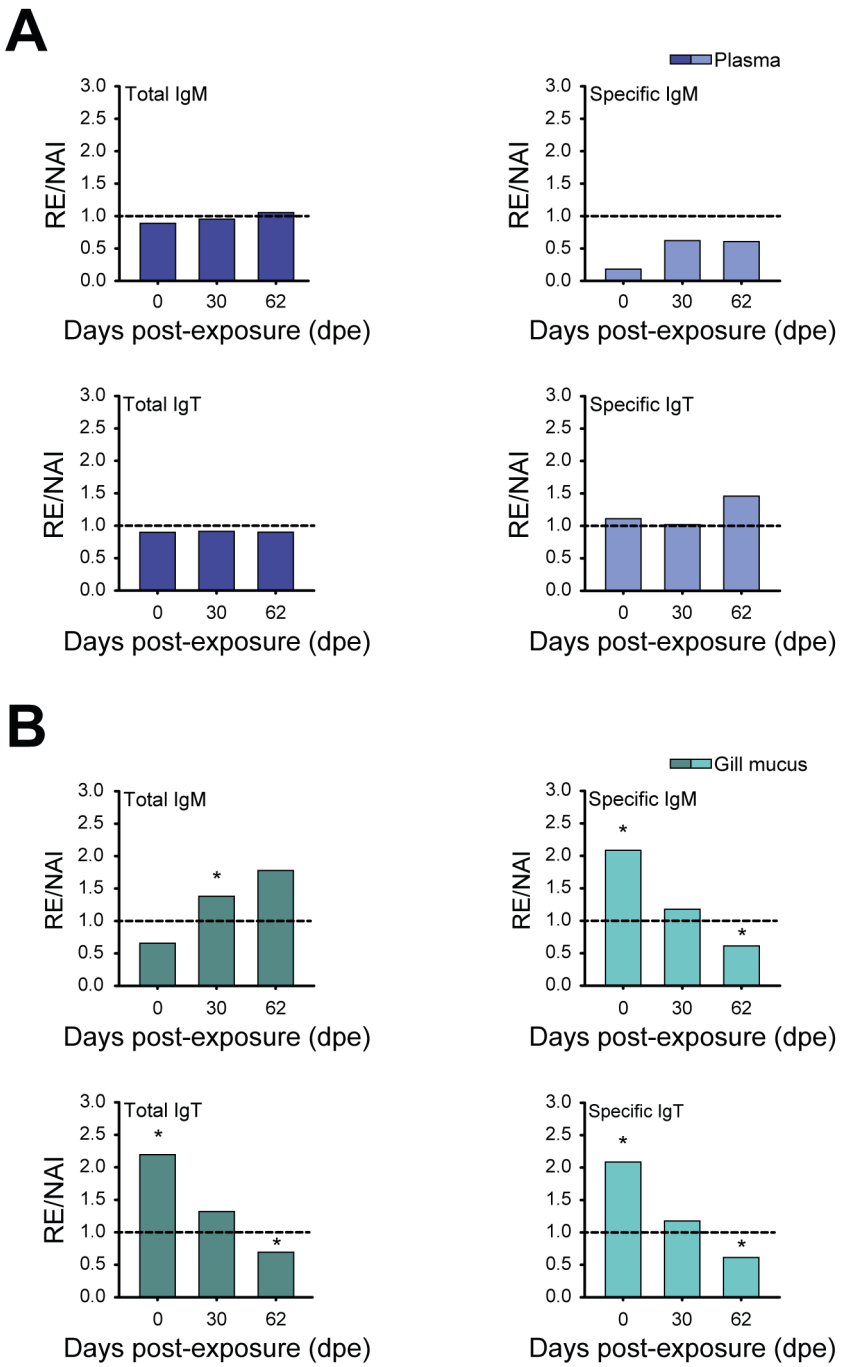

Figure 2. Total and specific IgM and IgT in reexposed (RE) and naïve (NAI) gilthead seabream throughout two months of exposure to *Sparicotyle chrysophrii*. A: Plasma ratios between RE and NAI. **B:** Gill mucus ratios between RE and NAI. **NOTE:** Values >1 correspond to higher titres in RE fish, whereas values <1 correspond to higher titres in NAI fish. Asterisks (*) indicate statistically significant differences between RE and NAI (t-test, p <0.05).

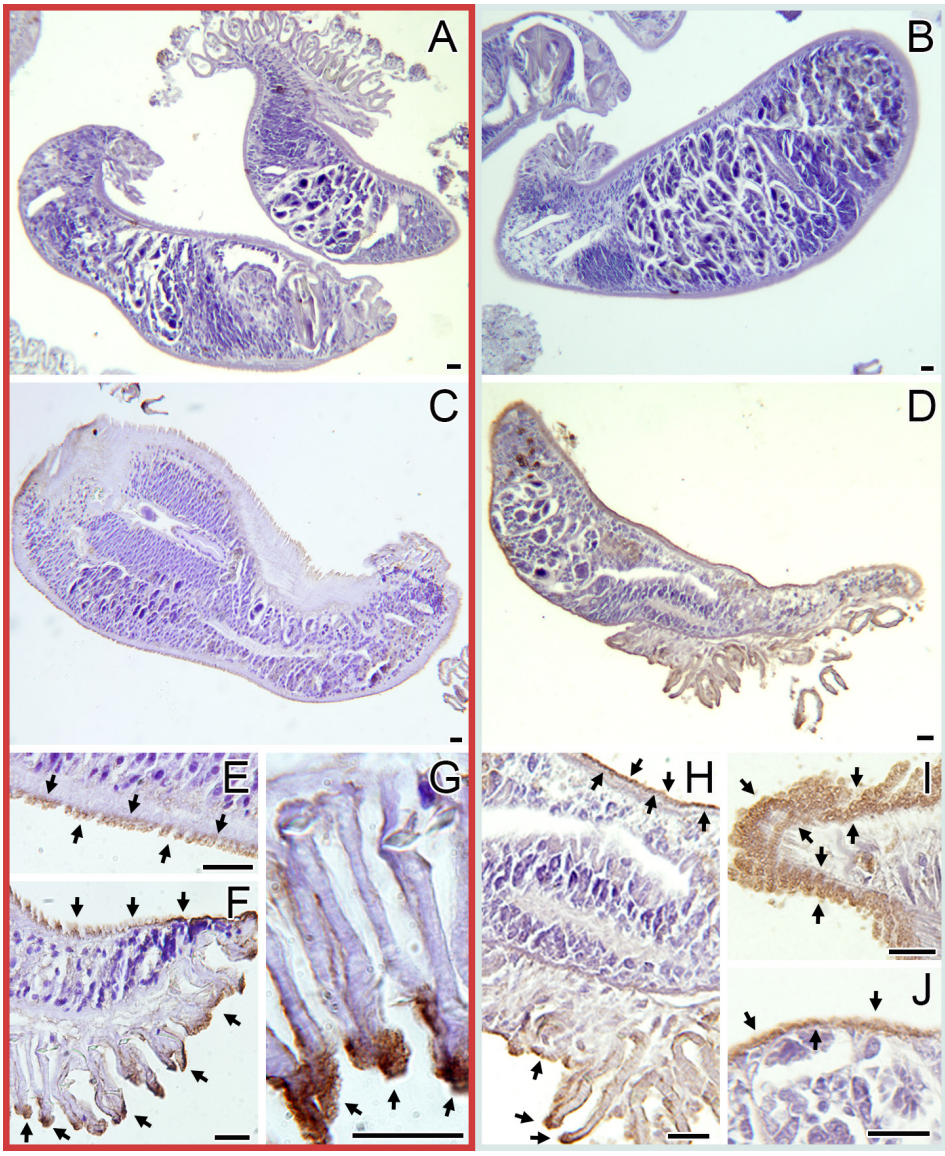

Figure 3. Specific IgM binding to *Sparicotyle chrysophrii* histological sections. Red-framed images were immunolabelled with samples of reexposed fish (RE) and pale turquoise-framed images with naïve fish (NAI) samples at 62 days post exposure. A, **B:** Absence of IgM immunoreactivity with mucus samples of RE and NAI fish. **C-J:** Plasma specific IgM binding to *S. chrysophrii*. Note the immunoreactivity (black arrows) of the parasite's outer tegument (neodermis) (**E**, **H-J**) and the syncytial lining covering the clamps (**F**, **G**, **H**) with plasma of both, RE and NAI fish. Scale bars = 20 µm.

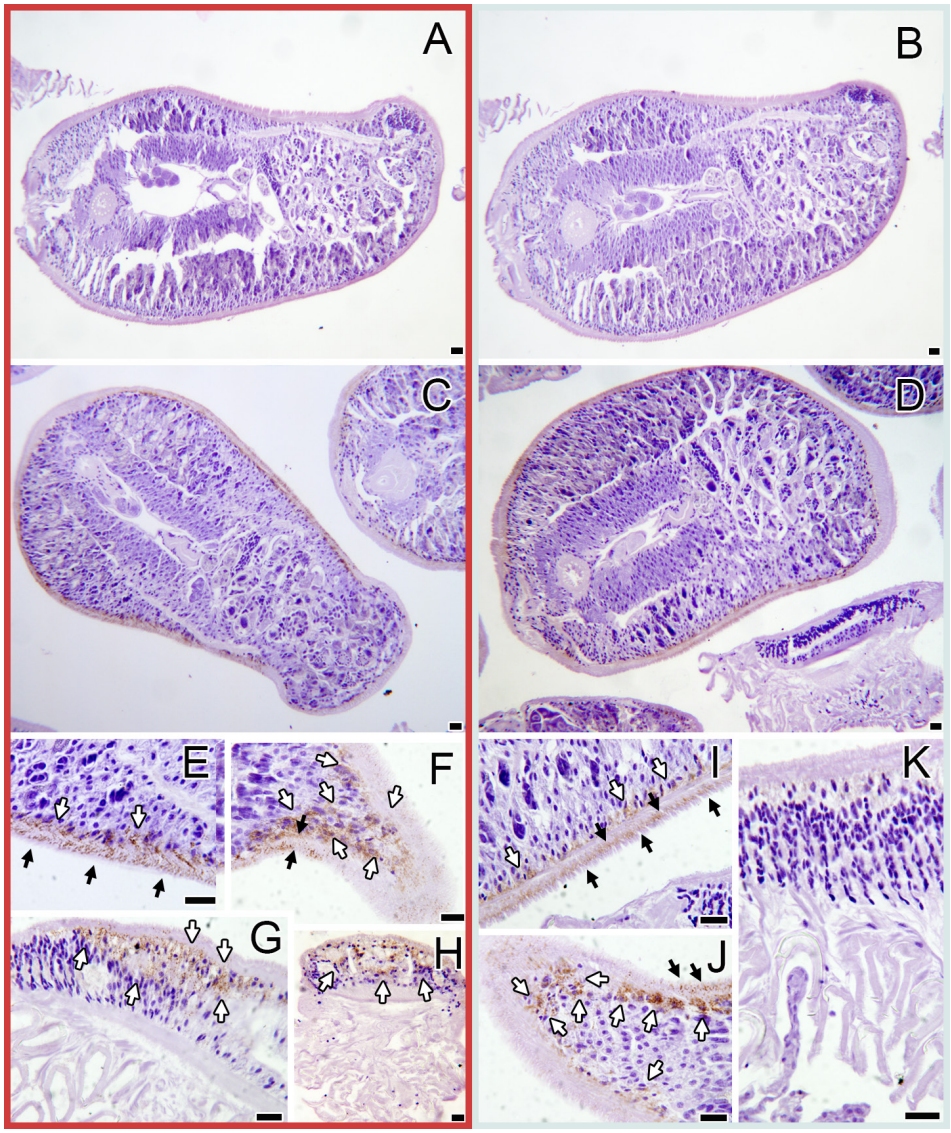

Figure 4. Specific IgT binding to *Sparicotyle chrysophrii* histological sections. Red-framed images were immunolabelled with samples of reexposed fish (RE) and pale turquoise-framed images with naïve fish (NAI) samples at 62 days post exposure. A, **B:** Absence of IgT immunoreactivity with plasma samples of RE and NAI fish. **C-K:** Gill mucus-specific IgT binding to *S. chrysophrii*. Note the immunoreactivity of the parasite's outer (black arrows) and inner (white arrows) tegument (**E**, **I**, **J**) with mucus samples of both RE and NAI fish, and in the haptoral region of RE fish (**G**, **H**). Note the absence of immunoreactivity on the clamps of RE and NAI fish (**G**, **H**, **K**). Scale bars = 20 µm.

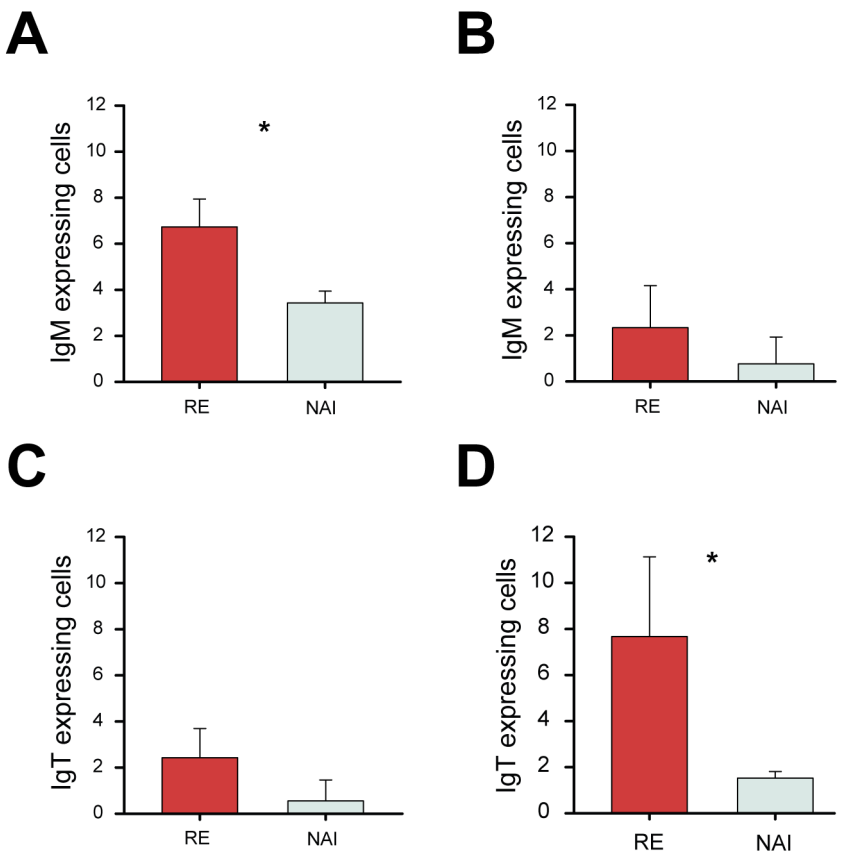

Figure 5. IgM and IgT expressing cells (mean ± SD) in reexposed (RE) and naïve (NAI) gilthead seabream upon 62 days of exposure to *Sparicotyle chrysophrii*. A: IgM expressing cell counts in the spleen. **B:** IgM expressing cell counts in gill filaments. **C:** IgT expressing cell counts in the spleen. **D:** IgT expressing cell counts in gill filaments. Asterisks (*****) indicate statistically significant differences between RE and NAI (t-test, p <0.05). For each fish (n=5 RE and n=4 NAI) and tissue, average number in ten radom microscope fields at 625× magnification were counted.

plasma and gill mucus bound to the parasite. IgM in gill mucus from RE and NAI fish did not bind to *S. chrysophrii* (**Figure 3A**, **B**). By contrast, plasma IgM from both RE (**Figure 3C**, **E** and **F**) and NAI fish (**Figure 3D**, **H-J**) at 62 dpe displayed immunoreactivity against the outer tegument of *S. chrysophrii*. This plasma IgM from both RE (**Figure 3F**, **G**) and NAI fish (**Figure 3D**, **H**) also showed immunoreactivity against the syncytium lining the clamps in the haptoral region of the parasite. Interestingly, the labelling was more intense in the distal region of the clamps, suggesting greater immunoreactivity of that area.

Furthermore, plasma IgT from RE and NAI fish did not show any specific binding to *S. chrysophrii* (**Figure 4A**, **B**). However, the 0 dpe and 62 dpe gill mucus of RE and only the 62 dpe gill mucus of NAI fish demonstrated IgT immunoreactivity against the outer and inner tegument (**Figure 4C-J**) but not against the parasite's haptoral region (**Figure 4G**, **H**, **K**).

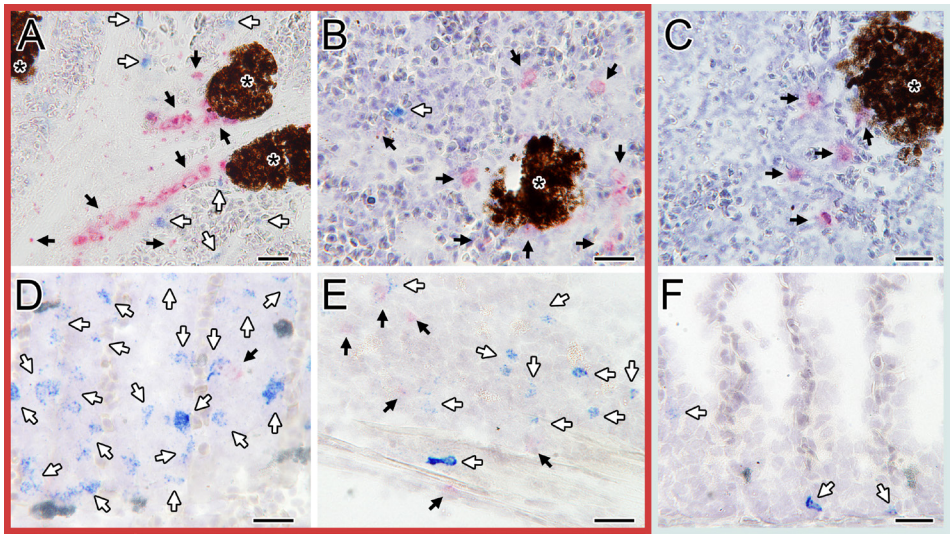

Figrue 6. IgM and IgT RNA *in situ* hybridisation in reexposed (RE, red-framed images) and naïve (NAI, pale turquioise-framed images) gilthead seabream after 62 days of exposure to *Sparicotyle chrysophrii*. A-C: Spleen. **D-F:** Gill filaments. **A:** IgM expressing cells (red-labelled; white arrows) apparently leaving melanomacrophagic centres in the spleen into splenic capillaries, and few scattered IgT expressing cells (blue labelled; black arrows) in the splenic parenchyma. **B:** IgM expressing cells (red-labelled; white arrows) in close contact with a melanomacrophage centre in the spleen and a single IgT expressing cell (blue labelled; black arrow) in the periphery. **C:** IgM-expressing cells (red-labelled; white arrows) in close contact with a melanomacrophage centre, and where no IgT-expressing cells are identified. **D:** gill filaments showing high abundancy of IgT expressing cells (blue labelled), and with a single IgM expressing cell (red-labelled; white arrow). **E:** Branchial epithelium at the interfilamental pockets showing high abundancy of IgT expressing cells (blue labelled) and few IgM expressing cells (red-labelled; white arrows). **F:** Gill filaments showing a single IgT-expressing cell (blue labelled; black arrow). **NOTE:** melanomacrophage centres are labelled with an asterisk (*****). Scale bars = 20 µm.

IgM and IgT expressing cells

Overall, RE fish exhibited a higher number of Ig expressing cells in the spleen and gill filaments at 62 dpe than NAI (**Figure 5** and **Figure 6**). However, these differences were only statistically significant for IgM expressing cells in the spleen (**Figure 5A** and **Figure 6A-C**) and IgT expressing cells in gill filaments (**Figure 5D** and **Figure 6D-F**). In the spleen, IgM expressing cells were mostly located close to blood vessels and around melanomacrophage centres, in both, RE and NAI. This IgM expressing cell subset was the most abundant in the spleen, whereas IgT expressing cells were scarce and mostly spread across the splenic pulp. By contrast, in the gills, IgT expressing cells were the most prevalent B cell subset, mostly located infiltrated in the lamellar epithelium, in both RE and NAI. IgM expressing cells were scarce in the gills and mostly located in the lamellar epithelium.

Discussion

In aquaculture, the intensive farming of gilthead seabream often results in high stocking densities, restricting the fish's natural behaviour, such as migration and dispersal. These culture conditions create an environment favourable for the spread and amplification of parasitic infections, particularly the polyopisthocotylan flatworm *S. chrysophrii*, a major threat to seabream health[1]. In this scenario, implementing prophylactic measures is crucial to ensure fish welfare and the industry's sustainability during the fish grow-out period in sea-cages, which lasts about 1-2 years. The current study demonstrates that gilthead seabream can develop an adaptive immune response against *S. chrysophrii* following initial exposure, which provides partial protection against the parasitosis. These findings underscore the pivotal role of the mucosal immunity in teleosts, and will set the base for the future research on immunoprophylactic strategies against S. chrysophrii.

At the start of the secondary exposure, the size and condition factor of RE fish were lower than those of NAI fish. This difference can be attributed to the previous infection/disease process experienced by RE, which arrested their growth compared to NAI, similar to the effect observed in gilthead seabream infected by an enteric myxozoan parasite[40]. Upon the first month of exposure to *S. chrysophrii*, no significant differences in infection intensity or prevalence were observed between NAI and RE. However, at 62 dpe, a significant increase in infection intensity was noted in NAI, while a significant decrease was seen in RE (**Figure 1D**). Hence, initial parasite establishment was not hampered in RE fish, but after the first month of exposure, RE were able to restrain parasite infection in contrast to NAI. Although prevalence of infection reached 100% in both groups at the end of the experiment, the lower intensity of infection and the improved biometrical values of RE suggest that gilthead seabream acquire a certain degree of protection against *S. chrysophrii* following a primary exposure. Indeed, RE fish improved their condition factor and haemoglobin values, whereas growth was stagnated in NAI (**Figure 1A-C**, **E**, **F**). Interestingly, in the current study, even after 2 months of exposure, haematocrit and haemoglobin remained within normal range values in NAI fish[52], in contrast with a previous study that reported a stronger negative correlation of *S. chrysophrii* infection intensity with fish haemoglobin values[32]. This discrepancy could be attributed to the larger host size (~500 g; **Figure 1A**) and the lower infection intensity (45 ± 24 parasites·fish^{-1}; median ± IQR), since large fish hosts can cope better with the blood loss inflicted by the parasite than smaller fish[7].

In order to shed some light on the underlying protective mechanisms triggered in RE hosts, we studied their differential Ig response, at both, systemic and mucosal levels. B cells are main effectors of the adaptative immune response, and express Igs, which are secreted in polymeric or monomeric form (humoral defence) or remain membrane-bound

on the B cell surface (cellular defence). In most teleosts, the predominant Ig isotype is IgM, followed by IgT, whereas IgD expression is usually minor, and secreted Ig forms are typically the most prevalent. Lymphohaematopoietic organs, blood and mucosae are the main compartments where B cell and Ig responses are orchestrated against pathogen offenders. The mucosal epithelial barriers of fish actively participate in immune responses, with IgT^+ B cells as the main B cell subset in mucosal-associated lymphoid tissues (MALTs)[53–55]. However, each fish species may respond differently to distinct pathogens, and these may also rely on unique immunomodulative strategies for invasion, colonisation or exploitation of host resources. Thus, detailed immunologic studies on each specific host-pathogen model are required to design the most effective immunoprophylactic strategies for disease control.

Our results revealed a paramount mucosal immune response against *S. chrysophrii* in the gills of RE gilthead seabream, which was absent in NAI gills and was not detectable in the plasma of recipient (RE and NAI) fish. In RE gill mucus, a long lasting high local secretion of parasite-specific Igs was found. Five months after the first parasite exposure of RE, their gill mucus still presented significantly higher specific IgM and IgT titers than NAI, before the secondary challenge took place. Along the secondary exposure to *S. chrysophrii*, both specific Ig isotypes decreased gradually in RE and by the end of the trial, their gill mucosal levels were significantly lower than in NAI (**Figure 2B**). Besides the gill mucus ELISAs, the binding specificity of the anti-*S. chrysophrii* IgT in RE gill mucus (at 0 and 62 dpe) was confirmed by parasite immunolabelling (**Figure 4C-K**). Furthermore, higher numbers of IgM and IgT expressing cells were found in RE gills than in NAI, being the difference significant for IgT expressing cells (**Figure 5D** and **Figure 6D-F**). Apparently, only total IgM in RE gill mucus followed a prototypical secondary response pattern, with a short latency phase for B memory cell activation and higher antibody levels attained earlier than in NAI.

Immunoglobulins in teleost mucus, particularly IgT, have been associated with immune responses against parasites[18]. Though reports on monogenean immunogenicity remain limited, some studies demonstrating acquired protective responses in fish upon monogenean reinfections are available. The mucosal immune response found in the current study in gilthead seabream aligns with previous findings from other teleost species exposed to monogenean parasites. For example, Nile tilapia infected by the monopisthocotylan *G. cichlidarum* exhibited an early IgT response in the skin mucus (based on skin mucus ELISA and supported by Ig gene expression in skin), which helped to reduce parasite loads[45]. Similarly, in Japanese pufferfish infected with *H. okamotoi*, serum IgM titers were elevated, contributing to a reduction in parasite burdens upon secondary exposure[40]. However, not all teleost species respond similarly to monogenean infections. In rainbow trout infected with *Gyrodactylus derjavini* (Monopisthocotyla: Gyrodactyli-

dae), circulating antibodies did not develop[56]. Additionally, in European seabass (*Dicentrarchus labrax*) infected with *Diplectanum aequans* (Monopisthocotyla: Diplectanidae), IgM levels were found to increase in serum but not in mucosal tissues, highlighting species-specific differences in mucosal versus systemic immunity[28].

Japanese flounder was able to reduce *Neobenedenia girellae* (Monopisthocotyla: Capsalidae) load and worm size upon secondary exposure to the monopisthocotylan, though no circulating antibodies could be detected in the fish hosts[57,58]. These were, however, primed for 10 days by exposure to parasite eggs, then subjected to fresh-water treatment, and reexposed 10 days later to parasite eggs for 10 further days. The fact that those fish did not naturally overcome the primary infection over an extended time as in our experiment, was probably determinant for their null systemic antibody response after 10 days. A local mucosal Ig response might have been triggered already, but mucosal Igs from the primed fish skin were not checked. Reduced susceptibility to *N. girellae* re-infection was reported for Japanese flounder, greater amberjack (*Seriola dumerili*) and Japanese amberjack (*S. quinqueradiata*) similarly primed by exposure to oncomiracidia, after 10 days treated by fresh-water bath, and 10 days later reexposed to oncomiracidia[58], but no immune factors were analysed in this work. However, it is worth mentioning that in this study much younger fish (29-56 g) than the current adult gilthead seabream were used. Thus, differences in the acquired immune responses upon monogenean reexposure could be driven by differential maturity stages of the hosts' immune system. Furthermore, acquired protection was reported from *N. girellae*-reexposed greater amberjack, resulting in lower parasite burden and smaller parasite size than in NAI fish, which was attributed to an increase of the epidermal thickness and goblet cell numbers in specific skin locations[59]. Those fish were primed with the same procedure as in the previously mentioned work[58], but Hirazawa et al.[59] used significantly larger fish (263 g).

Japanese pufferfish persistently infected with the gill polyopisthocotylan *H. okamotoi* effectively restrained parasite load and presented higher titers of specific serum IgM (until 70 dpe) than NAI hosts[42]. This study suggested that acquired protection was based on the inhibition of oncomiracidial establishment, of parasite development into mature adults, or of adult establishment on their definitive gill location, but the possible contribution of innate immune mechanisms could not be discarded. Rainbow trout in which *G. derjavini* infection was declining at 34 dpe, were set to cohabit with NAI rainbow trout, resulting in significantly higher parasite burden in NAI[56]. However, passive immunisation of NAI rainbow trout by intraperitoneal injection of sera from fish with a persistent infection did not confer protection, and authors suspected no circulating specific antibodies were expressed in the fish in response to *G. derjavini*. In any case, no Ig detection was included in this study. Nevertheless, lower *D. sagittata* burdens and high specific IgM in serum

were achieved in rainbow trout after secondary exposure, only if the primary infection was a three-month continuous parasite exposure, followed by praziquantel treatment, one-month recovery and then reexposure to the parasite for a further month[27]. Shorter primary exposure or direct secondary super-infection without application of treatment for parasite clearance and recovery period did not result in an acquired protective response.

The presence of significantly high numbers of Ig expressing cells in RE spleens reported in this study suggests an activation of an acquired immune response. Recently, it was reported that Ig transcripts are upregulated, not only locally but also systemically in the spleen, following a mild infection with *S. chrysophrii* in gilthead seabream[34]. The spleen, a secondary lymphoid tissue, is a site for B cell activation upon antigen trapping and presentation, but also for plasmablast differentiation into plasma cells[53]. The presence of cells, predominantly positive for IgM RNA transcripts, close to melanomacrophage centres, primitive germinal centres involved in maintaining humoral memory[60,61], might indicate a systemic IgM^+ B cell activation. Indeed, the number of splenic melanomacrophage centres increased in naïve gilthead seabream experimentally infected with *S. chrysophrii* after two months of exposure, which was related to antigen retention and processing for specific immune response development[32]. Activated B cells, would then migrate through the blood stream to be recruited into the local infection site, and accordingly, we detected also Ig expressing cells around and within blood vessels in the spleen (**Figure 6A**).

The current study not only identified specific IgT and IgM against *S. crhysophrii* in the gill mucus of recipient fish by ELISA, but also showed the binding specificity of the mucosal and plasmatic Igs by immunohistochemistry. It was evidenced that the immunogenicity of *S. chrysophrii* mainly relies on the outer tegumental layers of the parasite. Antigenic epitopes in the outer syncytial layer lining the worm's surface seemed to bind the specific plasma IgM, which was detectable only at 62 dpe in NAI and RE. Interestingly, immunoreactivity of the syncytium was especially intense on the parasite's clamps which are the structures that penetrate the fish mucosal barrier and tissue for parasite attachment to the gill lamellae. Only immunolabelling with specific IgM from fish plasma was within the visible threshold, but plasma IgT specific binding could not be detected by immunohistochemistry although a light specific IgT response was found in RE plasma by ELISA. This was a predictable result, since secreted IgM is the most prevalent Ig form in the blood of gilthead seabream[51].

Specific gill mucus IgT bound to the parasite's tegument, on the surface but also in some deeper tegumental layers, and showed no immunoreactivity on the parasite's clamps. Such specific binding was detected at 0 dpe only in the gill mucus of RE, but by 62 dpe, the specific IgT labelling was detected in NAI and RE. The differential immunore-

activity of gilthead seabream IgM and IgT against *S. chrysophrii* highlights the complexity of the immune response. Moreover, the increased abundances of IgM and IgT expressing cells (**Figure 5**), along with the differential specific IgM and IgT immunoreactivity observed (**Figure 3A**, **B** and **Figure 4A**, **B**), emphasise the distinct yet complementary roles of these Igs: IgM in systemic immunity and IgT in mucosal defence. Interestingly, different parasite antigens seemed to trigger IgM and IgT responses. These results also indicate the development of an effective adaptive immune response in NAI after two months of parasite exposure, as previously suggested by the upregulation of Ig transcripts, including light chains and variable Ig genes, in the gills of gilthead seabream upon a mild *S. chrysophrii* infection[51].

The long-lasting specific mucosal Ig titres involve active B cell secretion during the recovery phase even in the absence of parasite antigens, but as total mucosal IgM increased significantly in RE earlier than in NAI, memory B cell activation upon reexposure to *S. chrysophrii* also likely occurred and should be further studied in detail. Memory cells and long-lived plasma cells from gilthead seabream mucosal tissues have never been characterised and whether B cells found in gills are recruited from lymphoid tissues or proliferate locally needs to be revealed.

Regarding the systemic response, Igs in the plasma of RE did not differ significantly from those in NAI. However, we were able to locate the binding specificity of plasmatic anti-*S. chrysophrii* IgM in the 62 dpe plasma of RE and NAI, evidencing the presence of high specific circulating IgM levels. Specific Igs have been identified in various fish hosts against monopisthocotylan parasites such as *Dactylogyrus vastator* (Monopisthocotyla: Dactylogyridae), *Pseudactylogyrus bini* (Monopisthocotyla: Pseudodactylogyridae), *Pseudodactylogyrus anguillae* (Monopisthocotyla: Pseudodactylogyridae), *D. aequans*, *G. cichlidarum*, *N. girellae*, and *Neobenedenia melleni* (Monopisthocotyla: Capsalidae)[47,57,62–66], though not against *G. derjavini* [67]. Most research, however, has focused on systemic IgM responses[57,64,66], rather than mucosal IgT responses[18], and often no significant differences are reported between parasitised and healthy control fish. Interestingly, some studies have shown upregulation of Ig heavy and light chain genes in peripheral blood leukocytes of Japanese flounder following an experimental infection with *Neoheterobothrium hirame* (Polyopisthocotyla: Diclidophoridae)[68]. Additionally, Fernández-Montero et al.[69] described the significant increase of Igs in skin mucus of greater amberjack infected by *N. girellae* through a Gene Ontology (GO) analysis, and Zhi et al.[47] suggested an active role for IgT in the skin mucosal immunity of Nile tilapia against *G. cichlidarum*. Similarly, specific Igs in serum have been identified in Japanese flounder against *H. okamotoi* upon a natural infection[70], and in rainbow trout against *D. sagittata*[45] upon an experimental infection. However, no specific antibodies were identi-

fied in spot croaker against *Neoheteraxinoides xanthophilis* (formerly *Heteraxinoides xanthophilis*) (Polyopisthocotyla: Heteraxinidae)[71]. These findings collectively underscore the importance of mucosal humoral immunity, in the defence against monopisthocotylan parasites, as previously suggested[72]. Nevertheless, specific anti-*S. chrysophrii* IgT in plasma was slightly higher in RE than in NAI before the secondary challenge took place, and this difference increased (not significantly) by 62 dpe. Although IgM is the predominant secreted Ig isotype in the blood of gilthead seabream, the systemic response of secreted IgT has been reported upon primary mucosal challenges in this species. Namely, an enteric myxozoan parasite triggered the overexpression of secreted IgT in the head kidney, but also a bacterial bath challenge in previously orally vaccinated fish increased specific IgT in serum[51]. Thus, antigen exposure at mucosal sites seems to trigger a systemic IgT response, although mild when compared to the systemic IgM response. However, total serum IgT levels barely responded in RE gilthead seabream upon secondary exposure to the enteric myxozoan parasite[40], but no data on specific IgT levels were reported.

Overall, the acquired immune response encompassing a strong local immune response in the gill mucosa of gilthead seabream was evidenced upon the current secondary exposure to *S. chrysophrii*. To what extent the observed Ig response contributes to the fish host protection, helping to restrain parasite establishment in the target organ, calls for further exploration. The discrepancy between the high IgT titres in RE at 0 dpe (**Figure 2B**) and the prevalence and intensity of infection one month later (**Figure 1D**) strongly suggests that, despite the development of a partially effective humoral immune response against adult *S. chrysophrii*, the host is unable to prevent the establishment of larval stages (oncomiracidia). This finding aligns with previous observations by Tinsley et al.[73], indicating that *S. chrysophrii* can establish reservoirs within host populations.

Mucosal tissues are immunological barriers constantly challenged by pathogen-rich environments, thus, adaptive mucosal immune responses are constantly shaped by mucosal innate effectors, like cytokines and chemokines that activate and recruit local immune cells[54]. In the case of the adaptive secondary immune response against sparicotylosis, protection was probably also mediated by upholding innate immune factors, which have been reported during the primary response against the flatworm, such as mucin hypersecretion, changes in mucin glycosylation, recruitment/proliferation of eosinophilic granular cells in the gills, plasma complement C3 and alternative complement pathway, and serum respiratory burst, myeloperoxidase activity and nitric oxide[31–33,36]. Also, the shift in gill microbiota induced during the parasitosis[35] involving a possible translocation of bacteria could affect polyclonal expansion of diverse Ig repertoires[54]. In fact, a shift in the Ig repertoire of B cells was suggested based on the changes in the variable regions of the Ig light chains found in the plasma proteome of gilthead seabream

upon sparicotylosis[33], further highlighting the complex immune response elicited by this parasite. Immunisation trials have demonstrated partial protection against *D. sagittata* in rainbow trout[45] and against *Microcotyle sebastis* (Polyopisthocotyla: Microcotylidae) in Korean rockfish (*Sebastes schlegelii*)[74], based on a significant reduction in the infection intensity, but little experience has been gathered on monogenean immunogenicity and vaccination.

Conclusions

This study highlights the adaptive immune response of gilthead seabream to *S. chrysophrii*, with a focus on mucosal immunity in the gills. The observed increase in IgT and IgM levels, particularly in gill mucus, highlights the importance of mucosal defence in teleost fish. We have evidenced that a secondary antibody response and long lasting specific Igs occur in the gill mucosa. While partial protection was achieved, the inability to fully prevent larval establishment indicates the need for further research to optimise immunoprophylactic measures. This study provides a foundational understanding of the immune mechanisms at play and lays the groundwork for developing more effective control measures against *S. chrysophrii* and other parasitic threats in aquaculture. Therefore, much research remains to decipher the role of each specific immune effector in the gilthead seabream's protective response against *S. chrysophrii*, paving the way for new strategies in disease control through mucosal vaccination.

Funding

This work was supported by the following projects of the Spanish Ministry of Science and Innovation [MCIN/AEI/10.13039/501100011033]: SpariControl [RTI2018-098664-B-I00, AEI/FEDER, UE], MucosalFrontier [PID2020-115070RA-I00], Target4cotyle [PID2022-136914OB-100 AEI/FEDER, UE] and LinfoBream [CNS2022-135433, NextGenerationEU, PRTR]. Additional funding was obtained from the Spanish Ministry of Science and Innovation with funding from European Union NextGenerationEU project ThinkInAzul [PRTR-C17·I1] and from Generalitat Valenciana to the project REMEDISA-PARASITE [GVA-THINKINAZUL/2021/022, CIAICO/2022/144]. ERF was supported by a PRE2019-087409 contract, funded by [MCIN/AEI/10.13039/501100011033] and co-funded by the European Social Fund (ESF). We acknowledge support of the publication fee by the CSIC Open Access Publication Support Initiative through URICI.

Acknowledgements

We thank J. Monfort and L. Rodríguez for their technical assistance on the histological processing and I. Vicente for the technical assistance with fish husbandry and samplings.

References

1. Brabec J, Salomaki ED, Kolísko M, Scholz T, Kuchta R. The evolution of endoparasitism and complex life cycles in parasitic platyhelminths. Curr Biol. 2023;33:4269-4275.e3.

2. Caña-Bozada V, Robinson MW, Hernández-Mena DI, Morales-Serna FN. Exploring evolutionary relationships within neodermata using putative orthologous groups of proteins, with emphasis on peptidases. Trop Med Infect Dis. 2023;8:59.

3. Ogawa K. Diseases of cultured marine fishes caused by Platyhelminthes (Monogenea, Digenea, Cestoda). Parasitology. 2015;142:178–95.

4. Kawatsu H. Studies on the anemia of fish - IX: hypochromic microcytic anemia of crucian carp caused by infestation with a trematode, *Diplozoon nipponicum*. B Jpn Soc Sci Fish. 1978;44:1315–9.

5. Muniesa A, Basurco B, Aguilera C, Furones D, Reverté C, Sanjuan-Vilaplana A, et al. Mapping the knowledge of the main diseases affecting sea bass and sea bream in Mediterranean. Transbound Emerg Dis. 2020;67:1089–100.

6. Mladineo I, Volpatti D, Beraldo P, Rigos G, Katharios P, Padrós F. Monogenean *Sparicotyle chrysophrii*: The major pathogen of the Mediterranean gilthead seabream aquaculture. Rev Aquac. 2024;16:287–308.

7. Riera-Ferrer E, Estensoro I, López-Gurillo B, Del Pozo R, Esteban-Montero F, Sitjà-Bobadilla A, et al. Hooked on fish blood: the reliance of a gill parasite on haematophagy. Proc R Soc B. 2024;291:20241611

8. Sitjà-Bobadilla A, Estensoro I, Pérez-Sánchez J. Immunity to gastrointestinal microparasites of fish. Dev Comp Immunol. 2016;64:187–201.

9. Fast MD. Fish immune responses to parasitic copepod (namely sea lice) infection. Dev Comp Immunol. 2014;43:300–12.

10. Moreira M, Costas B, Rodrigues PM, Lourenço-Marques C, Sousa R, Schrama D, et al. Amyloodiniosis in aquaculture: A review. Rev Aquac. 2024;16:1042–68.

11. Masud N, Williams C, James J, Cable J. Infectivity of an emerging fish parasite *Gyrodactylus sprostonae* in juvenile carp (*Cyprinus carpio*). Aqua fish fish. 2024;4:e170.

12. Akram N, El-Matbouli M, Saleh M. The immune response to the myxozoan parasite *Myxobolus cerebralis* in salmonids: a review on whirling disease. Int J Mol Sci. 2023;24:17392.

13. Rigos G, Padrós F, Golomazou E, Zarza C. Antiparasitic approaches and strategies in European aquaculture, with emphasis on Mediterranean marine finfish farming: present scenarios and future visions. Rev Aquac. 2024;16:622–43.

14. Jiang S, Huang X. Host responses against the fish parasitizing ciliate *Cryptocaryon irritans*. Parasite Immunol. 2023;45:e12967.

15. Madsen H, Stauffer JR. Aquaculture of animal species: their eukaryotic parasites and the control of parasitic infections. Biology (Basel). 2024;13:41.

16. Dezfuli BS, Lorenzoni M, Carosi A, Giari L, Bosi G. Teleost innate immunity, an intricate game between immune cells and parasites of fish organs: who wins, who loses. Front Immunol. 2023;14:1250835.

17. Gómez D, Bartholomew J, Sunyer JO. Biology and mucosal immunity to myxozoans. Dev Comp Immunol. 2014;43:243–56.

18. Zhang YA, Salinas I, Li J, Parra D, Bjork S, Xu Z, et al. IgT, a primitive immunoglobulin class specialized in mucosal immunity. Nat Immunol. 2010;11:827–35.

19. Holzer AS, Piazzon MC, Barrett D, Bartholomew JL, Sitjà-Bobadilla A. To react or not to react: the dilemma of fish immune systems facing myxozoan infections. Front Immunol. 2021;12:734238.

20. de Melo Souza DC, dos Santos MC, Chagas EC. Immune response of teleost fish to helminth parasite infection. Rev Bras Parasitol Vet. 2019;28:533–47.

21. Dezfuli BS, Bosi G, DePasquale JA, Manera M, Giari L. Fish innate immunity against intestinal helminths. Fish Shellfish Immunol. 2016;50:274–87.

22. Aaltonen TM, Valtonen ET, Jokinen EI. Humoral response of roach (*Rutilus rutilus*) to digenean *Rhipidocotyle fennica* infection. Parasitology. 1997;114:285–91.

23. Nakayasu C, Tsutsumi N, Yoshitomi T, Yoshinaga T, Kumagai A. Identification of Japanese flounder leucocytes involved in the host response to *Neoheterobothrium hirame*. Fish Pathol. 2003.

24. Lindenstrøm T, Buchmann K, Secombes CJ. *Gyrodactylus derjavini* infection elicits IL-1β expression in rainbow trout skin. Fish Shellfish Immunol. 2003;15:107–15.

25. Lindenstrøm T, Secombes CJ, Buchmann K. Expression of immune response genes in rainbow trout skin induced by *Gyrodactylus derjavini* infections. Vet Immunol Immunopathol. 2004;97:137–48.

26. Buchmann K, Lindenstrøm T. Interactions between monogenean parasites and their fish hosts. Int J Parasitol. 2002;32:309–19.

27. Rubio-Godoy M, Porter R, Tinsley RC. Evidence of complement-mediated killing of *Discocotyle sagittata* (Platyhelminthes, Monogenea) oncomiracidia. Fish Shellfish Immunol. 2004;17:95–103.

28. Faliex E, Da Silva C, Simon G, Sasal P. Dynamic expression of immune response genes in the sea bass, *Dicentrarchus labrax*, experimentally infected with the monogenean *Diplectanum aequans*. Fish Shellfish Immunol. 2008;24:759–67.

29. Paul A, Sahoo PK. A host choosy gill parasite (*Dactylogyrus* spp.) in fish: an insight into host-parasite interaction for developing control strategies. Aquacult Int. 2024;32:4619–45.

30. Valles-Vega I, Pérez-Urbiola JC, Tovar-Ramírez D, Graham AL, Sicard-González T, Ascencio F. Immune response of the Almaco jack (*Seriola rivoliana*) against the infestation with *Neobenedenia* sp. in three cultivated temperatures. Parasitol Res. 2024;123:127.

31. Henry MA, Nikoloudaki C, Tsigenopoulos C, Rigos G. Strong effect of long-term *Sparicotyle chrysophrii* infection on the cellular and innate immune responses of gilthead sea bream, *Sparus aurata*. Dev Comp Immunol. 2015;51:185–93.

32. Riera-Ferrer E, Del Pozo R, Piazzon MC, Sitjà-Bobadilla A, Estensoro I, Palenzuela O. *Sparicotyle chrysophrii* experimental infection of gilthead seabream (*Sparus aurata*): establishment of an in vivo model reproducing the pathological outcomes of sparicotylosis. Aquaculture. 2023;573.

33. Riera-Ferrer E, Piazzon MC, Del Pozo R, Palenzuela O, Estensoro I, Sitjà-Bobadilla A. A bloody interaction: plasma proteomics reveals gilthead sea bream (*Sparus aurata*) impairment caused by *Sparicotyle chrysophrii*. Parasit Vectors. 2022;15:322.

34. Piazzon MC, Mladineo I, Naya-Català F, Dirks RP, Jong-Raadsen S, Vrbatović A, et al. Acting locally- Affecting globally: RNA sequencing of gilthead sea bream with a mild *Sparicotyle chrysophrii* infection reveals effects on apoptosis, immune and hypoxia related genes. BMC Genomics. 2019;20:1–16.

35. Toxqui-Rodríguez S, Riera-Ferrer E, Del Pozo R, Palenzuela O, Sitjà-Bobadilla A, Estensoro I, et al. Molecular interactions in an holobiont-pathogen model: integromics in gilthead seabream infected with *Sparicotyle chrysophrii*. Aquaculture. 2024;581:740365.

36. Riera-Ferrer E, Del Pozo R, Muñoz-Berruezo U, Palenzuela O, Sitjà-Bobadilla A, Estensoro I, et al. Mucosal affairs: glycosylation and expression changes of gill goblet cells and mucins in a fish–polyopisthocotylidan interaction. Front Vet Sci. 2024;11:1347707.

37. Xu DH, Klesius PH. Protective effect of cutaneous antibody produced by channel catfish, *Ictalurus punctatus* (Rafinesque), immune to *Ichthyophthirius multifiliis* Fouquet on cohabited non-immune catfish. J Fish Dis. 2003;26:287–91.

38. Sitjà-Bobadilla A, Palenzuela O, Riaza A, Macías MA, Álvarez-Pellitero P. Protective acquired immunity to *Enteromyxum scophthalmi* (Myxozoa) is related to specific antibodies in *Psetta maxima* (L.) (Teleostei). Scand J Immunol. 2007;66:26–34.

39. Woo PTK, Ardelli BF. Immunity against selected piscine flagellates. Dev Comp Immunol. 2014;43:268–79.

40. Picard-Sánchez A, Estensoro I, del Pozo R, Piazzon MC, Palenzuela O, Sitjà-Bobadilla A. Acquired protective immune response in a fish-myxozoan model encompasses specific antibodies and inflammation resolution. Fish Shellfish Immunol. 2019;90:349–62.

41. Rubio-Godoy M. Fish host-monogenean parasite interactions, with special reference to Polyopisthocotylea. In: Terrazas LI, editor. Advances in the Immunobiology of Parasitic Diseases. Kerala,India: Research Signpost; 2007. p. 91–109.

42. Nakane M, Ogawa K, Fujita T, Sameshima M, Wakabayashi H. Acquired Protection of Tiger Puffer *Takifugu rubripes* against Infection with *Heterobothrium okamotoi* (Monogenea: Diclidophoridae). Fish Pathol. 2005;40:95–101.

43. Chaves IS, Luvizotto-Santos R, Sampaio LAN, Bianchini A, Martínez PE. Immune adaptive response induced by *Bicotylophora trachinoti* (Monogenea: Diclidophoridae) infestation in pompano *Trachinotus marginatus* (Perciformes: Carangidae). Fish Shellfish Immunol. 2006;21:242–50.

44. Cable J, Van Oosterhout C. The role of innate and acquired resistance in two natural populations of guppies (*Poecilia reticulata*) infected with the ectoparasite *Gyrodactylus turnbulli*. Biol J Linn Soc. 2007;90:647–55.

45. Rubio-Godoy M, Sigh J, Buchmann K, Tinsley RC. Immunization of rainbow trout *Oncorhynchus mykiss* against *Discocotyle sagittata* (Monogenea). Dis Aquat Organ. 2003;2003:23–30.

46. Sandoval-Gío JJ, Rodríguez-Canul R, Vidal-Martínez VM. Humoral antibody response of the tilapia *Oreochromis niloticus* against *Cichlidogyrus* spp. (Monogenea). J Parasitol. 2008;94:404–9.

47. Zhi T, Huang C, Sun R, Zheng Y, Chen J, Xu X, et al. Mucosal immune response of Nile tilapia *Oreochromis niloticus* during *Gyrodactylus cichlidarum* infection. Fish Shellfish Immunol. 2020;106:21–7.

48. Widdicombe M, Coff L, Nowak BF, Ramsland PA, Bott NJ. Understanding the host response of farmed fish to blood flukes (Trematoda: Aporocotylidae) for developing new treatment strategies. Fish Shellfish Immunol. 2024;149:109613.

49. Riera-Ferrer E, Estensoro I, Del Pozo R, Piazzon MC, Moreno-Estruch P, Sitjà-Bobadilla A, et al. A non-lethal approach upon *Sparicotyle chrysophrii* burden prediction in gilthead sea bream (*Sparus aurata*). Aquaculture Europe 2021. 2021.

50. Palenzuela O, Sitjà-Bobadilla A, Álvarez-Pellitero P. Isolation and partial characterization of serum immunoglobulins from sea bass (*Dicentrarchus labrax* L.) and gilthead sea bream (*Sparus aurata* L.). Fish Shellfish Immunol. 1996;6:81–94.

51. Piazzon MC, Galindo-Villegas J, Pereiro P, Estensoro I, Calduch-Giner JA, Gómez-Casado E, et al. Differential modulation of IgT and IgM upon parasitic, bacterial, viral, and dietary challenges in a perciform fish. Front Immunol. 2016;7:637.

52. Michail G, Berillis P, Nakas C, Henry M, Mente E. Haematology reference values for *Dicentrarchus labrax* and *Sparus aurata*: A systematic review and meta-analysis. J Fish Dis. 2022;45:1549–70.

53. Salinas I, Zhang YA, Sunyer JO. Mucosal immunoglobulins and B cells of teleost fish. Dev Comp Immunol. 2011;35:1346–65.

54. Salinas I, Fernández-Montero Á, Ding Y, Sunyer JO. Mucosal immunoglobulins of teleost fish: a decade of advances. Dev Comp Immunol. 2021;121:104079.

55. Rombout JHWM, Yang G, Kiron V. Adaptive immune responses at mucosal surfaces of teleost fish. Fish Shellfish Immunol. 2014;40:634–43.

56. Lindenstrøm T, Buchmann K. Acquired resistance in rainbow trout against *Gyrodactylus derjavinii*. J Helminthol. 2000;74:155–60.

57. Bondad-Reantaso MG, Ogawa K, Yoshinaga T, Wakabayashi H. Acquired protection against *Neobenedenia girellae* in Japanese flounder. FishPathology. 1995;30:233–8.

58. Ohno Y, Kawano F, Hirazawa N. Susceptibility by amberjack (*Seriola dumerili*), yellowtail (*S. quinqueradiata*) and Japanese flounder (*Paralichthys olivaceus*) to *Neobenedenia girellae* (Monogenea) infection and their acquired protection. Aquaculture. 2008;274:30–5.

59. Hirazawa N, Hagiwara H, Takano R, Noguchi M, Narita M. Assessment of acquired protection levels against the parasite *Neobenedenia girellae* (Monogenea) between body surface sites including fins of amberjack *Seriola dumerili* (Carangidae) and the skin in response to the parasite infection. Aquaculture. 2011;310:252–8.

60. Vigliano FA, Bermúdez R, Quiroga MI, Nieto JM. Evidence for melano-macrophage centres of teleost as evolutionary precursors of germinal centres of higher vertebrates: an immunohistochemical study. Fish Shellfish Immunol. 2006;21:467–71.

61. Shibasaki Y, Afanasyev S, Fernández-Montero A, Ding Y, Watanabe S, Takizawa F, et al. Cold-blooded vertebrates evolved organized germinal center–like structures. Sci Immunol. 2023;8:eadf1627.

62. Vladimirov VL. Immunity of fishes in the case of dactylogyrosis. Parazitologiya. 1971;5:51–8.

63. Buchmann K. A note on the humoral immune response of infected *Anguilla anguilla* against the gill monogenean *Pseudodactylogyrus bini*. Fish Shellfish Immunol. 1993;3:397–9.

64. Mazzanti C, Monni G, Cognetti-Varriale AM. Observations on antigenic activity of *Pseudodactylogyrus anguillae* (Monogenea) on the European eel (*Anguilla anguilla*). Bull Eur Assoc Fish Pathol. 1999;19:57–9.

65. Monni G, Cognetti-Varriale AM. Antigenic activity of *Diplectanum aequans* (Monogenea) in sea bass (*Dicentrarchus labrax* L.) held under different oxygenation conditions. Bull Eur Assoc Fish Pathol. 2001;21:241.

66. Reyes-Becerril M, Alamillo E, Trasviña A, Hirono I, Kondo H, Jirapongpairoj W, et al. *In vivo* and *in vitro* studies using larval and adult antigens from *Neobenedenia melleni* on immune response in yellowtail (*Seriola lalandi*). J Fish Dis. 2017;40:1497–509.

67. Buchmann K. Binding and lethal effect of complement from *Oncorhynchus mykiss* on *Gyrodactylus derjavini* (Platyhelminthes: Monogenea). Dis Aquat Organ. 1998;32:195–200.

68. Matsuyama T, Fujiwara A, Nakayasu C, Kamaishi T, Oseko N, Tsutsumi N, et al. Microarray analyses of gene expression in Japanese flounder *Paralichthys olivaceus* leucocytes during monogenean parasite *Neoheterobothrium hirame* infection. Dis Aquat Organ. 2007;75:79.

69. Fernández-Montero Á, Torrecillas S, Montero D, Acosta F, Prieto-Álamo MJ, Abril N, et al. Proteomic profile and protease activity in the skin mucus of greater amberjack (*Seriola dumerili*) infected with the ectoparasite *Neobenedenia girellae* — an immunological approach. Fish Shellfish Immunol. 2021;110:100–15.

70. Wang EG, Kim J-H, Sameshima M, Ogawa K. Detection of antibodies against the monogenean *Heterobothrium okamotoi* in Tiger Puffer by ELISA. Fish Pathol. 1997;32:179.

71. Thoney DA, Burreson EM. Lack of a specific humoral antibody response in *Leiostomus xanthurus* (Pisces: Sciaenidae) to parasitic copepods and monogeneans. J Parasitol. 1988;74:191–4.

72. Scott ME. Experimental epidemiology of *Gyrodactylus bullatarudis* (Monogenea) on guppies (*Poecilia reticulata*): short and long term studies. In: Rollinson D, Anderson RM, editors. Ecology and genetics of host-parasite interactions. London: Academic Press; 1985. p. 21.

73. Tinsley R, Stott L, York J, Everard A, Chapple S, Jackson J, et al. Acquired immunity protects against helminth infection in a natural host population: long-term field and laboratory evidence. Int J Parasitol. 2012;42:931–8.

74. Hong Kim K, Jung Hwang Y, Bum Cho J. Immunization of cultured juvenile rockfish *Sebastes schlegeli* against *Microcotyle sebastis* (Monogenea). Dis Aquat Organ. 2000;40:29–32.

Chapter 7

Hooked on fish blood: The reliance of a gill parasite on haematophagy

Enrique Riera-Ferrer[1†], Itziar Estensoro[1†], Beatriz López-Gurillo[1], Raquel Del Pozo[1], Francisco Esteban Montero[2], Ariadna Sitjà-Bobadilla[1] and Oswaldo Palenzuela[1]

[1]Fish Pathology Group, Institute of Aquaculture Torre de la Sal (IATS, CSIC), Consejo Superior de Investigaciones Científicas, Castellón, Spain

[2]Cavanilles Institute for Biodiversity and Evolutionary Biology, Science Park, University of Valencia, Valencia 46071, Spain

[†]These authors contributed equally to the study

Proceedings of the Royal Society B: Biological Sciences , 16 October 2024
https://doi.org/10.1098/rspb.2024.1611

Abstract

Parasitism involves diverse evolutionary strategies, including adaptations for blood feeding, which provides essential nutrients for growth and reproduction. *Sparicotyle chrysophrii* (Polyopisthocotyla: Microcotylidae), an ectoparasitic flatworm, infects the gills of gilthead seabream (*Sparus aurata*), significantly affecting fish health, welfare and Mediterranean cage farm profitability. Despite its impact, limited information exists on its feeding behaviour. This study demonstrates the presence of blood and exogenous haem groups in *S. chrysophrii* and explores its digestive tract using light and electron microscopy, elucidating its internal morphology and spatial arrangement. Elemental analysis of the digestive haematin cells shows residual oxidised haem depots as haematin crystals. Additionally, we studied the impact of the blood feeding on the host by estimating the average volume of blood intake for an adult parasite ($2.84 \pm 2.12 \mu L \cdot 24h^{-1}$), and we described the significant drop of the plasmatic free iron levels in infected hosts. Overall, we demonstrate the parasite's reliance on its host blood, the parasite's buccal and digestive morphological adaptations for blood feeding, and the provoked effect on the fish host health.

Introduction

Haematophagy has evolved multiple times as a nutritional strategy associated with a parasitic lifestyle. Blood provides a rich source of carbohydrates for the production of energy and amino acids required for growth and reproduction purposes[1]. However, obligate haematophagy encompasses several functional and metabolic challenges to overcome. One of the main constraints threatening blood-feeding parasites is haemoglobin digestion, as the resulting free haem is highly toxic due to its pro-oxidant nature and causes tissue damage and protein degradation. Among other effects, free radicals induced by haem interfere with phospholipid bilayer stability and accelerate cytolysis[2]. Consequently, haematophagous organisms have developed efficient haem-detoxification and storage routes.

Haematophagous organisms affecting terrestrial animals are diverse and include obligate and facultative parasites as well as micropredators, from the class Insecta Linnaeus, 1758 to the class Arachnida Lamarck, 1801. Among the phylum Annelida Lamarck, 1809, haematophagy is common in leeches (Hirudinia Lamarck, 1818), and has also been described in several helminths. Aquatic animals and fish are also infected by haematophagous parasites, such as some copepods, isopods, branchiurans, and polyopisthocotylans, that lead health and welfare concerns in freshwater and marine aquaculture regimes.

Monogeneans, formerly considered a platyhelminth class (Monogenea Carus, 1863) within Neodermata Ehlers, 1985 and recently reclassified into two independent classes, Monopisthocotyla Brabec, Salomaki, Kolísko, Scholz, Kuchta, 2023 and Polyopisthocotyla Brabec, Salomaki, Kolísko, Scholz, Kuchta, 2023[3,4], are mainly ectoparasites in aquatic environments. Some of them have a major impact on fish health and welfare. Infections by these parasites can cause tissue disruption, anaemia and respiratory and osmotic distress, and often trigger secondary infections and increased fish mortality[5,6]. In the aquaculture industry, some monogeneans cause significant economic losses[5,7–10] including *Sparicotyle chrysophrii* Van Beneden and Hesse, 1863 in gilthead seabream (*Sparus aurata* Linnaeus, 1758)[11]. In terms of pathogenicity, the scientific literature is dominated by the class Polyopisthocotyla, most probably due to their large size, prolificacy and presumed haematophagous lifestyle[12].

In *S. aurata* aquaculture industry, *S. chrysophrii* is considered by far the most devastating pathogen across the Mediterranean Sea. Up to 30% of the mortality during the on-growing culture in sea cages has been attributed to this parasitic flatworm[11,13], and its management implies extensive use of resources and manpower devoted to parasite monitoring and application of chemical treatments when infection intensity thresholds are reached. Infections by *S. chrysophrii* and by other polyopisthocotylans have been linked to severe host anaemia, locally reflected in pale gills, and it is generally accepted

these parasites are haematophagous. However, direct evidence of blood feeding by these parasites is scarce[12,14] and has not been demonstrated for *S. chrysophrii*, yet.

Unlike haematophagous arthropods, polyopisthocotylans lack any true piercing anatomical appendages. Instead, ultrastructure studies have described that the anterior end in these flatworms presents a buccal complex consisting of a pair of buccal suckers, a mouth cavity, a pharynx, a putative taste organ and associated structures such as glandular ducts, and a valve apparatus in some species[15,16]. The pair of buccal suckers are strongly muscular, each anatomically situated within a buccal capsule, probably allowing the protrusion of the suckers, improving their attachment to the host and sealing, and with their lumina connecting to the mouth cavity[15–17]. The access to host blood would be facilitated by the secretion of histolytic enzymes through the glandular ducts and the mouth cavity, and the blood intake would be regulated by the pharynx/valve apparatus[15–18]. Given the scarce functional studies on blood ingestion by polyopisthocotylans, it remains unclear to what extent the observed host anaemia can be attributed to haematophagy or the microhaemorrhages caused by mechanical injuries from the parasite's attachment organ, known as the haptor.

Haem and iron are crucial for growth and reproduction of many organisms. Moreover, vitellogenins are primary constituents of yolk proteins in eggs and have been described as iron-binding proteins related to haem detoxification and embryogenesis in haematophagous parasitic and micropredator arthopods[19,20]. Similarly, yolk ferritins were identified in *Clonorchis sinensis* Cobbold, 1875[21] and *Schistosoma mansoni* Sambon, 1907[22], and later it was determined that haem is essential for *S. mansoni* egg production[23]. However, free-living flatworms were described to have specific yolk ferritins that supply aluminium rather than iron to the vitellaria[24].

The focus of the current study encompasses the direct demonstration and the quantification of host blood intake, a detailed study of the parasite´s buccal complex, digestive tract and the elemental composition of its digestive cells. The investigation further reveals exogenous haem groups, the close association of iron with vitelline cells and vitellogenin, and assesses the parasite's impact on the host's plasmatic free iron levels.

Material and methods

In vivo maintenance of *Sparicotyle chrysophrii* in *Sparus aurata*

Sparus aurata were experimentally exposed to *S. chrysophrii* in the Fish Pathology facilities at the Institute of Aquaculture Torre de la Sal (IATS) located at 40°5´N; 0°10´E. Details of the *in vivo* parasite maintenance setup were previously described in Riera-Ferrer et al.[25]. Infected fish were used as parasite source in the subsequent assays.

Haemochromogen crystal assay—parasite *intra vitam* observations

An infected host was euthanised by tricaine methanesulfonate (MS-222; Sigma-Aldrich, MO, USA) overexposure (0.1 $g \cdot L^{-1}$). Gill arches were dissected, and live adult parasites were retrieved under the stereomicroscope. Adult specimens are easily distinguishable by having more than six pairs of clamps and vitellaria, and their location at the distal end of gill filaments. Worms (n = 5) with internalised fresh bloodmeal (**Figure 1**) were chosen to quickly apply the *intra vitam* haemochromogen crystal assay[26], for haem group confirmation. A few drops of the haemochromogen crystal assay reagent (5 mL saturated glucose solution, 5 mL 10% sodium hydroxide solution, 5 mL pyridine (Sigma-Aldrich, MO, USA) and 10 mL distilled water) were applied onto worms on a slide, and observed under light microscopy. Additionally, two positive controls were performed with fresh host blood drawn from caudal vessels using heparinised syringes. In the first positive control, a blood smear was prepared and directly treated with the haemochromogen crystal reagent. In the second, a smear of lysed peripheral blood cells (PBC) was treated with the reagent. For this, washed PBCs were mechanically lysed in a Bullet Blender® (Next Advance, NY, USA) with a combination of 0.5 and 0.15 mm zirconium oxide beads, centrifuged 30 s at 3,500× *g*, and the supernatant used for the smear.

Blood intake

A modified method of Ogawa et al.[14] was applied to demonstrate and quantify blood intake by *S. chrysophrii*. Briefly, 10 mL of Fluoro-Max™ green fluorescent polymer microspheres (FPMs; Thermo Scientific™, Fremont, CA, USA) (1.81×10^{10} FPMs$\cdot mL^{-1}$) were washed in Hank's Balanced Salt Solution (HBSS), centrifuged 5 min at 7000x *g*, and resuspended to the same volume. Infected fish (n = 7) were sedated in eugenol (30 ppm; Guinalima, Valencia, Spain). First, blood (100 µL) was withdrawn from the caudal vessels to determine haemoglobin, haematocrit and circulating erythrocyte (RBC) count. Then,

Figure 1. A-C: Stereomicroscope images of different fresh *Sparicotyle chrysophrii* adult stages with internalised fresh bloodmeal**.** Note bloodmeal in differentlocations, indicative of the parasites' digestive tract. Scale bars = 500 µm.

FPMs (2 µL per body weight g) were injected into the fish bloodstream. Fish were individually allocated in 100 L sea-water tanks. At 3 h post-injection (hPI), fish were sedated and blood (100 µL) was withdrawn for RBC and FPM counts. At 18 hPI, fish were euthanised as before, blood was withdrawn to perform RBC and FPM counts and all gill arches were excised. RBC and FPM counts were performed using a haemocytometer at 312.5×, and the FPMs·RBCs^{-1} coefficient was calculated to assess the efficiency of FPMs perfusion in the fish vascular system. Gill arches were inspected under the stereomicroscope and worms (n = 98) manually detached. Fish biometry, blood values before FPM injection and parasite numbers are detailed in **Table 1**. Worms were treated in ethanol 70% (*v/v*) at 38°C for 1 min, preventing body contraction, and rinsed in HBSS to remove external FPMs.

Since few FPMs were detected inside the worms under a BX51 fluorescence microscope (Olympus Corporation, Tokyo, Japan), parasites were individually placed in Eppendorf tubes® (Eppendorf, Hamburg, Germany) containing 10 µL of lysis buffer (5M NaCl, 1M Tris, 10% SDS, 0.5M EDTA, pH8) and 10 µL proteinase K, and digested overnight at 38°C in agitation. Ingested FPMs were counted from the digestion product of each lysed parasite under fluorescence microscopy.

The blood volume ingested by each parasite per day was calculated from the internal FPMs, and the mean circulating FMP concentration at 3 and 18 h in their fish host.

Parasite histology and histochemistry

Eighty adult worms were harvested from infected fish, fixed in Bouin's solution and processed for routine paraffin histology. Sections (4 µm) were mounted on Superfrost™ Plus slides (Menzel-Gläser, Braunschweig, Germany) and stained with haematoxylin-eosin for anatomical observations on parasites. For *in situ* detection of free ionic iron (Fe^{3+}) LeVine et al.[27] method was modified. Briefly, sections were deparaffinised, hydrated and

Table 1. Biometrical and haematological values of sampled *Sparus aurata* before fluorescent polymer microsphere injection and number of retrieved adult *Sparicotyle chrysophrii*.

Fish	Weight (g)	Length (cm)	Hb (g·dL^{-1})	Hct (%)	Retrieved adult parasites
1	147	18	3.5	31	8
2	134.5	17.6	3.5	22	3
3	557	28	3.1	19	10
4	125	17.5	5.7	35	15
5	103	16	3.1	21	4
6	216	20.7	9.1	51	9
7	162.5	18.4	2.9	19	49

endogenous peroxidase activity quenched with 0.3% H_2O_2 for 30 min. Slides were incubated 20 min in potassium hexacyanoferrate (II) solution with hydrochloric acid (HEMATOGNOST Fe™ staining kit, Sigma-Aldrich, MO, USA) and incubated 30 min with 3,3′-diaminobenzidine tetrahydrochloride chromogen (DAB; Sigma-Aldrich, MO, USA), then washed in deionised water. Sections were counterstained with nuclear fast red solution, dehydrated and mounted with di-N-butyl phthalate in xylene. Negative controls were solely quenched and incubated in DAB, without HEMATOGNOST Fe™ procedure. Also, iron-depleted sections (incubated overnight in 250 µL 0.1M sodium-citrate/hydrochloric acid buffer, pH 1) were processed as described above to verify absence of Fe^{3+} staining. To identify vitellogenin and its potential associations with Fe^{3+}, further sections were stained using Cleveland-Wolfe[28,29].

Transmission electron microscopy (TEM) and energy dispersive X-ray spectroscopy (EDX) TEM of the parasitedigestive tract

In order to locate iron in the parasite at ultrastructural level, ten specimens were retrieved, immediately fixed in 2.5% glutaraldehyde in 0.1M sodium cacodylate buffer at pH 7.2 for 24 h at 4°C, and washed in the same buffer. Sample post-fixation was performed 1 h in 1% osmium tetroxide in the same buffer, before dehydration and embedding in Spurr´s resin (Sigma-Aldrich, MO, USA). Ultrathin sections were contrasted in uranyl acetate and viewed using a Hitachi HT7800 transmission electron microscope (TEM) at an accelerating voltage of 120 kV (Hitachi Ltd., Tokyo, Japan).

TEM coordinates of grid sections were registered for further analysis of their elemental composition. The sites of interest were analysed by energy dispersive x-ray spectroscopy (EDX) TEM, using a high-resolution FEI Tecnai G2 F20 S-Twin microscope at an accelerating voltage of 200 kV (FEI, OR, USA).

Plasma Fe^{2+}/Fe^{3+} levels in parasite-infected fish

To determine the effects of *S. chrysophrii* on fish-free plasmatic iron concentration, blood was withdrawn from infected (R; n = 28; 81 days post parasite exposure) and control (C; n = 23) fish with heparinised syringes, centrifuged at 2000× *g* 10 min, and plasma was retrieved and frozen at −20°C.

Plasma Fe^{2+}/Fe^{3+} levels were determined with an Iron Cromazurol kit (Linear Chemicals, Barcelona, Spain). Briefly, cromazurol reagent (100 µL) and each plasma sample (5 µL) or standard (5 µL) were placed in 96-well plates and incubated for 3 min at 37°C. Absorbances were measured at 635 nm (Infinite® M Plex; Tecan Group Ltd., Männedorf, Switzerland), and optical density (OD) was interpolated into a standard curve calculated according to manufacturer's instructions. Two plasma sample replicates were run.

Statistical analyses

Blood intake data in the seven hosts was checked for normal distribution and equal variance and compared using the Kruskal–Wallis H-test (one-way ANOVA on ranks) with SigmaPlot v14.5 software (Systat Software Inc., San Jose, CA, USA). The median and interquartile range were employed to calculate volume estimates of blood ingested by *S. chrysophrii*.

Generalised linear models (GLM) with a gamma distribution were used and compared to study the relation between infection intensity (continuous predictor) and free iron concentration in plasma (response variable). Outliers were removed based on Cook's distance (>0.5) (**Supplementary material: Figure S2**). The model quality was visually assessed by analysing predictive power, variance homogeneity, influential observations, residual uniformity and its performance (**Supplementary material: Figure S3**, **Figure S4**, **Table S1**).

Normality was assessed using Shapiro–Wilk, Anderson–Darling and Kolomogorov–Smirnov tests for both C and R groups separately and combined. Additionally, diagnostic plots, including density and quantile-quantile plots, were analysed together with the skewness, kurtosis, and the equality of variances between C and R groups (Brown–Forsythe test).

Mann–Whitney U-test (Wilcoxon rank sum test) and Welch's t-test were used to determine differences in plasma Fe^{2+}/Fe^{3+} between R and C fish. Statistically significant differences were considered at $p < 0.05$. Statistical analyses were conducted with R v4.4.0 (R Foundation for Statistical Computing, Vienna, Austria)[30] using R packages: MASS[31], ggplot2[32], performance[33], patchwork[34], DHARMa[35], car[36], nortest[37], moments[38], onewaytests[39] and dplyr[40].

Ethics statement

Experiments were carried out according to current Spanish (Royal Decree 53/2013) and EU (Directive 2010/63/EU) legislation on experimental fish handling. Procedures were approved by the Ethics and Animal Welfare Committee of the Institute of Aquaculture Torre de la Sal (IATS-CSIC, Castellón, Spain), CSIC and 'Generalitat Valenciana' (permit number 2021/VSC/PEA/0194).

Results

Haemochromogen crystal assay—parasite *intra vitam* observations

Parasites with internalised fresh blood showing the bloodmeal along their digestive system (**Figure 1**) were used for the haemochromogen crystal assay. A few seconds after adding the reagent, pyridine haemochromogen orange/red precipitate started to develop, and in approximately 1 min, the characteristic typical flame-like pyridine ferropro-

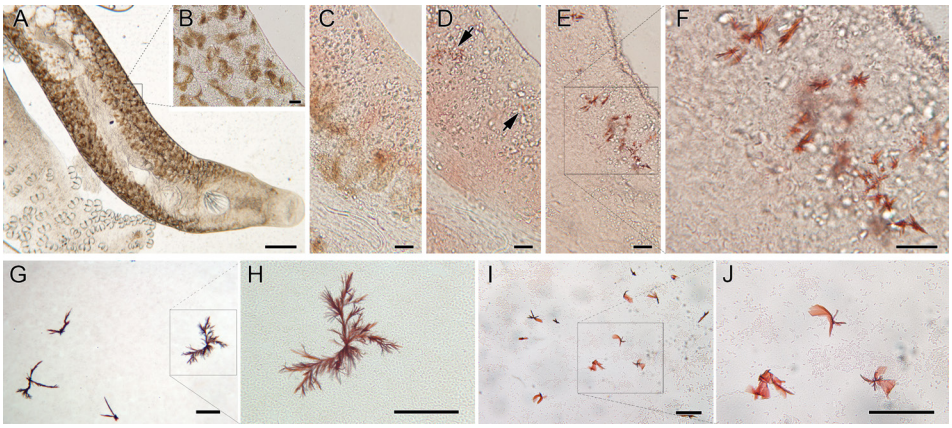

Figure 2. Haemochromogen crystal assay. A-F: Haem group detection in *Sparicotyle chrysophrii*. **G-J:** Haem group detection in blood smears. **A:** Wet mount of an adult specimen before reagent application. **B:** Magnified section of the square in (**A**). **C:** After adding the haemochromogen crystal assay reagent it diffused along the parasite's body, acquiring a reddish colour. **D:** After one minute, orange-red precipitates (black arrows) started to develop. **E:** Red flame-like crystals developed from the precipitates in (**D**). **F:** Magnified section of the dashed square in (**E**). **G:** Red precipitates in *Sparus aurata* whole blood smears. **H:** Magnified section of the square in (**G**). **I:** Red precipitates in mechanically lysed *Sparus aurata* peripheral blood cells. **J:** Magnified section of the square in (**I**). Scale bars: **A**=200 µm, **B-F** = 20 µm, **G-J**=100 µm.

toporphyrin crystals precipitated and polymerised. The crystals were located along the parasite's body, adjacent to the digestive caeca and the pigmented haematin cells, indicating the presence of residual iron-porphyrin complexes, also known as haem- groups (**Figure 2**). In the first positive control using S. aurata blood smears, it took about 2 h for the flame-like pyridine ferroprotoporphyrin crystals to precipitate, whereas it took about 30 min for the mechanically lysed PBC smears.

Blood intake

The FPMs·RBCs^{-1} coefficient remained stable throughout the experiment indicating success in the FPMs perfusion in the fish vascular system (**Figure 3A**). The parasites' blood-meal ingestion was calculated in regard to FPMs·RBCs^{-1} coefficient of each fish (n = 7; **Figure 3B**). For this purpose, individual digestion of specimens (n = 98) enabled ingested FPM counts (**Figure 3E**). Since no statistically significant differences were observed in the blood ingested by parasites in the different fish according to the Kruskal–Wallis U test ($p < 0.05$; p value = 0.054) (**Figure 3B**), the average blood ingestion of adult worms was calculated, resulting in 2.84 ± 2.12 µL·24 h^{-1} (median ± IQR).

Detection of free ionic iron (Fe^{3+}), vitellogenin and parasite histology

Bilateral iron (Fe^{3+}) deposits in *S. chrysophrii* were visible as an intense brown DAB precipitate longitudinally distributed from the rostral to caudal regions along the parasite's digestive caeca (**Figure 4A–C**). The specificity of the Fe^{3+} labelling was confirmed by the

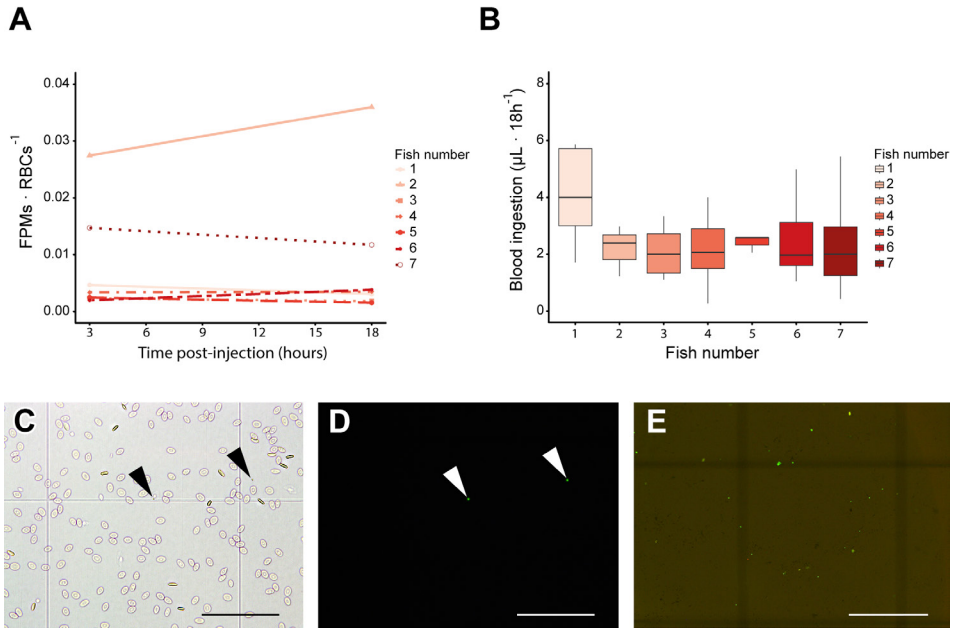

Figure 3. Fluorescent polymer microspheres (FPM) count. A: FMP–erythrocyte coefficient throughout the experiment for the seven fish used. **B:** Boxplot representing the ingested blood volume by adult *Sparicotyle chrysophrii* population from each fish. **C:** Bright-field microphotograph of a blood sample at 18 h post FPMs injection. **D:** Fluorescence microphotograph of the same field as in (**C**). Note the presence of two FPMs (arrows). **E:** FPMs present in digested parasite (bright-field+fluorescence overlap). Scale bars=100 µm.

absence of staining after iron depletion (**Figure 4D**). Moreover, the Cleveland–Wolfe stain revealed that the main Fe^{3+} deposits overlapped with the location of vitellogenin (**Figure 4E–G**), indicating a potential association between them.

Anatomy of the parasite buccal complex

The foregut of *S. chrysophrii* is located subterminally at the anterior end. It is constituted by the mouth cavity, two lateral buccal suckers and the pharynx, placed centrally behind the mouth cavity (**Figure 5**). A complex network of nerves and ducts, the latter probably excretory, can be distinguished in the anterior cephalic region (**Figure 5A**, **B**). Behind the pharynx, the digestive tract bifurcates around the male copulatory organ and gonopore into the two main digestive caeca, which run laterally along the parasite's body. The paired buccal suckers are formed by radial muscle fibres (**Figure 5D–H**). Depending on the orientation and depth of the section, a septum can be observed in the lumen of the suckers linking their facing muscles (**Figure 5E**, **F**, **H**). Although suckers appear subcircular in fresh specimens, in histological sections the entire annulus is rarely seen, probably because of their folded shape and angled position. Anteriorly to the buccal suckers, two refringent slightly protruding papillae-like structures were observed, which were intense-

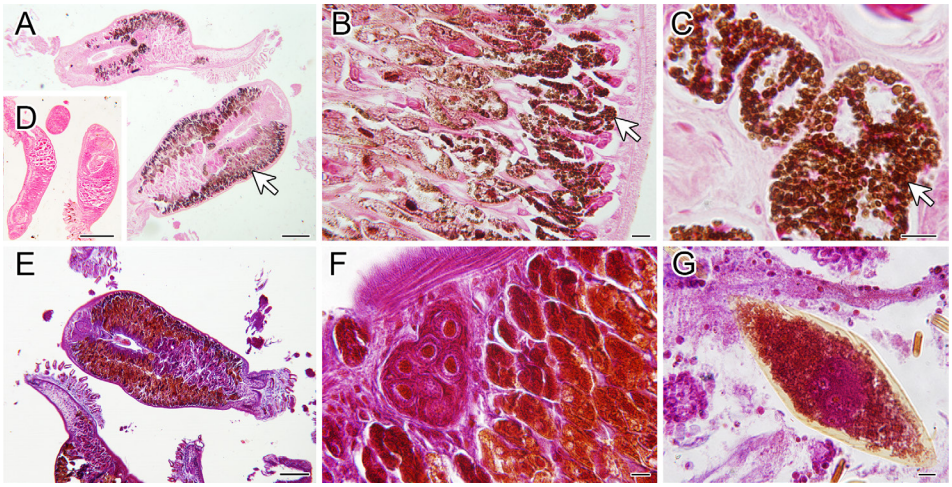

Figure 4. *Sparicotyle chrysophrii* microphotographs. A-C: Free ionic iron (Fe^{3+}) staining (brown colour; arrows) in adult specimens counterstained with nuclear fast red. **D:** Negative control shows the absence of free ionic iron staining after iron depletion. **E-F:** Adult specimens with vitellogenin-positive staining (orange-brown) with Cleveland-Wolfe. **G:** Eggs with vitellogenin-positive staining with Cleveland-Wolfe.
Scale bars in **A**, **D**, **E** = 200 µm; **B** ,**C** ,**F** ,**G** = 10 µm.

ly orange-stained with Cleveland–Wolfe (**Figure 5B–D**, **G**, **I**). Also, some cells resembling glandular cells, with an enlarged and granular or coarse cytoplasm, were observed close to the mouth cavity and the pharynx (**Figure 5G**,**H**). The pharynx is located posteriorly and slightly dorsally of the suckers. In cross-section, a slightly off-centred pharyngeal canal was distinguished with a convoluted lumen inside a fibrous tube (**Figure 5I–K**). The buccal suckers and the pharynx are each located in a fibrous capsule surrounding them (**Figure 5F**, **H**, **J**, **K**). Fan-shaped muscle fibres inserting buccal suckers were evident (**Figure 5C**, **E**).

Transmission electron microscopy (TEM) and energy dispersive X-ray spectroscopy (EDX) TEM of the parasite digestive tract

The digestive tract of *S. chrysophrii* adult specimens presented numerous branched caeca extending between vitellaria and testis (**Figure 6A–C**). The ultrastructure of the gastrodermis lining the gut lumen consisted of cup-shaped digestive cells, the haematin cells, interconnected by a digestive syncytium. Continuity between haematin cells and the digestive syncytium was noted (**Figure 6I**, **L**). The haematin cells had a basal nucleus and an apical opening, and their cytoplasm presented extensive areas of endoplasmic reticulum and numerous lysosomal vesicles with coarse material or electron-dense crystals inside, the haematin pigment (**Figure 6B**, **F**, **G**, **N**, **O**). Free haematin aggregates were also observed in the gut lumen, together with lipid-like droplets, undifferentiated debris and membrane-bound vacuoles, but fish erythrocytes were not identified (**Figure 6D**, **H**, **L**, **P**). The diverticula formed by the haematin cells and the connecting syncytium were mostly

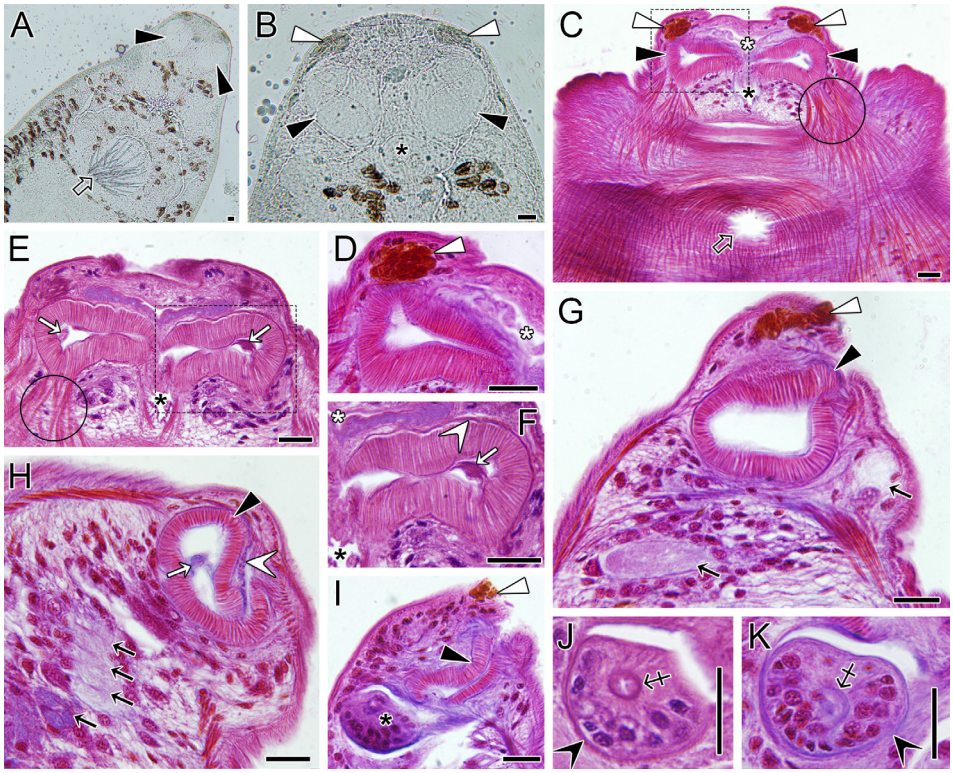

Figure 5. Light microscopy of the buccal complex of *Sparicotyle chrysophrii*. A-B: Live specimen with two oval subterminal buccal suckers (black arrowheads), taste organs (white arrowheads) and central pharynx (black asterisk). Note the male genital atrium in ventral central position (hollow arrow) and the complex network of nerves and ducts occupying the cephalic region. **C:** Ventral surface section at longitudinal transversal orientation showing both buccal suckers (black arrowheads), taste organs (white arrowheads), mouth cavity (white asterisk) and pharynx lumen (black asterisk). Note the prominent muscle fibres, especially the fan-shaped fibres binding to the radial muscles of the suckers (circle). The gonopore appears in a central position (hollow arrow). **D:** Magnified section of the dashed square in (**C**). **E:** Longitudinal transversal section across the buccal suckers showing the pharynx lumen (black asterisk) and fan-shaped muscle fibres (circle). Note the septum across each sucker lumen (white arrows). **F:** Magnified section of the dashed square in (**E**), showing the mouth cavity (white asterisk) and the fibrous capsule around the buccal sucker (white arrowhead). **G:** Longitudinal sagittal section across the taste organ (white arrowhead) and buccal sucker (black arrowhead). Note the presence of putative giant glandular cells with light or coarse cytoplasm (black arrows). **H:** Buccal sucker (black arrowhead) surrounded by a fibrous capsule (white arrowhead) and with a septum across the lumen (white arrow). Note the presence of numerous glandular cells with different cytoplasm contents (black arrows). **I:** Cephalic section across taste organ (white arrowhead), buccal sucker (black arrowhead) and pharynx (black asterisk). Note the slightly off-centred pharynx lumen. **J-K:** Detail of pharynx cross-sections surrounded by a fibrous capsule (black arrowheads) containing numerous cells and the pharynx convoluted lumen inside a fibrous wall (cross-arrow). Stainings: Cleveland-Wolfe **C**, **D**, **G**, **H**, **I**, **K**; haematoxylin-eosin **E**, **F**, **J**. Scale bars=20 µm.

covered by numerous, branched and unbranched lamellar projections on the gut luminal surface, which greatly increase the absorptive surface (**Figure 6F**, **I**, **J**, **L**, **N**, **P**). Also, areas with a smooth syncytial layer lining on vitelline cells were observed and some extended lamellae formedballoon-like structures enclosing luminal contents (**Figure 6K**, **M**). The spectral analysis of the emission of electron-dense crystalsin haematin cells by EDX-TEM showed iron as the main component (**Supplementary material: Figure S1**). The spectra of the haematin cell cytoplasm, vitelline cells and worm sclerites inside the clamps were also analysed, but no iron could be detected (**Supplementary material: Figure S1**).

Parasite effect on fish plasma Fe^{2+}/Fe^{3+} levels

The best gamma-distributed GLM (**Figure 7A**; **Supplementary material: Table S1**, **Figure S3**) obtained after removing three outliers (one C, n = 22, and two R, n = 26) identified using Cook's distance (**Supplementary material: Figure S2**), was used to determine the effects of *S. chrysophrii* on its host plasmatic free iron concentration. This model met validity assumptions, including predictive power, variance homogeneity, influential observations, and residual uniformity (**Supplementary material: Figure S4**). Overall, the model performed well, presenting an adequate fit with an akaike information criterion (AIC), AICc and bayesian information criterion (BIC) values of 472.995, 473.541, and 478.609, respectively (**Supplementary material: Table S1**), and moderate explanatory power with a Nagelkerke's R^2 (R^2_N) of 0.263, indicating that 26.3% of the variance in plasma free iron concentrations is explained by parasite infection intensity. The model also showed reasonable prediction accuracy with a root mean squared error value of 33.456, and consistent reliability with a Sigma value of 0.536 (**Supplementary material: Table S1** and **Figure S3**). The infection intensity significantly affected plasma free iron concentration, with higher parasitic burdens associated to lower iron levels, according to the Wald test ($p < 0.05$; p value = $8.84e^{-04}$) (**Figure 7A**). Normality and variance equality were checked (**Supplementary material: Figure S5**, **Table S2**). Additionally, the Mann–Whitney U-test ($p < 0.05$; p value = 0.03221) and the Welch's t-test ($p < 0.05$; p value = 0.02197) (**Figure 7B**) showed statistically significant differences between C (n = 22) and R (n = 26), providing robust evidence of the effects of these parasites on their hosts' plasmatic free iron concentration.

Discussion

Erythrocytes are the major cellular constituent in the blood tissue, and as such, the globin moiety present in haemoglobin poses the main source of peptide and amino acid acquisition for haematophagous parasites[41,42]. Moreover, iron is indispensable for life and haem is a prosthetic group consisting of an iron atom bound to the ring of porphyrin with-

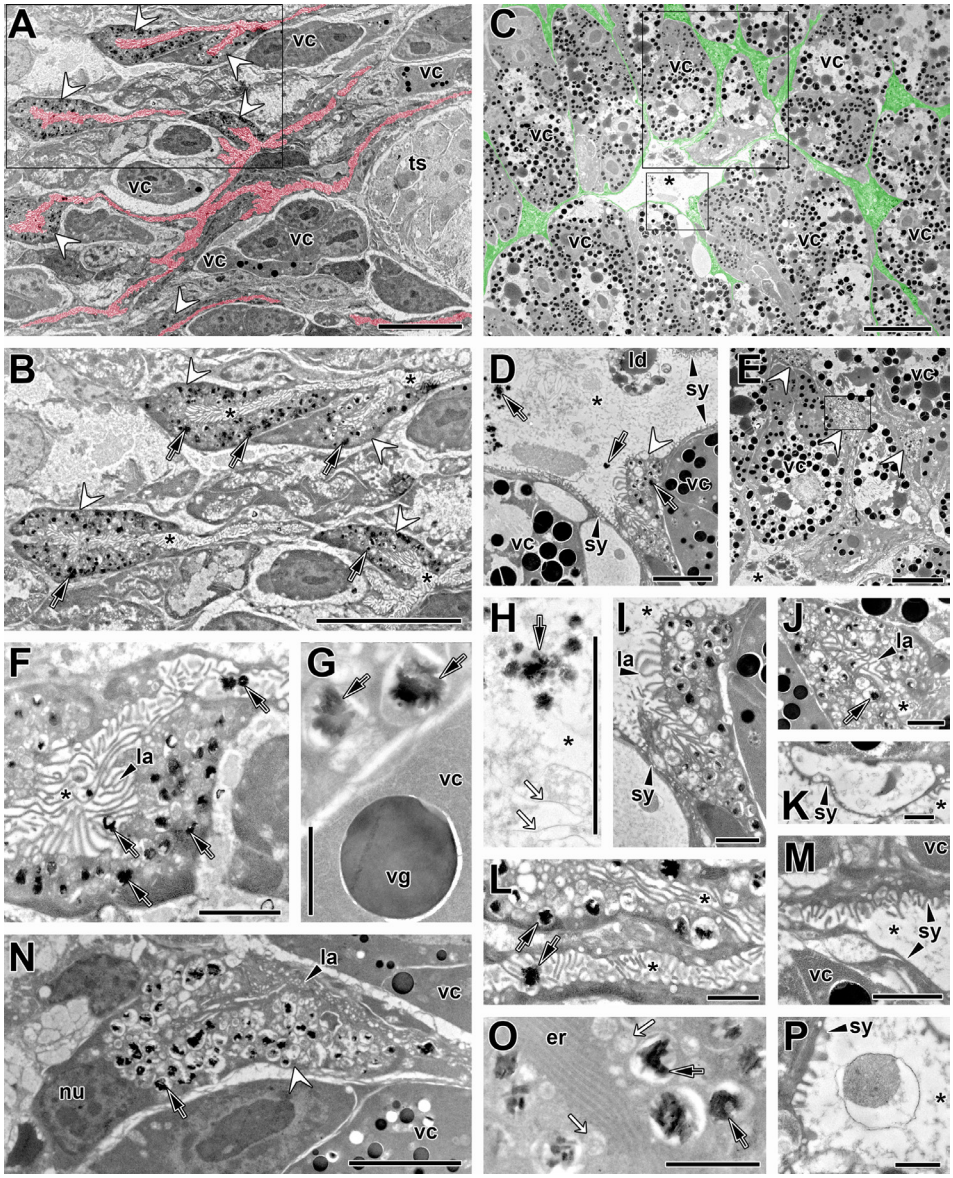

Figure 6. Transmission electron microscopy of *Sparicotyle chrysophrii* gastrodermis. A: Gut lumen (highlighted in red) lined by a syncytium interconnecting the pigmented digestive cells (haematin cells). Vitelline cells (mature and immature) and testis can be observed close to the gastrodermis. The framed box indicates the area magnified in **B**. **B:** Haematin cells forming gut diverticula. Note their abundant electron-dense inclusions and lamellar projections into the gut lumen. **C:** Haematin cells and the connecting syncytium (highlighted in green) branching in between vitelline cells in vitelline follicles. Note the broad gut luminal opening in the centre. The small framed box indicates the area magnified in **D**, the larger framed box indicates the area magnified in **E**. **D:** Portion of the gut lumen lined by the connecting syncytium and haematin cell. Note the presence of intracellular haematin crystals inside lysosomal vesicles and extracellular haematin crystals in the gut lumen, together with lipid-like droplets and undifferentiated debris. **E:** Three haematin cells between vitelline cells in vitelline follicles. The framed box indicates the area magnified in **J**. **Continued on the next page.**

Figure 6. (Continued). F: Haematin cell with abundant lysosomal vesicles, many containing haematin inclusions. Haematin crystals are also present in the gut lumen, together with numerous branched and unbranched lamellae projecting from the haematin cell. **G:** Haematin crystals inside lysosomal vesicles in a digestive cell close to a vitelline cell with vitelline granule. **H:** Free haematin aggregates in the gut lumen together with some fibrous and coarse material (white arrows). **I:** Haematin cell with abundant digestive lysosomes, haematin granules and apical lamellae. Note the continuity between the haematin cell and the connecting syncytium with shorter luminal lamellae. **J:** Haematin cell forming a gut diverticulum full of lamellar projections. **K:** Connecting syncytium forming balloon-like structure enclosing luminal contents. **L:** Confluence of digestive channel with luminal haematin crystal and caecum formed by haematin cell with abundant lysosomal vacuoles, some containing haematin crystals. Note the continuity between the haematin cell and the connecting syncytium. **M:** Connecting syncytium overlying vitelline cells. Note the upper syncytial layer with some electron-lucent vesicles and abundant short lamellae projected into the gut lumen, in contrast to the smooth syncytial layer lining on the lower vitelline cell. **N:** Cross-section of haematin cell including the nucleus at basal position, some apical lamellae and abundant cytoplasmic vesicles, many containing haematin crystals. **O:** Haematin cell cytoplasm with lysosomal vesicles with and without (white arrows) haematin crystals and endoplasmic reticulum. **P:** Gut lumen with membrane-bound vacuole containing coarse undifferentiated material. White arrowheads = Haematin cells; black arrows = haematin crystals; asterisk = gut lumen; endoplasmic reticulum (**er**); luminal lamellae (**la**); lipid-like droplets (**ld**); nucleus (**nu**); syncytium (**sy**); testis (**ts**); vitelline cells (**vc**); vitelline granule (**vg**). Scale bars: **A**, **B**, **E** = 10 µm; C = 20 µm; **D**, **H**, **N** = 5 µm; **F**, **I**, **J**, **M** = 2 µm; **G**, **K**, **L**, **O**, **P** = 1 µm.

in haemoglobin[43,44]. However, free haem is highly cytotoxic[2] and must be detoxified by haematophagous parasites[1]. In parasitic flatworms, this is accomplished by either haem breakdown by catabolic enzymes (glutathione *S*-transferase or reduced glutathione), or by the synthesis of inert haem aggregate crystals (haemozoin)[1,45–47]. An additional strategy for mitigating haem toxicity is to efficiently sequester these prosthetic groups into developing oocytes for egg formation and embryogenesis, thus regulating reproduction and ultimately increasing the iron concentration in eggs[19,20]. Haem binding proteins involved in such process were first described in haematophagous arthropods belonging to the classes Insecta and Arachnida[40,41], but have also been identified in trematode parasites[1,23,48–51], suggesting neodermatans may also follow this strategy.

Polyopisthocotylans including *S. chrysoprhii*, are considered haematophagous, mostly on the basis of a recognised association between high adult parasite burdens and host anaemia[52]. However, it remains uncertain to which extent the anaemia can be attributed to a direct haematophagy or to traumatic haemorrhagic lesions inflicted by the parasite's haptor in the gill tissue. In this study, we describe for the first time the presence of bloodmeal content in the gut of adult *S. chrysophrii* specimens (**Figure 1**) and the *in vivo* location of haem by the haemochromogen crystal assay (**Figure 2**). Similar results were reported in other polyospisthocotylans[26] where flame-like crystals were observed in the same location as in *S. chrysophrii*. Interestingly, the observed time differences for ferroprotoporphyrin crystal precipitation in live worms (1 min) compared to whole blood (2 h) and lysed fish blood (30 min) (**Figure 2**) suggest the existence of a highly active haemolytic machinery in this parasite. Similar results have been reported in the polyopisthocotylan *Eudiplozoon nipponicum* Goto, 1891, the blood fluke *S. mansoni* and the hard tick *Ixodes ricinus* Linnaeus, 1758[10,42,53]. Accordingly, large bilateral iron deposits were identified by

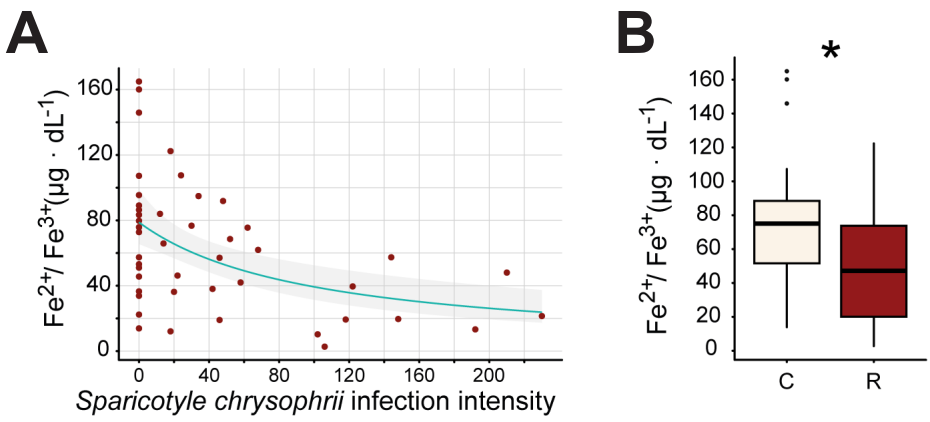

Figure 7. Plasmatic free ionic iron concentration in *Sparus aurata*. A: Scatterplot showing the relation between the plasmatic free ionic iron concentration and *Sparicotyle chrysophrii* infection intensity. The green line represents the generalised linear model fit on the observed data and the grey area the model's 95% confidence intervals. **B:** Boxplot showing plasmatic free ionic iron concentration. Asterisk indicates significant differences between C (control) and R (infected) fish (Mann-Withney U-test, Welch's t-test; $p < 0.05$).

histology along the parasite's digestive caeca (**Figure 4**).

TEM evidenced the structural distribution of the digestive caeca and their associated diverticula in a complex interweaving network between gonadal tissues, the male follicular testes and female vitelline follicles (**Figure 6**). The syncytial lamellar grid lining the gastrodermis was termed the apical pinocytotic fibrous surface complex and documented in other polyopisthocotylans[17,54]. It increases the digestive surface and engulfs food material from the gut lumen into the haematin cells through membrane-bound vesicles by endocytosis. The connecting syncytium, with internal vesicles and with luminal lamellae and balloon-like structures entrapping digestive material, apparently plays an active role in nutrient absorption and distribution beyond a mere structural supporting role. The cytoplasm of adult *S. chrysophrii* haematin cells bears abundant lysosomal vesicles mostly containing electron-dense haematin crystals, and TEM-EDX revealed its main elemental component was iron (**Supplementary material: Figure S1**). The lysosomal vesicles with coarse material probably contain endocytosed haemoglobin prior to digestion. Overall, this parasite's gastrodermis morphologically resembles that of other studied polyopisthocotylans[55–59]. The luminal surface of haematin cells, with numerous vesicles and pits, suggests macromolecule uptake through endocytosis and subsequent intracellular digestion within a lysosomal system. Dalton et al.[41] described for monogenean blood-feeders this so-called intracellular digestive tract, which first endocytoses haemoglobin upon a receptor-mediated selective ingestion. After the intracellular digestion of the globin moiety, the residual oxidised haem accumulates as the insoluble ferriporphyrin haematin, which is eventually extruded into the gut lumen and regurgitated. Accordingly, extracellu-

lar haematin crystals were observed in the caecal lumen of parasites, together with other undifferentiated debris.

No erythrocytes were observed in the caecal lumen of *S. chrysophrii*, suggesting that bloodmeal is haemolysed before it reaches the gastrodermis in the gut caeca for effective absorption and intracellular digestion. The absence of blood cells in the gut lumen of other polyopisthocotylans has been reported[26,41,54,56,60] and haemolysis by gland secretions in the parasite's pharynx/ foregut was suggested[17]. Giant cells, considered unicellular glands located below buccal suckers and around the pharynx, were described in other polyopisthocotylans, namely, *E. nipponicum* and *Paradiplozoon homoion* Bychowsky and Nagibina, 1959[18,61,62], similar to our observations in the buccal complex of *S. chrysophrii* (**Figure 5**). The released proteolytic secretions would be responsible for the extraintestinal digestion. Furthermore, the taste organ, a tegument invagination with numerous sensory receptors and glandular ducts at the anterior end of the polyopisthocotylidan *Pricea multae* Chauhan, 1945[16], resembles the stained protrusions observed in *S. chrysophrii*. Those authors suggested that the taste organ might be protruded and directly contact the gill tissue so that its histolytic secretions would help to access surface blood capillaries. These observations are further supported by the proteomic work of Riera-Ferrer et al., which suggests that this parasite causes haemolytic anaemia in *S. aurata* based on a positive correlation of plasmatic alpha−1-microglobulin with infection intensity[63]. In addition, about 14% of the proteins identified in *S. chrysophrii* purified extracellular vesicles correspond to hydrolytic enzymes, including leucyl and alanyl aminopeptidases, thought to be involved in the final steps of haemoglobin lysis. Glutathione *S*-transferase was identified in these extracellular vesicles as well, evidencing the participation of extracellular vesicles in biological processes such as haem detoxification and Fe transport[64].

Overall, the buccal complex of *S. chrysophrii* fulfils apparently a triple function during blood feeding: sensory, attachment and haemolysis. The muscle action of buccal suckers assists in attachment of the anterior end to the feeding area. The prominent body musculature bound to the capsules holding buccal suckers and the pharynx allows them to be everted during sucking and the fan-shaped muscle fibres have an opener and stretcher function for the buccal suckers, as previously described for *E. nipponicum* and *P. homoion*[61,62]. The septum, a transverse band of musculature in the lumen of buccal suckers[62] has been suggested to generate negative pressure contributing to attachment and sucking in other polyopisthocotylans[17].

Iron is an essential micronutrient for sustaining life. It is generally thought that haem-auxotrophic blood-feeding parasites have developed haematophagy as an alternative strategy for iron acquisition; however, not all acquired bioavailable iron originates from haemoglobin-derived haem. Previous studies in the tick *I. ricinus* have demonstrat-

ed that (i) feeding and oviposition do not rely on the intake of host blood haemoglobin, yet it is indispensable for embryogenesis, (ii) haemoglobin is an indispensable source of haem, but not a source of iron, (iii) haemoglobin-derived haem is transported from the guts to the ovaries, and (iv) vitellins are the major haem-binding proteins in the ovaries[65]. Although these aspects are largely unexplored for most haematophagous parasitic helminths, recent work on the transcriptome and proteome of *E. nipponicum* has demonstrated an abundance of ferritin transcripts, which suggests an interesting parallelism with ticks, possibly associated with blood-feeding strategy[10].

Functional studies in *S. mansoni* have shown that haem and iron are key for growth, sexual maturity, fecundity, oogenesis, and egg deposition and viability[23,48]. Recently, Toh et al.[23] described that haem could be taken into the ovary and vitellaria by transmembrane haem transporters and in the trematode *Fasciola hepatica* Linnaeus, 1758 it was reported that haem-sequestering proteins could bind haem in maturing vitelline cells within vitellaria[49]. Moreover, exogenous haem trafficking and homeostasis pathways were identified using the free-living haem-auxotroph nematode *Caenorhabditis elegans* Maupas, 1900 as a model, where proteins related to haem uptake in the nematode's intestine and haem transporter proteins trafficking haem from the intestine to developing oocytes were identified[50]. Our histological observations suggest a close association between iron deposits and vitellogenin (**Figure 4**), indicating a critical requirement for this trace element for reproductive purposes, which could simultaneously act as a haem detoxification pathway. However, iron was not detected in vitelline cells (cytoplasm and vitelline granule) of *S. chrysophrii* by EDX-TEM (**Supplementary material: Figure S1**), possibly due to the maturation stage of the sampled cells[49].

Our current study evidences a statistically significant iron impairment in hosts that is directly related to *S. chrysophrii* infection intensity (**Figure 7**), building onto the previously reported decrease in haemoglobin levels in infected fish[25,63]. The current findings correlate with the requirements of non-haem-derived iron for metabolic processes and with the necessity of haem for reproductive purposes as described above. These lower iron levels in hosts might hint at a specific specialised ferritin machinery in this parasite working in deep iron exploitation from host plasma.

In this study, we provide further direct evidence of *S. chrysophrii* haematophagy through intravascular injection of FPMs into the fish host and their recovery from adult parasite specimens feeding on the fish for 18 h. Our results estimate an average blood intake rate by an adult worm of 2.84 ± 2.12 µL·24 h^{-1}, up to 1.5 times as much as reported for *Heterobothrium okamotoi* Ogawa, 1991[14]. Considering that blood comprises about 5% of the fish mass[66], it can be estimated that a 30 g *S. aurata* parasitised by 100 *S. chrysophrii* adults would lose 4.80–33.07% of its blood volume daily. In market-size

fish (e.g., 350 g), the same infection intensity would result in a daily 0.41–2.83% blood loss. These levels of blood loss pose a severe threat to newly introduced juvenile fish in sea cages. Monthly blood extractions should not exceed 10% of the body weight[66], and become life-threatening if blood loss surpasses 30–50% of the body weight[67]. The continuous daily blood loss caused by the parasites can quickly be fatal, given that the daily blood depletion rates far exceed the safe thresholds over a shorter time span, indicating the potentially deadly impact of the parasite on its host.

In the case of *S. aurata* reaching market size, the parasite impact would be relatively lower, as fish would be able to cope with the blood loss produced by relatively high parasitic burdens, thus becoming reservoirs. In Mediterranean sea cages, the common fish farming practice overlaps different year-class groups in the same sites to cater for a wide range of harvest sizes and dates. From a health surveillance perspective, adopting an *all-in*, *all-out* system is crucial. This approach ensures that different year-class fish stocks do not cohabit in the same farming site, thereby preventing older animals from infecting newly introduced ones in the cages. Furthermore, integrating current *S. chrysophrii* control measures[13] with additional strategies to mitigate the anaemia and plasmatic iron decrease in parasitised *S. aurata* could significantly improve their health.

Iron homeostasis in fish is crucial for various biological functions, including respiration, energy metabolism, immune function, DNA synthesis and repair, detoxification and overall optimal cellular function maintenance[68]. Dietary iron requirements have been studied for different cultured species, including *S. aurata*. These studies indicate that low iron levels reduce growth performance, depress erythropoiesis, and worsen heat-induced hypoxia[69–71]. However, these iron concentration values have been determined in very few cases based on serum or plasmatic iron levels. In *S. aurata*, iron supplementation enhanced the performance mainly from a haematological and immunological point of view[72]. Trials involving iron overload suggest that the iron homeostasis seems to be much more complex than in other vertebrates, probably due to the involvement of the different mediators between iron metabolism and host immune response[73]. Therefore, future research should prioritise establishing the correlation between plasma iron levels and the health status of fish.

Conclusions

In this study, we demonstrate the presence of blood and exogenous haem groups, estimate the average volume of blood intake in *S. chrysophrii* and describe the functional anatomy of its buccal and gastrodermal apparatus. Moreover, our results suggest the necessity of an iron source other than haem for the flatworm's survival, and an intimate relationship between blood intake, haem detoxification and parasite reproduction, com-

patible with strategies already described in other haematophagous parasites.

Funding

The Spanish Government supported this work: 1) the Spanish Ministry of Science and Innovation [MCIN/AEI/10.13039/501100011033] through three projects RTI2018-098664-B-I00, PID2019- 10730RB-I00 and PID2022-136914OB-100), which also had funding from 2) EU AEI/FEDER, MINECO/FEDER and by FEDER A way to make Europe; 3) the Generalitat Valenciana through ThinkInAzul programme supported by MICIN with funding from Next-Generation EU [PRTR-C17.I1] [THINKINAZUL/2021/022 and THINKINAZUL/2021/029] and CIAICO/2022/144 and AICO/2021/279. ERF was supported by a PRE2019-087409 contract, funded by MCIN/AEI/10.13039/501100011033 and co-funded by the European Social Fund (ESF). We acknowledge support of the publication fee by the CSIC Open Access Publication Support Initiative through URICI.

Acknowledgements

We dedicate this article to the memory of Dr. Panos Varvarigos, a renowned Greek fish pathologist who significantly contributed to diagnostics and health management in Mediterranean marine aquaculture and inspired our study on this parasite's bloodfeeding nature. We thank J. Monfort, L. Rodríguez, and I. Vicente for technical assistance, and the microscopy staff at SCSIE (University of Valencia, Spain) for their support.

Supplementary material

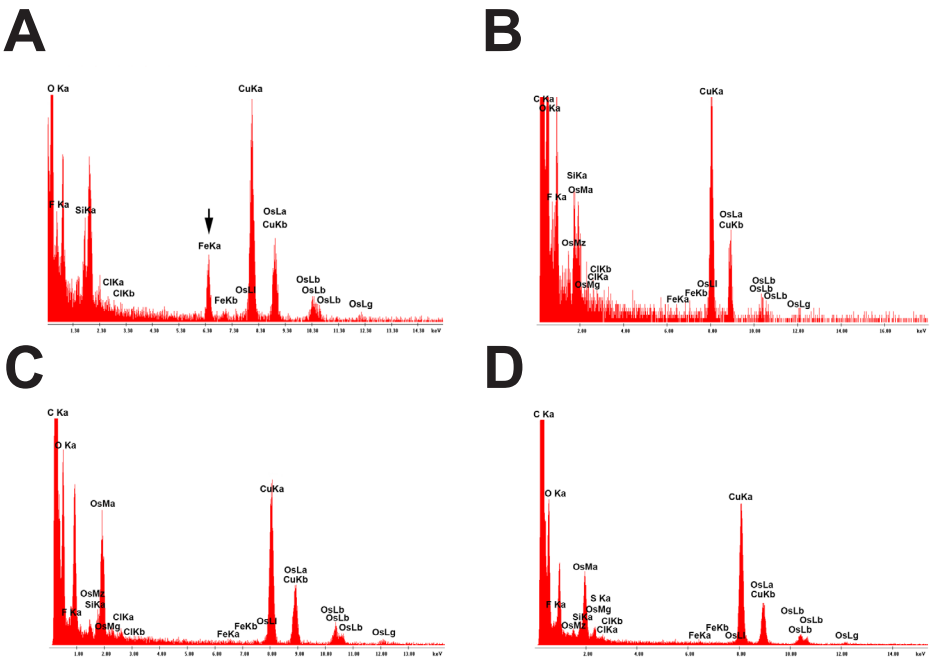

Figure S1. X-ray energy spectrum analysis in *Sparicotyle chrysophrii* cells and structures. X-ray energy spectrum analysis in *Sparicotyle chrysophrii* cells and structures. A: X-ray energy spectrum of an electron-dense haematin crystal in a digestive cell. The Ka (black arrow) and Kb peaks from iron (Fe) represent the principal constituent element. Note the absence of Fe Ka and Fe Kb peaks in **B:** a haematin cell cytoplasm. **C:** vitelline cells and **D:** sclerites. The copper (Cu) and silicon (Si) element peaks are derived from the sample grid and microscope column, respectively, and the osmium (Os) peaks from the embedding medium.

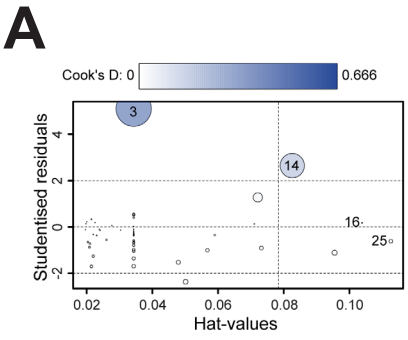

Observation	StuRes	Hat	CookD
3 ▲	5.1038484	0.03431774	0.6664382084
14	2.6462656	0.08259433	0.3152477012
16	0.1731340	0.10384837	0.0007994266
25	-0.6178392	0.11262999	0.0071703093

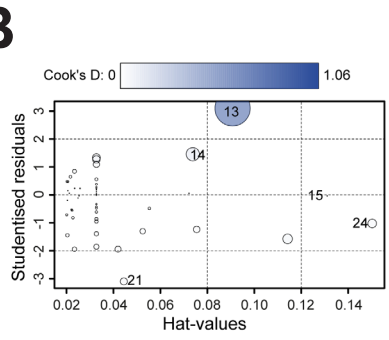

Observation	StuRes	Hat	CookD
13 ▲	3.10038109	0.09073538	1.0598132838
14	1.45921158	0.07380012	0.1481306716
15	-0.03681666	0.13107235	0.0001065959
21	-3.09563888	0.04442043	0.0432313430
24	-1.02242399	0.15024406	0.0617041134

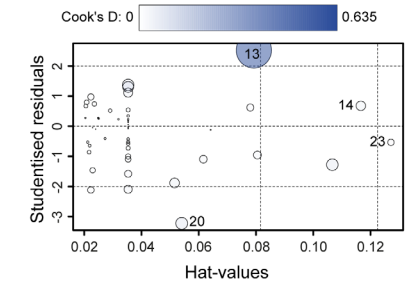

Observation	StuRes	Hat	CookD
13 ▲	2.5211173	0.07925490	0.63504879
14	0.6785119	0.11662121	0.04671087
20	-3.2245350	0.05405126	0.07252262
23	-0.5364200	0.12713015	0.02079624

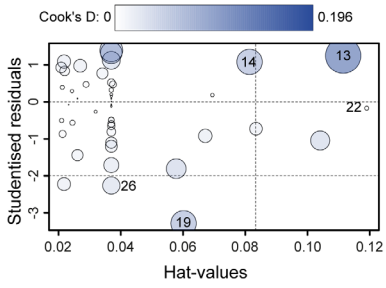

Observation	StuRes	Hat	CookD
13	1.2504029	0.11145692	0.19647616
14	1.0828474	0.08136738	0.10237657
19	-3.2830458	0.06017706	0.10217683
22	-0.1716283	0.11902525	0.00262800
26	-2.2602584	0.03694604	0.04698168

Figure S2. Influential-outlier removal. A: Identification of outliers in a gamma-distributed generalised linear model (GLM) with raw data (g_model_A). **B:** Identification of outliers in a gamma-distributed GLM after removing initial outliers identified in **A** (g_model_B). **C:** Identification of outliers in a gamma-distributed GLM after removing outliers identified in **A** and **B** (g_model_C). **D:** Identification of outliers in a gamma-distributed GLM after removing outliers identified in **A**, **B** and **C** (g_model_D). **NOTE:** The symbol ▲ indicates outliers (Cook's distance > 0.5). Observations 3 (**A**), 13 (**B**) and 13 (**C**) correspond to observations 3 (Control- C), 14 (Infected – R) and 15 (Infected – R) in the raw data available at https://doi.org/10.5281/zenodo.12666600. The generated gamma-distribute GLM in D (g_model_D as stated in the available R script) was the one selected to analyse the effects of *Sparicotyle chrysophrii* on *Sparus aurata* plasmatic free iron concentration.

Table S1. Assessment of the generalised linear model (GLM) performance.

GLM	AIC	AICc	BIC	Nagelkerke's R^2	RMSE	Sigma
g_model_A	555.471	555.982	561.266	0.126	134.294	1.430
g_model_B	513.187	513.709	518.923	0.035	43.139	0.715
g_model_C	490.554	491.088	496.230	0.160	35.577	0.607
g_model_D	472.995	473.541	478.609	0.263	33.456	0.536

AIC: Akaike's information criterion. **AICc:** Secondary-order (or small sample) AIC with a correction for small sample sizes. **BIC:** Bayesian information criterion. **Nagelkerke's R^2:** Pseudo R-squared measure for logistic regression models. **RMSE:** Root mean squared error. **Sigma:** Residual standard deviation. **NOTE:** The GLM g_model_D was the one selected to analyse the effects of *Sparicotyle chrysophrii* on *Sparus aurata* plasmatic free iron concentration.

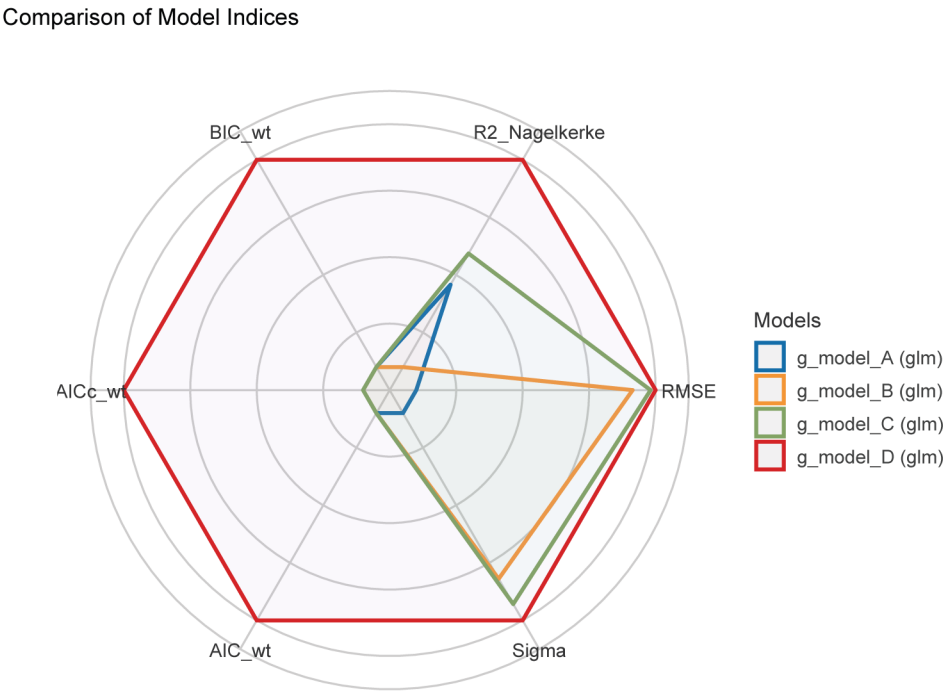

Figure S3. Visual representation of the generalised linear model (GLM) performance assessment. The models are compared in terms of the assessed performance parameters previously stated in **Table S1.**

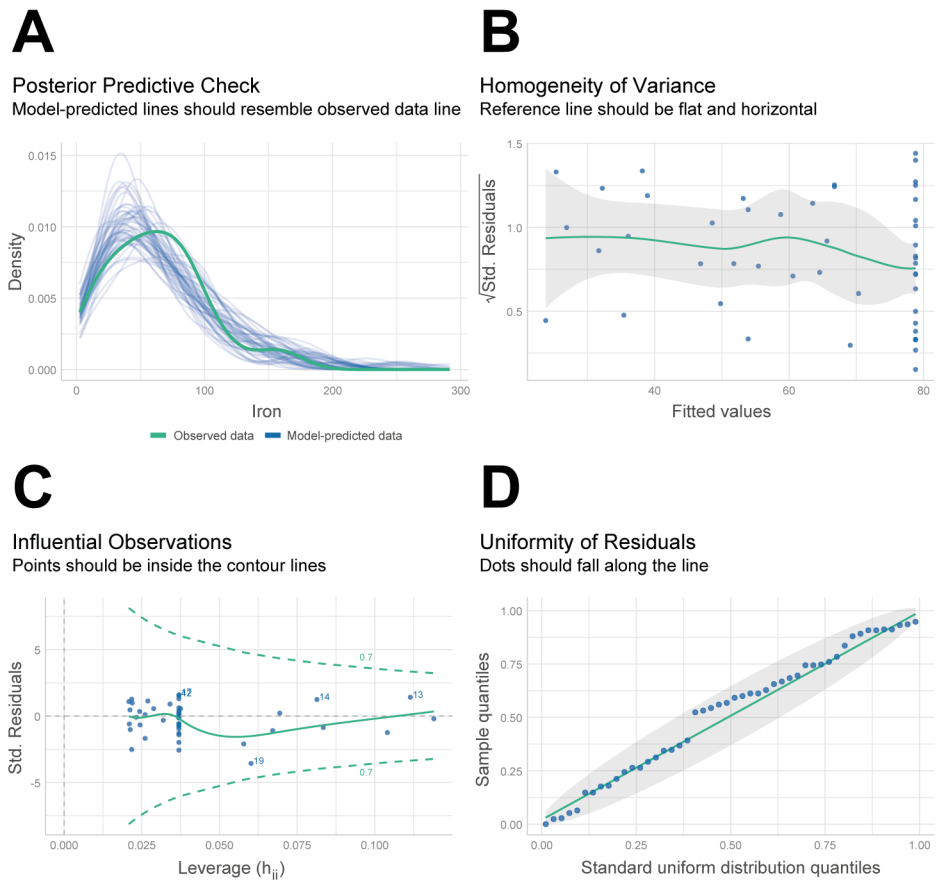

Figure S4. Quality assessment analyses of the gamma-distributed generalised linear model (GLM; g_model_D). A: Analysis of the predictive power of the produced GLM. **B:** Homogeneity of the variance assessment. The grey area represents the confidence intervals (CI) at 95%. **C:** Influential-outlier observations. Green dashed lines represent Cook's distance set at 0.7. Values placed over the green dashed lines are considered influential observations in the GLM. **D:** Assessment of the uniformity of the residuals using a quantile-quantile plot. The grey area represents the CI at 95%.

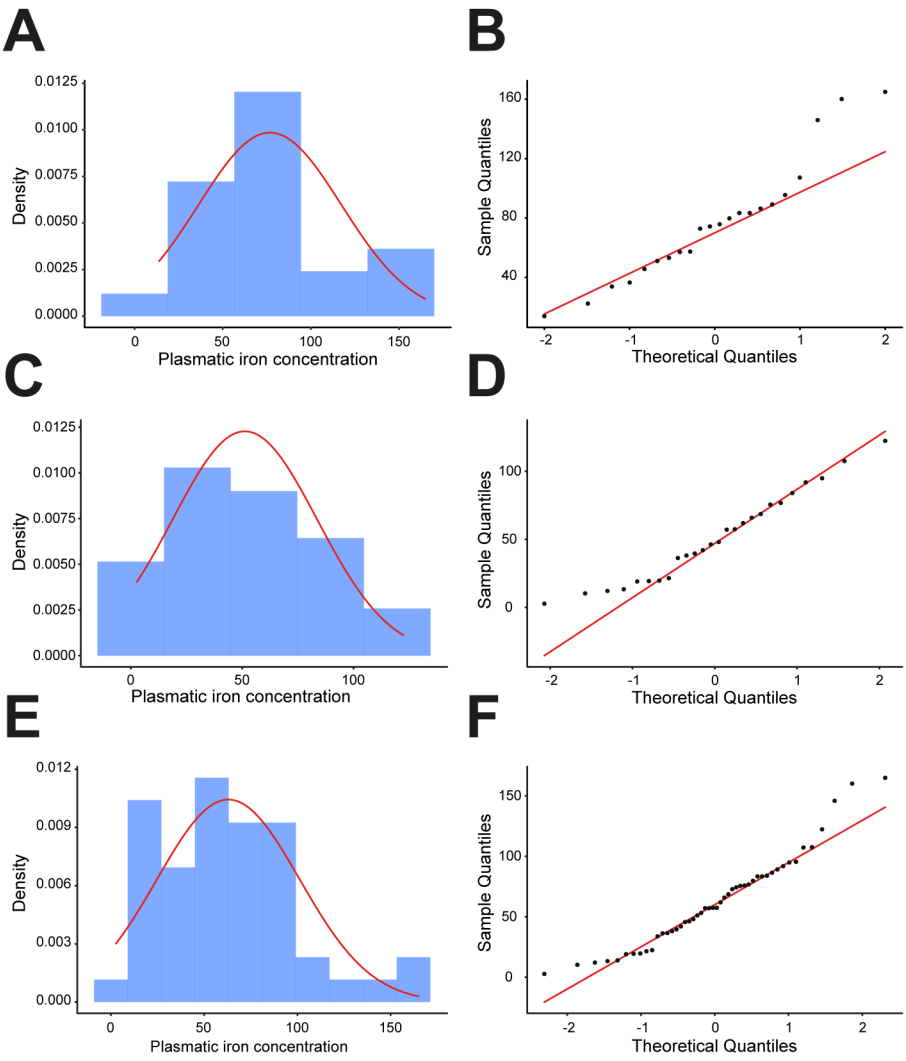

Figure S5. Visual assessment of normality for free plasmatic iron levels in control (C) *Sparus aurata* and *S. aurata* infected (R) with *Sparicotyle chrysophrii* after removing influential – outlier observations. A: Density plot for free plasmatic iron levels in C *S. aurata*. **B:** Quantile-quantile plot for free plasmatic iron levels in C *S. aurata*. **C:** Density plot for free plasmatic iron levels in R *S. aurata*. **D:** Quantile-quantile plot for free plasmatic iron levels in R *S. aurata*. **E:** Density plot for free plasmatic iron levels in C and R *S. aurata* combined. **D:** Quantile-quantile plot for free plasmatic iron levels in C and R *S. aurata* combined.

Table S2. Normality assessment of the free iron concentration in plasma of *Sparus aurata* parasitised with *S. chrysophrii*.

	Normality tests			Descriptive assessment of normality		Analysis of the variance
Group	**Shapiro-Wilk**	**Anderson-Darling**	**Kolmogorov-Smirnov**	**Skewness**	**Kurtosis**	**Brown-Forsythe**
C	*p* value=0.1212 Normal	*p* value=0.1277 Normal	*p* value=0.1962 Normal	0.7334672 Right-skew	3.052045 Mesokurtic	
R	*p* value=0.3941 Normal	*p* value=0.5147 Normal	*p* value=0.3351 Normal	0.399585 Symmetrical	2.271103 Mesokurtic	
C+R	*p* value=0.0394 Not normal	*p* value=0.1748 Normal	*p* value=0.6483 Normal	0.7154499 Right-skew	3.341355 Mesokurtic	*p* value=0.02197148 Unequal variances

Data, code and materials supporting this paper are publicly available in Zenodo repository at https://doi.org/10.5281/zenodo.12666600.

References

1. Toh SQ, Glanfield A, Gobert GN, Jones MK. Heme and blood-feeding parasites: friends or foes? Parasit Vectors. 2010;3:108.

2. Schmitt TH, Frezzatti WA, Schreier S. Hemin-induced lipid membrane disorder and increased permeability: a molecular model for the mechanism of cell lysis. Arch Biochem Biophys. 1993;307:96–103.

3. Brabec J, Salomaki ED, Kolísko M, Scholz T, Kuchta R. The evolution of endoparasitism and complex life cycles in parasitic platyhelminths. Curr Biol. 2023;33:4269-4275.e3.

4. Caña-Bozada V, Robinson MW, Hernández-Mena DI, Morales-Serna FN. Exploring evolutionary relationships within neodermata using putative orthologous groups of proteins, with emphasis on peptidases. Trop Med Infect Dis. 2023;8:59.

5. Ogawa K. Diseases of cultured marine fishes caused by Platyhelminthes (Monogenea, Digenea, Cestoda). Parasitology. 2015;142:178–95.

6. Kawatsu H. Studies on the anemia of fish - IX: hypochromic microcytic anemia of crucian carp caused by infestation with a trematode, *Diplozoon nipponicum*. Bull J Soc Sci Fish. 1978;44:1315–9.

7. Bakke TA, Harris PD, Hansen H, Cable J, Hansen LP. Susceptibility of Baltic and East Atlantic salmon *Salmo salar* stocks to *Gyrodactylus salaris* (Monogenea). Dis Aquat Organ. 2004;58:171–7.

8. Grau A, Crespo S, Pastor E, González P, Carbonell E. High infection by *Zeuxapta seriolae* (Monogenea: Heteraxinidae) associated with mass mortalities of amberjack *Seriola dumerili* Risso reared in sea cages in the Balearic islands (western Mediterranean). Bull Eur Ass Fish Pathol. 2003;23:139–42.

9. Ternengo S, Agostini S, Quilichini Y, Euzet L, Marchand B. Intensive infestations of *Sciaenocotyle pancerii* (monogenea, microcotylidae) on *Argyrosomus regius* (Asso) under fish-farming conditions. J Fish Dis. 2010;33:89–92.

10. Vorel J, Cwiklinski K, Roudnický P, Ilgová J, Jedličková L, Dalton JP, et al. *Eudiplozoon nipponicum* (Monogenea, Diplozoidae) and its adaptation to haematophagy as revealed by transcriptome and secretome profiling. BMC Genomics. 2021;22:274.

11. Muniesa A, Basurco B, Aguilera C, Furones D, Reverté C, Sanjuan-Vilaplana A, et al. Mapping the knowledge of the main diseases affecting sea bass and sea bream in Mediterranean. Transbound Emerg Dis. 2020;67:1089–100.

12. Kearn GC. Monogenean gill parasites- Polyopisthocotyleans. Leeches, lice and lampreys: a natural history of skin and gill parasites of fishes. 1st ed. Dordrecht: Springer; 2004. p. 103–30.

13. Mladineo I, Volpatti D, Beraldo P, Rigos G, Katharios P, Padrós F. Monogenean *Sparicotyle chrysophrii*: the major pathogen of the Mediterranean gilthead seabream aquaculture. Rev Aquac. 2024;16:287–308.

14. Ogawa K, Yasuzaki M, Yoshinaga T. Experiments on the evaluation of the blood feeding of *Heterobothrium okamotoi* (Monogenea: Diclidophoridae). Fish Pathol. 2005;40:169–74.

15. Rohde K, Watson NA. Ultrastructure of the buccal complex of *Polylabroides australis* (Monogenea, Polyopisthocotylea, Microcotylidae). Int J Parasitol. 1995;25:307–18.

16. Rohde K, Watson NA. Ultrastructure of the buccal complex of *Pricea multae* (Monogenea: Ployopisthocotylea, Gastrocotylidae). Folia Parasitol (Praha). 1996;43:117–32.

17. Konstanzová V, Koubková B, Kašný M, Ilgová J, Dzika E, Gelnar M. Ultrastructure of the digestive tract of *Paradiplozoon homoion* (Monogenea). Parasitol Res. 2015;114:1485–94.

18. Valigurová A, Vaškovicová N, Gelnar M, Kováčiková M, Hodová I. *Eudiplozoon nipponicum*: morphofunctional adaptations of diplozoid monogeneans for confronting their host. BMC Zool. 2021;6:23.

19. Donohue K V., Khalil SMS, Sonenshine DE, Roe RM. Heme-binding storage proteins in the Chelicerata. J Insect Physiol. 2009;55:287–96

20. Whiten SR, Eggleston H, Adelman ZN. Ironing out the details: exploring the role of iron and heme in blood-sucking arthropods. Front Physiol. 2018;8:1134.

21. Tang Y, Pyo YC, Tae IK, Hong SJ. *Clonorchis sinensis*: molecular cloning, enzymatic activity, and localization of yolk ferritin. J Parasitol. 2006;92:1275–80.

22. Schüßler P, Pötters E, Winnen R, Bottke W, Kunz W. An isoform of ferritin as a component of protein yolk platelets in *Schistosoma mansoni*. Mol Reprod Dev. 1995;41:325–30.

23. Toh SQ, Gobert GN, Malagón Martínez D, Jones MK. Haem uptake is essential for egg production in the haematophagous blood fluke of humans, *Schistosoma mansoni*. FEBS J. 2015;282:3632–46.

24. Kawase O, Iwaya H, Asano Y, Inoue H, Kudo S, Sasahira M, et al. Identification of novel yolk ferritins unique to planarians: planarians supply aluminum rather than iron to vitellaria in egg capsules. Cell Tissue Res. 2021;386:391–413.

25. Riera-Ferrer E, Del Pozo R, Piazzon MC, Sitjà-Bobadilla A, Estensoro I, Palenzuela O. *Sparicotyle chrysophrii* experimental infection of gilthead seabream (*Sparus aurata*): establishment of an *in vivo* model reproducing the pathological outcomes of sparicotylosis. Aquaculture. 2023;573.

26. Llewellyn J. Observations on the food and the gut pigment of the polyopisthocotylea (Trematoda: Monogenea). Parasitology. 1954;44:428–37.

27. LeVine SM, Zhu H, Tague SE. A simplified method for the histochemical detection of iron in paraffin sections: intracellular iron deposits in central nervous system tissue. ASN Neuro. 2021;13:1759091420982169.

28. Mayer I, Shackley SE, Ryland JS. Aspects of the reproductive biology of the bass, *Dicentrarchus labrax* L. I. An histological and histochemical study of oocyte development. J Fish Biol. 1988;33:609–22.

29. Cleveland R, Wolfe JM. A differential stain for the anterior lobe of the hypophysis. Anat Rec. 1932;51:409–13.

30. R Core Team. R: a language and environment for statistical computing [Internet]. Vienna, Austria: R Foundation for Statistical Computing; 2021. Available from: https://www.R-project.org/

31. Venables WN, Ripley BD. Modern Applied Statistics with S. Fourth edition. New York: Springer; 2002.

32. Wickham H. ggplot2: elegant graphics for data analysis. New York: Springer-Verlag; 2016.

33. Lüdecke D, Ben-Shachar M, Patil I, Waggoner P, Makowski D. performance: an R package for assessment, comparison and testing of statistical models. J Open Source Softw. 2021;6:3139.

34. Pedersen T. Patchwork: the composer of plots . R package version 1.3.0.9000. 2024.

35. Hartig F. DHARMa: residual diagnostics for hierarchical (multi-level / mixed) regression models. R package version 0.4.6.1. 2022.

36. Fox J, Weisberg S. An R companion to applied regression. Third edition. Thousand Oaks: Sage; 2019.

37. Gross J, Ligges U. Nortest: tests for normality. R package version 1.0-4. 2015.

38. Komsta L, Novomestky F. Moments: moments, cumulants, skewness, kurtosis and related tests. R package version 0.14.1. 2022.

39. Dag O, Dolgun A, Meric Konar N. Onewaytests: an R package for one-way tests in independent groups designs. R J. 2018;10:175–99.

40. Wickham H, François R, Henry L, Müller K, Vaughan D. Dplyr: a grammar of data manipulation. R package version 1.1.4.. 2023. A

41. Dalton JP, Skelly P, Halton DW. Role of the tegument and gut in nutrient uptake by parasitic platyhelminths. Can J Zool. 2004;82:211–32.

42. Sojka D, Franta Z, Horn M, Caffrey CR, Mareš M, Kopáček P. New insights into the machinery of blood digestion by ticks. Trends Parasitol. 2013;29:276–85.

43. Pishchany G, Skaar EP. Taste for blood: hemoglobin as a nutrient source for pathogens. PLoS Pathpgens. 2012;8:e1002535.

44. Sánchez M, Sabio L, Gálvez N, Capdevila M, Dominguez-Vera JM. Iron chemistry at the service of life. IUBMB Life. 2017;69:382–8

45. Xiao S hua, Sun J. *Schistosoma* hemozoin and its possible roles. Int J Parasitol. 2017;47:171–83

46. Lvova M, Zhukova M, Kiseleva E, Mayboroda O, Hensbergen P, Kizilova E, et al. Hemozoin is a product of heme detoxification in the gut of the most medically important species of the family Opisthorchiidae. Int J Parasitol. 2016;46:147–56.

47. Martínez-González J de J, Guevara-Flores A, Del Arenal Mena IP. Evolutionary adaptations of parasitic flatworms to different oxygen tensions. Antioxidants. 2022;11:1102.

48. Abdelgelil NH, Abdellatif MZM, Abdel-Hafeez EH, Belal US, Mohamed RM, Abdel-Razik ARH, et al. Effects of iron chelating agent on *Schistosoma mansoni* infected murine model. Biomed Pharmacother. 2019;109:28–38.

49. Martínez-Sernández V, Mezo M, González-Warleta M, Perteguer MJ, Muiño L, Guitián E, et al. The MF6p/FhHDM-1 major antigen secreted by the trematode parasite *Fasciola hepatica* is a heme-binding protein. J Biol Chem. 2014;289:1441–56.

50. Reddi AR, Hamza I. Heme mobilization in animals: a metallolipid's journey. Acc Chem Res. 2016;49:1104–10.

51. Gobert GN, Tran MH, Moertel L, Mulvenna J, Jones MK, McManus DP, et al. Transcriptional changes in *Schistosoma mansoni* during early schistosomula development and in the presence of erythrocytes. PLoS Negl Trop Dis. 2010;4:e600.

52. Sitjà-Bobadilla A, Álvarez-Pellitero P. Experimental transmission of *Sparicotyle chrysophrii* (Monogenea: Polyopisthocotylea) to gilthead seabream (*Sparus aurata*) and histopathology of the infection. Folia Parasitol (Praha). 2009;56:143–51.

53. Delcroix M, Sajid M, Caffrey CR, Lim KC, Dvořák J, Hsieh I, et al. A multienzyme network functions in intestinal protein digestion by a platyhelminth parasite. J Biol Chem. 2006;281:39316–29.

54. Santos CP, Souto-Padrón T, Lanfredi RM. The ultrastructure of the gastrodermis and the nutrition of the gill parasitic *Atriaster heterodus* Lebedev and Paruchin, 1969 (Platyhelminthes: Monogenea). Mem Inst Oswaldo Cruz. 1998;93:277–82.

55. Halton DW, Morris GP. Ultrastructure of the anterior alimentary tract of a monogenean, *Diclidophora merlangi*. Int J Parasitol. 1975;5:407–19.

56. Brennan GP, Ramasamy P. Ultrastructure of the gut caecal epithelium of *Pricea multae* (Monogenea: Polyopisthocotylea). Parasitol Res. 1996;82:312–8.

57. Halton DW. Nutritional adaptations to parasitism within the Platyhelminthes. Int J Parasitol. 1997;27:693–704.

58. Poddubnaya LG, Hemmingsen W, Reed C, Gibson DI. Ultrastructural characteristics of the caeca of basal polyopisthocotylean monogeneans of the families Chimaericolidae and Hexabothriidae parasitic on cartilaginous fishes. Parasitol Res. 2015;114:2599–610.

59. Cable J, El-Naggar MM. Gastrodermis ultrastructure of the different life stages of the polyopisthocotylean monogenean gill parasite *Discocotyle sagittata*. Parasitol Res. 2021;120:3181–93.

60. Jennings JB. Studies on digestion in the monogenetic trematode *Polystoma integerrimum*. J Helminthol. 1959;33:197–204.

61. Hodová I, Sonnek R, Gelnar M, Valigurová A. Architecture of *Paradiplozoon homoion*: a diplozoid monogenean exhibiting highly-developed equipment for ectoparasitism. PLoS One. 2018;13.

62. Valigurová A, Hodová I, Sonnek R, Koubková B, Gelnar M. *Eudiplozoon nipponicum* in focus: monogenean exhibiting a highly specialized adaptation for ectoparasitic lifestyle. Parasitol Res. 2011;108:383–94.

63. Riera-Ferrer E, Piazzon MC, Del Pozo R, Palenzuela O, Estensoro I, Sitjà-Bobadilla A. A bloody interaction: plasma proteomics reveals gilthead sea bream (*Sparus aurata*) impairment caused by *Sparicotyle chrysophrii*. Parasit Vectors. 2022;15:322.

64. Riera-Ferrer E, Mazanec H, Mladineo I, Konik P, Piazzon MC, Kuchta R, et al. An inside out journey: biogenesis, ultrastructure and proteomic characterisation of the ectoparasitic flatworm *Sparicotyle chrysophrii* extracellular vesicles. Parasit Vectors. 2024;17:175.

65. Perner J, Sobotka R, Sima R, Konvickova J, Sojka D, Lagerblad De Oliveira P, et al. Acquisition of exogenous haem is essential for tick reproduction. Elife. 2016;5:e12318.

66. Witeska M, Kondera E, Ługowska K, Bojarski B. Hematological methods in fish – not only for beginners. Aquaculture. 2022;547:737498.

67. Groff JM, Zinkl JG. Hematology and clinical chemistry of cyprinid fish: common carp and goldfish. Vet Clin North Am Exot Anim Pract. 1999;2:741–76.

68. Farrell AP. Encyclopedia of fish physiology: from genome to environment. Farrell AP, Stevens ED, Cech Jr. JJ, Richards JG, editors. London: Academic Press; 2011.

69. Prabhu PAJ, Schrama JW, Kaushik SJ. Mineral requirements of fish: a systematic review. Rev Aquac. 2016;8:172–219.

70. Makwinja R, Geremew A. Roles and requirements of trace elements in tilapia nutrition: review. Egypt J Aquat Res. 2020;46:281–7.

71. Wang Z, Li X, Lu K, Wang L, Ma X, Song K, et al. Effects of dietary iron levels on growth performance, iron metabolism and antioxidant status in spotted seabass (*Lateolabrax maculatus*) reared at two temperatures. Aquaculture. 2023;562:738717.

72. Rigos G, Samartzis A, Henry M, Fountoulaki E, Cotou E, Sweetman J, et al. Effects of additive iron on growth, tissue distribution, haematology and immunology of gilthead sea bream, *Sparus aurata*. Aquacult Int. 2010;18:1093–104.

73. Serna-Duque JA, Espinosa Ruiz C, Martínez Lopez S, Sánchez-Ferrer Á, Esteban MÁ. Immunometabolic involvement of hepcidin genes in iron homeostasis, storage, and regulation in gilthead seabream (*Sparus aurata*). Front Mar Sci. 2022;9:1073060.

Chapter 8

An inside out journey: Biogenesis, ultrastructure and proteomic characterisation of the ectoparasitic flatworm *Sparicotyle chrysophrii* extracellular vesicles

Enrique Riera-Ferrer[1], Hynek Mazanec[2], Ivona Mladineo[3], Peter Konik[4], M. Carla Piazzon[1], Roman Kuchta[2], Oswaldo Palenzuela[1], Itziar Estensoro[1], Javier Sotillo[5] and Ariadna Sitjà-Bobadilla[1]

[1]Fish Pathology Group, Institute of Aquaculture Torre de la Sal (IATS, CSIC), Consejo Superior de Investigaciones Científicas, Castellón, Spain

[2]Laboratory of Helminthology, Institute of Parasitology, Biology Centre, Czech Academy of Sciences, (BC CAS), České Budějovice, Czech Republic.

[3]Laboratory of Functional Helminthology, Institute of Parasitology, Biology Centre Czech Academy of Sciences (BC CAS), České Budějovice, Czech Republic.

[4]Faculty of Science, University of South Bohemia, Branišovská 1160/31, 370 05 České Budějovice, Czech Republic.

[5]Parasitology Reference and Research Laboratory, National Centre for Microbiology, Instituto de Salud Carlos III, Majadahonda, Madrid, Spain.

Parasites & Vectors, 3 April 2024
https://doi.org/10.1186/s13071-024-06257-x

Abstract

Helminth extracellular vesicles (EVs) are known to have a three-way communication function among parasitic helminths, their host and the host-associated microbiota. They are considered biological containers that may carry virulence factors, being therefore appealing as therapeutic and prophylactic target candidates. This study aims to describe and characterise EVs secreted by *Sparicotyle chrysophrii* (Polyopisthocotyla: Microcotylidae), a blood-feeding gill parasite of gilthead seabream (*Sparus aurata*), causing significant economic losses in Mediterranean aquaculture.

To identify proteins involved in extracellular vesicle biogenesis, genomic datasets from *S. chrysophrii* were mined *in silico* using known protein sequences from *Clonorchis* spp., *Echinococcus* spp., *Fasciola* spp., *Fasciolopsis* spp., *Opisthorchis* spp., *Paragonimus* spp. and *Schistosoma* spp. The location and ultrastructure of EVs were visualised by transmission electron microscopy after fixing adult *S. chrysophrii* specimens by high-pressure freezing and freeze substitution. EVs were isolated and purified from adult *S. chrysophrii* (n = 200) using a newly developed ultracentrifugation-size-exclusion chromatography protocol for Polyopisthocotyla, and EVs were characterised via nanoparticle tracking analysis and tandem mass spectrometry.

Fifty-nine proteins involved in EV biogenesis were identified in *S. chrysophrii*, and EVs compatible with ectosomes were observed in the syncytial layer of the haptoral region lining the clamps. The isolated and purified nanoparticles had a mean size of 251.8 nm and yielded 1.71×10^8 particles·mL^{-1}. The protein composition analysis identified proteins related to peptide hydrolases, GTPases, EF-hand domain proteins, aerobic energy metabolism, anticoagulant/lipid-binding, haem detoxification, iron transport, EV biogenesis-related, vesicle-trafficking and other cytoskeletal-related proteins. Several identified proteins, such as leucyl and alanyl aminopeptidases, calpain, ferritin, dynein light chain, 14–3–3, heat shock protein 70, annexin, tubulin, glutathione *S*-transferase, superoxide dismutase, enolase and fructose-bisphosphate aldolase, have already been proposed as target candidates for therapeutic or prophylactic purposes.

We have unambiguously demonstrated for the first time to our knowledge the secretion of EVs by an ectoparasitic flatworm, inferring their biogenesis machinery at a genomic and transcriptomic level, and by identifying their location and protein composition. The identification of multiple therapeutic targets among EVs' protein repertoire provides opportunities for target-based drug discovery and vaccine development for the first time in Polyopisthocotyla (*sensu* Monogenea), and in a fish-ectoparasite model.

Introduction

Monogeneans, recently reclassified into two unrelated classes, Monopisthocotyla and Polyopisthocotyla[1,2], are important aquatic, mainly ectoparasitic neodermatans whose presence in fish farms pose a significant bottleneck for fish health, welfare, performance and economic revenue due to the artificial environment in which livestock is set[3].

Currently, the gill-infecting *Sparicotyle chrysophrii* (Van Beneden and Hesse, 1863) (Polyopisthocotyla: Microcotylidae) is among the most threatening pathogens in farmed gilthead seabream (*Sparus aurata*) across the Mediterranean Sea[4,5]. The urge to find solutions for this parasitosis is clearly reflected in the scientific knowledge produced in the past decades. Epidemiological surveys[4] and distribution models have been established[6] and various anthelmintics have been tested[5,7,8].

Recently, a growing interest in *sensu* Monogenea secretome, composed of a soluble and a vesicular fraction, has emerged, leading to the *in silico* identification and characterisation of drug target candidates, such as peptidases and peptidase inhibitors considered as virulence factors, in several species[9–17]. In the last decade, the vesicular fraction of the secretome, which contains extracellular vesicles (EVs), has been extensively studied in human-associated and zoonotic flatworms and nematodes infecting mammals[18]. EVs have been assigned roles in host-parasite interactions, intraspecies communication and communication with the surrounding microbiota[18,19].

EVs include exosomes and ectosomes, depending on their origin[20], and they follow different biogenesis pathways that ultimately determine the composition, cargo and function of EVs. Exosome formation following an endocytic pathway involves both the ESCRT (Endosomal Sorting Complex Required for Transport)-dependent and ESCRT-independent pathways and comprises intraluminal vesicles (ILVs) within multivesicular bodies (MVBs)[21–23]. The ESCRT-dependent pathway produces ILVs through tandem recruitment of members of the ESCRT machinery and associated proteins to the endosomal membrane, which subsequently control the process of membrane curvature as well as the cargo and final ILV scission.

The ESCRT-independent pathway, on the other hand, requires proteins of the tetraspanin family for its regulation, sphingomyelinases to promote a spontaneous negative curvature of membranes and sphingosine kinase for the MVBs maturation and cargo loading[24]. Ectosomes, however, form as a result of direct outward budding and scission of the plasma membrane upon cytoskeletal rearrangement and Ca^{2+} influx as well as activation of scramblases, flippases and translocases[25].

The EV biogenesis machinery required for the different pathways is reported to be generally conserved in Neodermata. However, differences have been found between different classes. In particular, the machinery involved in the ESCRT-dependent pathway

appears to be highly conserved in tapeworms (Cestoda), whereas it appears to be mostly incomplete in monogeneans (Polyopisthocotyla), akin to Trematoda. Similarly, proteins involved in the non-canonical ESCRT-dependent pathway and ectosome formation are conserved in Neodermata. Conversely, the protein machinery required for the ESCRT-independent pathway appears to be the least conserved of all known pathways, regardless of the Neodermata class[26].

The heterogeneity of the helminth EV population is not only limited to its size but also to its protein composition, which differs depending on the site of formation. The role of helminth EVs in cell-to-cell communication involves the transfer of effector molecules including proteins, lipids, small RNAs (mRNA, miRNA and non-coding RNA species) and glycans[18]. The protein composition of EVs may include structural and biogenesis-related proteins as well as enzymatic proteins critical for parasite survival. Additionally, lipids within helminth vesicles not only contribute to the viability of EVs in the extracellular space but also may serve as bioactive immunomodulators. Furthermore, miRNAs are known to play immunomodulatory roles, while glycans are associated with EV internalisation[18]. Studies on helminth EVs have mainly focused on mammalian models. Notably, according to the latest research, EVs have been isolated only in the L3 stage of the nematode *Anisakis pegreffi* among marine fish parasites[27], adding another layer to the complexity of parasite-fish host-microbiome interactions.

In light of increasing resistance to known anthelmintics, EVs seem promising research targets due not only to their roles in essential parasite physiological processes but also to virulence factors contained in their cargo involved in the pathogenesis. In general, excretory/secretory products (ESPs), including EVs, are appealing targets for prophylactic, therapeutic and/or diagnostic purposes due to their extracellular localisation and theoretical presence in the host. Nevertheless, due to the co-evolution of parasitic helminths with their hosts, the mechanisms of action of essential biological functions such as parasite adhesion, invasion, nutrition or immune evasion may differ in each species. So far, EVs have been studied only in endoparasitic helminths (Cestoda, Trematoda and Nematoda), while no EVs have been studied in ectoparasitic flatworms. Though gill polyopisthocotylans may have developed similar feeding and anchoring strategies, species-specific approaches are needed to decipher their unique pathogenic mechanisms so that effective therapies can be developed. In the current study, genomic and transcriptomic data of *S. chrysophrii* were generated for the identification of the protein machinery involved in different pathways of EV biogenesis and cargo sorting. The presence and tissular location of EVs in *S. chrysophrii* specimens was studied by transmission electron microscopy (TEM). Subsequently, EVs were isolated from adult *S. chrysophrii*, and their protein composition was characterised to identify therapeutic candidates for this parasite.

Material and methods

In silico scanning of proteins involved in extracellular vesicle biogenesis

A dataset of 82 sequences of known proteins involved in different EV biogenesis pathways in mammals (ESCRTdependent pathway: 31 proteins; non-canonical ESCRTassociated pathway: 5 proteins; ESCRT-independent mechanisms: 21 proteins; proteins involved in ectosome formation: 9 proteins; EV membrane organisers: 9 proteins; and proteins involved in RNA sorting into EV: 7 proteins)[26] were retrieved from UniProt (www.uniprot.org)[28]. These sequences were used to interrogate the *S. chrysophrii* draft genome and transcriptome datasets by translated nucleotide basic alignment search tool (tBLASTn)[29] under the Geneious Prime v2023.1.2 software framework with default settings (BLOSUM62, gap cost: 11 1; limited to 20 hits). The best BLAST hits for each protein query were selected considering a combination of E-value, bit score, pairwise identity and query coverage values. The best hits were then aligned with the queries via multiple sequence comparison by log-expectation (MUSCLE), and functionally important domains were assessed and compared using the InterProScan plug-in. Additionally, the predicted secondary structure of the hits was assessed and compared to that of the human protein queries (PSIPRED 4.0; http://bioinf.cs.ucl.ac.uk/psipred)[30]. The hypothetical orthologues were then used as queries to the NCBI database (https://www.ncbi.nlm.nih.gov) by translated nucleotide sequence searched against protein sequences (BLASTx). When significant hits were not found in *S. chrysophrii* datasets, or when confident prediction of *S. chrysophrii* protein sequences from the aligned regions was not feasible, available neodermatan homologues were retrieved from the NCBI database (https://www.ncbi.nlm.nih.gov). These homologues were sourced from *Clonorchis* spp., *Echinococcus* spp., *Fasciola* spp., *Fasciolopsis* spp., *Opisthorchis* spp., *Paragonimus* spp. and *Schistosoma* spp. because of the phylogenetic proximity among Trematoda, Cestoda and Polyopisthocotyla[1,2] and considering their genomic quality based on individual genome assembly statistics. The same steps and criteria as described above were employed to interrogate *S. chrysophrii* datasets for these neodermatan homologues. Finally, when different protein isoforms presented hit with the same *S. chrysophrii* contig, a single protein was considered (**Supplementary material: Dataset S1**). A representation of the entire data mining workflow is provided in **Figure 1**.

Parasite and fish maintenance

Gilthead seabream experimentally infected with *S. chrysophrii* were maintained in the Fish Pathology facilities at the Institute of Aquaculture Torre de la Sal under natural photoperiod and temperature conditions of the latitude (40°5'N; 0°10'E). The experimental infection was performed in a recirculating aquaculture system (RAS) where recipient *S.*

aurata received water effluent from infected donor *S. aurata* tanks, and the infective pressure within the system and the experimental units was modulated using egg collectors[31]. Infected fish (n = 5) were euthanised by tricaine methanesulfonate (MS-222; Sigma, St. Louis, MO, USA) overexposure (0.1 $g \cdot L^{-1}$) and bled from the caudal vessels. Gill arches were dissected and adult *S. chrysophrii* specimens were gently detached from the gill filaments under a stereomicroscope using fine paintbrushes for subsequent *in vitro* maintenance. Additionally, a piece of one gill arch bearing adult parasite stages was fixed in 10% neutral buffered formalin, dehydrated in graded ethanol series for routine histological procedures, embedded in Technovit resin (Kulzer, Heraeus, Germany), 2 µm-sectioned, stained with toluidine blue and examined by light microscopy.

Transmission electron microscopy (TEM)

Three adult *S. chrysophrii* specimens kept *in vitro* in complete Schnider's Drosophila medium (non-supplemented with chicken serum) were collected and processed for high-pressure freezing (HPF) and freeze substitution as reported in Mladineo et al.[32]. After cold fixation, samples were washed in acetone 3× for 15 min, infiltrated in mixtures of 25, 50 and 75% low viscosity Spurr resin (SPI Chem, West Chester, PA, USA) and anhydrous acetone for 1 h each and incubated overnight in 100% resin. The samples were left for polymerisation at 60 °C for 48 h in embedding moulds; afterwards, 1% toluidine blue-stained semithin sections (0.5 µm) were checked for orientation under the light microscope. Areas of interest were cut at 70 nm, mounted on Formvar-coated single-slot grids and contrasted for 30 min in ethanolic uranyl acetate and 20 min in lead citrate. Ultrathin sections were observed under a JEOL JEM-1400 microscope (JEOL, Akishima, Tokyo, Japan) operating at an accelerating voltage of 120 kV. The images were taken with a XAROSA 20-megapixel CMOS camera (EMSIS GmbH, Münster, Germany) and assembled and annotated in Inkscape 1.0 software (https:// inkscape. org).

Isolation and purification of extracellular vesicles

Two hundred adult *S. chrysophrii* specimens were kept *in vitro* for EV collection. Ten parasites per well were cultured in a 24 well-plate in 2.5 mL of 0.2 µm-filtered seawater (salinity 38 ppt) and kept at 18 °C. The medium from all wells was collected, pooled and

(See figure on next page.)

Figure 1. Workflow for *in silico* scanning of proteins involved in extracellular vesicle biogenesis. Protein sequences from *Homo sapiens* involved in EV biogenesis were collected from the UniProt database and used to interrogate *Sparicotyle chrysophrii* genome and transcriptome datasets, simultaneously using tBLASTn. Functional domains of *H. sapiens* and *S. chrysophrii* hypothetical orthologues were compared using InterPro, Pfam domains were retrieved, and PsiPred was used to compare their secondary structures. The chosen *S. chrysophrii* sequences were then used in a BLASTx search against the NCBI database. Orthologue protein sequences from Neodermata were used to interrogate *S. chrysophrii* draft genome by tBLASTn and the same methodology was applied to identify hypothetical proteins.

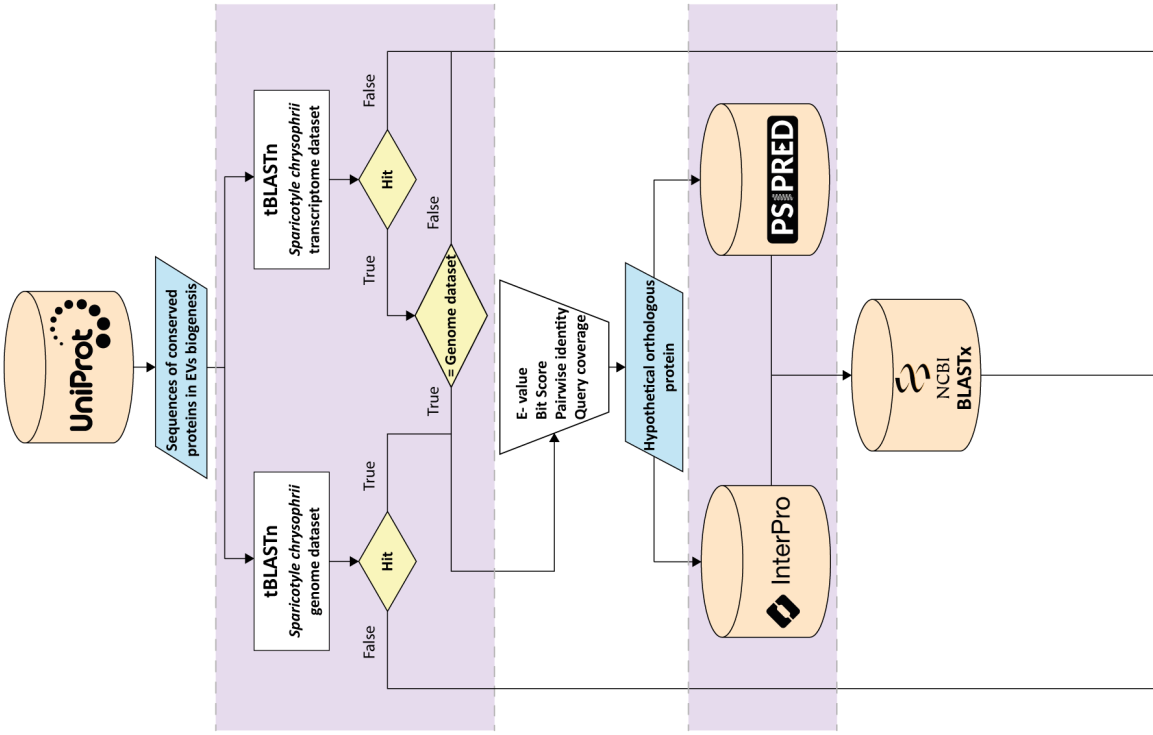
UniProt
Sequences of conserved proteins in EVs biogenesis
tBLASTn
Sparicotyle chrysophrii
genome dataset
Hit
True
False
tBLASTn
Sparicotyle chrysophrii
transcriptome dataset
Hit
True
False
= Genome dataset
True
False
E- value
Bit Score
Pairwise identity
Query coverage
Hypothetical orthologous protein
PSIPRED
InterPro
NCBI
BLASTx

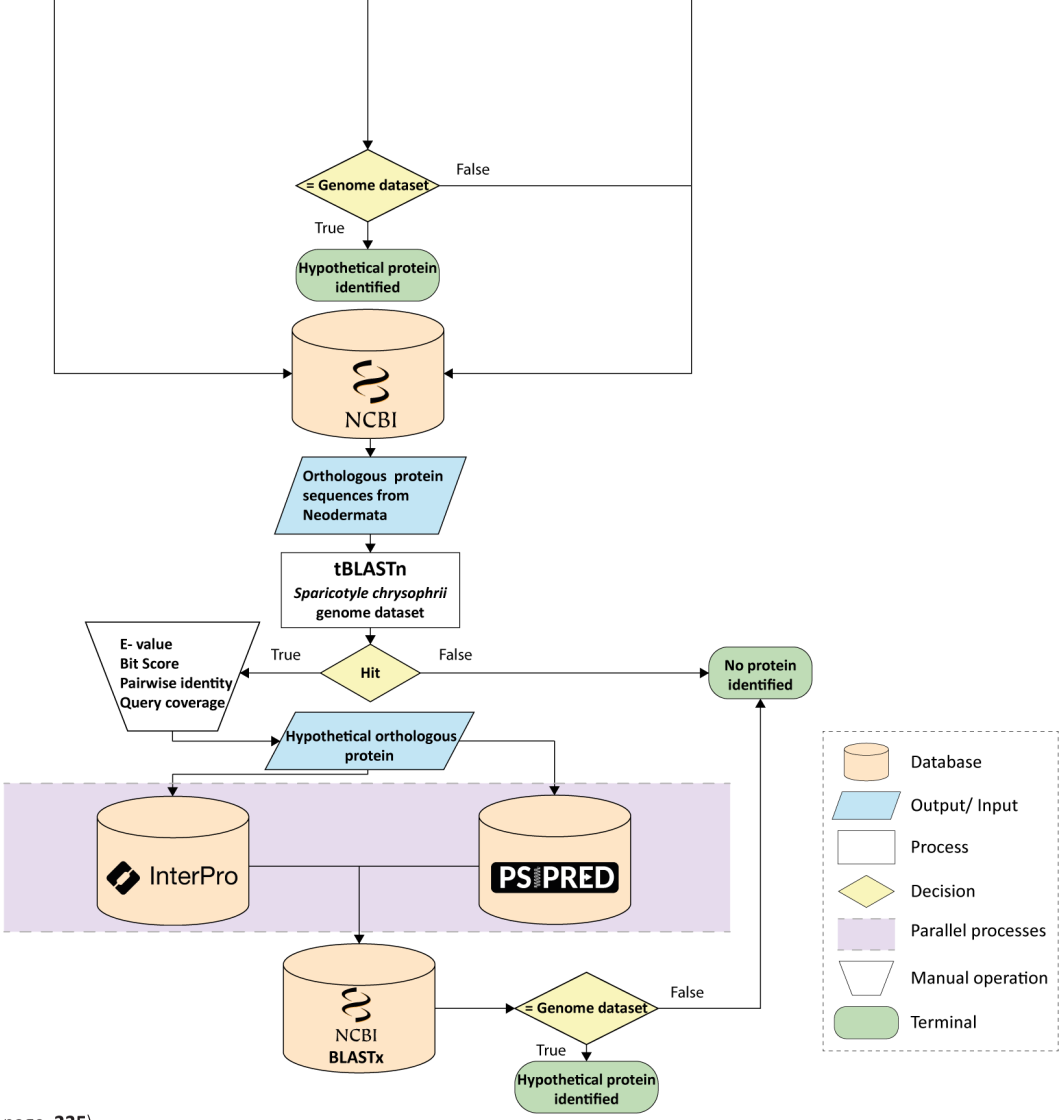

Figure 1. (See legend on page **235**).

replaced every 24 h for 3 days. Pooled samples from the three different sampling points (24 h, 48 h and 72 h) were processed separately. Initially, serial centrifugations were performed at 500, 2000 and 3500× *g* at 4°C for 30 min each, after which the supernatant containing ESPs was collected. The protein concentration in each ESP sample was quantified with the Pierce™ BCA protein assay kit (ThermoFisher Scientific, Waltham, MA, USA), and once the presence of proteins was confirmed, the samples were processed for a subsequent ultracentrifugation-size exclusion chromatography (UC-SEC) protocol.

ESPs were concentrated with an Amicon® Ultra-15 Centrifugal Filter Units 10 kDa (Amicon®, Miami, USA) to a final volume of 14 mL by centrifuging samples at 2500× *g* for 30 min at 12 °C. The resulting volume was centrifuged at 100,000× *g* for 8 h at 4 °C in a Beckman Optima XPN-90 Ultracentrifuge using a SW 40 Ti swinging-bucket rotor. The obtained pellets were resuspended in 500 µL of PBS and then processed by size-exclusion chromatography using qEVoriginal/70 nm Gen2 Columns (Izon Science, Christchurch, NZ). Finally, isolated EV samples were concentrated to a final volume of 250 µL by centrifuging samples at 3500× *g* for 1 h at 12 °C in Amicon® Ultra-4 Centrifugal Filter Units 10 kDa (Amicon®, Miami, FL, USA). In parallel, a 50 mL sample of the maintenance medium used and 0.2 µm-filtered PBS were processed similarly as a negative and quality control.

Isolated EV aliquots were diluted in PBS (1:5 *v/v*) and analysed via nanoparticle tracking analysis (NTA) using NanoSight (NS300; Malvern Panalytical, Malvern, UK) and software v3.4 to determine their nanoparticle concentration (particles·mL^{-1}). The protein concentration from the resulting isolated EV samples was quantified with the Bradford protein assay (ThermoFisher Scientific, Waltham, USA) together with the nanoparticle concentration, their purity (particles·µg protein^{-1}) was calculated according to Webber and Clayton[33].

Extracellular vesicle protein cargo analysis and therapeutic target candidate exploration

For EV samples proteomic analysis, 20 µL of the sample was mixed 1:1 with 100 mM ammonium bicarbonate; Rapigest (Waters, Milford, MA, USA) surfactant was added at a final concentration of 0.1% (*v/v*) and incubated at 60 °C for 45 min. The mixture was cooled to room temperature, and proteomic grade trypsin (Sigma, St. Louis, USA) was added at a final concentration of 10 ng·µL^{-1} and incubated at 37 °C. After 12 h, samples were acidified by addition of formic acid (Sigma, St. Louis, MO, USA) and peptides were isolated by StageTip procedure[34] to produce 30 µL of sample.

Liquid chromatography with tandem mass spectrometry (LC–MS/MS) was performed using an UltiMate 3000 UHPLC (ThermoFisher Scientific, Waltham, MA, USA) coupled online to a TimsTOF pro (Bruker, Billerica, MA, USA) mass spectrometer. Two µL of sample

was trapped on a ThermoFisher trap column (0.3 × 5 mm, C18, 5 µm) for 1 min and then separated by reverse phase liquid chromatography on an Acclaim PepMap RSLC column (75 µm × 15 cm, C18, 2 µm, 100 Å; ThermoFisher Scientific, Waltham, MA, USA). The gradient ran for 30 min, during which the acetonitrile in 0.1% formic acid vs 0.1% formic acid ratio rose from 3 to 50%. Peptides were ionised using CaptiveSpray. Spectra were acquired in data-dependent PASEF (Parallel Accumulation/SErial Fragmentation) mode with an accuracy of 0.2 ppm for precursors and 0.5 ppm for fragments.

Raw data were processed using MaxQuant/Andromeda software[35, 36] and compared to a custom protein database constituted by a *S. chrysophrii* translation of our draft transcriptome and UniProt databases 9PLAT/37945 (Monogenea class specific proteins) and 9TELE/8174 (*Sparus* genus-specific proteins). Statistical analysis was performed with Perseus software v1.6.14.0[37].

From the resulting statistical analysis, only the proteins with ≥ 2 unique peptides were considered for further analyses. Sequences of the selected proteins were retrieved from *S. chrysophrii* proteome and protein basic alignment search tool (BLASTp) was used against UniProt database with standard settings (BLOSUM62, gap cost: 11 1) to identify the proteins detected in the EV samples. The best BLAST hits for each protein query were selected considering a combination of E-value, bit score, pairwise identity and query coverage values, considering the E-value as the most determinant variable, limited to a value ≤ 1.00e−05. The hypothetical orthologues were further analysed for domain structure with InterPro (https://www.ebi.ac.uk/interpro)[38] and PfamScan (https://www.ebi.ac.uk/jdispatcher/pfa/pfamscan)[39], and for secondary structure with PSIPRED 4.0 (http://bioinf.cs.ucl.ac.uk/psipred)[30]. Furthermore, the identified proteins were used to perform BLASTp against the NCBI database (https://www.ncbi.nlm.nih.gov) with the aim to identify high-identity orthologue sequences from other haematophagous parasites, mainly in the Platyhelminthes, Nematoda and Arthropoda phyla.

Gene Ontology (GO) terms were obtained for each identified protein with Blast2GO v6.0.3[40], and biological processes, molecular functions and cellular components were plotted using ReviGO v1.8.1 (http://revigo.irb.hr)[41], a web tool to visualise GO terms using semantic similarity-based scatterplots.

Finally, the proteins present in the EV samples were classified into non-enzymatic and enzymatic proteins and their corresponding subclasses with ECPred v1.1[42]. Subsequently, those protein sequences classified within the peptide hydrolases/peptidases subclass underwent a BLASTp analysis with standard settings against the MEROPS database[43] to determine their peptidase nature.

Results

In silico scanning of proteins involved in extracellular vesicle biogenesis

Of the 82 selected and analysed known proteins involved in EV biogenesis pathways, a total of 59 proteins were identified in *S. chrysphrii* genome datasets. These proteins are represented in **Table 1**. Of the 31 known proteins that comprise the four ESCRT complexes (ESCRT-0, I, II and III) and ESCRT-accessory proteins of the ESCRTdependent pathway, only one protein (VPS37) remained unidentified. Among the ESCRT-accessory proteins, although the PDCD6IP/ALIX protein appears to be present and its functional interaction domains were present, its homology with the protein orthologues of *Homo sapiens* and *Echinococcus granulosus* (Batsch, 1786) (Cestoda: Taeniidae) was low (E-value: 1.20E−01 and 1.41E−03, respectively; **Supplementary material: Dataset S1**). Within the ESCRT-dependent pathway, proteins involved in the non-canonical ESCRT-associated pathway were well conserved. In contrast, proteins involved in the ESCRTindependent pathway did not appear to be conserved in *S. chrysophrii*, as eight out of 14 proteins remained unidentified, among which S1PR1/3, SMPD1/3, SMPDL3a/b and PLA2 were identified.

According to the assessed proteins, the ectosome biogenesis pathway appeared to be preserved, with solely a single protein (ARRDC1) missing in *S. chrysophrii*. Soluble N-ethylmaleimide-sensitive factor-activating protein receptor (SNARE) proteins were well conserved in *S. chrysophrii*, VAMP7 being the only unidentified protein in the parasite. From all proteins analysed involved in cargo loading, such as those implicated in RNA sorting, i.e. hnRNPA2B1, NSEP1, hnRNPQ, Ago2, MVP and other vault-complex proteins (PARP4 and TEP1), the only unidentified protein in *S. chrysophrii* was TEP1.

Light and transmission electron microscopy (TEM)

EVs with a diameter of approximately 200 nm consisting of a bilayer with coarse, moderately electrodense inner material are observed by TEM in the luminal space of clamps, either free or detaching from the tegumental syncytial layer lining the clamp surface (**Figure 2**). The clamp ultrastructure consists of radially oriented bundles of myofilaments and mitochondria, extended among clamp sclerites. The syncytium, the outer layer of the tegument (neodermis), which covers the whole clamp sclerites and myofilaments, forms a thin layer (300 nm–2.5 µm) on the luminal clamp side. Abundant vesicles of different sizes and densities, granules, large vacuoles, mitochondria and multivesicular structures are observed in the cytoplasm of the EV-producing syncytium. The syncytium is also noticeable by light microscopy, especially at the clamp openings, in close contact with the gill lamellar tissues.

Table 1. List of proteins involved in EV biogenesis present in *Sparicotyle chrysophrii*

Machinery	Gene name	Species	E-Value Genome	E-Value Transcriptome[1]
ESCRT-0	**HGS** [a]	*Schistosoma mansoni*	6.38E-33	-
	STAM [a]	*Schistosoma japonicum*	3.56E-19	-
	STAMBP [a]	*Clonorchis sinensis*	2.92E-63	2.47E-57
ESCRT-I	**TSG101** [a]	*Schistosoma japonicum*	2.70E-18	8.25E-22
	VPS28 [a]	*Schistosoma japonicum*	5.35E-35	1.09E-13
	MVB12 [a]	*Fasciola gigantica*	1.66E-40	-
ESCRT-II	**VPS SNF8** [a]	*Paragonimus westermani*	2.22E-40	2.34E-66
	VPS25 [a]	*Schistosoma haematobium*	2.07E-74	-
	VPS36 [a]	*Homo sapiens*	7.08E-44	9.67E-48
ESCRT-III	**CHMP1a** [a]	*Homo sapiens*	4.53E-41	2.05E-58
	CHMP1b [a]	*Fasciolopsis buski*	2.40E-47	-
	CHMP2a [a]	*Homo sapiens*	1.62E-24	-
	CHMP2b [a]	*Homo sapiens*	1.10E-35	3.84E-41
	CHMP3 [a]	*Clonorchis sinensis*	2.04E-20	-
	CHMP4 [a]	*Homo sapiens*	3.17E-21	1.10E-32
	CHMP5 [a]	*Homo sapiens*	3.64E-46	-
	CHMP6 [a]	*Homo sapiens*	4.69E-10	1.48E-17
	IST1 [a]	*Homo sapiens*	2.97E-45	1.81E-57
ESCRT-associated proteins	**VPS4** [a]	*Homo sapiens*	1.25E-45	0
	VTA1 [a]	*Paragonimus heterotremus*	8.08E-25	-
	ALIX [a, b]	*Echinococcus granulosus*	1.41E-03	-
	LITAF [a]	*Paragonimus heterotremus*	3.37E-11	-
Non-canonical ESCRT-associated	SDC1 [b]	*Schistosoma mansoni*	1.70E-11	-
	SDCBP [b]	*Homo sapiens*	1.80E-08	-
	Ral-A [b]	*Homo sapiens*	6.66E-46	-
	ARF6 [b, d]	*Schistosoma japonicum*	8.52E-71	-
	PLD2 [b, d]	*Echinococcus granulosus*	8.28E-16	-
Lipid-modifying	**SMPD2** [c, d]	*Homo sapiens*	1.28E-04	8.86E-25
	SMS2 [c]	*Fasciola hepatica*	2.81E-105	-
	SPHK2 [c]	*Schistosoma haematobium*	1.57E-11	-
	LTA4H [c]	*Homo sapiens*	5.61E-140	1.74E-140
	DGK [c]	*Homo sapiens*	3.63E-18	3.50E-58
Lipid transport	**ABCA** [c, d]	*Homo sapiens*	8.22E-117	3.30E-152
	PLSCR [d]	*Schistosoma japonicum*	5.56E-12	-
	OSBP [c]	*Schistosoma bovis*	2.81E-49	-
	NPC1 [c]	*Homo sapiens*	1.90E-15	2.07E-66
	NPC2 [c]	*Clonorchis sinensis*	4.55E-10	3.3E-28
Signalling	**ARF1** [d]	*Homo sapiens*	1.13E-83	-
	ROCK1 [d]	*Fasciolopsis buski*	6.42E-65	-
	ROCK2 [d]	*Schistosoma japonicum*	1.24E-50	-
	DIAPH3 [d]	*Homo sapiens*	2.87E-62	1.87E-65
	MYLK3 [d]	*Paragonimus heterotremus*	0	2.99E-35
	MAPK3 [d]	*Fasciola hepatica*	2.06E-35	
Cytoskeleton remodelling	**CAPN**1 [d]	*Homo sapiens*	1.22E-38	2.62E-70
	GELS [d]	*Echinococcus multilocularis*	1.50E-10	3.74E-36
Membrane organisers	**CD63**	*Clonorchis sinensis*	2.09E-21	-
	FLOT1	*Homo sapiens*	2.13E-35	1.75E-115
	FLOT2	*Homo sapiens*	2.19E-28	1.54E-142
SNAREs	**STX1A**	*Echinococcus granulosus*	1.40E-42	-
	STX5	*Fasciola gigantica*	1.49E-17	-
	YKT6	*Paragonimus westermani*	9.34E-10	-
	SYT1	*Schistosoma japonicum*	3.20E-28	-
	VAMP3	*Homo sapiens*	4.34E-14	-
RNA sorting and transport	**hnRNPA2B1**	*Homo sapiens*	1.69E-52	6.73E-59
	NSEP1	*Homo sapiens*	1.83E-30	3.36E-38
	hnRNPQ	*Opisthorchis viverrini*	7.42E-90	-
	Ago2	*Homo sapiens*	1.48E-53	0
	MVP	*Schistosoma bovis*	1.06E-60	1.81E-116
Other vault complex proteins	PARP4	*Schistosoma mansoni*	4.92E-28	-

Lowercase superscript letters indicate the different EV biogenesis pathways. [a]ESCRT-dependent pathway; [b]non-canonical ESCRT-associated pathway; [c]ESCRTindependent pathway; [d]Ectosome formation pathways. **1:** E-values from the transcriptome were solely obtained using *Homo sapiens* protein sequences. Bold lettering corresponds to protein sequences with ≥ 20% query coverage.

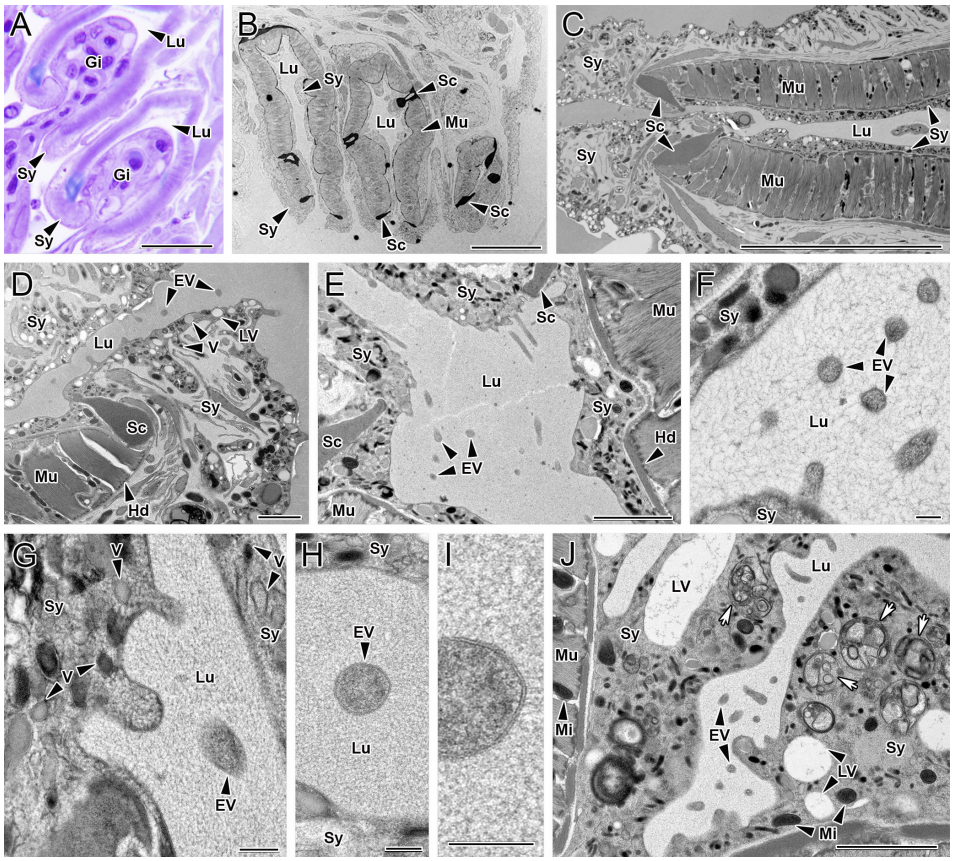

Figure 2. Microscopic images of the tegumental syncytial layer covering *Sparicotyle chrysophrii* clamps. **A:** Light microscopy. **B–J:** transmission electron microscopy. **A:** Toluidine blue-stained section of gilthead sea bream (*Sparus aurata*) gill lamellae pinched by the parasite's clamps. Note the syncytial layer covering the parasite's clamps in close contact with the host lamellar tissue. **B:** The three most distal clamps in the parasite's opisthaptor. Note the syncytium covering the luminal and outer surface of the clamps. **C:** Distal end of the clamp sclerites and associated myofilament bundles. Note the heterogeneity of the covering syncytium, which is a thin layer with flat surface at the clamp luminal side and thicker at the outer side and distal end, with an undulating surface. Higher magnification of the tegumental syncytium covering the clamp distal end at the tip (**D**) and luminal side (**E**). Note the presence of extracellular vesicles apparently emerging from the syncytial surface in the luminal part of the clamp and the abundance and diversity of vesicle types in the syncytium. **F:** Detail of free extracellular vesicles in the clamp lumen, close to the clamp syncytial surface. **G:** Detail of the undulating syncytial surface in the apparent process of secreting extracellular vesicles to the clamp lumen. **H**, **I:** Two magnifications of a free extracellular vesicle in the clamp lumen, close to its syncytial surface. Note the bilayer enclosing coarse, moderately electrodense material. **J:** Free extracellular vesicle in the clamp lumen in an area where the syncytium covering the clamp surface contains different vesicle types and multivesicular structures (arrows). **Gi**, gill filament; **Hd**, hemidesmosomes; **Lu**, clamp lumen; **LV**, large vacuoles; **Mi**, mitochondria; **Mu**, clamp myofilament bundles; **EV**, extracellular vesicles; **Sc**, sclerite; **Sy**, syncytial layer; **V**, syncytial vesicles. Scale bars: (**A–C**) = 20 µm, (**D–E** and **J**) = 2 µm, (**F–I**) = 200 nm.

Isolation and purification of extracellular vesicles

Sparicotyle chrysophrii specimens were kept for 3 days under *in vitro* conditions since parasites presented a mortality rate of 100% after the 3rd day without media supplementation. The NTA analyses indicated that the 2nd day of maintenance of *S. chrysophrii* was the most appropriate for EV collection, with the highest concentration and purity (**Figure 3**; **Table 2**). The nanoparticle size ranged between 53.5 and 918.5 nm with a mean size of 251.8 ± 2.2 nm (± SD) and concentration peak at 215 nm (**Figure 3**), yielding 1.71 × 10^8 ± 4.55 × 10^7 particles·mL^{-1} (mean ± SD; **Supplementary material: Dataset S2**). On the other hand, the concentration of particles·mL^{-1} in the maintenance medium without parasites was similar to filtered PBS, 1.53 × 10^7 ± 5.23 × 10^6 and 1.95 × 10^7 ± 1.86 × 10^6 particles·mL^{-1} (mean ± SD), respectively (**Supplementary material: Figure S1**).

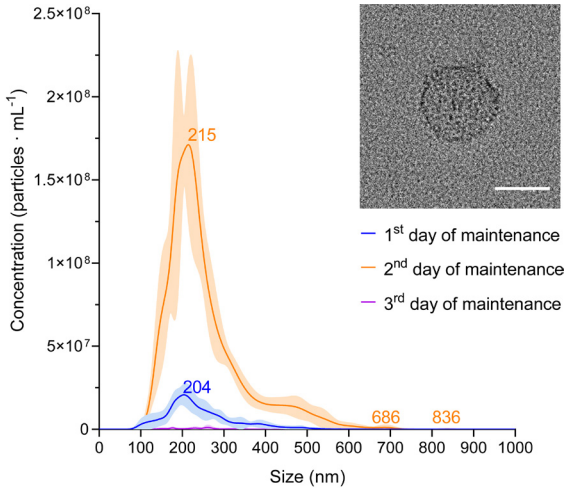

Figure 3. Nanoparticle concentration according to size of purified EVs from adult *Sparicotyle chrysophrii* collected after the 1st, 2nd and 3rd day of *in vitro* maintenance ± standard deviation. Insert shows an extracellular vesicle under transmission electron microscopy of the extracellular vesicle isolated samples. Scale bar = 200 nm.

Table 2. Nanoparticle concentration, protein concentration and nanoparticle purity of purified EV samples collected at three sampling points during *in vitro* maintenance.

***In vitro* maintenance** (days)	**Nanoparticle concentration** (mean particles · mL^{-1} ± SD)	**Protein concentration** (µg · mL^{-1})	**Purity** (particles · µg $protein^{-1}$)
1	2.81 × 10^9 ± 2.13 × 10^8	8.602	3.27 × 10^8
2	2.33 × 10^{10} ± 1.12 × 10^9	33.840	6.89 × 10^8
3	1.07 × 10^8 ± 1.21× 10^7	1.343	7.97 × 10^7

Extracellular vesicle proteome analysis

A total of 124 proteins were successfully identified in EVs released by *S. chrysophrii*. From these, 18 proteins could putatively be involved in the different exosome and ectosome biogenesis pathways (including 8 small GTPases). Ten proteins were chaperone-related proteins; 11 were involved in energy metabolism processes; two were related to detoxification processes, 17 to hydrolases and one to iron transport (**Supplementary material: Dataset S3**).

After performing GO analysis, various metabolic processes were enriched, including the ones related to energy metabolism (glycolytic process, gluconeogenesis, pentose-phosphate pathway), proteolysis, protein ubiquitination, phosphorylation and folding processes. Additionally, cytoskeleton organisation and exocytosis processes, vesicle-mediated and iron transport, and negative regulation of coagulation were identified (**Figure 4A**).

Regarding molecular functions, the analysis revealed glutathione transferase activity and catalytic activities such as oxidoreductase, transferase, hydrolase, lyase, isomerase and ligase activities, consistent with the results from the enzymatic classification analysis (**Figure 5**). In addition, peptidase activity, metal ion and ferric iron binding, ferroxidase activity and protein and nucleotide binding, along with GTP and GTPase-related activities, were identified (**Figure 4B**).

Moreover, the analysis indicated that cellular components related to the proteasome complex, the protein containing complex and extracellular exosome proteins were represented (**Supplementary material: Dataset S4**).

Further in-depth analysis of the enzymatic nature of the proteins resulting from the proteome analysis identified 17 hydrolase sequences, attaining 37.78% of the total identified enzymes (**Figure 5**), from which nine corresponded to peptidases: five proteasome subunits (threonine peptidases), three metallopeptidases and one cysteine peptidase were identified (**Table 3**).

Discussion

Extracellular vesicle biogenesis

Most studies regarding EV biogenesis in neodermatans have focused on the identification of the different proteins involved disregarding their biological functionality. Thus, neodermatan EV biogenesis in general remains poorly understood and has not been addressed in Polyopisthocotyla (*sensu* Monogenea) fish parasites before.

Recently, the proteins required for EV biogenesis in helminths have been considered well conserved throughout different phyla. However, the degree of conservation of these proteins in Polyopisthocotyla, with *Protopolystoma xenopodis* (Price, 1943) (Polyopisthocotyla: Polystomatidae) as the only representative of such class, raised questions due to

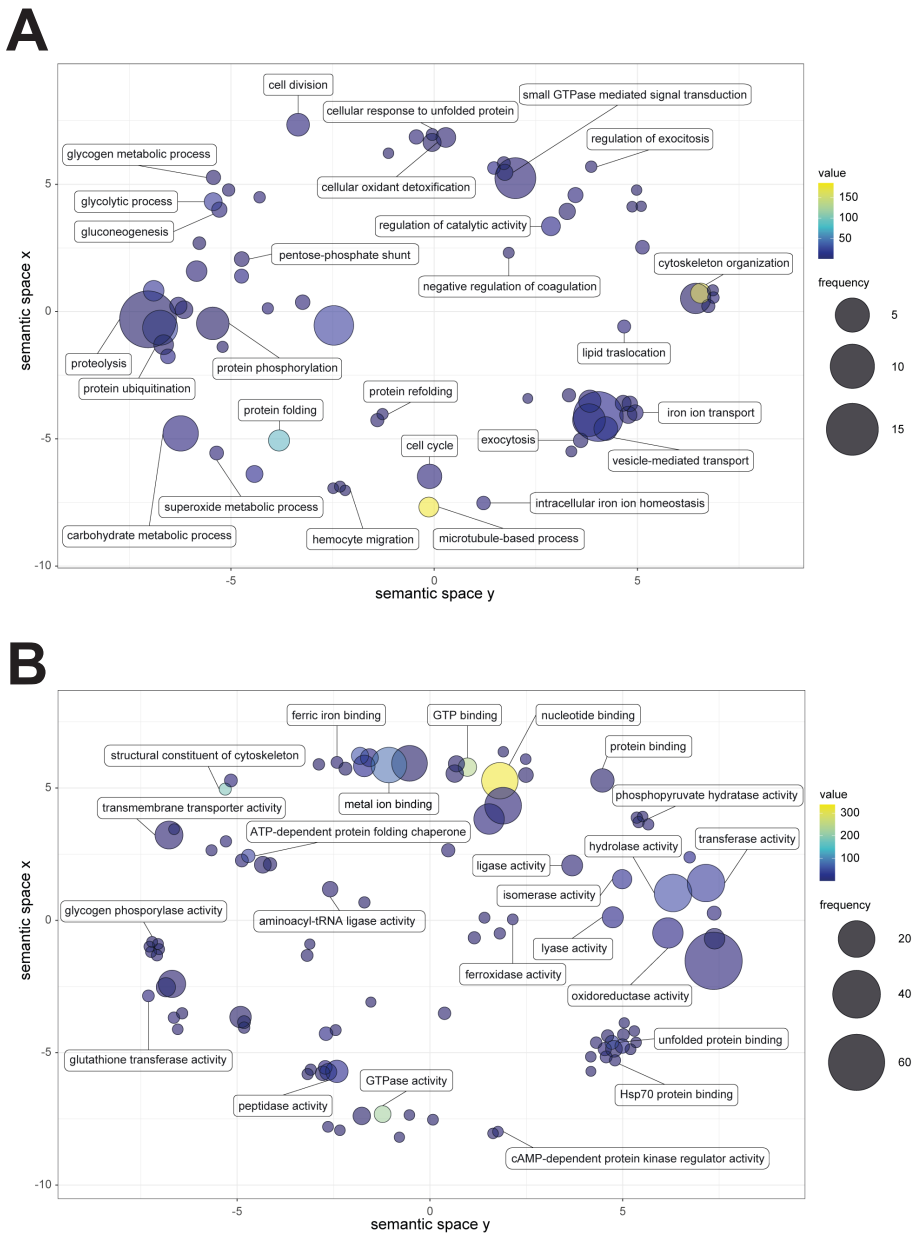

Figure 4. Gene ontology analysis of purified EV proteins from adult Sparicotyle chrysophrii. Semantically similar GO term scatterplots show the biological processes (**A**) and molecular function (**B**). The scatterplots show cluster representatives in a two-dimensional space where *x* and *y* coordinates are assigned to each GO term so that more semantically similar GO terms are set closer in the plot through a multidimensional scaling procedure. Circle size denotes the frequency of the GO term from the underlying database, and increasing heatmap score represents increasing node score from Blast2GO.

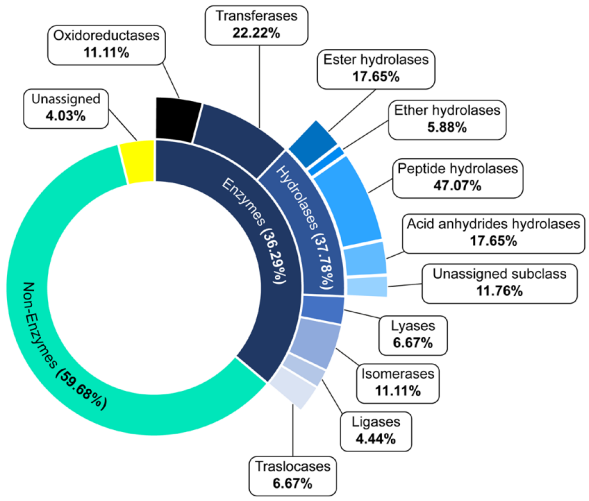

Figure 5. Enzymatic classification of the identified proteins in adult *Sparicotyle chrysophrii* EV samples. Represented percentages are calculated regarding each enzyme subclass.

the lack of orthologues and the low conservation of their interacting regions[26].

Regarding EV biogenesis by the ESCRT-dependent pathway, ESCRT-0, ESCRT-II and ESCRT auxiliary proteins are almost fully conserved in Neodermata, whereas some proteins involved in ESCRT-I and ESCRT-III appear to be lacking in Trematoda (ESCRT-I: VPS28, VPS37 and MVB12; ESCRT-III: CHMP6 and IST1) and Polyopisthocotyla (ESCRT-I: TSG101, VPS37 and MVB12; ESCRT-III: CHMP2, CHMP3, CHMP5 and IST1)[26]. In the *in silico* analysis of *S. chrysophrii*, the only missing protein required for EV biogenesis related to the ESCRT-dependent pathway seems to be VPS37 (ESCRT-I), as no orthologue of any *H. sapiens* isoform (UniProt: VPS37a: Q8NEZ2; VPAS37b: Q9H9H4; VPS37c: A5D8V6; VPS37d: Q86XT2) nor the VPS37 protein (GenBank: RTG90235.1) of *Schistosoma bovis* (Sonsino, 1876) (Trematoda: Schistosomatidae) could be confidently identified. Notably, FYVE and VHS domains for HGS (ESCRT-0) were found and a single isoform orthologue was found for STAM (ESCRT-0), MVB12 (ESCRT-I), CHMP4 (ESCRT-III) and VPS4 (ESCRT-related component) in *S. chrysophrii*, apparently as opposed to the several isoforms of these proteins present in *H. sapiens* (STAM1/2, MVB12a/b, CHMP4a/b/c and VPS4a/b). From the analysed SNAREs, YKT6 was identified unlike in *P. xenopodis*, and VAMP7 remained the only unidentified protein in *S. chrysophrii*, in agreement with most Nematoda and Neodermata[26]. In view of these findings, we hypothesise that exosome production in *S. chrysophrii* may be driven primarily by the ESCRT-dependent pathway as described for adult *Fasciola hepatica* (Linnaeus, 1758) (Trematoda: Fasciolidae)[44]. However, VPS37 is key for the modulation of the ternary complex formation of ESCRT-I and PDCD6IP/ALIX[45] and yet it is missing in *S. chrysophrii* and in trematodes, or at least highly divergent from

its *H. sapiens* homologues. Species-specific adaptations cannot be ruled out, and specific EV biogenesis pathways may acquire relevant roles depending on the parasite's life stage as observed in *Schistosoma japonicum* (Katsurada, 1904) (Trematoda: Schistosomatidae) [46]. In the context of the ESCRT-dependent pathway in mammals, a non-canonical ESCRT-associated route revolving around the programmed cell death 6-interacting protein (PDCD6IP/ALIX) has been identified in EV biogenesis. PDCD6IP/ALIX recruits ESCRT-III and facilitates the sorting and delivery of tetraspanins to exosomes. Additionally, PDCD6IP/ALIX can associate with transmembrane syndecan proteins via syntenin, promoting membrane budding steps of ILVs biogenesis[47–49]. In the current study, protein representatives of the non-canonical ESCRT-associated signalling pathway were identified, including syndecan, syntenin and a Bro1- domain containing protein, herein classified as PDCD6IP/ALIX. However, due to low homology (**Table 1**), further studies on *S. chrysophrii* PDCD6IP/ALIX are required. Tetraspanin CD63 and other membrane organiser proteins such as flotillin1/2 (FLOT1/2) appeared to be conserved in *S. chrysophrii*, in agreement with previous *in silico* studies[26].

Lipid-modifying proteins, involved in the ESCRT-independent pathway and ectosome formation (**Table 1**), seem to be the least conserved in Polyopisthocotyla and other helminths, probably because of the inability of helminth species to synthesise fatty acids *de novo*[50]. Thus, SMPD1/3, SMPDL3a/b, S1PR1/3 and PLA2 remained unidentified in our analysis and were consistent with the finding in *P. xenopodis*. However, three further aspects were noticed. Unlike in *P. xenopodis*, SMS2 and sphingosine kinase (SPHK) were identified. Interestingly, PLB-like 2 protein, apparently conserved Nematoda and Neodermata, including *P. xenopodis*[26], remained unidentified in *S. chrysophrii*. In addition, a single orthologue of the DGK isoform was identified in *S. chrysophrii* as opposed to the two isoforms present in *H. sapiens*.

The release of ectosomes is regulated by small Rab GTPases, including Rho-associated coiled coil-containing protein kinase and the GTP-binding protein ADPribosylation factor 6 (ARF6), which have been identified as positive regulators of vesicle budding in cancer cells[25,51]. In the current study, Rho-associated protein kinase 1 and 2 (ROCK1/2) were identified together with ARF6 and ARF1 (**Table 1**); interestingly, a third ARF protein besides ARF6/1 was identified in the protein cargo from *S. chrysophrii* EVs (**Supplementary material: Dataset S3**), raising questions about the possible presence of other ARF isoforms and their role in polyopisthocotylan EVs. Additionally, DIAPH3, previously reported in the neodermatans *Echinococcus multilocularis* (Leuckart, 1863) (Cestoda: Taeniidae) and *Schistosoma* spp.[26], was identified in *S. chrysophrii*, adding Polyopisthocotyla as the third class within Neodermata where DIAPH3 has been identified. Other signalling proteins such as ARRDC1, apparently absent in Neodermata, also remained absent in *S.*

Table 3. List of *Sparicotyle chrysophrii* peptidases present in EV samples, showing the peptidase clan and family according to MEROPS database, including their best hit.

***Sparicotyle chrysophrii* protein sequence**
augustus_masked-contig_1681_pilon_pilon-processed-gene-0.0-mRNA-1
maker-contig_20098_pilon_pilon-augustus-gene-0.16-mRNA-1
maker-contig_22363_pilon_pilon-exonerate_est2genome-gene-0.0-mRNA-1
maker-contig_24278_pilon_pilon-snap-gene-0.33-mRNA-1
maker-contig_28754_pilon_pilon-snap-gene-0.18-mRNA-1
maker-contig_46585_pilon_pilon-augustus-gene-0.2-mRNA-1
maker-contig_4765_pilon_pilon-exonerate_est2genome-gene-0.1-mRNA-1
maker-contig_6883_pilon_pilon-snap-gene-0.23-mRNA-1
maker-contig_7443_pilon_pilon-snap-gene-0.43-mRNA-1

***** Indicates ether hydrolases with peptidase activity included in MEROPS database. **Peptidase clan**. **MA:** includes different families with aminopeptidase (**M1**, **M16**), carboxypeptidase (**M2**, **M32**), peptidyl-dipeptidase (**M2**), oligopeptidase (**M3**, **M13**) and endopeptidase activity (**M4**, **M10**, **M12**). **MF:** Presents solely proteins belonging to the **M17** family, which have a predominant aminopeptidase activity. **PB:** Autocatalytic activation peptidase activity except for family **T1**. **CA:** Presents proteins with mostly endopeptidase activities; however, proteins belonging to C1 family present a predominant exopeptidase activity. **Peptidase family. M1:** Peptidase family mainly containing metallo-catalytic aminopeptidases dependent on a single zinc ion. **M17:** Peptidase family containing metallo-catalytic aminopeptidases with co-catalytic metal ions. **T1:** Peptidase family containing the peptidases components of proteasomes and related compound peptidases holding a threonine catalytic site. **C2:** Peptidase family containing endopeptidases termed "calpains" which hold a cysteine catalytic site

chrysophrii, once again in agreement with previous findings[26].

Finally, regarding the proteins required for RNA sorting into exosomes, hnRNPQ was previously reported to be exclusive to Nematoda[26]. However, it was also identified in the trematode *Opisthorchis viverrini* (Poirier, 1886) (Trematoda: Opisthorchiidae; GenBank: OON14851.1), of which a single orthologue was found in *S. chrysophrii*.

Extracellular vesicle isolation and transmission electron microscopy (TEM)

The present study showed that the 2nd day of *in vitro* maintenance of *S. chrysophrii* was the best time frame for EV collection with a nanoparticle concentration of $2.33 \times 10^{10} \pm 1.12 \times 10^{9}$particles·mL^{-1} (mean ± SD) and a sample purity of 6.89 × 108 particles µg·protein$^{-1.}$ Previous studies proposed that a purity of 1×10^{8} particles µg·protein^{-1} represent

Protein type	Peptidase		Species	E-value
	clan	family		
Leukotriene A-4 hydrolase*	MA	M1	*Schistosoma curassoni*	1.90E-175
Leucyl aminopeptidase	MF	M17	*Fasciola* spp.	5.20E-157
Proteasome subunit beta5i	PB	T1	*Schistosoma japonicum*	1.40E-120
Calpain	CA	C2	*Schistosoma margrebowiei*	1.80E-154
Proteasome alpha subunit G1	PB	T1	*Schistosoma mansoni*	3.40E-110
Proteasome subunit alpha 1	PB	T1	*Clonorchis sinensis*	1.70E-130
Proteasome alpha subunit G1	PB	T1	*Schistosoma mansoni*	2.90E-105
Cytosol alanyl aminopeptidase	MA	M1	*Echinococcus granulosus*	1.30E-138
Proteasome subunit alpha 6	PB	T1	*Schistosoma japonicum*	2.70E-62

high-quality vesicular preparations from *Schistosoma* spp. and other helminth parasites[52]. Since the purity of the analysed samples is in the same order of magnitude, given the target organism, we consider the EV samples to have a high purity.

So far, the presence of two different EV subpopulations according to their biogenesis pathways (exosomes and ectosomes) have been described in adult trematode *Fasciola* spp., *Schistosoma mansoni* (Sambon, 1907) (Trematoda: Schistosomatidae) and *O. viverrini*[44, 53–55].

In the current study, nanoparticles between 53.50 and 918.50 nm were isolated (**Supplementary material: Dataset S2**), and the EV protein composition of *S. chrysophrii* indicated the presence of proteins potentially involved in exosome and ectosome biogenesis pathways[20]. Moreover, TEM revealed EVs of ≈ 200 nm in diameter apparently budding off the syncytial lining covering *S. chrysophrii* clamps at the opisthaptor region, suggesting a possible ectosome biogenesis. However, the limited evidence precludes a conclusive determination of their exact biogenesis pathway.

The clamp covering syncytial cytoplasm containing different vesicle types, multivesicular structures and large vacuoles has been described in several polyopisthocotylans, and vesicles in the process of exocytosis from the syncytium surface were observed in *Gotocotyla bivaginalis* (Ramalingam, 1961) (Polyopisthocotyla: Gotocotylidae) and *Chi-*

maericola leptogaster (Leuckart, 1830) (Polyopisthocotyla: Chimaericolidae)[56–58]. For the latter, differences in the syncytial surface and composition were also described depending on its luminal or external orientation in the clamp, where the syncytial thickenings at the clamp distal tips were considered clamp lips. However, the excretory/secretory importance of the secreted vesicles was not further discussed. Yet, exocytosis of syncytial material, such as secretory granules, vesicles and vacuoles, was also suggested as a mechanism of polyopisthocotylan protection against immunological, ionic and osmotic damage caused by gill mucus secretion or water forces[58]. In *S. chrysophrii*, the occurrence of EVs in the tegument syncytium-lamellar membrane interphase could suggest a protective mechanism, but considering the tight host-parasite-microbiota contact, a mechanism of modulation on the fish host or host-associated microbiota via parasite's ESPs should not be ruled out.

Konstanzová et al.[57] found glandular cells with vesicles at the sclerite base, apparently responsible for the secreted vesicles in the syncytium cytoplasm, in *Paradiplozoon homoion* (Bychowsky and Nagibina, 1959) (Polyopisthocotyla: Diplozoidae). These authors described three clearly differentiated vesicle types by their electron density and diameter and suggested that vesicles may have a storage function. In our case, a more heterogenous vesicle population from 50 to 400 nm in diameter was found in the cytoplasm of the tegument syncytium, but the question of whether these have a storage or secretory fate remains unsolved. Regarding ultrastructure, Konstanzová et al.[57] and Mergo[59] also described that clamps were covered by a very thin syncytial layer compared to the overall body surface in *P. homoion* and *Diplostamenides spinicirrus* (MacCallum, 1918) (formerly *Microcotyle spinicirrus*; Polyopisthocotyla: Microcotylidae), respectively. The reduction of the syncytial thickness in clamps is a trait shared among other polyopisthocotylans and was attributed to an adaptation to increase the grasping ability to the host tissue in the limited space between gill lamellae[56–59]. In *S. chrysophrii*, no tegumental MVB containing ILVs nor exosomes on the outer body surface were identified, perhaps due to the way these parasites interact with their host, as opposed to endoparasitic helminths. However, the lack of secretion of EVs through tegument in other regions of the parasite's body attributed to the sample preparation should not be ruled out.

In any case, the intimate contact between *S. chrysophrii* clamps and their hosts' secondary lamellae pinpoints the opisthaptor as an optimal area for host recognition and continuous parasite-host-microbiota cross-talk, and haemorrhagic mechanical microlesions inflicted by the haptoral clamps in the gill epithelium[60] might facilitate host exposure to EVs. Future research might focus on the ability of *S. chrysophrii* EVs to internalise into host cells, especially since a cell-polarity regulator protein (LLGL scibble cell polarity complex component 2)[61] has been identified in the current EV proteome analysis.

Extracellular vesicle proteome analysis

In haematophagous parasites haemoglobin serves as a nutrient-rich source for obtaining iron and amino acids through the digestion of globins. For this purpose, haematophagous parasites employ a diverse set of peptidases. This process involves a multienzymatic network cascade, featuring clan CA (cathepsins B, C and L) and AA (cathepsin D) cysteine peptidases, alongside aminopeptidases[62,63]. So far, they have been identified in Nematoda, Trematoda, Cestoda[64–66], Monopisthocotyla and Polyopisthocotyla[9,11,15,16].

The liver fluke, *F. hepatica*, exhibits an extracellular digestion phase in its gut lumen[67], and a similar process is presumed in *Eudiplozoon nipponicum* (Goto, 1891) (Polyopisthocotyla: Diplozoidae)[10]. However, Riera-Ferrer et al.[68] suggested that *S. chrysophrii* induces an intravascular haemolysis in its host, prior to ingesting the resulting blood meal. Thus, ESPs and EV-originating peptidases and peptidase inhibitors might have a crucial role in this parasite's feeding strategies.

Gene Ontology analyses from the purified EVs indicated biological processes related to blood (negative regulation of coagulation, iron ion transport, haemocyte migration and intracellular iron ion homeostasis; **Figure 4A**), consistent with the negative haemostatic impact[68, 69] and catalytic process (regulation of catalytic activity and proteolysis) observed in infected *S. aurata*. Molecular functions revealed ferric and metal ion binding, ferroxidase activity, glutathione transferase and enzymatic activities related to oxidoreductase, transferase, hydrolase-peptidase, lyase, isomerase, ligase and translocase enzymes (**Figure 4B**). Eight peptidases, including calpain, involved in signal transduction, cellular differentiation, cytoskeletal remodelling, vesicular trafficking and ectosome biogenesis[70,71], two metallo- catalytic-type aminopeptidases, namely leucyl aminopeptidase and alanyl aminopeptidase, thought to be involved in the final steps of haemoglobin catabolism in *Plasmodium falciparum* (Welch, 1897) (Aconoidasida: Plasmodiidae)[72,73], and the aminopeptidase leukotriene A4 hydrolase, related to the ESCRT-independent EV biogenesis pathway and suggested to have an extracellular peptidase role[74,75], were identified in *S. chrysophrii* EVs (**Table 3**). Despite it is tempting to suggest an intravascular haemolytic event taking place, given the current findings and previous studies, further mechanistic, functionality, protein characterisation and EV internalisation studies are required. Notably, threonine proteasome-related peptidases (clan PB, family T1; **Table 3**) are the most represented among the identified peptidases, aligning with the observations in *E. nipponicum* secretome[16] and *F. hepatica*[44], implying that isolated EVs present a substantial role in protein turnover.

Free haem groups resulting from haemoglobin digestion elicit high toxicity and oxidative stress. To ensure their viability, hematophagous parasites require a haem detoxification route[76]. Glutathione *S*-transferase, identified in *S. chrysophrii* EVs (**Supplementary**

material: Dataset S3; **Figure 4B**), is known for engaging in haem catabolic processing[77,78]. Such results are consistent with observations in Trematoda[44,52,79–81] and in *E. nipponicum*[16], suggesting a significance in the haem detoxification pathway within Polyopisthocotyla.

Along the same line, haemoglobin remains the primary source of iron acquisition for parasitic blood-feeders, critical for multiple biological processes[82]. However, precise iron homeostasis is crucial, as both deficiency and excess pose survival challenges[83,84]. Ferritins, iron storage proteins, counteract the toxic free iron ions by binding to them[85]. In isolated *S. chrysophrii* EV samples, a single ferritin (EC 1.16.3.1) was identified (**Supplementary material: Dataset S3**). GO analyses inferred iron ion transport, intracellular iron ion homeostasis (**Figure 4A**) and ferric ion binding, metal ion binding and ferroxidase activities related to molecular function (**Figure 4B**). The origin of free iron is unknown; although it might result from haem catabolic detoxification by glutathione *S*-transferase, solid evidence is lacking. Interestingly, ferritins are among the most transcribed genes in *E. nipponicum*[16], and given their presence in EVs of several trematode species[52,80,86], it is suggested that these play a significant role in Trematoda.

Platelet-activating factor (PAF; 1-*O*-alkyl-2-acetyl-*sn*-glycero-3-phosphocholine) is a key inflammatory mediator in the mammalian immune system, promoting platelet aggregation and triggering various immune responses and cytokine synthesis[87,88]. In this study, we identified platelet-activating factor acetyl hydrolase (PAF-AH; EC 3.1.1.47), which by removing the *sn*-2 acetyl group from PAF silences its biological activity[89]. Thus, PAF-AH might ultimately inhibit the host's coagulation cascade and extravasation of granulocytes. GO analysis inferred a negative regulation of the coagulation (**Figure 4A**), overall aligning with the impaired haemostasis and immune system in *S. chrysophrii*-infected *S. aurata*[68]. Nevertheless, a significant increase in eosinophilic granular cells, the functional equivalent of mammalian neutrophils in *S. aurata*[90], was determined from 28 to 50 days post-parasite exposure[31]. In this context, the previously mentioned identification of a leukotriene A4 hydrolase suggests that *S. chrysophrii* might also secrete eicosanoids as proinflammatory mediators, as described for *S. japonicum*[91,92]. Furthermore, human PAF-AH has been described to bind to very low-density lipoproteins (VLDL), intermediate-density lipoproteins (IDL), low-density lipoproteins (LDL) and high-density lipoproteins (HDL)[93]. This is in line with the impact on the lipid transport and metabolism described in *S. chrysophrii*-infected *S. aurata*, which presented plasma apolipoprotein impairment and hypocholesterolaemia[68]. The role of PAF-AH in *Nippostrongylus brasilensis* (Yokogawa, 1920) (Nematoda: Heligmonellidae) was inconclusive[94], contrasting with *Leishmania major* (Yakimoff and Schokhor, 1914) (Kinetoplastea: Trypanosomatidae) where it acts as a virulence factor[95]. Altogether, these findings prompt further studies to explore the

potential pathogenic roles of PAF-AH in *S. chrysophrii*.

The understanding of the energy metabolism in Polyopisthocotyla remains elusive. Previous studies on *S. chrysophrii*, *E. nipponicum* and *Diclidophora merlangi* (Kuhn, 1829) (Polyopisthocotyla: Diclidophoridae) suggested an oxygen requirement and hypothesised an aerobic metabolism[16,31,96]. In this study, we identified oxidoreductases, transferases and lyases (**Supplementary material: Dataset S3**) related to energy metabolism, gathering more evidence on *S. chrysophrii* metabolism. GO analyses revealed biological processes related to glycolysis, gluconeogenesis and the pentose-phosphate pathways (**Figure 4A**), all indicative of an aerobic metabolism. Similar results were observed in other neodermatans, including other Polyopistocotyla at a transcriptomic level[16], ESPs of Trematoda[79] and EVs from Trematoda and Cestoda[44,97].

In addition to the previously discussed proteins, proposed EV-marker proteins such as 14–3-3 and heat shock protein 70 (HSP70), commonly found in eukaryotic EVs, were identified in *S. chrysophrii* vesicles (**Supplementary material: Dataset S3**), in agreement with other helminth species[54,81,86,98]. Heat shock protein 90 (HSP90), previously detected in *S. japonicum* EVs[99], and four out of eight subunits of the T-complex protein 1 (TCP1) ring complex, a group II chaperonin related to heat shock protein 60 (HSP60) exhibiting ATP-dependent protein folding (**Supplementary material: Dataset S3**) [100–102], and previously identified in *F. hepatica*[44], were also identified in *S. chrysophrii* EVs. The presence of HSP70/90 and TCP1 is reflected in the biological processes (**Figure 4A**) and molecular functions (**Figure 4B**) inferred from the GO analyses. Other suggested EV-marker proteins include those with an EF-hand domain (PF13499), potentially characteristic of Trematoda and Cestoda EVs protein cargo[98]. In the *S. chrysophrii*-derived EVs in this study, three proteins presenting an EF-hand domain (PF13499.9; sorcin, calmodulin and calcineurin B homologous protein 1; **Supplementary material: Dataset S3**) were identified.

Currently, treatment options for polyopisthocotylan infections in aquaculture, including *S. chrysophrii*, are limited, with hydrogen peroxide and formaldehyde baths in their licensed formulation being the sole available chemotherapeutants. However, formaldehyde baths have already been banned in Italy, among other countries, due to safety concerns, and its use will not be warranted worldwide in the coming years[5,103,104]. Coupled with the ongoing threat of anthelmintic drug resistance, these limitations underscore the need for further therapeutic or prophylactic strategies to address sparicotylosis and proactively combat emerging drug resistance. Most of the identified proteins in *S. chrysophrii* EVs have already been confirmed in other helminths including Neodermata [98]. Several proteins including the aforementioned peptidases, non-enzymatic proteins and energy metabolism-related proteins have been proposed as drug targets or vaccine candidates in

Trematoda, Nematoda and certain Apicomplexa parasitic species. **Table 4** compiles these protein target candidates from *S. chrysophrii* EVs, contributing to a comprehensive understanding of novel strategies against this parasite.

Table 4. List of orthologues described as drug and vaccine target candidates from different hematophagous parasites including Trematoda, Nematoda and Apicomplexa found in the EVs' proteomic study using *Sparicotyle chrysophrii*, *Protopolystoma xenopodis*, *Gyrodactylus salaris* and *Microcotyle sebastis* proteomes as reference.

Protein target candidates	References	Species and sequence hit
		Sparicotyle chrysophrii
Proteases		
Leucine aminopeptidase (M17 family)	[52], [73], [105-108]	maker-contig_20098_pilon_pilon-augustus-gene-0.16-mRNA-1
Alanyl aminopeptidase (M1 family)	[73], [109]	maker-contig_6883_pilon_pilon-snap-gene-0.23-mRNA-1
Calpain	[52]	maker-contig_24278_pilon_pilon-snap-gene-0.33-mRNA-1
Carrier proteins		
Ferritin	[84]	maker-contig_34520_pilon_pilon-augustus-gene-0.7-mRNA-1
Cytoskeleton		
Dynein light chain	[52], [107]	maker-contig_41206_pilon_pilon-augustus-gene-0.3-mRNA-1
14-3-3 protein	[52], [107]	maker-contig_34517_pilon_pilon-snap-gene-0.19-mRNA-1 maker-contig_34517_pilon_pilon-snap-gene-0.19-mRNA-1 maker-contig_30173_pilon_pilon-snap-gene-0.10-mRNA-1
Heat shock protein 70	[52], [107]	augustus_masked-contig_13257_pilon_pilon-processed-gene-0.1-mRNA-1 augustus_masked-contig_5207_pilon_pilon-processed-gene-0.2-mRNA-1
Annexin	[52]	maker-contig_38531_pilon_pilon-exonerate_est2genome-gene-0.0-mRNA-1 maker-contig_29652_pilon_pilon-augustus-gene-0.2-mRNA-1 maker-contig_12610_pilon_pilon-snap-gene-0.5-mRNA-1
Tubulin	[110]	maker-contig_8332_pilon_pilon-augustus-gene-0.19-mRNA-1 snap_masked-contig_2563_pilon_pilon-processed-gene-0.25-mRNA-1
Antioxidant/ Defence/ Detoxification		
Glutathione *S*-transferase	[52], [107]	maker-contig_7282_pilon_pilon-snap-gene-0.22-mRNA-1
Superoxide dismutase	[111]	maker-contig_45344_pilon_pilon-augustus-gene-0.2-mRNA-1
Metabolism		
Enolase	[52], [107]	snap_masked-contig_11270_pilon_pilon-processed-gene-0.1-mRNA-1
Fructose-bisphosphate aldolase	[107], [111]	maker-contig_31661_pilon_pilon-snap-gene-0.18-mRNA-1
		Protopolystoma xenopodis
Cytoskeleton		
Heat shock protein 70	[52], [107]	A0A448WN47
Tubulin	[110]	A0A448X3E2 A0A3S5FFD8 A0A448WX98 A0A448XD95
		Gyrodactylus salaris
Cytoskeleton		
Tubulin	[110]	Q709M4
		Microcotyle sebastis
Cytoskeleton		
Annexin	[52]	B3GQS3

Conclusions

In the current study, EVs have successfully been isolated and observed through TEM in the parasite's clamp syncytial tegument of the haptoral region. Further protein characterisation from isolated *S. chrysophrii* EVs revealed a similar protein profile as in other neodermatans, with several proteins related to EV biogenesis. The present findings allow the deepening of the understanding of aspects related to *S. chrysophrii* aerobic metabolism, iron transport, detoxification and proteolysis, among others, and overall identify therapeutic target candidates previously reported for other parasitic organisms.

Funding

Open Access funding provided thanks to the CRUE-CSIC agreement with Springer Nature. This work was supported by the Spanish Ministry of Science and Innovation (MICIN) through the projectsSpariControl(RTI2018-098664-B-I00), with AEI/FEDER; the ThinkInAzul programme supported by MICIN with funding from NextGenerationEU (PRTR-C17.I1) and by Generalitat Valenciana (THINKINAZUL/2021/022); the Generatitat Valenciana AICO2023 funding (CIAICO/2022/144); the Czech Science Foundation (grant no. 23-07990S); and by MEYSCR through the Czech-BioImaging large RI project (LM2023050 and OP VVV CZ.02.1.01/0.0/0.0/18_046/0016045). ERF was supported by an FPI contract PRE2019-087409 (MCIN/AEI/https://doi.org/10.13039/501100011033), JS was supported by a Ramón y Cajal fellowship (RYC2021-032443-I) and MCP by a Ramón y Cajal fellowship (RYC2021-2018-024049-I), all funded by MICIN. The authors acknowledged support of the publication fee by the CSIC Open Access Publication Support Initiative through its Unit of Information Resources for Research (URICI).

Acknowledgements

The authors thank I. Vicente for the technical assistance with fish husbandry and samplings at IATS and BC CAS core facility LEM for their support obtaining microscopy data.

Supplementary material

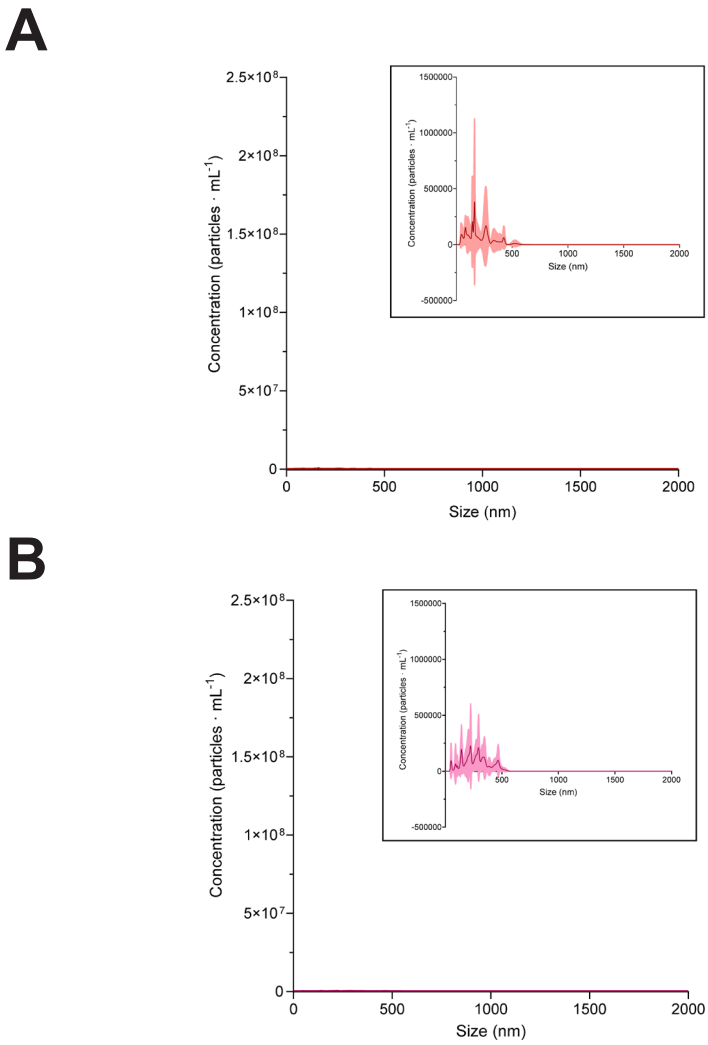

Figure S1. Nanoparticle concentration in the *Sparicotyle chrysophrii in vitro* maintenance media as a negative control (**A**), and 0.2 µm-filtered PBS as internal quality control (**B**). Shadowed areas correspond to the standard deviation.

The following supplementary material is freely available at https://doi.org/10.1186/s13071-024-06257-x:

- **Supplementary material: Dataset S1.** Spreadsheet containing information on the genomic *in silico* identification of proteins involved in multiple extracellular vesicle biogenesis pathways. **Tab A** has information on *Sparicotyle chrysophrii* genome and transcriptome dataset interrogation with *Homo sapiens* query sequences. **Tab B** has information about *Sparicotyle chrysophrii* genome dataset interrogation with query sequences belonging to diverse Neodermata species.

- **Supplementary material: Dataset S2.** Spreadsheet containing information from the nanoparticle tracking analysis about the excretory/secretory products nanoparticle concentration according to size at each sampling point (24 h: **Tab A**, 48 h: **Tab B** and 72 h: **Tab C**).

- **Supplementary material: Dataset S3.** Spreadsheet containing information on the proteome analysis of isolated extracellular vesicles from *Sparicotyle chrysophrii*. The spreadsheet contains sequences classified as non-enzyme proteins (**Tab A**), unassigned Enzyme Commission number (**Tab B**), oxidoreductase (**Tab C**), transferases (**Tab D**), hydrolases (**Tab E**), lyases (**Tab F**), isomerases (**Tab G**), ligases (**Tab H**) and translocases (**Tab I**).

- **Supplementary material: Dataset S4.** Spreadsheet containing information related to the ReviGO output. **Tab A** contains GO terms related to biological processes. **Tab B** contains GO terms related to cellular components. Tab C contains GO terms related to molecular functions.

The proteomic data that support the findings of this study are openly available in Mass Spectrometry Interactive Virtual Environment (MassIVE) repository at http://massive.ucsd.edu/ProteoSAFe/status.jsp?task=35be3c4268c243ac8b0b2ccc63656244.
Nucleotide and amino acid sequences from hypothetical proteins supporting the findings of this study are available upon request in ZENODO repository at https://doi.org/10.5281/zenodo.8405325.

References

1. Brabec J, Salomaki ED, Kolísko M, Scholz T, Kuchta R. The evolution of endoparasitism and complex life cycles in parasitic platyhelminths. Curr Biol. 2023;33:4269-75.e3.

2. Caña-Bozada V, Robinson MW, Hernández-Mena DI, Morales-Serna FN. Exploring evolutionary relationships within Neodermata using putative orthologous groups of proteins, with emphasis on peptidases. Trop Med Infect Dis. 2023;8:59.

3. Ogawa K. Diseases of cultured marine fishes caused by Platyhelminthes (Monogenea, Digenea, Cestoda). Parasitology. 2015;142:178–95.

4. Muniesa A, Basurco B, Aguilera C, Furones D, Reverté C, Sanjuan-Vilaplana A, et al. Mapping the knowledge of the main diseases affecting sea bass and sea bream in Mediterranean. Transbound Emerg Dis. 2020;67:1089–100.

5. Mladineo I, Volpatti D, Beraldo P, Rigos G, Katharios P, Padrós F. Monogenean *Sparicotyle chrysophrii*: the major pathogen of the Mediterranean gilthead seabream aquaculture. Rev Aquac. 2024;16:287–308.

6. Stella E, Pastres R, Pasetto D, Kolega M, Mejdandžić D, Čolak S, et al. A stratified compartmental model for the transmission of *Sparicotyle chrysophrii* (Platyhelminthes: Monogenea) in gilthead seabream (*Sparus aurata*) fish farms. R Soc Open Sci. 2023;10:221377.

7. Sitjà-Bobadilla A, de Felipe MC, Álvarez-Pellitero P. *In vivo* and *in vitro* treatments against *Sparicotyle chrysophrii* (Monogenea: Microcotylidae) parasitizing the gills of gilthead sea bream (*Sparus aurata* L.). Aquaculture. 2006;261:856–64.

8. Merella P, Montero FE, Burreddu C, Garippa G. In-feed trials of fenbendazole and other chemical/natural compounds against *Sparicotyle chrysophrii* (Monogenea) infections in *Sparus aurata* (Osteichthyes). Aquac Res. 2021;52:5908–11.

9. Jedličková L, Dvořáková H, Kašný M, Ilgová J, Potěšil D, Zdráhal Z, et al. Major acid endopeptidases of the blood-feeding monogenean *Eudiplozoon nipponicum* (Heteronchoinea: Diplozoidae). Parasitology. 2016;143:494–506.

10. Ilgová J, Jedličková L, Dvořáková H, Benovics M, Mikeš L, Janda L, et al. A novel type I cystatin of parasite origin with atypical legumain-binding domain. Sci Rep. 2017;7:1–12.

11. Jedličková L, Dvořáková H, Dvořák J, Kašný M, Ulrychová L, Vorel J, et al. Cysteine peptidases of *Eudiplozoon nipponicum*: a broad repertoire of structurally assorted cathepsins L in contrast to the scarcity of cathepsins B in an invasive species of haematophagous monogenean of common carp. Parasit Vectors. 2018;11:1–17.

12. Roudnický P, Vorel J, Ilgová J, Benovics M, Norek A, Jedličková L, et al. Identification and partial characterization of a novel serpin from *Eudiplozoon nipponicum* (Monogenea, Polyopisthocotylea). Parasite. 2018;25:61.

13. Jedličková L, Dvořák J, Hrachovinová I, Ulrychová L, Kašný M, Mikeš L. A novel Kunitz protein with proposed dual function from *Eudiplozoon nipponicum* (Monogenea) impairs haemostasis and action of complement *in vitro*. Int J Parasitol. 2019;49:337–46.

14. Ilgová J, Kavanová L, Matiašková K, Salát J, Kašný M. Effect of cysteine peptidase inhibitor of *Eudiplozoon nipponicum* (Monogenea) on cytokine expression of macrophages *in vitro*. Mol Biochem Parasitol. 2020;235:111248.

15. Caña-Bozada V, Chapa-López M, Díaz-Martín RD, García-Gasca A, Huerta-Ocampo JÁ, de Anda-Jáuregui G, et al. *In silico* identification of excretory/secretory proteins and drug targets in monogenean parasites. Infect Genet Evol. 2021;93:104931.

16. Vorel J, Cwiklinski K, Roudnický P, Ilgová J, Jedličková L, Dalton JP, et al. *Eudiplozoon nipponicum* (Monogenea, Diplozoidae) and its adaptation to haematophagy as revealed by transcriptome and secretome profiling. BMC Genomics. 2021;22:1–17.

17. Mirabent-Casals M, Caña-Bozada VH, Morales-Serna FN, García-Gasca A. Predicted secretome of the monogenean parasite *Rhabdosynochus viridisi*: hypothetical molecular mechanisms for host-parasite interactions. Parasitologia. 2023;3:33–45.

18. Drurey C, Coakley G, Maizels RM. Extracellular vesicles: new targets for vaccines against helminth parasites. Int J Parasitol. 2020;50:623–33.

19. Rooney J, Northcote HM, Williams TL, Cortés A, Cantacessi C, Morphew RM. Parasitic helminths and the host microbiome – a missing 'extracellular vesicle-sized' link? Trends Parasitol. 2022;38:737–47.

20. Welsh JA, Goberdhan DCI, O'Driscoll L, Buzas EI, Blenkiron C, Bussolati B, et al. Minimal information for studies of extracellular vesicles (MISEV2023): from basic to advanced approaches. J Extracell Vesicles. 2024;13:e12404.

21. Kalra H, Drummen GPC, Mathivanan S. Focus on extracellular vesicles: introducing the next small big thing. Int J Mol Sci. 2016;17:170.

22. Henne WM, Buchkovich NJ, Emr SD. The ESCRT Pathway. Dev Cell. 2011;21:77–91.

23. Hessvik NP, Llorente A. Current knowledge on exosome biogenesis and release. Cell Mol Life Sci. 2018;75:193–208.

24. Van Niel G, D'Angelo G, Raposo G. Shedding light on the cell biology of extracellular vesicles. Nat Rev Mol Cell Biol. 2018;19:213–28.

25. Anand S, Samuel M, Kumar S, Mathivanan S. Ticket to a bubble ride: cargo sorting into exosomes and extracellular vesicles. Biochim Biophys Acta Proteins Proteom. 2019;1867:140203.

26. Bennett APS, de la Torre-Escudero E, Robinson MW. Helminth genome analysis reveals conservation of extracellular vesicle biogenesis pathways but divergence of RNA loading machinery between phyla. Int J Parasitol. 2020;50:655–61.

27. Palomba M, Rughetti A, Mignogna G, Castrignanò T, Rahimi H, Masuelli L, et al. Proteomic characterization of extracellular vesicles released by third stage larvae of the zoonotic parasite *Anisakis pegreffii* (Nematoda: Anisakidae). Front Cell Infect Microbiol. 2023;13:1–15. 28. Consortium TU. UniProt: the universal protein knowledgebase in 2023. Nucleic Acids Res. 2023;51:D523–31.

29. Gertz EM, Yu YK, Agarwala R, Schäffer AA, Altschul SF. Composition based statistics and translated nucleotide searches: improving the TBLASTN module of BLAST. BMC Biol. 2006;4:41.

30. McGuffin LJ, Bryson K, Jones DT. The PSIPRED protein structure prediction server. Bioinformatics. 2000;16:404–5.

31. Riera-Ferrer E, Del Pozo R, Piazzon MC, Sitjà-Bobadilla A, Estensoro I, Palenzuela O. *Sparicotyle chrysophrii* experimental infection of gilthead seabream (*Sparus aurata*): establishment of an *in vivo* model reproducing the pathological outcomes of sparicotylosis. Aquaculture. 2023;573:739588.

32. Mladineo I, Charouli A, Jelić F, Chakroborty A, Hrabar J. *In vitro* culture of the zoonotic nematode *Anisakis pegreffii* (Nematoda, Anisakidae). Parasit Vectors. 2023;16:51.

33. Webber J, Clayton A. How pure are your vesicles? J Extracell Vesicles. 2013;2:19861.

34. Rappsilber J, Mann M, Ishihama Y. Protocol for micro-purification, enrichment, pre-fractionation and storage of peptides for proteomics using StageTips. Nat Protoc. 2007;2:1896–906.

35. Cox J, Mann M. MaxQuant enables high peptide identification rates, individualized p.p.b.-range mass accuracies and proteome-wide protein quantification. Nat Biotechnol. 2008;26:1367–72.

36. Tyanova S, Temu T, Cox J. The MaxQuant computational platform for mass spectrometry-based shotgun proteomics. Nat Protoc. 2016;11:2301–19.

37. Tyanova S, Temu T, Sinitcyn P, Carlson A, Hein MY, Geiger T, et al. The Perseus computational platform for comprehensive analysis of (prote)omics data. Nat Methods. 2016;13:731–40.

38. Paysan-Lafosse T, Blum M, Chuguransky S, Grego T, Pinto BL, Salazar GA, et al. InterPro in 2022. Nucleic Acids Res. 2023;51:D418–27.

39. Punta M, Coggill PC, Eberhardt RY, Mistry J, Tate J, Boursnell C, et al. The Pfam protein families database. Nucleic Acids Res. 2012;40:290–301.

40. Conesa A, Götz S, García-Gómez JM, Terol J, Talón M, Robles M. Blast2GO: A universal tool for annotation, visualization and analysis in functional genomics research. Bioinformatics. 2005;21:3674–6.

41. Supek F, Bošnjak M, Škunca N, Šmuc T. Revigo summarizes and visualizes long lists of gene ontology terms. PLoS ONE. 2011;6:e21800.

42. Dalkiran A, Rifaioglu AS, Martin MJ, Cetin-Atalay R, Atalay V, Doğan T. ECPred: a tool for the prediction of the enzymatic functions of protein sequences based on the EC nomenclature. BMC Bioinformatics. 2018;19:334.

43. Rawlings ND, Barrett AJ, Thomas PD, Huang X, Bateman A, Finn RD. The MEROPS database of proteolytic enzymes, their substrates and inhibitors in 2017 and a comparison with peptidases in the PANTHER database. Nucleic Acids Res. 2018;46:D624–32.

44. Cwiklinski K, De La Torre-Escudero E, Trelis M, Bernal D, Dufresne PJ, Brennan GP, et al. The extracellular vesicles of the helminth pathogen, *Fasciola hepatica*: biogenesis pathways and cargo molecules involved in parasite pathogenesis. Mol Cell Proteomics. 2015;14:3258–73.

45. Okumura M, Katsuyama AM, Shibata H, Maki M. VPS37 isoforms differentially modulate the ternary complex formation of ALIX, ALG-2, and ESCRT-I. Biosci Biotechnol Biochem. 2013;77:1715–21.

46. Qadeer A, Giri BR, Ullah H, Cheng G. Transcriptional profiles of genes potentially involved in extracellular vesicle biogenesis in *Schistosoma japonicum*. Acta Trop. 2021;217:105851.

47. Krylova SV, Feng D. The machinery of exosomes: biogenesis, release, and uptake. Int J Mol Sci. 2023;24:1337.

48. Larios J, Mercier V, Roux A, Gruenberg J. ALIX- and ESCRT-III-dependent sorting of tetraspanins to exosomes. J Cell Biol. 2020;219:e201904113.

49. Baietti MF, Zhang Z, Mortier E, Melchior A, Degeest G, Geeraerts A, et al. Syndecan-syntenin-ALIX regulates the biogenesis of exosomes. Nat Cell Biol. 2012;14:677–85.

50. Barrett J. Nutrition and Biosynthesis. Biochemistry of Parasitic Helminths. 1st ed. London and Basingstoke: Macmillan Publishers Ltd; 1981. p. 149–244.

51. Haraszti RA, Didiot MC, Sapp E, Leszyk J, Shaffer SA, Rockwell HE, et al. High-resolution proteomic and lipidomic analysis of exosomes and microvesicles from different cell sources. J Extracell Vesicles. 2016;5:32570.

52. Sotillo J, Pearson M, Potriquet J, Becker L, Pickering D, Mulvenna J, et al. Extracellular vesicles secreted by *Schistosoma mansoni* contain protein vaccine candidates. Int J Parasitol. 2016;46:1–5.

53. Kifle DW, Pearson MS, Becker L, Pickering D, Loukas A, Sotillo J. Proteomic analysis of two populations of *Schistosoma mansoni*-derived extracellular vesicles: 15k pellet and 120k pellet vesicles. Mol Biochem Parasitol. 2020;236:111264.

54. Sheng ZA, Wu CL, Wang DY, Zhong SH, Yang X, Rao GS, et al. Proteomic analysis of exosome-like vesicles from *Fasciola gigantica* adult worm provides support for new vaccine targets against fascioliasis. Parasit Vectors. 2023;16:62.

55. Chaiyadet S, Sotillo J, Smout M, Cooper M, Doolan DL, Waardenberg A, et al. Small extracellular vesicles but not microvesicles from *Opisthorchis viverrini* promote cell proliferation in human cholangiocytes. bioRxiv [Preprint] 2023;1–30. Available from: https://doi.org/10.1101/2023.05.22.540805.

56. Poddubnaya LG, Hemmingsen W, Gibson DI. Clamp ultrastructure of the basal monogenean *Chimaericola leptogaster* (Leuckart, 1830) (Polyopisthocotylea: Chimaericolidae). Parasitol Res. 2014;113:4023–32.

57. Konstanzová V, Koubková B, Kašný M, Ilgová J, Dzika E, Gelnar M. An ultrastructural study of the surface and attachment structures of *Paradiplozoon homoion* (Bychowsky & Nagibina, 1959) (Monogenea: Diplozoidae). Parasit Vectors. 2017;10:261.

58. Ramasamy P, Bhuvaneswari R. The ultrastructure of the tegument and clamp attachment organ of *Gotocotyla bivaginalis* (Monogenea, Polyopisthocotylea). Int J Parasitol. 1993;23:213–20.

59. Mergo JCJr. Studies on the life history, development, occurrence, and microhabitat of *Microcotyle spinicirrus*, (Monogenea: Microcotylidae) Maccallum 1819. 1983.

60. Colorni A, Padrós F. Diseases and health management. In: Pavlidis MA, Mylonas CC, editors. Sparidae: Biology and Aquaculture of Gilthead Sea Bream and other Species. 1st ed. Blackwell Publishing Ltd; 2011. p. 321–57.

61. Wirtz-Peitz F, Knoblich JA. Lethal giant larvae take on a life of their own. Trends Cell Biol. 2006;16:234–41.

62. Sojka D, Franta Z, Horn M, Caffrey CR, Mareš M, Kopáček P. New insights into the machinery of blood digestion by ticks. Trends Parasitol. 2013;29:276–85.

63. Delcroix M, Sajid M, Caffrey CR, Lim KC, Dvořák J, Hsieh I, et al. A multienzyme network functions in intestinal protein digestion by a platyhelminth parasite. J Biol Chem. 2006;281:39316–29.

64. Caffrey CR, Goupil L, Rebello KM, Dalton JP, Smith D. Cysteine proteases as digestive enzymes in parasitic helminths. PLoS Negl Trop Dis. 2018;12:e0005840.

65. Dalton JP, Neill SO, Stack C, Collins P, Walshe A, Sekiya M, et al. *Fasciola hepatica* cathepsin L-like proteases: biology, function, and potential in the development of first generation liver fluke vaccines. Int J Parasitol. 2003;33:1173–81.

66. Peterkova K, Vorel J, Ilgova J, Ostasov P, Fajtova P, Konecny L, et al. Proteases and their inhibitors involved in *Schistosoma mansoni* egg host interaction revealed by comparative transcriptomics with *Fasciola hepatica* eggs. Int J Parasitol. 2023;53:253–63.

67. Robinson MW, Dalton JP, Donnelly S. Helminth pathogen cathepsin proteases: it's a family affair. Trends Biochem Sci. 2008;33:601–8.

68. Riera-Ferrer E, Piazzon MC, Del Pozo R, Palenzuela O, Estensoro I, Sitjà-Bobadilla A. A bloody interaction: plasma proteomics reveals gilthead sea bream (*Sparus aurata*) impairment caused by *Sparicotyle chrysophrii*. Parasit Vectors. 2022;15:322.

69. Sitjà-Bobadilla A, Álvarez-Pellitero P. Experimental transmission of *Sparicotyle chrysophrii* (Monogenea: Polyopisthocotylea) to gilthead seabream (*Sparus aurata*) and histopathology of the infection. Folia Parasitol (Praha). 2009;56:143–51.

70. Chaimon S, Limpanont Y, Reamtong O, Ampawong S, Phuphisut O, Chusongsang P, et al. Molecular characterization and functional analysis of the *Schistosoma mekongi* Ca2+ -dependent cysteine protease (calpain). Parasit Vectors. 2019;12:383.

71. de la Torre-Escudero E, Bennett APS, Clarke A, Brennan GP, Robinson MW. Extracellular vesicle biogenesis in helminths: more than one route to the surface? Trends Parasitol. 2016;32:921–9.

72. Mathew R, Wunderlich J, Thivierge K, Cwiklinski K, Dumont C, Tilley L, et al. Biochemical and cellular characterisation of the *Plasmodium falciparum* M1 alanyl aminopeptidase (PfM1AAP) and M17 leucyl aminopeptidase (PfM17LAP). Sci Rep. 2021;11:2854.

73. Skinner-Adams TS, Stack CM, Trenholme KR, Brown CL, Grembecka J, Lowther J, et al. Plasmodium falciparum neutral aminopeptidases: new targets for anti-malarials. Trends Biochem Sci. 2010;35:53–61.

74. Esser J, Gehrmann U, D'Alexandri FL, Hidalgo-Estévez AM, Wheelock CE, Scheynius A, et al. Exosomes from human macrophages and dendritic cells contain enzymes for leukotriene biosynthesis and promote granulocyte migration. J Allergy Clin. 2010;126:1032–40.

75. Haeggström JZ, Kull F, Rudberg PC, Tholander F, Thunnissen MMGM. Leukotriene A 4 hydrolase. Prostaglandins Other Lipid Mediat. 2002;68–69:495–510.

76. Toh SQ, Glanfield A, Gobert GN, Jones MK. Heme and blood-feeding parasites: friends or foes? Parasit Vectors. 2010;3:108.

77. Nebert DW, Vasiliou V. Analysis of the glutathione *S*-transferase (GST) gene family. Hum Genomics. 2004;1:460–4.

78. Atamna H, Ginsburg H. Heme degradation in the presence of glutathione. A proposed mechanism to account for the high levels of non-heme iron found in the membranes of hemoglobinopathic red blood cells. J Biol Chem. 1995;270:24876–83.

79. Sotillo J, Pearson MS, Becker L, Mekonnen GG, Amoahid AS, van Dam G, et al. In-depth proteomic characterization of *Schistosoma haematobium*: towards the development of new tools for elimination. PLoS Negl Trop Dis. 2019;13:e0007362.

80. Zhu L, Liu J, Dao J, Lu K, Li H, Gu H, et al. Molecular characterization of *S. japonicum* exosome-like vesicles reveals their regulatory roles in parasite-host interactions. Sci Rep. 2016;6:25885.

81. Chaiyadet S, Sotillo J, Smout M, Cantacessi C, Jones MK, Johnson MS, et al. Carcinogenic liver fluke secretes extracellular vesicles that promote cholangiocytes to adopt a tumorigenic phenotype. J Infect Dis. 2015;212:1636–45.

82. Furuyama K, Kaneko K, Vargas PD. Heme as a magnificient molecule with multiple missions: heme determines its own fate and governs cellular homeostasis. Tohoku J Exp Med. 2007;213:1–16.

83. Jomova K, Valko M. Importance of iron chelation in free radical-induced oxidative stress and human disease. Curr Pharm Des. 2011;17:3460–73.

84. Glanfield A, McManus DP, Anderson GJ, Jones MK. Pumping iron: a potential target for novel therapeutics against schistosomes. Trends Parasitol. 2007;23:583–8.

85. Carmona F, Palacios Ò, Gálvez N, Cuesta R, Atrian S, Capdevila M, et al. Ferritin iron uptake and release in the presence of metals and metalloproteins: chemical implications in the brain. Coord Chem Rev. 2013;257:2752–64.

86. Pakharukova MY, Savina E, Ponomarev DV, Gubanova NV, Zaparina O, Zakirova EG, et al. Proteomic characterization of *Opisthorchis felineus* exosome-like vesicles and their uptake by human cholangiocytes. J Proteomics. 2023;283–284:104927.

87. Prescott SM, Zimmerman G, Stafforini DM, McIntyre TM. Platelet activating factor and related lipid mediators. Annu Rev Biochem. 2000;69:419–45.

88. Venable ME, Zimmerman GA, McIntyre TM, Prescott SM. Platelet-activating factor: a phospholipid autacoid with diverse actions. J Lipid Res. 1993;34:691–702.

89. Arai H, Koizumi H, Aoki J, Inoue K. Platelet-activating factor acetylhydrolase (PAF-AH). J Biochem. 2002;640:635–40.

90. Sepulcre M, Pelegrín P, Mulero V, Meseguer J. Characterisation of gilthead seabream acidophilic granulocytes by a monoclonal antibody unequivocally points to their involvement in fish phagocytic response. Cell Tissue Res. 2002;308:97–102.

91. Zhou Y, Zheng H, Chen Y, Zhang L, Wang K, Guo J, et al. The *Schistosoma japonicum* genome reveals features of host-parasite interplay. Nature. 2009;460:345–51.

92. Noverr MC, Erb-Downward JR, Huffnagle GB. Production of eicosanoids and other oxylipins by pathogenic eukaryotic microbes. Clin Microbiol Rev. 2003;16:517–33.

93. Noto H, Hara M, Karasawa K, Iso-O N, Satoh H, Togo M, et al. Human plasma platelet-activating factor acetylhydrolase binds to all the murine lipoproteins, conferring protection against oxidative stress. Arterioscler Thromb Vasc Biol. 2003;23:829–35.

94. Grigg ME, Gounaris K, Selkirk ME. Characterization of a platelet-activating factor acetylhydrolase secreted by the nematode parasite *Nippostrongylus brasiliensis*. Biochem J. 1996;317:541–7.

95. Pawlowic MC, Zhang K. Leishmania parasites possess a platelet-activating factor acetylhydrolase important for virulence. Mol Biochem Parasitol. 2012;186:11–20.

96. Arme C, Fox MG. Oxygen uptake by *Diclidophora merlangi* (Monogenea). Parasitology. 1974;69:201–5.

97. Mazanec H, Koník P, Gardian Z, Kuchta R. Extracellular vesicles secreted by model tapeworm *Hymenolepis diminuta*: biogenesis, ultrastructure and protein composition. Int J Parasitol. 2021;51:327–32.

98. Sotillo J, Robinson MW, Kimber MJ, Cucher M, Ancarola ME, Nejsum P, et al. The protein and microRNA cargo of extracellular vesicles from parasitic helminths – current status and research priorities. Int J Parasitol. 2020;50:635–45.

99. Liu J, Zhu L, Wang J, Qiu L, Chen Y, Davis RE, et al. *Schistosoma japonicum* extracellular vesicle miRNA cargo regulates host macrophage functions facilitating parasitism. PLoS Pathog. 2019;15:e1007817.

100. Hartl FU, Bracher A, Hayer-Hartl M. Molecular chaperones in protein folding and proteostasis. Nature. 2011;475:324–32.

101. Spiess C, Meyer AS, Reissmann S, Frydman J. Mechanism of the eukaryotic chaperonin: protein folding in the chamber of secrets. Trends Cell Biol. 2004;14:598–604.

102. Kubota H, Hynes G, Willison K. The chaperonin containing t-complex polypeptide 1 (TCP-1): multisubunit machinery assisting in protein folding and assembly in the eukaryotic cytosol. Eur J Biochem. 1995;230:3–16.

103. European Chemicals Agency - ECHA. Formaldehyde and formaldehyde releasers - Strategy for future work. 2018 [cited 2023 Aug 5]. Available from: https://echa.europa.eu/documents/10162/17233/formaldehyde_review_report_en.pdf/551df4a2-28c4-2fa9-98ec-c8d53e2bf0fc?t=1516170136797.

104. European Chemicals Agency - ECHA. Substance evaluation conclusion as require by REACH article 48 and evaluation report for formaldehyde. 2019 [cited 2023 Aug 5]. Available from: https://echa.europa.eu/documents/10162/cc0acabf-6e82-f2ed-5dbe-8058f48ce6c4.

105. Acosta D, Cancela M, Piacenza L, Roche L, Carmona C, Tort JF. *Fasciola hepatica* leucine aminopeptidase, a promising candidate for vaccination against ruminant fasciolosis. Mol Biochem Parasitol. 2008;158:52–64.

106. Maggioli G, Acosta D, Silveira F, Rossi S, Giacaman S, Basika T, et al. The recombinant gut-associated M17 leucine aminopeptidase in combination with different adjuvants confers a high level of protection against *Fasciola hepatica* infection in sheep. Vaccine. 2011;29:9057–63.

107. Mekonnen GG, Pearson M, Loukas A, Sotillo J. Extracellular vesicles from parasitic helminths and their potential utility as vaccines. Expert Rev Vaccines. 2018;17:197–205.

108. Edgar RCS, Siddiqui G, Hjerrild K, Malcolm TR, Vinh NB, Webb CT, et al. Genetic and chemical validation of *Plasmodium falciparum* aminopeptidase PfA-M17 as a drug target in the hemoglobin digestion pathway. Elife. 2022;11:e80813.

109. Drinkwater N, Lee J, Yang W, Malcolm TR, McGowan S. M1 aminopeptidases as drug targets: broad applications or therapeutic niche? FEBS J. 2017;284:1473–88.

110. Fennell BJ, Naughton JA, Barlow J, Brennan G, Fairweather I, Hoey E, et al. Microtubules as antiparasitic drug targets. Expert Opin Drug Discov. 2008;3:501–18.

111. Cwiklinski K, Dalton JP. Omics tools enabling vaccine discovery against fasciolosis. Trends Parasitol. 2022;38:1068–79.

Chapter 9

General discussion

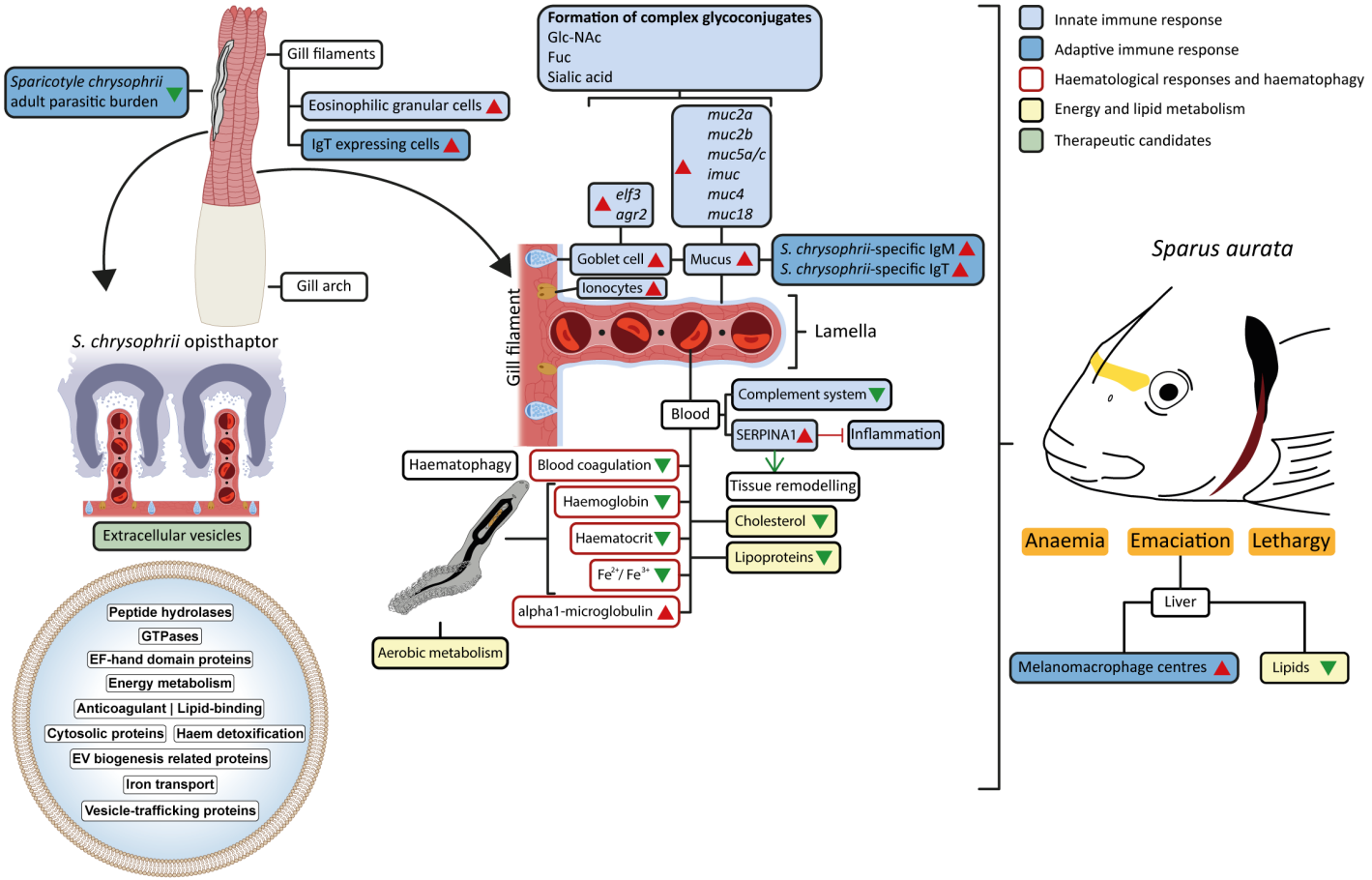

Figure illustrating the integration of key findings discussed in this section.

This multidisciplinary thesis comprehensively explores various aspects of the polyopisthocotylan ectoparasite *Sparicotyle chrysophrii* and its impact on the sparid teleost, gilthead seabream (*Sparus aurata*), given its effect on fish health and the economic challenge it represents to aquaculture in the Mediterranean basin. This final chapter intends to integrate the thorough findings from **Chapters 3** to **8**, providing a broad and clear understanding of the most relevant research outcomes.

Gilthead seabream growth performance

Sparicotylosis, a disease caused by *S. chrysophrii* gill infections, has been associated with lethargy, severe anaemia, and emaciation. Histopathological analyses of infected gilthead seabream revealed lamellar synechiae, clubbing and shortening of gill filaments, and epithelial hyperplasia leading to gill lamellae fusion[1,2]. These alterations, along with the anaemia, contribute to the hypoxic condition in affected hosts, explaining the observed lethargy. Additionally, the proliferation of ionocytes during sparicotylosis[2] highlights the osmoregulatory disruption caused by this disease.

A controlled *in vivo* infection model using *S. chrysophrii* and gilthead seabream was successfully developed (**Chapter 3**), providing the essential experimental framework and biological materials used in the subsequent chapters of this thesis. This model not only replicates the pathological effects and parasite loads observed in farmed gilthead seabream during their on-growing stage in sea cages under controlled laboratory conditions, but also effectively bypasses the need to source infected animals from sea cages that are often constrained by disease outbreaks and farmers' cooperation. Additionally, by incorporating non-lethal tools such as *S. chrysophrii* egg collectors to monitor the progression of parasitosis, the model contributes to the 3R strategy in experimental animal procedures, minimising harm and reducing the need for more invasive methods.

The results of this thesis indicate that *S. chrysophrii* has a more severe impact on juvenile gilthead seabream, which are more susceptible to infection by this flatworm than adults (**Chapter 3** and **Chapter 7**). Infected naïve adult gilthead seabream (484.9 ± 60.1 g; mean ± SD) showed stagnation in growth (both in weight and length) despite maintaining an optimal condition factor. In contrast, growth performance in adults (328.2 ± 29.6 g; mean ± SD) with acquired partial protection was better, gaining weight and growing in length while also maintaining an optimal condition factor (**Chapter 6**). In naïve juvenile gilthead seabream (20.22 ± 3.04 g; mean ± SD), although weight and length were positively correlated with infection intensity, the correlation for weight was not significant (**Chapter 3**). Conversely, the condition factor showed a significant negative correlation with infection intensity (**Chapter 3**). This suggests that, although juvenile gilthead seabream continue to grow in size, the characteristics of this growth may be compromised.

Growth may not be proportional to the total increase in body size, potentially due to fluid retention caused by an osmoregulatory impairment. Furthermore, hepatic fat depletion in infected gilthead seabream is another indicator of poor growth performance (**Chapter 3**).

Overall, juvenile gilthead seabream are highly susceptible to sparicotylosis following *S. chrysophrii* exposure and their growth performance remains significantly compromised. Interestingly, the proteomic analysis of the plasma of infected gilthead seabream (about 70 g) also reflected compensatory mechanisms aimed at restoring homeostasis as the infection progresses, since a reduced variability in plasmatic protein abundance was found in those fish with the highest infection intensities (**Chapter 4**).

Host immune response

Starting with the innate immune response, eosinophilic granular cells (EGCs) are pivotal innate immune cell effectors of teleost fish, particularly against gill parasites[3,4]. Among EGC populations in gilthead seabream, acidophilic granulocytes are considered functional equivalents of the mammalian neutrophils, serving as the predominant cell type recruited during immune responses[5,6], as observed in **Chapter 3**. These cells participate in various immune functions, including inflammation, vasodilation, neutrophil recruitment, and macrophage activation[3]. This thesis revealed a significant increase in branchial EGCs in the presence of adult *S. chrysophrii*, likely due to the tissue damage caused by the parasite's clamps on the host's gills (**Chapter 3**). In this context, the identification of leukotriene A4 hydrolase among *S. chrysophrii* excretory/secretory products (**Chapter 8**) suggests that the parasite might secrete eicosanoids as proinflammatory mediators targeting EGCs, similar to what has been described in some digenean trematodes[7,8].

Notably, *S. chrysophrii* has been associated with the modulation of SERPINA1, a serine protease inhibitor that inhibits neutrophil elastase, an enzyme involved in the acute phase of inflammation and tissue remodelling[9]. Elevated levels of SERPINA1 were observed in gilthead seabream with mild to low *S. chrysophrii* burdens (**Chapter 4**), suggesting that the parasite may impair the inflammatory response typically driven by EGCs. This highlights the complex interactions between *S. chrysophrii* and the host's immune system, wherein the parasite might modulate EGCs by promoting their activation (via eicosanoids) to induce localised inflammation, while simultaneously suppressing their tissue-degrading activities (via SERPINA1) to prevent excessive host tissue damage and ensure stable attachment to gill filaments.

Moreover, the complement system is a crucial component of the innate immune response, consisting of proteins that not only enhance pathogen clearance by promoting inflammation, opsonisation, and direct lysis through the formation of the membrane at-

tack complex, but also interact with the adaptive immune response. Known for its protective role, particularly against monopisthocotylan monogeneans at different life stages[10], the complement system was found to be inhibited by *S. chrysophrii* in infected gilthead seabream, as revealed by plasma proteomics (**Chapter 4**). This inhibition, which mirrors observations in other polyopisthocotylans[11], significantly compromises the host's immunocompetence. In addition, ceruloplasmin, an acute-phase protein associated with inflammation and tissue damage, shows altered activity in *S. chrysophrii*-infected gilthead seabream. An initial increase in plasma ceruloplasmin levels in mildly infected fish is followed by a decrease in heavily infected fish as the disease progresses (**Chapter 4**). These changes might reflect the different stages of the infection and the host's attempt to manage hypoxia and oxidative stress.

Additionally, gill-infecting monogeneans have been linked to host mucus hypersecretion at the infection site[12]. In this thesis, neutral mucin-secreting goblet cell hyperplasia was observed in gilthead seabream, directly associated with the presence of adult *S. chrysophrii* (**Chapter 3** and **Chapter 5**). This response likely serves as a defence mechanism, enhancing the protection of damaged gill tissue and maintaining gas exchange efficiency, counteracting parasite-induced hypoxia. The goblet cell hyperplasia was supported by the upregulation of genes related to both secreted (*muc2a*, *muc2b*, *muc5a/c*) and membrane-bound mucin genes (*imuc*, *muc4* and *muc18*) (**Chapter 5**). Moreover, the expression of regulatory factors involved in goblet cell differentiation (*elf3* and *agr2*) increased, and glycosylation patterns shifted toward more complex glycoconjugates featuring sialylated, fucosylated, and branched structures (**Chapter 5**). These modifications enhance the protective functions of mucus.

Regarding the adaptive immune response, melanomacrophage centres (MMCs), aggregations of phagocytes rich in melanin, haemosiderin, and lipofuscin[13–17] and considered to be evolutionary precursors of mammalian germinal centres[16,18,19], crucial for the differentiation and clonal expansion of memory B cells, were significantly more abundant in *S. chrysophrii*-infected gilthead seabream compared to healthy ones (**Chapter 3**). In this context, this observation suggests that *S. chrysophrii* infection triggers B cell activation, as previously indicated[20], pointing to the onset of a specific immune response likely accompanied by a shift in the Ig repertoire (**Chapter 4**).

Finally, upon reinfection with *S. chrysophrii*, while the prevalence of infection remained at 100%, the parasite burden was significantly lower in reexposed than in naïve gilthead seabream (**Chapter 6**). This suggests the acquisition of partial protection against adult specimens of the parasite. Reexposed gilthead seabream exhibited high specific IgT and IgM titres in gill mucus for months after the primary exposure to the parasite, alongside a significant increase in IgT expressing cells in gills. Binding specificity of specific

IgM in plasma and specific IgT in gill mucus were identified on *S. chrysophrii* specimens at various locations (**Chapter 6**).

The lack of a significant differential Ig response in the plasma of reexposed fish highlights the importance of the adaptive humoral immune response at mucosal level. However, changes in the Ig repertoire expression upon sparicotylosis (**Chapter 4**) might be driven by the shift of gill microbiota observed by Toxqui et al.[21], underscoring the systemic and local effects of this flatworm on its host.

Overall, *S. chrysophrii* elicits a complex immune response involving innate and adaptive mechanisms integrated at mucosal and systemic levels. The critical role of mucus in protecting gill tissue and mitigating the parasite's impact is underscored. Innate immunity modulation was evidenced by the significant increase in gill EGCs, plasma complement depletion, alterations in SERPINA1 and ceruloplasmin plasma levels, and gill mucus hypersecretion with shifts in mucin glycosylation. They all likely interact, coordinate and reshape the adaptive immunity, manifested through the presence of specific antibodies against the parasite, the increase of systemic and mucosal Ig expressing cells and the increase of splenic melanomacrophage centers. Thus, the multifaceted host immune response aimed at counteracting the parasite's pathogenic effects is illustrated. The observation of partial protection upon reinfection further highlights the potential for developing targeted vaccines. These findings offer a valuable foundation for advancing vaccine development and therapeutic strategies against this flatworm.

Host haematological responses and parasitic haematophagy

Sparicotylosis in gilthead seabream has been strongly associated with severe host anaemia, marked by reduced haemoglobin (Hb) levels, haematocrit (Hct), and red blood cell counts (RBCs), often visibly manifested as pale gills in infected fish[1,2]. This thesis consistently demonstrates the significant impact of *S. chrysophrii* on these haematological parameters (**Chapter 3**, **Chapter 4** and **Chapter 8**). While juvenile and post-larval stages of *S. chrysophrii* have a relatively minor effect on Hb and Hct levels, likely due to differing feeding strategies[22], a pronounced negative correlation was observed between Hb, Hct, and the infection intensity of adult *S. chrysophrii* (**Chapter 3**). However, the exact contribution to host anaemia of direct haematophagy *versus* traumatic haemorrhagic lesions caused by the parasite's haptor remains unclear.

In addition to anaemia, high *S. chrysophrii* burdens appear to modulate both the extrinsic and intrinsic pathways of the coagulation cascade. Modulation of the extrinsic coagulation pathway is likely due to the disruption of the gill epithelium caused by mechanical damage from the haptoral clamps or enzymatic damage prior to feeding, and of the intrinsic coagulation pathway by intravascular haemolysis (**Chapter 4**). These factors

ultimately impact the common pathway of the coagulation cascade (**Chapter 4**). Interestingly, in gilthead seabream presenting a high *S. chrysophrii* infection intensity, serine protease inhibitors, such as SERPIND1 and SERPING1 identified by plasma proteomics, were more abundant (**Chapter 4**). These inhibitors are known to interfere with the coagulation cascade, with SERPIND1 directly and indirectly inhibiting thrombin in the common pathway of the coagulation cascade, and SERPING1 inhibiting components within the intrinsic pathway[23–25]. Although it remains uncertain whether modulation of these inhibitors is a direct result of *S. chrysophrii* activity or a host response, their presence aligns with the observed disruptions in coagulation.

Further supporting this, gene ontology (GO) analysis of the proteins in purified *S. chrysophrii* extracellular vesicles (EVs) revealed a negative regulation of the coagulation (**Chapter 8**). This is consistent with the identification of platelet-activating factor acetylhydrolase (PAF-AH) in the EVs (**Chapter 8**). PAF-AH inhibits platelet aggregation[26], and along with SERPIND1 and SERPING1, may inhibit the host's coagulation cascade, thereby contributing to the parasite's ability to maintain a blood-feeding niche.

The effects of *S. chrysophrii* on its host extend beyond merely reducing Hb and Hct levels, as the parasite also depletes plasmatic free iron ions (Fe^{2+} / Fe^{3+}) from their hosts. These ions, along with haem-derived iron, are likely tied to the flatworm's utilisation of iron for its own biological functions, including metabolic processes and reproduction (**Chapter 7**). This is further supported by GO analysis from purified EV proteins, which indicated roles in iron transport and metal ion binding (**Chapter 8**).

The blood-feeding strategy of *S. chrysophrii* is closely tied to its buccal complex, which serves three main functions: sensory detection, host attachment, and haemolysis (**Chapter 7**). This complex contains giant cells (unicellular glands) that secrete digestive enzymes for extraintestinal digestion, similar to those in other blood-feeding monogeneans[27–29] (**Chapter 7**). Additionally, the taste organ aids the parasite in accessing blood capillaries in the host's gills, and the buccal sucker's muscular structure enhances attachment and suction supported by a retractile pharynx (**Chapter 7**). Moreover, the absence of blood cells in *S. chrysophrii* gut lumen (**Chapter 7**), as reported in other polyopisthocotylans[30–34], aligns with the probable haemolytic anaemia caused by *S. chrysophrii* blood meal intake, as suggested by the significant positive correlation between infection intensity and alpha-1-microglobulin levels (**Chapter 4**).

The haematophagous nature of *S. chrysophrii* was confirmed by identifying bloodmeal and haem groups in the parasite's gut, with its blood intake estimated at 2.84 ± 2.12 $\mu L \cdot 24h^{-1}$ (median ± IQR) (**Chapter 7**), a rate particularly concerning for juvenile gilthead seabream given their small total blood volume. Haematophagy involves a multienzymatic network cascade to acquire iron and amino acids. This process employs a diverse set of

peptidases, including cysteine peptidases from clans CA (cathepsins B, C, and L) and AA (cathepsin D), alongside aminopeptidases[35,36]. *In silico* studies on the protein composition of purified *S. chrysophrii* EVs, identified two metallo-catalytic-type aminopeptidases, namely leucyl aminopeptidase and alanyl aminopeptidase (**Chapter 8**), thought to be involved in the final steps of haemoglobin catabolism in some apicomplexans[37,38].

The management of free haem, a byproduct of haemoglobin digestion, presents a significant challenge for blood-feeding parasites due to its toxicity and pro-oxidant properties, which can lead to tissue damage and protein degradation[39]. To mitigate these harmful effects, haematophagous parasites must efficiently detoxify free haem groups. In monogenean blood-feeders, intracellular digestion of haemoglobin has been described[31], and was also inferred for *S. chrysophrii* from EV proteome GO analysis as intracellular iron ion homeostasis (**Chapter 8**). In this process, oxidised haem accumulates as insoluble ferriporphyrin haematin crystals, which are eventually excreted into the gut lumen and regurgitated[31]. *Sparicotyle chrysophrii* seems to utilise this haem detoxification strategy, as extracellular haematin crystals were observed in the flatworm's gut lumen (**Chapter 7**). Furthermore, the identification of glutathione *S*-transferase, an enzyme associated with haem detoxification, in *S. chrysophrii* EVs (**Chapter 8**), further evidences the role of these vesicles in managing haem toxicity. Additionally, the close association between iron deposits and vitellogenin underscores the critical importance of this trace element for reproductive purposes, which may simultaneously function as a haem detoxification pathway (**Chapter 7**).

Iron homeostasis is another critical aspect of *S. chrysophrii*'s survival, as both iron deficiency and excess pose significant challenges[40,41]. As mentioned before, the parasite depletes plasmatic free iron ions (Fe^{2+} / Fe^{3+}) from their hosts for its own biological functions (**Chapter 7**). Ferritins, which serve as iron storage proteins, help counteract the toxic effects of free iron ions by binding to them[42]. While a single ferritin was identified in purified *S. chrysophrii* EVs (**Chapter 8**), its precise role in the iron acquisition or the neutralisation of toxic effects remains to be fully understood.

Overall, *S. chrysophrii* significantly disrupts the haematological balance in gilthead seabream, contributing to severe anaemia and interfering with the host's coagulation pathways. This impact is particularly pronounced in juvenile gilthead seabream, more susceptible to the parasite's blood-feeding behaviour (**Chapter 7**). The parasite likely employs a multifaceted approach, including mechanical damage, enzymatic activity, and the release of extracellular vesicles that manipulate host processes. These adaptations, particularly in iron metabolism and haem detoxification, demonstrate the parasite's ability to maintain a stable blood-feeding environment. Understanding these mechanisms offers insights into potential strategies for managing sparicotylosis in affected fish populations.

Host and parasite energy and lipid metabolism

Previous studies on polyopisthocotylans, have suggested that these parasites require oxygen and likely rely on aerobic metabolism[43,44]. For instance, they are believed to derive their energy from aerobic respiration rather than from the glycogen reserves of their hosts[44]. Consistent with these findings, hepatic glycogen levels in *S. chrysophrii*-infected gilthead seabream remained unaltered (**Chapter 3**), further suggesting that *S. chrysophrii* also relies on aerobic metabolism. This need for oxygen could explain why adult *S. chrysophrii* specimens are typically located within the gills (**Chapter 3**), particularly near the gill filament apex and downstream in the ventilating water flow, where oxygen intake is maximised. Additionally, oxygen present in the blood meal consumed by the parasite could further supplement its needs, a strategy observed in other polyopisthocotylans[45]. Further supporting this notion, the presence of enzymes such as oxidoreductases, transferases, and lyases identified in *S. chrysophrii* EVs provides additional evidence of the parasite's reliance on aerobic metabolic processes (**Chapter 8**). Gene ontology analyses revealed biological processes associated with glycolysis, gluconeogenesis, and the pentose phosphate pathways, all indicative of an aerobic metabolism. These findings are in line with observations in other neodermatans, including polyopisthocotylans, digenean trematodes, and cestodes[43,46–48]. Interestingly, despite the initial assumptions that *S. chrysophrii* might not rely on glycogen (**Chapter 3**), GO analyses of the proteins in purified EVs inferred biological processes and molecular functions related to glycogen metabolism, such as the glycogen metabolic process and glycogen phosphorylase activity, respectively (**Chapter 8**). This suggests that while *S. chrysophrii* may utilise glycogen for its own needs, it does so without significantly depleting the host's glycogen stores, as observed in **Chapter 3**.

Concerning the impact on further metabolic processes, sparicotylosis in gilthead seabream significantly affects the fish's lipid metabolism. The emaciation observed in infected fish, evidenced by a reduction in hepatic lipid deposits and poor growth performance (**Chapter 3**), likely reflects the high energy demands imposed by the disease. The depletion of hepatic lipid stores suggests that the fish may be using these reserves as an energy source to meet the infection's metabolic costs. Similar findings have been reported in other parasitic infections[49], where nutrient absorption is impaired, making the hepatic lipid content a reliable indicator of the fish's overall health.

Parasitic platyhelminths are unable to synthesise fatty acids *de novo*[50], making them reliant on the host's lipid reserves. The role of *S. chrysophrii* in this metabolic disruption is further highlighted by its apparent reliance on the host's lipid reserves. The parasite's feeding behaviour might involve consuming these lipid reservoirs, as suggested by the observed hypocholesterolaemia and the significant reduction in plasma levels of ApoB-100,

a crucial structural component in very-low density lipoproteins (VLDL) and low-density lipoproteins (LDL), and ApoA-II, associated with high-density lipoproteins (HDL) (**Chapter 4**). These changes in lipid profiles are consistent with previously reported observations[20]. Since these lipoproteins play essential roles in various host physiological functions, including maintaining erythrocyte membrane stability[51], their alteration could affect the host's susceptibility to haemolytic events and immune responses as observed in mammals[52–54]. Interestingly, neodermatan's dependency on their host's lipid reservoir has been related to host immunomodulation and immune evasion[43,55,56].

Notably, some digenean trematodes have been shown to bind LDL to its surface, possibly as an immune evasion strategy, while also ingesting LDL to distribute lipids throughout its body[56]. It is plausible that *S. chrysophrii* employs comparable mechanisms, relying on the more readily digestible and transportable VLDLs and LDLs from its host. However, direct evidence of the worm feeding on or displacing the host's lipoproteins remains to be fully elucidated. The involvement of lipid transport in the parasite-host interaction is further supported by findings related to PAF-AH, an enzyme known to bind to various lipoproteins, including VLDL, LDL, and HDL[8]. This binding activity aligns with the lipid transport and metabolic disruptions observed in *S. chrysophrii*-infected gilthead seabream, providing a clearer understanding of the complex metabolic interactions between the parasite and its host.

Overall, the findings suggest that *S. chrysophrii* may rely on aerobic metabolism, as evidenced by stable hepatic glycogen levels in infected gilthead seabream and by the presence of enzymes linked to aerobic pathways in the parasite's EVs. Despite this, GO analyses hint at the parasite involvement in glycogen metabolism without significantly depleting the host's reserves. Additionally, sparicotylosis appears to disrupt the host's lipid metabolism, evidenced by the depletion of hepatic lipid reserves and reduction of key plasma lipoproteins, which might reflect the parasite's dependence on the host's lipid resources.

Management of sparicotylosis and potential therapeutic targets against *Sparicotyle chrysophrii*

Experimental evidence suggests that adult gilthead seabream are more resilient to sparicotylosis than juveniles, as the parasite's blood-feeding behaviour has a less severe impact on adult fish (**Chapter 7**). Additionally, research indicates that gilthead seabream infected with *S. chrysophrii* can develop a long-lasting, partial immunity, leading to a reduced parasitic burden despite a 100% prevalence of the parasite (**Chapter 6**). These findings imply that second-year class gilthead seabream may act as reservoirs of *S. chrysophrii* in enzootic farming sites, posing a risk to newly introduced juveniles in the same site and

that partial immunisation of gilthead seabream against *S. chrysphrii* is possible.

In Mediterranean sea cages, gilthead seabream farming often involves rearing different year-class groups in the same locations. This approach provides flexibility in harvest size and timing, ensuring a steady supply for market demand. However, while fallowing strategies can temporarily improve the health status of farming sites in *S. chrysophrii* enzootic locations, relapses are frequently observed within a year after resuming gilthead seabream production (personal observation). To effectively reduce the impact of *S. chrysophrii* and maintain fish health, adopting an *all-in*, *all-out* farming system seems critical.

Therapeutic strategies should focus on targeting specific molecules, pathways, genes, or proteins that are essential to the parasite's development but absent in the host. Targeting these parasite-specific elements could drive the development of effective drugs or vaccines, aiming to disrupt the parasite's biological processes. However, addressing *S. chrysophrii* is particularly challenging due to its ectoparasitic nature. Bath therapies in sea cages can lead to significant environmental impact and inconsistent dosing, while feed-based treatments face similar issues with dosage uniformity and potential environmental impact. These challenges emphasise the importance of innovative approaches that balance efficacy and environmental sustainability. In this context, extracellular vesicles (EVs) offer a promising therapeutic avenue. Acting as biological containers that carry virulence factors and facilitate host-parasite interactions, intraspecies communication, and interactions with the surrounding microbiota[57,58], EVs could enable more targeted treatments while reducing the overall environmental footprint.

In this thesis, *S. chrysophrii* EVs were successfully isolated and identified via transmission electron microscopy (TEM) in the haptoral region of adult specimens, where they appear to bud off from the syncytial lining covering the parasite's clamps (**Chapter 8**). This region displayed strong immunoreactivity to *S. chrysophrii*-specific host plasma IgM (**Chapter 6**), which also reacted against the parasite's outer tegument (**Chapter 6**). These findings suggest that EVs could be promising targets for pharmacological or prophylactic treatments aimed at reducing parasite load or eliminating the parasite. Further supporting this approach, GO analysis of purified *S. chrysophrii* EVs identified processes related to energy metabolism, iron transport, detoxification, and proteolysis. Notably, 13 proteins found in these EVs have been already been proposed as drug targets or vaccine candidates in other parasites, including digenean trematodes, nematodes, and apicomplexans (**Chapter 8**). Additionally, *S. chrysophrii*-specific host mucus IgT also exhibited immunoreactivity with the outer and inner tegument of the parasite, though not against the syncytial lining covering the parasite's clamps (**Chapter 6**). The presence of diverse immunogenic antigens detected by both, specific host plasma IgM and specific gill mucus IgT, demonstrates significant potential for vaccine development against adult *S. chrysophrii* specimens.

The proteomic analysis of *S. chrysophrii* EVs and the subsequent GO analyses, further suggests EV involvement in the essential parasite process of haem/iron detoxification, as indicated by the presence of leucyl aminopeptidase, alanyl aminopeptidase and glutathione *S*-transferase (**Chapter 8**). In this context, digestive enzymes from the haemoglobinolytic pathway, such as cathepsins (B, C, L, and D) and aminopeptidases[35,36], some of which have already been identified in the polyopisthocotylans[43], emerge as appealing targets against *S. chrysophrii*.

Moreover, considering *S. chrysophrii*'s impact on the host's lipid metabolism and reservoirs (**Chapter 3** and **Chapter 4**), and its apparent reliance on them, fatty acid-binding proteins (FABPs) also represent relevant targets. These proteins, previously described in trematode species and more recently in polyopisthocotylans[43,55], remain largely unexplored in monogeneans but hold potential as therapeutic targets.

Finally, platelet-activating factor acetylhydrolase (PAF-AH) (**Chapter 8**) stands out as an intriguing target. Despite the lack of knowledge about its role as a virulence factor or its function in Neodermata, its potential dual impact on haemostasis and lipid metabolism makes it particularly worthy of further investigation.

Overall, while managing *S. chrysophrii* poses significant challenges, innovative strategies such as targeting EVs, proteases, and fatty acid-binding proteins (FABPs) present valuable opportunities for therapeutic and prophylactic interventions. Continued research into these molecular targets, along with vaccine development, has the potential to yield more effective and sustainable methods for controlling this parasite and ensuring the health of farmed gilthead seabream.

References

1. Sitjà-Bobadilla A, de Felipe MC, Álvarez-Pellitero P. *In vivo* and *in vitro* treatments against *Sparicotyle chrysophrii* (Monogenea: Microcotylidae) parasitizing the gills of gilthead sea bream (*Sparus aurata* L.). Aquaculture. 2006;261:856–64.

2. Sitjà-Bobadilla A, Álvarez-Pellitero P. Experimental transmission of *Sparicotyle chrysophrii* (Monogenea: Polyopisthocotylea) to gilthead seabream (*Sparus aurata*) and histopathology of the infection. Folia Parasitol (Praha). 2009;56:143–51.

3. Reite OB, Evensen Ø. Inflammatory cells of teleostean fish: a review focusing on mast cells/eosinophilic granule cells and rodlet cells. Fish Shellfish Immunol. 2006;20:192–208.

4. Dezfuli BS, Giari L. Mast cells in the gills and intestines of naturally infected fish: evidence of migration and degranulation. J Fish Dis. 2008;31:845–52.

5. Mulero I, Chaves-Pozo E, García-Alcázar A, Meseguer J, Mulero V, García Ayala A. Distribution of the professional phagocytic granulocytes of the bony fish gilthead seabream (*Sparus aurata* L.) during the ontogeny of lymphomyeloid organs and pathogen entry sites. Dev Comp Immunol. 2007;31:1024–33.

6. Sepulcre M, Pelegrín P, Mulero V, Meseguer J. Characterisation of gilthead seabream acidophilic granulocytes by a monoclonal antibody unequivocally points to their involvement in fish phagocytic response. Cell Tissue Res. 2002;308:97–102.

7. Zhou Y, Zheng H, Chen Y, Zhang L, Wang K, Guo J, et al. The *Schistosoma japonicum* genome reveals features of host-parasite interplay. Nature. 2009;460:345–51.

8. Noverr MC, Erb-Downward JR, Huffnagle GB. Production of eicosanoids and other oxylipins by pathogenic eukaryotic microbes. Clin Microbiol Rev. 2003;16:517–33.

9. Pham CTN. Neutrophil serine proteases: specific regulators of inflammation. Nat Rev Immunol. 2006;6:541–50.

10. Ilgová J, Salát J, Kašný M. Molecular communication between the monogenea and fish immune system. Fish Shellfish Immunol. 2021;112:179–90.

11. Jedličková L, Dvořák J, Hrachovinová I, Ulrychová L, Kašný M, Mikeš L. A novel Kunitz protein with proposed dual function from *Eudiplozoon nipponicum* (Monogenea) impairs haemostasis and action of complement in vitro. Int J Parasitol. 2019;49:337–46.

12. Ogawa K. Diseases of cultured marine fishes caused by Platyhelminthes (Monogenea, Digenea, Cestoda). Parasitology. 2015;142:178–95.

13. Agius C. The role of melano-macrophage centres in iron storage in normal and diseased fish. J Fish Dis. 1979;2:337–43.

14. Agius C, Roberts RJ. Melano-macrophage centres and their role in fish pathology. J Fish Dis. 2003;26:499–509.

15. Wolke RE. Piscine macrophage aggregates: a review. Annu Rev Fish Dis. 1992;2:91–108.

16. Steinel NC, Bolnick DI. Melanomacrophage centers as a histological indicator of immune function in fish and other poikilotherms. Front Immunol. 2017;8:1–8.

17. Uribe C, Folch H, Enriquez R, Moran G. Innate and adaptive immunity in teleost fish: a review. Vet Med (Praha). 2011;56:486–503.

18. Buchmann K. Mucosal Immunity in Fish. In: Buchmann K, Secombes CJ, editors. Principles of Fish Immunology: From Cells and Molecules to Host Protection. 1st ed. 2022. p. 387–443.

19. Stosik MP, Tokarz-Deptuła B, Deptuła W. Melanomacrophages and melanomacrophage centres in Osteichthyes. Central European Journal of Immunology. 2019;44:201–5.

20. Piazzon MC, Mladineo I, Naya-Català F, Dirks RP, Jong-Raadsen S, Vrbatović A, et al. Acting locally- Affecting globally: RNA sequencing of gilthead sea bream with a mild *Sparicotyle chrysophrii* infection reveals effects on apoptosis, immune and hypoxia related genes. BMC Genomics. 2019;20:1–16.

21. Toxqui-Rodríguez S, Riera-Ferrer E, Del Pozo R, Palenzuela O, Sitjà-Bobadilla A, Estensoro I, et al. Molecular interactions in an holobiont-pathogen model: integromics in gilthead seabream infected with *Sparicotyle chrysophrii*. Aquaculture. 2024;581:740365.

22. Antonelli L, Quilichini Y, Marchand B. *Sparicotyle chrysophrii* (Van Beneden and Hesse 1863) (Monogenea: Polyopisthocotylea) parasite of cultured Gilthead sea bream *Sparus aurata* (Linnaeus 1758) (Pisces: Teleostei) from Corsica: ecological and morphological study. Parasitol Res. 2010;107:389–98.

23. Gettins PGW. Serpin structure, mechanism, and function. Chem Rev. 2002;102:4751–803.

24. Law RHP, Zhang Q, McGowan S, Buckle AM, Silverman GA, Wong W, et al. An overview of the serpin superfamily. Genome Biol. 2006;7:1–11.

25. Rau JC, Mitchell JW, Fortenberry YM, Church FC. Heparin Cofactor II: discovery, properties, and role in controlling vascular homeostasis. Semin Thromb Hemost. 2011;37:339–48.

26. Arai H, Koizumi H, Aoki J, Inoue K. Platelet-activating factor acetylhydrolase (PAF-AH). J Biochem. 2002;640:635–40.

27. Valigurová A, Vaškovicová N, Gelnar M, Kováčiková M, Hodová I. *Eudiplozoon nipponicum*: morphofunctional adaptations of diplozoid monogeneans for confronting their host. BMC Zool. 2021;6.

28. Valigurová A, Hodová I, Sonnek R, Koubková B, Gelnar M. *Eudiplozoon nipponicum* in focus: monogenean exhibiting a highly specialized adaptation for ectoparasitic lifestyle. Parasitol Res. 2011;108:383–94.

29. Hodová I, Sonnek R, Gelnar M, Valigurová A. Architecture of *Paradiplozoon homoion*: a diplozoid monogenean exhibiting highly-developed equipment for ectoparasitism. PLoS One. 2018;13.

30. Llewellyn J. Observations on the food and the gut pigment of the polyopisthocotylea (Trematoda: Monogenea). Parasitology. 1954;44:428–37.

31. Dalton JP, Skelly P, Halton DW. Role of the tegument and gut in nutrient uptake by parasitic platyhelminths. Can J Zool. 2004;82:211–32.

32. Santos CP, Souto-Padrón T, Lanfredi RM. The ultrastructure of the gastrodermis and the nutrition of the gill parasitic *Atriaster heterodus* Lebedev and Paruchin, 1969 (Platyhelminthes: Monogenea). Mem Inst Oswaldo Cruz. 1998;93:277–82.

33. Brennan GP, Ramasamy P. Ultrastructure of the gut caecal epithelium of *Pricea multae* (Monogenea: Polyopisthocotylea). Parasitol Res. 1996;82:312–8.

34. Jennings JB. Studies on digestion in the monogenetic trematode *Polystoma integerrimum*. J Helminthol. 1959;33:197–204.

35. Sojka D, Franta Z, Horn M, Caffrey CR, Mareš M, Kopáček P. New insights into the machinery of blood digestion by ticks. Trends Parasitol. 2013;29:276–85.

36. Delcroix M, Sajid M, Caffrey CR, Lim KC, Dvořák J, Hsieh I, et al. A multienzyme network functions in intestinal protein digestion by a platyhelminth parasite. Journal of Biological Chemistry. 2006;281:39316–29.

37. Mathew R, Wunderlich J, Thivierge K, Cwiklinski K, Dumont C, Tilley L, et al. Biochemical and cellular characterisation of the *Plasmodium falciparum* M1 alanyl aminopeptidase (PfM1AAP) and M17 leucyl aminopeptidase (PfM17LAP). Sci Rep. 2021;11:1–17.

38. Skinner-Adams TS, Stack CM, Trenholme KR, Brown CL, Grembecka J, Lowther J, et al. *Plasmodium falciparum* neutral aminopeptidases: new targets for anti-malarials. Trends Biochem Sci. 2010;35:53–61.

39. Schmitt TH, Frezzatti WA, Schreier S. Hemin-induced lipid membrane disorder and increased permeability: a molecular model for the mechanism of cell lysis. Arch Biochem Biophys. 1993;307:96–103.

40. Jomova K, Valko M. Importance of iron chelation in free radical-induced oxidative stress and human disease. Curr Pharm Des. 2011;17:3460–73.

41. Glanfield A, McManus DP, Anderson GJ, Jones MK. Pumping iron: a potential target for novel therapeutics against schistosomes. Trends Parasitol. 2007;23:583–8.

42. Carmona F, Palacios Ò, Gálvez N, Cuesta R, Atrian S, Capdevila M, et al. Ferritin iron uptake and release in the presence of metals and metalloproteins: chemical implications in the brain. Coord Chem Rev. 2013;257:2752–64.

43. Vorel J, Cwiklinski K, Roudnický P, Ilgová J, Jedličková L, Dalton JP, et al. *Eudiplozoon nipponicum* (Monogenea, Diplozoidae) and its adaptation to haematophagy as revealed by transcriptome and secretome profiling. BMC Genomics. 2021;22:1–17.

44. Arme C, Fox MG. Oxygen uptake by *Diclidophora merlangi* (Monogenea). Parasitology. 1974;69:201–5.

45. Houlihan DF, Macdonald S. *Diclidophora merlangi* and *Entobdella soleae*: egg production and oxygen consumption at different oxygen partial pressures. Exp Parasitol. 1979;48:109–17.

46. Sotillo J, Pearson MS, Becker L, Mekonnen GG, Amoahid AS, van Dam G, et al. In-depth proteomic characterization of *Schistosoma haematobium*: towards the development of new tools for elimination. PLoS Negl Trop Dis. 2019;13:1–23.

47. Cwiklinski K, De La Torre-Escudero E, Trelis M, Bernal D, Dufresne PJ, Brennan GP, et al. The extracellular vesicles of the helminth pathogen, *Fasciola hepatica*: biogenesis pathways and cargo molecules involved in parasite pathogenesis. Molecular and Cellular Proteomics. 2015;14:3258–73.

48. Mazanec H, Koník P, Gardian Z, Kuchta R. Extracellular vesicles secreted by model tapeworm *Hymenolepis diminuta*: biogenesis, ultrastructure and protein composition. Int J Parasitol. 2021;51:327–32.

49. Picard-Sánchez A, Estensoro I, Perdiguero P, del Pozo R, Tafalla C, Piazzon MC, et al. Passive immunization delays disease outcome in gilthead sea bream infected with *Enteromyxum leei* (Myxozoa), despite the moderate changes in IgM and IgT repertoire. Front Immunol. 2020;11:1–14.

50. Barrett J. Nutrition and Biosynthesis. Biochemistry of Parasitic Helminths. 1st ed. London and Basingstoke: Macmillan Publishers Ltd; 1981. p. 149–244.

51. Van Der Stoep M, Korporaal SJA, Van Eck M. High-density lipoprotein as a modulator of platelet and coagulation responses. Cardiovasc Res. 2014;103:362–71.

52. Han R. Plasma lipoproteins are important components of the immune system. Microbiol Immunol. 2010;54:246–53.

53. Norata GD, Pirillo A, Ammirati E, Catapano AL. Emerging role of high density lipoproteins as a player in the immune system. Atherosclerosis. 2012;220:11–21.

54. Grao-Cruces E, Lopez-Enriquez S, Martin ME, Montserrat-de la Paz S. High-density lipoproteins and immune response: a review. Int J Biol Macromol. 2022;195:117–23.

55. Lombardo JF, Pórfido JL, Sisti MS, Giorello AN, Rodríguez S, Córsico B, et al. Function of lipid binding proteins of parasitic helminths: still a long road. Parasitol Res. 2022;121:1117–29.

56. Bennett MW, Caulfield JP. Specific binding of human low-density lipoprotein to the surface of schistosomula of *Schistosoma mansoni* and ingestion by the parasite. American Journal of Pathology. 1991;138:1173–82.

57. Drurey C, Coakley G, Maizels RM. Extracellular vesicles: new targets for vaccines against helminth parasites. Int J Parasitol. 2020;50:623–33.

58. Rooney J, Northcote HM, Williams TL, Cortés A, Cantacessi C, Morphew RM. Parasitic helminths and the host microbiome – a missing 'extracellular vesicle-sized' link? Trends Parasitol. 2022;38:737–47.

Chapter 10

Conclusions

1. The achieved experimental *in vivo* transmission model successfully maintains *Sparicotyle chrysophrii* under experimental conditions, with temperature and biomass as key factors, replicating the pathological effects and parasite loads in farmed gilthead seabream and providing a controlled environment, providing biological material to study the parasite's biology, host-parasite interactions and for testing treatments.

2. The *Sparicotyle chrysophrii* egg collector, a practical and reliable non-lethal tool, proves to be effective in monitoring the progression of the parasitosis without the need to handle or euthanise fish, in compliance with the 3R strategy in experimental animal procedures (reduce, reuse, and recycle).

3. Haemostasis, the immune system, and lipid metabolism in infected fish are the main altered biological processes, as revealed by the plasma proteome of *Sparicotyle chrysophrii*-infected gilthead seabream.

4. Gilthead seabream presenting high *Sparicotyle chrysophrii* burdens attempt to restore some of the alterations suffered during the acute stage of the disease, as evidenced by their reduced variability in plasmatic protein abundance.

5. Infected gilthead seabream show increased goblet cell numbers and activity, leading to more mucus production, driven by upregulated mucin and regulatory genes, for protection against *Sparicotyle chrysophrii*.

6. Mucus secreted during infection is less viscous and rich in neutral glycoconjugates, facilitating water flow and gas exchange in the gills, critical for counterbalancing parasite-induced hypoxia.

7. Gilthead seabream develop an adaptive immune response against *Sparicotyle chrysophrii* after initial exposure, providing partial protection, and those that recovered from a prior infection exhibit better growth than naïve gilthead seabream upon subsequent exposure to the parasite.

8. The protective mucosal response in reexposed gilthead seabream involves specific immunoglobulins, particularly IgT, in the gill mucus and increased IgT-expressing cells in the gill filaments.

9. The haematophagous nature of *Sparicotyle chrysophrii* is demonstrated by the presence of blood and exogenous haem groups and by estimating the average daily blood volume intake by the parasite.

10. The functional anatomy of the parasite's buccal and gastrodermal apparatus is described, highlighting the absence of blood cells and the presence of haematin crystals.

11. A close relationship between blood intake, haem detoxification, and reproduction of *Sparicotyle chrysophrii* is revealed, including the necessity of an alternative iron source beyond haem for survival.

12. Extracellular vesicles are successfully isolated and observed via transmission electron microscopy in the syncytial tegument of *Sparicotyle chrysophrii*'s haptoral region.

13. Protein characterisation of isolated extracellular vesicles, showing similarities to those in other neodermatans, reveals proteins associated with vesicle biogenesis and enhances understanding of *Sparicotyle chrysophrii*'s aerobic metabolism, iron transport, detoxification, and proteolysis, while also identifying potential therapeutic targets found in other parasitic organisms.